UNIVERSITY OF LIVERPOOL

Understanding the role of two conserved, but hypothetical bacteriophage genes, in controlling the biology of their host cells

Thesis submitted in accordance with the requirements of the University of Liverpool for the degree of Doctor in Philosophy by

Hashim Felemban

February 2022

Acknowledgements

Thanks to God (Allah) for his saving and blessing me and my family upon our life.

There are really no words can describe my fully appreciation and gratitude to my supervisor Dr Heather Allison who has been a guidance, motivator, supporter, advisor, and supervisor me from the first day in the PhD to the end. It was a generous time to work under her supervision. I would like to appreciate my appreciation my secondary supervisors Professor Alan McCarthy, and Professor Jay Hinton for their helpful advice. I would like also to thank Professor Waldemar Vollmer and his research group in Newcastle University for giving me a chance of collaboration work in lab to run some peptidoglycan studies, Dr Mohammed Mohaisen for his useful lab skills advises in my first year of PhD, Dr Nicolas Wenner for sharing his knowledge in some experiments, and Mr Paul Loughnane for his help in the lab.

I acknowledge the Ministry of Education and King abdulaziz University, Saudi Arabia for sponsoring the PhD in University of Liverpool.

My appreciation to my role model Mr Reda Felemban who is my dad, and Mrs Jawahir Bamahfouz who is my mam for their supporting, and I pray god to save them always. Massive shout of appreciation goes to my love and wife Mrs Nibras Abu lnaja for her patient on living away and far distance from each other during the PhD years and carring and growing up our kids (Abdulmalik, and Mohmmed) who I love them and I am excited to live again together in one home.

I am grateful to every member in lab H in University of Liverpool colleagues for timing and sharing experiences. I want to mention all the names in lab H. Special thanks to my flatmate Mr Ammar Basabrain for sharing and living together in one flat for more than three years.

In sports side but it was happened during my PhD years, I want to send my greeting to the football teams members that I have played with them during my PhD and we won many titles which positively impacts on my mental health during the PhD. The teams are Futsal men University of Liverpool who won the Northern British Universities and Collages Sport (BUCS) cup 2020, Parkway Villa FC who won the East Cheshire Sunday Football league (ECSFL) league and cup 2018, and AFC Didsbury.

Abstract

Stx phages convert their bacterial hosts, providing them with shigatoxigenic potential. All *E. coli* carrying Stx phage are known as Shiga toxin-encoding *Escherichia coli* (STEC) and have become a global challenge to food safety. Around 74% of the genes carried by the model Stx phage, $\phi 24_B$ (vB_EcoP_24_B), are annotated as hypothetical, and we have been ascribing function to many of these genes. The expression of some hypothetical genes has been shown to be uncoupled from viral replication, but function to aid the lysogen in surviving environmental stresses such as antibiotic and acid exposures. Two genes are examined in this study, gene 21 (vB _24_B_21) and gene 48 (vB _24_B_48). The former is expressed only at the end of the lytic cycle and the latter only during the lysogenic cycle.

We have created a series of isogenic mutants to establish whether P21 impacts upon phage release. Though, the crystal structure of P21 was recently solved and we demonstrated that this protein has the previously unknown ability to modify peptidoglycan and to bind to it. Work is currently ongoing to better understand if and how the action of P21 controls phage release. Why the phage would do this is left to speculation, but it could be a mechanism to hold on to the phage due to the significant fitness advantage provided to the lysogen when the Stx phage exists as a resident prophage. The initial data presented in this work has demonstred that an induced lysogen carrying a phage producing P21 releases fewer progeny phages than an induced lysogen that does not produce P21, even though the same number of phages are made intracellularly. We examined whether the difference in phage release happened at the cell level or at the population level. We demonstrated that there were differences in cell morphology and different live and dead cell ratios showing that phage release was impacted across the population.

The $\phi 24_B$ lysogen has been shown phenotypic microarray to confer a multitude of low-level resistances to its bacterial host cell. Gene 48 is an enormous hypothetical gene that is predicted to encode a protein of 2808 a.a. It is located at the right end of the integrated prophage $\phi 24_B$. However, this protein has many of the conserved features of the bacterial “giant genes” that usually encode a surface protein associated in bacterial fitness. It was hypothesised that this gene might be behind some not all of these resistant phenotypes. A synthetic plasmid carrying gene 48 was constructed and *E.coli* naiive MC1061 cells were transformed and compared with naiive and lysogen cells in the six antimicrobial agents resistance assays. The bacterial cells that carry the plasmid possessing gene 48 showed more resistance to 8-hydroxyquinoline than naïve cells in an arabinose inducible manner, indicating that gene 48 is involved in this resistance. As a result, it may explain which gene that is encoded by $\phi 24_B$ lysogen modulates the phage-mediated resistance to 8-hydroxyquinoline that has been previously described.

Table of Contents

List of Figures

List of Table

List of Abbreviations

2D-PAGE	Two-dimensional polyacrylamide gel electrophoresis
4-MUFAc	4-methylumbelliferyl-acetate
4-MUFac	4-Methylumbelliferyl acetate
a.a.	Amino acids
A/E	Attaching and Effacing
AAF	Aggregative adherence factors
Amox	Amoxicillin
Amp	Ampicillin
Ape	Acetylpeptidoglycan esterase
Arp	Actin related protein
ATP	Adenosine Tri Phosphate
att	attachment site
BFP	Bundle-forming pilus
cAMP	Cyclic adenosine monophosphate
Car	Carbenicillin
Cat	Chloramphenicol
CAZy	Carbohydrate-Active Enzyme database
CBD	Carbohydrate binding domian
CCl_3	Chloroform
cDNA	Copy DNA
CDS	Coding sequences
Cef	Cefoxitin
cGMP	Cyclic guanosine monophosphate
CMAT	Change Mediated Antigen Technology
Ct	Cycle threshold
DAEC	Diffuse-Adherant *Escherichia coli*
DAF	decay Decay accelerating factor
ddH_2O	Double distilled water
$DiSC_3$ (5)	3,3'-dipropylthiadicarbocyanine iodide
DNA	Deoxyribonucleic acid
DUF	Domain unknown function
EaeA	Intimin
EAF	*Escherichia coli* adherence factor
EAST1	Heat-satable toxin
EDTA	Ethylenediaminetetraacetic acid
EHEC	Enterohaemorrhagic *Escherichia coli*
Ehx	Enterohaemolysin
EIEC	Enteroinvasive *Escherichia coli*
EPEC	Enterpathogenic *Escherichia coli*
ER	Endoplasmic reticulum
Esp	Extracellular serine protease
EspP	Extracellular serine protease
ETEC	Enterotoxigenic *Escherichia coli*
FACS	Fluorescence activated cell sorting
GAD	Glutamic acid decarboxylase
Gb_3	Globotriaosylceramide 3
GlcNAc	*N*- acetylglucosamine
HPLC	High Performance Liquid Chromotography

HRP	Horse Radish Peroxidase
HUS	Haemolytic uremic syndrome
IL	Interleukin
IMAC	Immobilized metal affinity chromatography
Kan	Kanamycin
KatP	Catalase-peroxidase
LB	Luria Burtani
LEE	Locus of Enterocyte Effacement
Ler	LEE encoded regulator
LPS	Lipopolysaccharide
LT	Heat labile enterotoxin
LT	Lytic transglycosylase
MIC	Minimum inhibitory concentration
MOPS	3-(N-morpholino) propanesulfonic acid
mRNA	Massenger
MRSA	Methicillin-resistant *Staphylococcus aureus*
MurNAc	N-acetylmuramic acid
Nan S	N-acetylneuraminate esterase
nt	Nucleotide(s)
Ni^{+2}	Nickle ion
Nor	Norfoxacin
N-WASP	neuronal Wiscott Aldrich syndrome protein
OMV	outer membrane vesicles
OMVs	outer membrane vesicles
ONPG	ortho-nitrophenyl-β-D-galactoside
ORFs	Open reading frames
p	Promotor
PAI	Pathogenicity Associated Island
PBP	Penicillin binding protein
PBS	Phosphate buffered saline
Per	Plasmid encoded regulator
Pet	Autotransporter protease toxin
PG	Peptidoglycan
Pgd	Peptidoglycan deacetylase
pic	serine protease precursor
PLS-DA	Partial least discriminant analysis
qPCR	Quantitative (Real-time) PCR
Rif	Rifampicin
RNA	Ribonucleic
RT-PCR	Reverse transcription polymerase chain reaction
RTX	Repeat in toxin
S.O.C.	Super optimal broth
SCC	Saline sodium citrate
SDS	Sodium Dodecyl Sulphate
SDS-PAGE	Sodium dodecyl-sulfate-polyacrylamide gel electrophoresis
SEM	Standard error of mean
ShET1	*Shigella* enterotoxin 1
SIB	Sub inhibitory concentration
sIgA	Secretory Immunoglobin A
SLT	Shiga-like toxin

SOB	Super optimal broth
SPATE	serine protease auto-transporter of the *Enterobateriaceae*
ST	Heat stable enterotoxin
Stx	Shiga toxin
t	Terminator
T2SS	Type II Secretion System
T3SS	Type III Secretion System
TAE	Tris-acetate-EDTA
TBS	Tris Buffer Saline
Tet	Tetracycline
Tir	Translocated intimin receptor
TNF-α	Tumour necrosis factor-α
ToxB	Clostridium difficile-like toxin
Tris	Tris (hydroxymethyl) methylanime
TSS	Transcription start sites
TTP	Thrombocytopenic purpura
Tween 20	Polysorbate 20
U-2-P	Uridine-2-monophosphate
UV	Ultraviolet
Vav	Vancomycin
VP	Virulence plasmid
VT	Verocytotoxin
WB	Western blotting
α-hlyA	α-hemolysin
λ	Lambda phage
ϕ	Bacteriophage

List of units

Unit	Definition
µJ	Microjoule
µF	Microfarad
µg	Microgram
µl	Microlitre
µm	Micrometre
min	Minutes
bp	Base pair
℃	Degree Centigrade
c.f.u	Colony forming unit
cm	Centimetre
g	Gram
h	Hour
Hg	Hectogram
kb	Kilobases
kbp	Kilobases pair
kDa	Kilodaltons
kn	Kiloneuclotide
L	litre
M	Moles per liter
mA	Milliamperes
mg	Milligram
min	minute
mL	Millilitre
mM	Millimoles per litre
mV	Millivolt
ng	Nanogram
nm	Nanometer
OD	Optical densities
P	P value
p.f.u	Plaque forming unit
r.p.m	Revolution per minute
RT	Room temprature
V	Volt
v/v	Volume to volume
W	Watt
w/v	Weight to volume
λ_{em}	Emission wavelenght
λ_{ex}	Excitation wavelength
µM	Micromoles per litre
Ω	Electrical resistance
U	Dalton
sec	Second

CHAPTER 1:

INTRODUCTION

1.1. *Escherichia coli*

Escherichia coli (*E. coli*) is a Gram negative bacterium that is classified within the family of the *Enterobacteriaceae* (Brenner, 1981). *E. coli* cells are viewed under the light microscope as rods with rounded ends (Fig 1.1) that are approximately 2.0-6.0 µm in length and 1.1-1.5 µm in width (Percival and Williams, 2014). *E. coli* is a facultative anaerobic organism that is motile via peritrichous flagella. It is non-spore forming, lactose fermenting and produces gas from carbohydrate fermentation. *E. coli* normally produces a positive ortho-nitrophenyl-β-D-galactoside (ONPG) reaction, indicating the production of β -galactosidase. Moreover, it produces a positive methyl red reaction that maintains the acidic pH after carbohydrate fermentation, produces indole, is catalase positive, oxidase negative and doesn't hydrolyse urea (Percival and Williams, 2014). Many *E. coli* cells are encapsulated or micro-encapsulated through the production of acidic polysaccharides comprised of K or M antigens that help identify these strains through serology (Jiménez et al., 2012). In addition, the fimbriae or pili that can decorate the outer surface of *E. coli* are hydrophobic and play a role in host adhesion properties (Percival and Williams, 2014). *E. coli* are divided into many distinct groups based on serotype and genotype that vary in their pathogenic profile with many groups comprising part of the healthy gut microbiota in humans (Savage, 1977a, Savage, 1977b) to pathogenic groups (Fig 1.2) like the *enterohaemorrhagic E. coli* (EHEC) serogroups that cause bloody diarrhoea and even death in humans (Allison, 2007).

1.1.1. Non- Pathogenic *E. coli*

The human gut microbiota is comprised of an estimated 500+ taxa of bacteria which amounts to a total of ~10^{13} – 10^{14} cells per gram of the gastrointestinal tract of which 0.4% of the overall bacteria are *E. coli* cells (Tenaillon et al., 2010, Sender, 2016). Commensal *E. coli* have many important functions that impact upon the health of their human host including: antimicrobial protection, nutrient metabolism, and immunomodulation (Jandhyala et al., 2015). Commensal *E. coli* cells are found in the large intestine, they are placed on the mucus layer that coats the epithelial cells

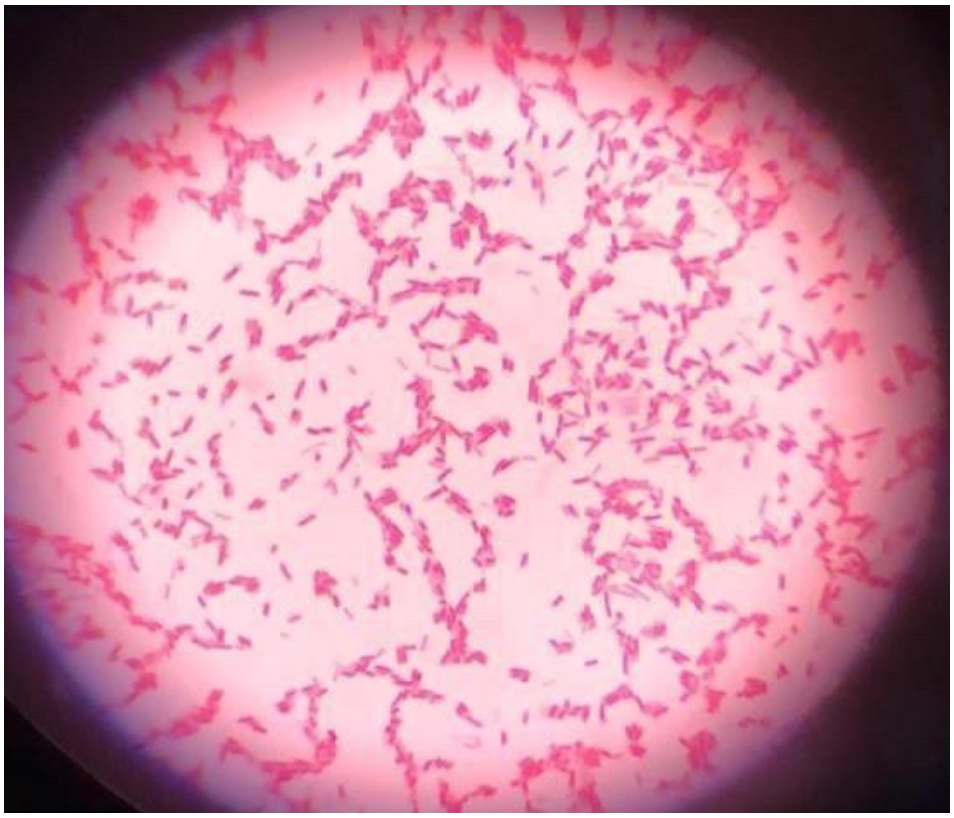

Figure 1. 1. *E. coli* cells under light microscope with magnification 1000×.
Gram stain showing *E. coli* cells, pink stained cells with rod shape rounded ends are typical characteristic of most gram negative bacteria.

throughout the digestive tract. As a result, the advantage of presence *E.coli* in epithelial cells is inhbiting pathogen colonization by keeping away the pathogenic microbes to contact the epithelial cells via double tiered mucus layers.

Commensal *E. coli* colonising the intestinal wall play an important role in maintaining equilibrium within the gut microbiotum by facilitating the production of trefoil-factor and resistin-like molecule-β from goblet cells (Johansson, Phillipson et al. 2008, Kim and Ho 2010). Trefoil-factor and resistin-like molecule-β maintain the integrity of the host cells by stabilisation of the mucin polymers stable thereby creating a barrier (Johansson, Larsson et al. 2011). Moreover, they ferment carbohydrates by synthesising short chain fatty acids like butyrate that provide a significant source for energy for the intestinal cells (Macfarlane and Macfarlane, 2003, Sartor, 2008).The host cell uses this energy to interact with the short chain fatty acids and a G protein-coupled receptor, Gpr41, via a ligand receptor (Samuel et al., 2008). As a result, the butyrate production is inhibiting the accumulation of toxic metabolism like D-lactate (Bourriaud et al., 2002). Commensal *E. coli* can improve the host cell immunity in activation of the intestinal dendritic cells by inducing plasma cells of the intestinal mucosa via MY-D88 signaling to express secretory IgA (sIgA) that turn coating the gut microbiota especially in subclass sIgA2 that exceedingly resists the bacterial protease degradation (He et al., 2007).

1.1.2. Pathogenic *E. coli* Pathotypes

1.1.2.1. Enterotoxigenic *E. coli* (ETEC)

Enterotoxigenic *E. coli* (ETEC) is named because the disease symptoms it causes are related to its production of toxins. ETEC is associated with watery diarrhoeal symptoms that can be mild to fatal. This disease is often referred to as travellers' diarrhoea (Nataro and Kaper, 1998). These organisms are commonly found in developing countries with limited sanitation systems and access to clean water. Young children less than 2 years of age (Qadri et al., 2005) are most affected by ETEC because they undergo rapid dehydration, as a result of diarrhoea (Kotloff et al., 2013). ETEC can be associated with > 22 colonization factors that are presented as *E. coli* surface antigens (Gaastra and Svennerholm, 1996): fimbrial, fibrillar, nonfimbrial and helical proteins (Qadri et al., 2005). As a result, ETEC cells colonise the small intestine using colonization factors and produce and secrete the enterotoxins (Aziz et al., 2008, Kaper et al., 2004b). There are two distinct types of enterotoxins: heat-labile (LT) and

heat-stable (ST). These toxins are the main virulence factors causing diarrhoea (Fig 1.2A) (Fleckenstein et al., 2010).

LT shares similarity with cholera toxin at the physiological, structural, and antigenic levels. LT contains A subunit surrounded by five similar binding B subunits (Gill and Richardson, 1980, Holmgren, 1981). The B subunits enable the toxin to interact with a susceptible cell using a host cell receptor GM1 ganglioside. The A subunit is responsible for activation of adenylate cyclase. As a result, the level of cAMP (cyclic adenosine monophosphate) increases which leads to a stimulation of chloride ion secretion in the crypt cells and prevents sodium chloride in the villus tips. From this action, the bowel's absorptive capacity is exceeded which results in watery diarrhoea (Gill and Richardson, 1980). There are two classes of ST (STh that was discovered first in relation to human disease, and STp that was initially discovered in pigs). STh can reversibly bind to guanylate cyclase which raises levels of cGMP (cyclic guanosine monophosphate) in the intestinal lumen (Rao, 1985). ST is also involved in cell proliferation control, as a result, raising intracellular calcium levels. ST activates chloride secretion in the crypt cells and prevents sodium chloride absorption. As a result, watery diarrhoea symptom is caused (Sears and Kaper, 1996).

1.1.2.2. Diffusely adherent *E. coli* (DAEC)

Diffusely adherent *E. coli* (DAEC) is a common cause of diarrhoea affecting children under 12 months age (Nataro and Kaper, 1998). It is characterised as diffusely adherent to human intestine Caco-2 cells *in vitro* (Kaper et al., 2004b). The main virulence factor of DAEC are fimbrae which bind to the cell surface of enterocytes, specifically their glycosylphosphatidylinositol-anchored protein known as decay accelerating factor (DAF) (Hasan et al., 2002, Peiffer et al., 1998). This binding results in the stimulation of DAF (also known as CD55) and through signal transduction promotes cytoskeleton F-actin rearrangement (Peiffer et al., 1998). The cytoskeletal rearrangement leads to the development and extrusion of long microvilli that surround and hold DAEC, attaching them to the Caco-2 cell surface (Fig 1.2B) (Bernet-Camard et al., 1996, Cookson and Nataro, 1996, Yamamoto et al., 1992). As a result, the infection of intestinal cells by DAF binding, results in the reduction of the activity and abundance of brush-border-associated hydrolases that impact on the mechanism of the adsorption and secretion, leading to the symptom of diarrhoea (Peiffer et al., 2001).

1.1.2.3. Enteropathogenic *E. coli* (EPEC)

Younger children less than five years are most affected by Enteropathogenic *E. coli* (EPEC) (Black et al., 2010). EPEC is also associated with infantile diarrhoea in the developing countries (Nataro and Kaper, 1998). A pathogenicity island (PAI) called the locus of enterocyte effacement (LEE) is the main virulence associated of EPEC (Trabulsi et al., 2002). The LEE genes encode a T3SS to release locus proteins into host's gut epithelial cells, destroying host cell activities and producing attaching and effacing (A/E) lesion (Iguchi et al., 2009, Nataro and Kaper, 1998). Effacement of intestinal epithelial cell microvilli that results from rearrangement of the cytoskeleton is facilitated by EPEC-mediated A/E lesions on epithelial cells via an outer membrane protein by the EPEC called intimin to form a pedestal beneath. Effacing (A/E) lesion causes a disturbance of the gut epithelial cell surface that result in lose of surface area thereby reducing fluid absorbtion by the cells (Fig 1.2C) (Nataro and Kaper 1998). When this is combined with increased intestinal permeability and inflammation it can lead to diarrhoea (Nataro and Kaper, 1998). Another factor that contributes to the virulence of EPEC is the plasmid *E.coli* adherence factor (EAF) which encodes two crucial operons: the *bfp* operon that encodes the type IV bundle-forming pilus (BFP), and the *per* operon that encodes a plasmid encoded transcriptional activator regulator (Per) (Ochoa and Contreras, 2011). Moreover, some strains of EPEC encode toxins such as heat-labile enterotoxin that stimulates secretion of fluid from epithelial cells into the large intestine (Scotland et al., 1981), cytotoxic necrotising factor that impacts on the cytoskeleton leading to cellular necrosis (Caprioli et al., 1983), and cytolethal distending toxin that stops mitosis (Bouzari and Varghese, 1990).

1.1.2.4. Enteroaggregative *E. coli* (EAEC)

Enteroaggregative *E. coli* (EAEC) is associated with persistent diarrhoea in malnourished children and immunosuppressed people in developed countries (Nataro et al., 2006). EAEC is characterized by its intestinal colonisation strategy that results in a "stacked-brick", aggregative adherence on Hep-2 epithelial cells (Nataro et al., 1998). There are three stages describing EAEC pathogenesis: 1) EAEC cells adhere to HE-p2 epithelial cells in the intestinal mucosa. 2) EAEC cells encrusted on the surface of enterocytes stimulate the production of mucus. 3) toxins are released that stimulate an inflammatory response, and derive to intestinal secretion and mucosal toxicity (Harrington et al., 2005, Nataro, 2005). The first stage involves the function of

a large cluster of genes encoded on the EAEC chromosome. Amongst these genes is *aggR*, which encodes a regulator that controls expression of *aap* (encoding Dispersion (Aap) protein), and other adherence factors (Nataro et al., 2006). Aap mediates the antiaggregation phenotype of EAEC by inducing a change in the polarization of the bacterial outer membrane (Velarde et al., 2007). The pAA plasmid also encodes fimbrial structures named aggregative adherence factors (AAF) that allow EAEC cells to adhere the HE-p2 intestinal mucosa (Nataro et al., 1993). The second stage occurs when the EAEC cells adhere to the mucosa, characterised by an aggregating biofilm (Wakimoto et al., 2004). *AggR* regulates this biofilm production and requires a few other genes including: Fis a DNA-binding protein required for growth regulation (Sheikh et al., 2001), and *air* a gene that encodes a predicted outer membrane protein associated with biofilm formation (Sheikh et al., 2006). The third stage involoves the release of toxins that are encoded by a large virluence palsmid named pAA (Boisen et al., 2013), or locus chromosome on opposite strands (Kaper et al., 2004b), are caused stimulation of inflamatory response (Harrington et al., 2006). Three EAEC toxins damage the tips and sides of intestinal villi. The first toxin is the plasmid encoded autotransporter protease toxin (Pet) that breaks down alpha III spectrin inside the epithelial cytoskeleton resulting in exfoliation of clonocytes and cell extension (Navarro-García et al., 2001, Boisen et al., 2013). The second toxin is similar to *Shigella* enterotoxin 1 (ShET1) (Ménard and Dubreuil, 2002) whose mode of action is not understood, but may be involved in secretory diarrhoea which results from both EAEC and *Shigella* infection (Kaper et al., 2004b, Boisen et al., 2013). This thought is based on ShET1 encoded in serine protease precursor (*pic*) open reading frame that are expressed in the intestinal luman (Harrington et al., 2009). The expression of *pic* has been associated with increased *E. coli* growth in a mouse moodle, while *pic* mutant showed a decrease in cellular colonisation (Henderson et al., 2001). The last toxin is a heat- stable toxin (EAST1) that is encoded by the *astA* gene (Ménard and Dubreuil, 2002), and is involved in the production of watery diarrohea (Kaper et al., 2004b). EAEC infection leads to mucosal damage, resulting in the induction of interleukin-8 (IL-8). As a result, the cytokine is released and neutrophil transmigration is stimulated which cause watery diarrohea and tissue disturbance (Fig 1.2D) (Kaper et al., 2004b).

1.1.2.5. Enteroinvasive *E. coli* (EIEC)

The genetics, biochemical and pathological features of the Enteroinvasive *E. coli* (EIEC) pathotype are almost identical to those associated with *Shigella spp*. (Wei et al., 2003, Pupo et al., 2000). EIEC and bacteria in the *Shigella* genus cause shigellosis, a disease that results from invasion of the mucosal tissue lining as well as the further exacerbation of the inflammatory response from the gut (Kotloff et al., 1999, Lan and Reeves, 2002). A virulence plasmid (VP) of ~220 kb in size harbours the main virulence factor encoded by EIEC. These virulence factors enable EIEC cells to enter into epithelial cells of the gut lining where the organisms can spread from cell to cell in a manner that hides them from the host cell immune system. Amongst the genes carried on the VP are a set of genes that encode a type III secretion system (TTSS) which includes a type three secretion apparatus (TTSA) that extends from the bacterial envelope, and secreted protein effectors that move through the TTSA and are injected directly into the eukaryotic target cell's cytoplasm through a pore created by the TTSA (translocon). The protein effectors are injected inside the eukaryotic cell along with chaperones that escort effector proteins to the translocon structure (Parsot, 2005). Once the bacterial effectors reach the enterocyte's cytoplasm, they direct rearrangement of the cell cytoskeleton. These cytoskeletal rearrangements cause the enterocyte's membrane to expand beyond the area of contact between the EIEC cells, resulting in enterocycte membrane ruffling. Ultimately the enterocytes are forced to engulf the EIEC cells inside a vacuole (Tran Van Nhieu et al., 2000). EIEC cells then lyse the membrane of vacuole, and the EIEC cells escape into the enterocyte's cytoplasm. Once in the cytoplasm, the EIEC cells access the actin at one of its polar ends and direct the polymerisation of the actin from this pole. This polymerisation propels the EIEC through the cell, resembling a rocket tail. In this way EIEC cells are able to move from one host cell into neighbouring cell through actin-mediated motility avoiding much of the intestinal immune response (Fig 1.2F) (Girardin et al., 2001).

1.1.2.6. Enterohaemorrhagic *E. coli* (EHEC)

Enterohaemorrhagic *E. coli* (EHEC) is associated with intestinal disease that is often defined by the production of bloody diarrhoea. The symptoms of an EHEC infection range from mild diarrhoea to severe symptoms such as haemorrhagic colitis, haemolytic uremic syndrome (HUS), and thrombocytopenic purpura (TTP) (Kaper et al., 2004a). It is classified as a subset of Shigatoxigenic *E. coli* (STEC), but the EHEC

pathogroup not only carries *stx* gene to be the main virulence factors of STEC. They also carry additional host colonisation factors *e.g.* the LEE encoding PAI (Nataro and Kaper, 1998) and other virulence factors *e.g.* pO157 virulence plasmid that encodes enterohaemolysin (Ehx) and catalase-peroxidase (KatP) (Burland et al., 1998a).

1.2. EHEC Virulence Factors

1.2.1. Locus of Enterocyte Effacement

The 35 kb LEE PAI encodes 41 open reading frames (ORFs) and is defined as a genetic characteristic of the A/E pathogens *e.g.* EPEC and EHEC (McDaniel et al., 1995). Like some of the virulence-associated elements detected in the pathogenic *E. coli*, the lower GC content of the LEE (38.3%) compared to the whole *E. coli* chromosome (50.8%), indicate that it was acquired through horizontal gene transfer (McDaniel and Kaper, 1997, Frankel et al., 1998). The T3SS of EHEC, including the outer membrane protein intimin (EaeA) and effector proteins such as translocated intimin receptor (Tir) are encoded by LEE genes, and drive the intimate attachment of EHEC to colonic enterocytes, resulting in the production of A/E lesions (Kenny et al., 1997). Moreover, the regulator of control expression of LEE genes is Ler, a 15 kDa protein encoded by the first gene of the LEE1 operon. Ler is important for creation of A/E lesions (Mellies et al., 1999, Elliott et al., 2000, Friedberg et al., 1999, Mellies et al., 2007). Regulation of LEE gene expression is also controlled by environmental factors such as temperature and quorum sensing (Franzin and Sircili, 2015). The 41 ORFs of LEE are organised into five operons called LEE1, LEE2, LEE3, LEE4, and LEE5 (Mellies et al., 1999). The *esc* and *sep* genes, which encode the major structure of the T3SS, are harboured in LEE1, LEE2, and LEE3 (Jarvis et al., 1995). The genes which are located at LEE4 operon (Knutton et al., 1989, Donnenberg et al., 1993), form a hollow tubular structure and using EspA to link the bacterium to the host cell, and form a pore in the host cell membrane by proteins encoded by *espB* and *espD* (Kenny, 2001, Vallance and Finlay, 2000) A hairpin loop structure is formed in the host cell membrane by Tir, which is encoded in LEE5 operon (Donnenberg et al., 1993, Kenny, 2001, Knutton et al., 1989), and translocated to the host cell by the T3SS.

LEE is responsible for the A/E lesion phenotype by encoding the T3SS genes and effector proteins. A/E lesion features are defined by intimate attachment of the bacteria to the enterocyte membrane, damage to the brush border microvilli,

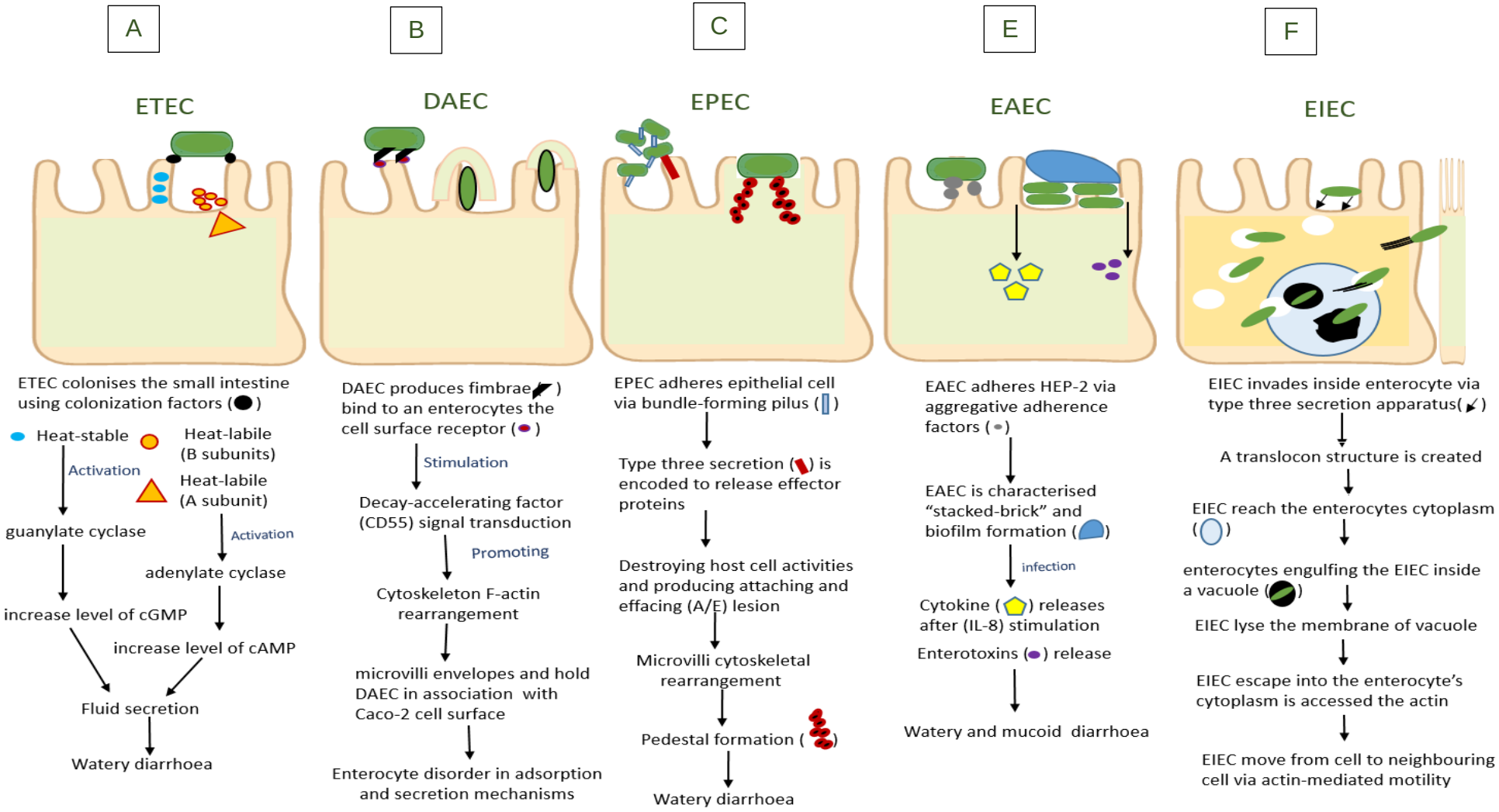

Figure 1. 2. Mechanistic schema of pathogenic *E. coli*.

The five characterised types of pathogenic *E. coli* have different methods in pathogenesis of human host cells. A) ETEC firstly colonises the small intestine, and then it produces and secretes the enterotoxins. B) DAEC firstly produces fimbrae that binds to enterocyte cell surface receptor that stimulates the (CD55) signal transduction, and then the microvilli envelope surrounds and holds DAEC in attaching with Caco-2 cell surface. C) EPEC firstly adheres epithelial cells resulting in the destruction of microvillar structure and producing attaching and effacing lesion, and finally because the cytoskeletal rearrangement, the pedestal formation is caused. D) EAEC firstly adheres to epithelial cells in the intestinal mucosa that results EAEC encrusts on enterocytes surface by stimulation of the enterocytes' production of mucus, and then enterotoxins and inflammatory response are released. F) EIEC firstly invades inside enterocyte, and then lyse the phagosome and moves to neighbouring cells.

rearrangement of cytoskeletal by binding bacterial intimin to *Tir*, and creating pedestal-like structures on which the bacteria attach to the host cells (Knutton et al., 1989, Kaper et al., 2004b, Moon et al., 1983). Although the consequence of the Tir-intimin interaction is similar in EHEC and EPEC, the mechanisms of A/E formation are not identical (Goosney et al., 2001), and there also different in host cells adherence, which is EPEC adheres to small intestine enterocytes and EHEC attaches to colon epithelial cells (Kaper et al., 2004a). The caboxy-terminus of Tir produced by EHEC is only 41% similar at the amino acid level to the carboxy-terminus of EPEC Tir, compared to an overall similarity of 60% across the entire proteins (Gruenheid et al., 2001). The mechanism of EPEC interaction with Tir begins when Tir has been introduced into the host cell membrane, host cell kinases phosphorylate a tyrosine residue in the carboxy-terminus of Tir that permit Nck (a host cell signalling protein) to bind Tir and N-WASP (neuronal Wiscott Aldrich syndrome protein) which induces the Arp2/3 complex (actin related protein) (Gruenheid et al., 2001, Caron et al., 2006). As a result, actin polymerisation occurs, which drives pedestal formation (Fig 1.3A) (Caron et al., 2006, Campellone et al., 2004). The difference in the EHEC mechanism of action is the caboxy-terminus of EHEC encoded Tir does not possess a tyrosine residue that becomes phosphorylated and the Nck binding site is missing (Goosney et al., 2001, DeVinney et al., 1999). Instead it is activated when it enters the cell and N-WASP can interact with it without modification immediately directing actin polymerisation (Goosney et al., 2001) with the help of an additional effector protein encoded by EHEC, $EspF_{U,}$ that binds the host membrane remodelling protein IRSp53 (Fig 1.3B) (Campellone et al., 2004, de Groot et al., 2011).

Moreover, there are 21 other effector proteins that are translocated by EPEC and EHEC and have been described in (Table.1.1). The genes encoding these effectors are scattered across the genome residing in: LEE elements, insertion sequences, random chromosomal locations, or prophages (Dean and Kenny, 2009). Examples of LEE encoded effector proteins are *EspF* (implicated in host cell intestinal barrier function and apoptosis), and EspG (implicated in microtubule disturbance) (Dean and Kenny, 2009, Elliott et al., 2001, Yoshida and Sasakawa, 2003). Examples of non-LEE encoded effector proteins are Cif (cycle-inhibiting factor, causes mitosis arrest and cell death), and EspJ (inhibits phagocytosis) (Marchès et al., 2008, Dahan et al., 2005).

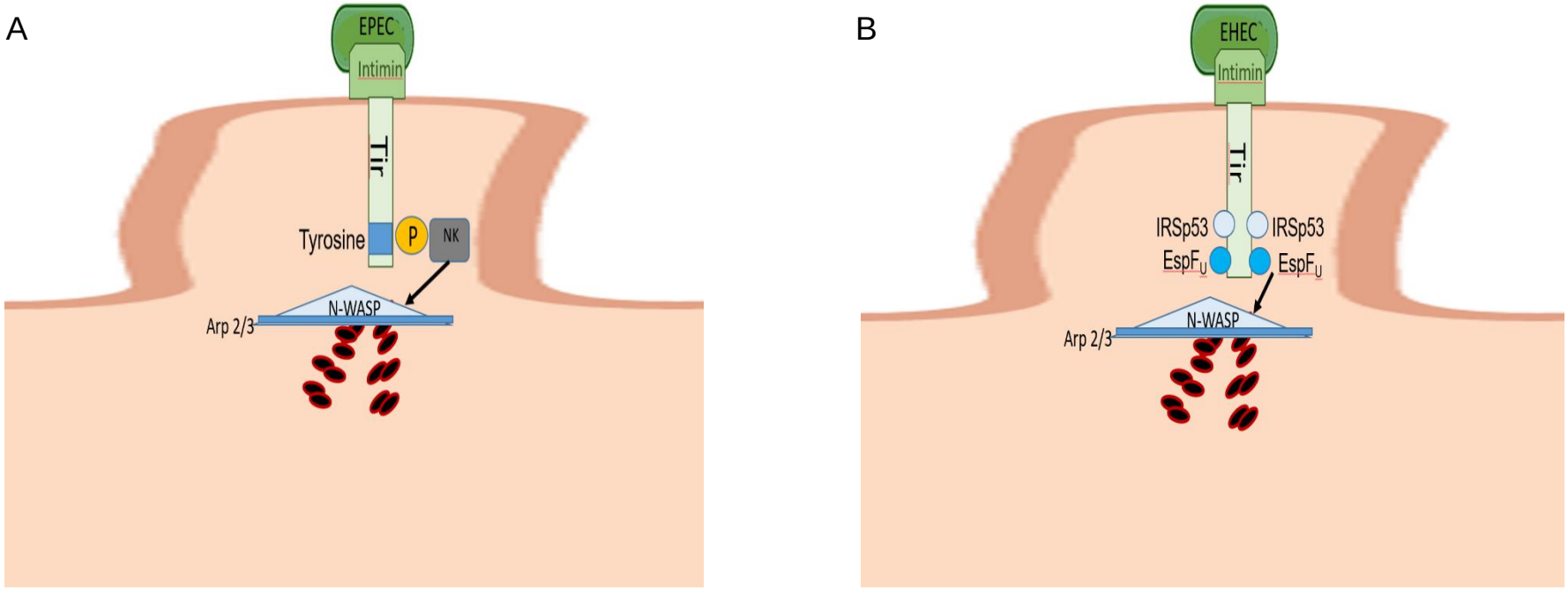

Figure 1. 3. Mechanism of action of pedestal formation by EPEC and EHEC.

The mechanism of interaction in EPEC and EHEC starts when *Tir* has injected into the host cell membrane, but the difference of action is the tyrosine residue in the carboxy-terminus has phosphorylated or not. A) In EPEC, the host cell kinases phosphorylates a tyrosine residue in the carboxy-terminus that permits *Nck* which is the host cell signalling protein to bind *Tir* and N-WASP (neuronal Wiscott Aldrich syndrome protein) that inducts the Arp2/3 complex (actin related protein) , as a result, actin polymerisation occurs, and pedestal formation. B) In EHEC, the caboxy-terminus of *Tir* of EHEC does not phosphorylate tyrosine residue. The N-WASP is still inducted and participated in actin polymerisation by effector protein namely $EspF_U$ that is encoded by EHEC, and binds the host membrane remodelling protein IRSp53.

Table 1.1. The effector proteins encoded by EPEC and EHEC, and their mobile genetic elements. (Dean and Kenny, 2009)

Effector protein	Function	Location
Tir	Intimin receptor	LEE5
Map	Cellular tight Junction disruption, cytoskeletal rearrangement	LEE3
EspB	Inhibition of phagocytosis, pore formation	LEE4
EspF	Apoptosis, N-WASP activation, tight Junction disruption	LEE4
EspH	Cytoskeletal rearrangement	LEE3
EspG	Microtubule disruption, tight Junction disruption	LEE1
EspG2/ORF3	Microtubule disruption	Insertion element
EspJ	Inhibition of phagocytosis	Prophage
EspL2	Modulate the cellular cytoskeleton (Tobe, 2010)	Insertion element
NIeA	Inhibition of protein secretion	Prophage
NIeB1	Inhibit Apoptosis (Pollock et al., 2017)	Insertion element
NleB2	Catalytic activitiy (Giogha et al., 2021)	Prophage
NIeC	Pro-inflammatory (Sham et al., 2011)	Prophage
NleD	Pro-inflammatory (Clements et al., 2012)	Prophage
NIeE1	Induction of innate immune system	Insertion element
NIeE2	Induction of innate immune system	Insertion element
NleF	Inhibit Apoptosis (Pollock et al., 2017)	Prophage
NleG	Unknown	Prophage
NIeH1	Pro-inflammatory	Prophage
NIeH2	Pro-inflammatory	Prophage
Cif	Inhibition of mitosis	Prophage

1.2.2. pO157 plasmid

A plasmid is an extrachromosomal molecule of DNA that can replicate independently from the chromosome. It can equip its bacterial host with different beneficial functions, for example: antibiotic resistance, toxin production and virulence factors or even additional metabolic pathways (Frost et al., 2005). Plasmid-encoded genes that are necessary to maintain a pathogenic profile are found across many enteropathogenic bacteria such as *Yersinia*, *Salmonella*, pathogenic *E. coli*, and *Shigella* (Lim et al., 2010).

EHEC O157:H7 isolates often carry a highly conserved plasmid which is called pO157. The size of pO157 from *E. coli* O157:H7 isolates is usually ~92 kb and has been completely sequenced (Burland et al., 1998a, Makino et al., 1998). It encodes ~100 ORFs (Burland et al., 1998a). Of these: 43 ORFs are orthologs of genes characterised elsewhere; 22 ORFs are completely hypothetical, lacking homology to anything in the current gene databases; and 35 ORFs encode proteins that are presumably related to the pathogenesis of *E. coli* O157:H7 infections, but only 19 genes have been previously identified as virulence factors, including enterohaemolysin (Ehx), catalase-peroxidase (KatP), a Clostridium difficile-like toxin (ToxB), as well as a type-II secretion system, and an extracellular serine protease (Burland et al., 1998a).

1.2.3. Enterohaemolysin

The first sequence had described virulence factor of encoding pO157 was enterohaemolysin (Ehx) (Bauer and Welch, 1996, Schmidt et al., 1995). When pO157 had sequenced, the results have shown two ORFs have 60% homology to *ehxA* and *ehxC* genes with the *E. coli* α-hemolysin (*α-hlyA*) operon (Schmidt et al., 1995). The EHEC-*ehx* operon harbours 4 genes which are: *ehxA* encodes protein which is classified as a member of the RTX (Repeat in toxin) family that are characterised as pore-forming cytolysins with haemolytic function (Schmidt et al., 1995) in some pathogenic Gram negative bacteria (Bauer and Welch, 1996), *ehxC* whose production is involved in posttranslational modification of the toxin (Castanie-Cornet et al., 1999, Delahay et al., 2001), and *ehxB* and *ehxD* that is required for transporting toxin outside the bacteria (Schmidt et al., 1996, Bauer and Welch, 1996). Moreover, these genes appear to be involved in a defective secretion system in *E. coli* O157 (Schmidt et al., 1995). Moreover, the production of Ehx flourishes in an anaerobic condition at 37 ℃

in laboratory experiments, which is the same environmental conditions found in the human colon (Chart, 1998, Law, 2000a). Ehx is frequently associated with infections that lead to HUS symptoms more than just those leading to simple diarrhoeic symptoms, but it is not the main virulence factor associated with more severe disease (Schmidt and Karch, 1996). Ehx induces the production of interleukin-1β (IL-1 β) in human monocytes (Taneike et al., 2002), and also induces the production of interleukin-1β (IL-1 β) in human macrophages and shares to the cytotoxicity of these cells (Zhang et al., 2012). Moreover, Ehx is also associated with the production of a biologically active form of outer membrane vesicle (OMVs) that transports bacterial toxins and other molecules from Gram negative bacteria to various targets (Aldick et al., 2009, Kuehn and Kesty, 2005) However, it is still unclear if some Ehx remains associated with the bacterial cell surface (Schwidder et al., 2019).

1.2.4. Catalase-peroxidase

The *katP* is a 2.2 kb gene that encodes a periplasmic protein, KatP, which is responsible for the bacterial bifunctional catalase-peroxidase (Lim et al., 2010). Catalase plays important role in protecting bacterial from oxidative stress. Oxygen metabolism produces reactive oxygen molecules that are toxic to bacterial cells (Farr and Kogoma, 1991). Moreover, phagocytes produce reactive oxygen molecules for oxidative damage purposes to destroy bacterial pathogens (Welch, 1987, Bortolussi et al., 1987, Beaman and Beaman, 1984) that they engulf so bacteria have evolved the ability to produce enzymes like catalases and peroxidases to protect themselves. Examples of KatP homologs have been annotated in pathogens like *Legionella pneumophila* (KatA), *Yersinia pestis* and *Yersinia tuberculosis* (KatY) (Bandyopadhyay and Steinman, 2000, Garcia et al., 1999). KatY is associated with pathogenic bacterial strains, and it expressed only when environmental temperatures shift from 26℃ to 37℃ (Garcia et al., 1999). KatP and KatY share only 75% homology at the nucleotide level, and unlike KatP, KatY is chromosomally encoded (Garcia et al., 1999). It is suggested that horizontal genetic transfer of these genes has involoved to the oraganism pathogensis (Faguy and Doolittle, 2000). However, beside the function of enzymes in oxidative stress respond is thoughtful to have a role in abloishing the neutrophil response to bacterial infection (Varnado et al., 2004).

1.2.5. Clostridium difficile-like toxin (ToxB)

The *toxB* gene size is 9.5 kb and at the amino acid level, it shares 20% identify

with toxin B of *Clostridium difficile* (Barroso et al., 1990, Makino et al., 1998) that is classified to the large clostridial toxin family (von Eichel-Streiber et al., 1996). Because the sequence of the *toxB* had demonstrated strong similar to the N-terminus of the member of the large clostridial family that is associated with cytoskeletal disruption, it can be assumed that ToxB has a similar function to toxin B of *Clostridium difficile* (Law, 2000b, Burland et al., 1998b). *ToxB* production has contributed to the adherence of EHEC O157 to Caco-2 cells through the promotion production of T3SS effector proteins (Tatsuno et al., 2001). In addition, the ToxB protein has shared homology with proteins that are encoded in EPEC and non-O157 EHEC strains (Morabito et al., 2003, Stevens et al., 2004). The first protein is LifA in EPEC which prevents the gastrointestinal lymphocytes activation in human (Klapproth et al., 2000). The second protein component of EPEC is Efa-1, which plays an important role in intestinal colonization in calves (Stevens et al., 2002). It is postulated that ToxB protein has a role to prevent interleukin synthesis as the encoded proteins from pO157 (Abu-Median et al., 2006, Stevens et al., 2004). However, a mutation of the *toxB* and *efa-1* genes have not shown any influences on the intestinal colonization of calves (Stevens et al., 2004).

1.2.6. Type II secretion pathway

The pO157 *etp* operon encodes a type 2 secretion system (T2SS) (Schmidt et al., 1997) with homologies to the T2SS of some Gram negative bacterial pathogens *e.g. Klebsiella pneumoniae* and *Erwinia carotovora* (Schmidt et al., 1997, Burland et al., 1998a, Sandkvist, 2001). The *etp* operon in pO157 is located near to the *ehx* operon (Lim et al., 2010). There is a gene called *stcE* that resides within the *etp* operon, encoding a metalloprotease, which is responsible for cleaving the C1 esterase inhibitor (Lathem et al., 2002). The C1 esterase inhibitor which is encoded by C1 host complement system, acts as a host regulator for many proteolytic cascades involves in inflammatory pathways, such as: complement activation, intrinsic coagulation, and contact activation betwwen leukocytes and host cells (Lim et al., 2010, Davis III et al., 2010). As a result, the production of *stcE* leads to the inhibition of cytokine release and the limitation of the establishment of the innate immune response cascade (Lathem et al., 2002). StcE also contributes to the C1 esterase inhibitor binding to host cell membrane, impacting upon C1 esterase inhibitor function, protecting host and bacterial cells from complexes of the activated complement system (Lathem et al.,

2004, Grys et al., 2005). Moreover, the metalloprotease has been noticed to breakdown salivary proteins, glycoproteins 340, and mucin 7. At the point of initiating an infection, StcE can promote survival of the bacteria during passage in the mouth by digesting salivary glycoproteins, then StcE facilitates bacterial adherence to epithelial cells in colon by damaging the protective layers of glycoprotien and mucin that covers the epithelium (Grys et al., 2005, Grys et al., 2006).

1.2.7. Extracellular serine protease

Extracellular serine protease (EspP) is encoded on pO157, and is classified as an serine protease auto-transporter of the *Enterobateriaceae* (SPATE) superfamily (Law, 2000a, Velarde and Nataro, 2004). Auto-transporters encode a signal sequence that passes through the bacterial cell's inner membrane and the periplasm. As a result, a β-barrel pore is formed by carboxy-terminus across the outer membrane, while amino-terminus of protein can pass and be release (Velarde and Nataro, 2004). When the SPATEs are analysed phylogenetically the results place the EspP of EHEC close to EspC in EPEC (Guignot et al., 2015, Dautin, 2010). The sequence alignments between EspP and EspC demnostates 48% amino acid sequence identity, and 65% similarity in the protease domain, while 45% identity and 62% similarity for the remaining of proteins including an identical catalytic site (GDSGS). According to these similarities sequencing between EspP and EspC, it can suggest that EspP may behave as EspC function which is acting as an enterotoxin and effecting colonic epithelial ion and water transport (Tse et al., 2018). Secretion of (SPATE) is governed by expression of the type V secretion system in EPEC and EHEC (Mellies et al., 2001), but before secretion, SPTA is produced as a precursor protein that has to pass N-terminal and C-terminal processing (Velarde and Nataro, 2004, Brunder et al., 1997b). Signal sequence that is encoded by autotransporters, as a result, the EspP can pass both the inner membrane and the periplasm, and release to damage human coagulation factor V and pepsin A (Brunder et al., 1997a). This may understand the cascade of clotting blood that can be associated with haemorrhagic manifestation in EHEC. Moreover, examining sera of infected EHEC patients has identified antibodies reactive to EspP, whereas the sera of healthy person lacked antibodies reactive to EspP (Brunder et al., 1997a, Jarvis and Kaper, 1996). EspP is also involved in the colonization in calves intestine and the adherence of primary epithelial cells of bovine intestine (van Diemen et al., 2005).

1.2.8. Bacterial Toxins

Bacterial toxins are produced by pathogenic bacterial strains that benefit from these toxins through one or more mechanisms: disturbing host cell functions, protection from innate immune response of host cells, crossing mucosal barriers, dissemination in or from the host, replication in the host (Bergsten et al., 2004, Merrell and Falkow, 2004). Bacterial toxins are classified into three categories dependent on toxic mode of action. The first category of toxin disrupts host cells without entering to the cells *e.g.* superantigens that are produced by *Staphylococcus aureus* and *Streptococcus pyogenes* (Proft et al., 2003). The second category of toxin damages the host cell membrane disturbing the host cell function, *e.g*. phospholipases which is produced by *Clostridium perfringens*, breaks down the cell membrane , and hemolysin which is produced by *Staphylococcus aureus* or *E. coli*, forms pores in the host cell membrane (van der Poll and Opal, 2008, Schmidt et al., 1999). The third category of toxin is called an A/B toxin due its subunit structure that damages host cell's biology. The B component is associated with specific binding to the host cell surface, while the A component is responsible for the activity of the toxin, often mediated by an enzymatic activity *e.g.* cholera toxin that is produced by *Vibrio cholera* (van der Poll and Opal, 2008), alters cell signalling pathway by ADP-ribosylation of G protien which leads to increase level of cAMP in the host cell. As a result, imbalanced electrolyte is occurred due quick effux chloride ions and reducing influx of sodium ions (Bharati and Ganguly, 2011).

However, bacterial toxins are often encoded by genes which are carried on mobile genetics elements (Hacker et al., 1997) *e.g.* cholera toxin is encoded on the filamentous phage, CTXφ (Boyd, 2012), the β2-toxin (CPB2) and Epsilon-toxin of *Clostridium perfringens* are encoded on large plasmids (between 45 kb to 140 kb) (Li et al., 2013). The possessing of toxin genes on mobile elements play important role in the evolution bacterial pathogenic and emergence of new pathogens (Boyd and Brüssow, 2002).

1.2.8.1. Shiga Toxin

Professor Kiyoshi Shiga in 1898 was credited with identifying *Bacillus dysenteriae* as the causative agent of dysentery (Shiga, 1898). It was renamed *Shigella dysenteriae* in 1930 (Trofa et al., 1999). The toxin production was demonstrated to cause death in rabbits and guinea pigs in 1903 (Conradi, 1903). It

was debated if the toxin was an exo-toxic product or an endo-toxic product (Flexner and Sweet, 1906, Kraus, 1905). Then, it was identified that *Shigella dysenteriae* expressed an exotoxin which was responsible for the death in rabbits (Engley Jr, 1952), and this toxin was renamed *Shiga toxin* (Dubos and Geiger, 1946). Later in 1977, product was discovered from some strains of *E. coli* that was toxic to vero cells (Konowalchuk et al., 1977); the toxin was named verocytotoxin (VT). VT was presumed to be a cause of some *E. coli* mediated diarrhoeal diseases. Then in 1983, an *E. coli* O157:H7 strain was isolated that produced a toxin which was neutralised by antisera raised to the exotoxin, Shiga toxin, of *Shigella dysenteriae* (O'brien et al., 1983). It was discovered that same year that *E. coli* H19 produced VT which was encoded on a temperate phage integrated with chromosomal of bacteria (Scotland et al., 1983, Smith et al., 1984), and this pathogenic *E. coli* strain expressed two distinct verotoxins, VT1 and VT2 (Scotland et al., 1985). Both toxins were renamed to Shiga-like toxin (SLT) based on recognising the association of the *E. coli* and *Shigella dysenteriae* toxins (O'brien et al., 1983, Paton and Paton, 1998). In 1982, there was an outbreak of disease in United States caused by an *E. coli* O157:H7 isolate, strain EDL933, which harboured various phages integrated in its chromosome and produced both SLT1 and SLT2 (Strockbine et al., 1986). The symptoms of disease varied from mild diarrhoea to haemolytic uremic syndrome (HUS). Recently, the nomenclature of these toxins has been simplified to Shiga toxin (Stx). There is a great degree of diversity recognised across the Stxs beyond the simplicity of Stx1 and Stx2 (Allison, 2007). Stx1 is different in sequence identity from *Shigellea dysenteriae* type I toxin (Allison, 2007). Recently, there are only two variants of Stx1 are defined: Stx1c and Stx1d which are seldom present in human disease in isolation STEC from patients (Friedrich et al., 2003, Kumar et al., 2012, Melton-Celsa, 2014). While, the Stx2 has many varients and are associated with severe human diseases *e.g*. Stx2a is defined in human disease (Melton-Celsa, 2014), Stx2c displays decreased cytotoxicity on Vero cells (Schmitt et al., 1991), and Stxd is highly virulent producing in a mouse model of infection which is streptomycin treated (Melton-Celsa et al., 1996, Lindgren et al., 1993). The two genes *stxA* and *stxB* which encode Stx are expressed along with the late genes of Stx phages which characteristic of transcribing only in the phage lytic cycle (Herold et al., 2004).

The structure of Stx contains a one A subunit and five B subunits as demonstrated by X-ray crystallography (Fraser et al., 1994, Stein et al., 1992). The A

subunit is the catalytic subunit and is non-covalently connected with a pentamer of symmetric B subunits, comprising the AB_5 holotoxin. Each subunit of B contains two anti-parallel β-sheets and one α-helix shaping a pentameric ring. β-sheets form the outer surface of the pentamer, while the α-helix forms the inner pore boundary. The B subunit is involved in binding to globotriaosylceramide 3 (Gb_3), the toxin receptor on the eukaryotic host cell (Jacewicz et al., 1986, Stein et al., 1992, Lindberg et al., 1987). Binding to Gb_3 results in endocytosis (Fig. 1.4) of the holotoxin where moves from endosome to the Golgi apparatus and then is transported to the endoplasmic reticulum (ER) (Garred et al., 1995b, Garred et al., 1997, Garred et al., 1995a, LaPointe et al., 2005). The A subunit is cleaved by the host-encoded protease (furin) to A_1 and A_2 fragments at a disulphide bond (Garred et al., 1995; Olsnes et al., 1981; Suh et al., 1998). The A_1 component possesses an RNA *N*-glycosidase activity that cleaves an adenine base at position 4,324 of the host cells' 28S ribosomal RNA (Endo et al., 1988, Saxena et al., 1989). This action prevents elongation factor-dependent amino-acyl tRNA binding and subsequent chain extension (Hale and Formal, 1980). Following by translocating the A subunits into cytoplasm which results in the prevention of protein synthesis, simulation of the ribotoxic stress and the ER stress response, and additionally in some conditions, can induce cytokines *e.g.* IL-8, GRO-α, IL-1β, chemokines *e.g.* TNF-α (Jandhyala et al., 2011) and ultimately apoptosis (Fig. 1.4) (Johannes and Römer, 2010).

Stx can move from the intestinal lumen to blood circulation system via transferring from the lumen to the basolateral side of the cells through the lumen to the cell borders, without shown any cytotoxicity imapct (Philpott et al., 1997, Acheson et al., 1996). As a result, vascular tissues can be damaged resulting in microvascular thrombosis, affecting other vessels covering the caecum and colon in infected rabbits as a direct effect of Stx (Sjogren et al., 1994). The (Sjogren et al., 1994) study showed that rabbits which were infected with *E. coli* carrying the *stxAB* operon had symptoms of bloody diarrhoea along with damage to the mucosal caecum and colon post mortem, while control animals infected with an *E. coli* strain lacking the *stxAB* operon lacked symptoms of bloody diarrhoea and showed no microvascular injuries (Sjogren et al., 1994). The symptoms in humans are similar to the symptoms in rabbits *e.g.* colon damage involving oedema of the mucosa and haemorrhage (Griffin et al., 1990). When Stx producing cells are present in the human gastrointestinal tract, the inflammatory response is induced, which causes damage of mucosa (Thorpe et al.,

1999). As a result, cytokines are released in local sites of damage that stimulates leukocytes (O'Loughlin and Robins-Browne, 2001). Moreover, when Stx is incubated with tumour necrosis factor-α (TNF-α) or interleukin-1β (IL-1β), Gb_3 expression is up-regulated on endothelial cells in laboratory experiments (Kaye et al., 1993, Louise and Obrig, 1991). In addition, vascular or intracellular adhesion molecules may be expressed as endothelial cells are broken. Followed by leukocytes adhere to endothelial cells, as a result, flow reduces through vessels. Thrombocytopenia and erythrocytosis which are both symptoms of HUS, are caused by damage to endothelial cells (O'Loughlin and Robins-Browne, 2001). The resulting inflammatory response also increases the overall impact of Stx, mediating damage to organs *e.g.* liver in increasing IL-1β response, and lung in increasing TNF-α, and tissues (Tesh et al., 1994, van Setten et al., 1996, Chen et al., 2018).

The kidneys are the worst affected organ by Stx, because the kidney cells are highly concentrated of Gb_3 that is a receptor molecule in endothelial cells (Uchida et al., 1999, Boyd and Lingwood, 1989), and the toxin binds and cytotoxics both endothelial and epithelial cells (Uchida et al., 1999, Karpman et al., 1998). However, Stx2 is more cytotoxic of kidney endothelial cells than Stx1 (Louise and Obrig, 1995).

1.3. Bacteriophage

A bacteriophage, also known simply as a phage, is a virus that can infect bacteria. This name is taken from the Greek word *phagin* that means "to eat" (Gravitz, 2012). They were first identified in 1896 (Hankin, 1896a). Bacteriophages, being viruses, are obligate intercellular parasites that require a host cell in which to replicate. They are considered to number ~ 10^{31} tailed bacteriophages on the planet (Katsamba and Lauga, 2019). If the phage is a temperate phage, replication can follow one of two pathways, lytic or lysogenic depending on the host cell and its environment. If the bacteriophage is virulent then the phage follows a strictly lytic replication pathway. Lytic or virulent phages cause the destruction of their bacterial host cell following the bacteriophage is virulent then the phage follows a strictly lytic replication pathway. Lytic or virulent phages cause the destruction of their bacterial host cell following the production, assembly and release of progeny phages. Temperate phages can replicate like lytic phage or, under certain condition, they can direct the incorporation

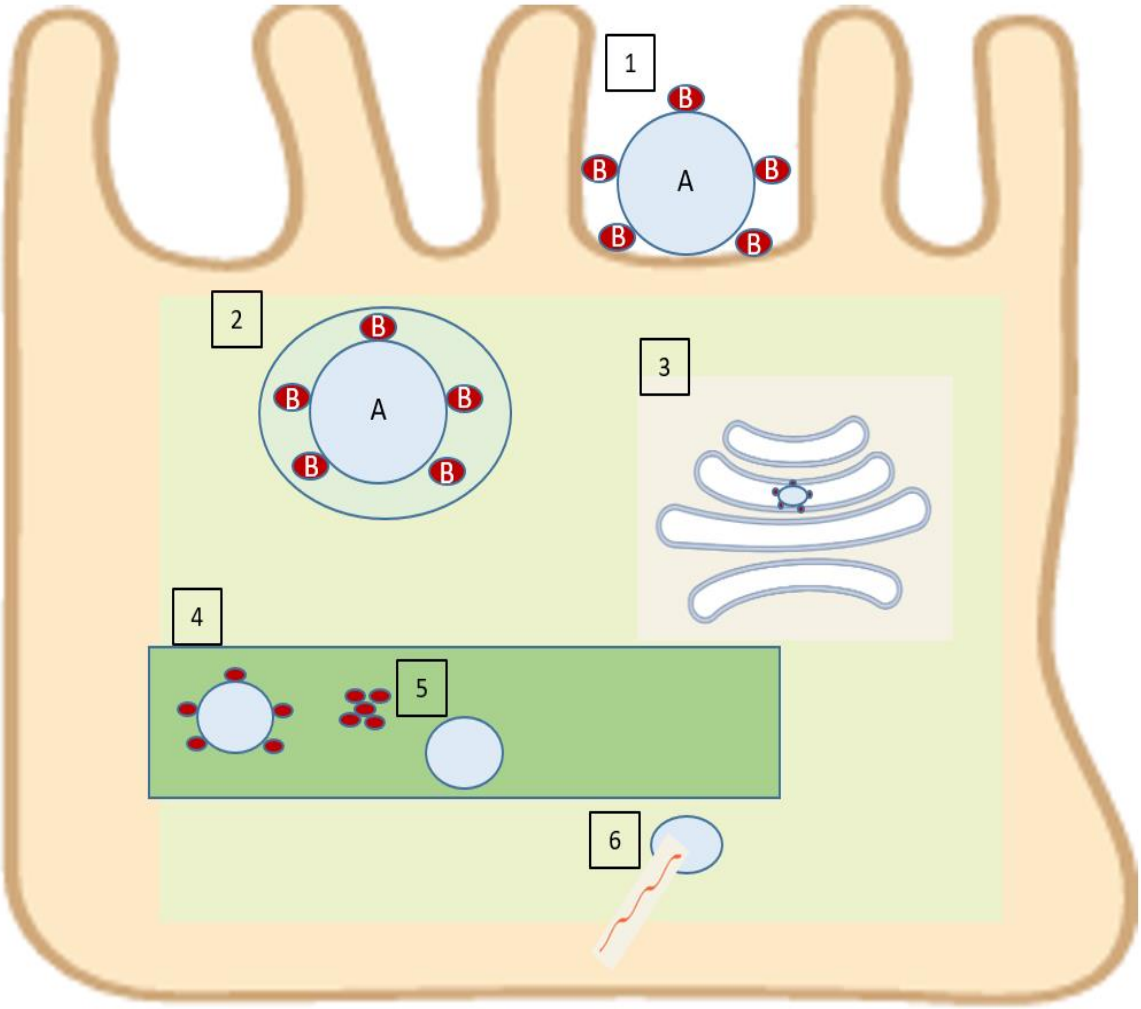

Figure 1. 4. The Stx mechanism of action: from entry of the host cell to apoptosis.

1) Stx binds to host cell receptor (Gb_3), and enters the host cell via endocytosis. 2) Stx is coated in a clathrin-enveloped vesicle. 3) The toxin travels to the Golgi apparatus. 4) The toxin moves into the endoplasmic reticulum. 5) The toxic subunits are separated and the A subunit is cleaved by furin into A_1 and A_2. 6) The A_1 subunit (*N*-glycosidase) inhibits protein synthesis by removing 400 bp of 28S ribosomal RNA that ultimately results in apoptosis (cell death) due to stopping translation of the mRNA molecule.

their viral genome into the genome of the bacterial host. This latter condition results in the phage becoming a prophage, and its bacterial host becoming a lysogen. All daughter cells of the lysogen will carry the prophage (Weinbauer, 2004). Prophages have been shown to play significant roles in the diversification, virulence and evolution of bacteria (Canchaya et al., 2004, Ohnishi et al., 2001). New pathogenic serogroups of bacteria can emerge following bacteriophage infection (Brüssow et al., 2004a, Allison, 2007). Moreover, bacteriophages can convert commensal bacteria and other non-pathogenic bacteria to virulent, pathogenic forms. Bacteriophages with these properties are known as converting phages (Bae et al., 2006, Allison, 2007).

1.3.1. The phage life cycle

In order to infect a host cell there are two key steps : adsorption, and entry of the phage genome into the host (Weinbauer, 2004). Firstly, the phage adsorption has occurred in two stages. The first stage of adsorption is a reversible connection of the phage to the surface of the host cell surface. While the second stage of adsorption is an irreversible connection between tail fibers of the phage and host cell receptors until full adsorption has been achieved (Weinbauer, 2004). Secondly, the host cell wall is penetrated by phage enzymes that are located in the tail or capsid. As a result, the phage DNA is transmitted inside the cell, while the phage capsid part stays outside the cell (Weinbauer, 2004). Then if the phage is a virulent phage or a temperate phage that is to enter the lytic replication pathway, the phage genomes will be actively transcribed and then replicated. The phage utilizes the host cell for initiating some or all of these processes and then the cell begins to synthesie newly encoded phage proteins. These proteins are assembled and packed with new phage genome copies to create new daughter phage particles (Ackermann, 1998). Finally, host cell lysis directed by phage encoded proteins, occurs and releases new progeny phage step. This step occurs when the host cell has become weak by phage enzymes *e.g.* tailed phages use a lytic system that includes a peptidoglycan hydrolase (endolysin) that targets the murein part of the cell wall and proteins called holins that damaged the cell membrane (Ackermann, 1998). The new progeny phage in extracellular stage can start a new infections or can die (Fig.1.5) (Weinbauer, 2004). While if the infecting phage is a temperate phage and it enters the lysogenic replication pathway, the phage chromosome integrates into bacterial host genome (Fig.1.6) that genome resulting in the formation of the prophage (Fig.1.6). The prophages are stable within the host cell

until they are induced to the lytic pathway spontaneously or by inducer *e.g* antibiotics (Fig.1.5) (Clokie et al., 2011). The prophage DNA is packaged into head that produces new particles which is called progeny phage (Susskind and Botstein, 1978). The progeny phages are assembled then subjected to the lytic pathway to be release (Weinbauer, 2004).

There is an additional state some phages exist in called pseudolysogeny which is the phage infection status does not enter either lysis pathway or lysogenic pathway (Fig.1.7) (Łoś and Węgrzyn, 2012). The reasons of this status is that the unfavorable bacterial growth conditions are applied in the bacterial enviroment such as depleted nutrition, or changed temprature (Łoś and Węgrzyn, 2012). As the growth conditons are fixed, the pseudolysogenic status is over, and phages return to the lysis or lysogenic pathways (Latino, 2016).

1.3.2. Genome replication of lysis or lysogeny in Bacteriophage λ (lambda)

Lambda phage (λ) was discovered as a prophage that was integrated within the genome of an *E. coli* K-12 58F^+ strain (Bachmann, 1972, Lederberg and Lederberg, 1953). The size of the λ genome is 48,502 bp and it encodes 60 protiens (Sanger et al., 1982). The gene regulatory systems of this phage are quite complex because this is a temperate phage that uses a set of regulators and sensors to “decide” whether or not to enter the lysogenic pathway or lytic pathway at the point it infects its host. It also uses this same set of genes, whilst a prophage, to escape its host through prophage induction if it senses that the cell might die (Little, 2007).

At the onset of an infection, *N* which is an intial gene in very early experssion, which is chratectrised as an anti-terminator, is transcribed from promotor L (*p*L) ,and controls terminator R1 (*t*R1), and terminator L1 (*t*L1) (Fig.1.8) (Court et al., 2007). The anti-termination feature of *N* is associatated with host cell encoded Nus factors which combine with N and the *E. coli* RNA polymerase at the *nut*R and *nuf*L sites (Fig.1.9) to termination of the new transcript at *t*L1 and *t*R1. As a result, the genes are transcribed to invoke in lytic pathway such as *O*, *P*, and *Q* , or lysogenic pathway such as *cII* and *cIII* (Fig.1.9). Transcription from *p*R prodominantly leads to lytic pathway, while transcription from pL primarily leads to lysogenic pathway (Court et al., 2007, Oppenheim et al., 2005).

There is a hairpin loop forms which locates between *N* and nutL region, inhibits *N* gene translation (Fig.1.9). The translation of *N* gene occurs when the loop has

broken by increasing concentration of host protien called Rnase III, so the production of N becomes high. The phage decision to enter lytic or lysogenic pathway depends on transcription level of pL or pR which are responsible from concentration of Rnase III (Oppenheim et al., 2005, Court et al., 2007, Campbell, 1994).

1.3.2.1. The lytic pathway

When the λ enters the lytic pathway, Cro binds to the right operator sites O_R2 and O_R3 as well as the left operator binding sites O_L2 and O_L3 which effectively inhibits expression from *p*L and *p*RM (Fig.1.10A). The occupancy of these regions by Cro inhibits making of the repressor and N. Moreover, when Cro concentration has increased, Cro links to the O_L1 and O_R1, so that *p*R is downregulated (Fig.1.10A) (Court et al., 2007).

The expression of the *Q* gene, which results in the production of another protein with antiterminator function, permits expression to be completed from *p*R', which is important for the transcription of late genes and completion of the lytic cycle (Fig.1.9). When transcription has started from *p*R', the lysis cycle is irreversible. The threshold level of Q that needs for anti-termination and commits the phage to the lysis cycle requires more time than that required to reach the lower concentrations of N required for antitermination activities (Court et al., 2007)

1.3.2.2. The lysogenic pathway

There are several expressed genes that are essential in the lysogenic pathway: *cI*, *cII*, *cIII*, and *int*. Expression of the *cII* gene is begun from pR (Fig.1.8), enabled by the action of N on *t*R1. CII is responsible for activation of the promoters *p*I, *p*aQ and *p*RE and drives the cell into lysogenic cycle. The transcription of CIII from *p*L, enabled by the action of N on *t*L1, is indirectly responsible for extending the half life of CII, by blocking the activity of the host protease HfIB. The *p*I promotor (Fig.1.9) controls the expression of the of *int* gene (encoding the site-specific recombinase, integrase) which drives the integration of the phage genome into the host cell's genome. Transcription of an antisense RNA from *p*aQ (Fig.1.9) prevents translation of the *Q* gene transcript (Court et al., 2007). The expression of CI, which is a phage repressor protein, is initated from *p*RE as is *cro* antisense RNA (Spiegelman et al., 1972) (Fig.1.9). CI dimers bind to and connect O_L1 to O_R1 O_L2 and to O_R2 operator binding regions (Stayrook et al., 2008) (Fig.10B) becoming tetramers, forming a complex DNA looping that is responsible for stability of repressor connecting at the operator region. This

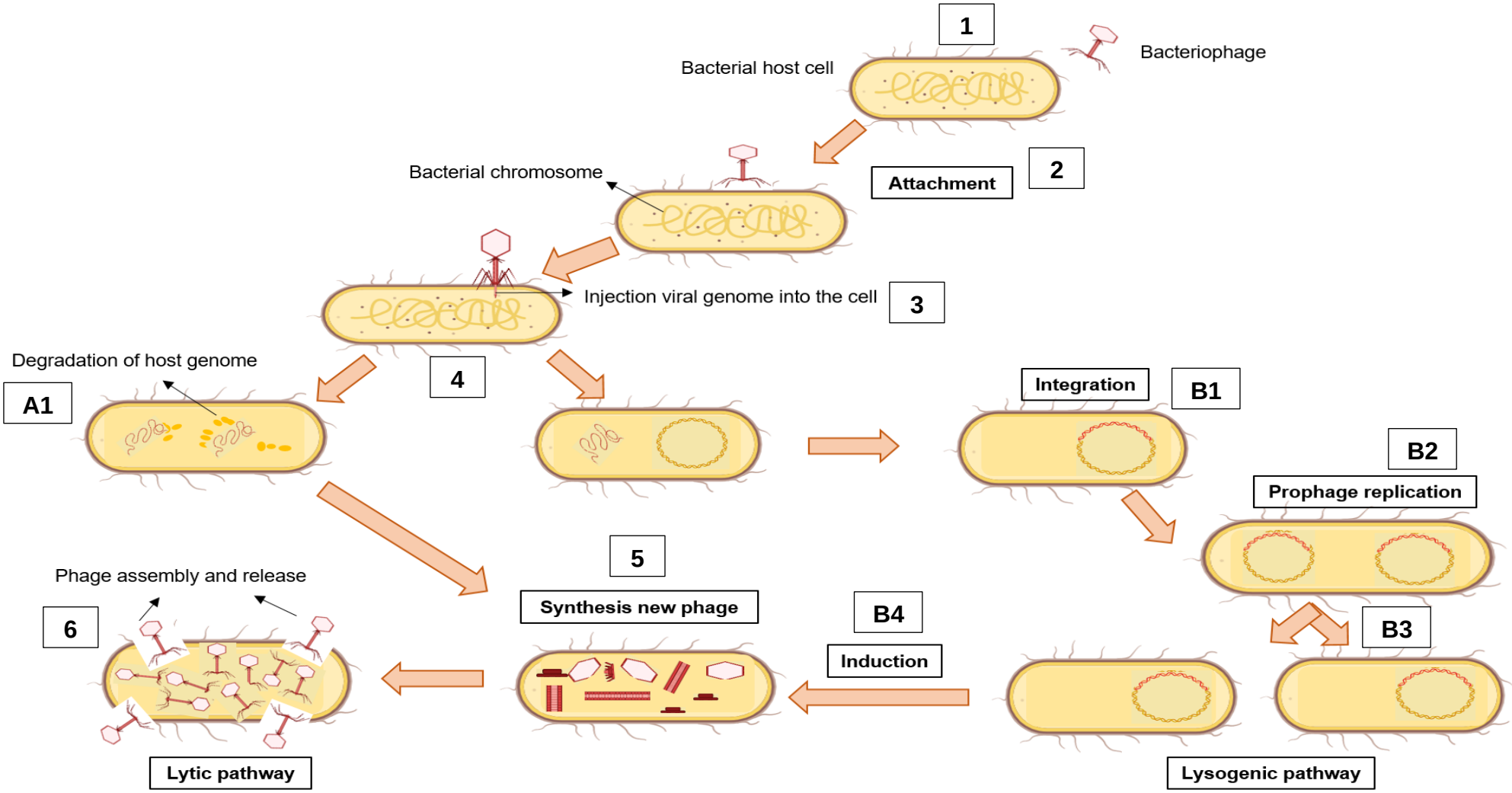

Figure 1. 5. Phage life cycle pathways.

1) Bateriophage attempt to recognise bacterial host cell receptors. 2) After initial attachment between phage and bacterial host cell, phage promotes recognizing an adsorption site on the cell surface structure.3) The phage injects the viral genome into the cell by phage enzymes in the tail or capsid that penetrate bacterial host cell wall. 4) The phage decides to have a lytic pathway or a lysogenic pathway. A1) The phage enters the lytic pathway which is irreversible, and the phage genome replicates, and the genes demended for the lytic cycle have transcribed. B1) The phage enters the lysogenic pathway, and the phage genome integrates into host chromosome. B2) The prophage replication with host chromosome. B3) The prophage passes to daughters cells. B4) The prophages status is stable inside the host cell until to be induced to the lytic pathway. 5) New phage particles are formed after the phage DNA is packaged into the head. 6) The bacterial host cell is lysed, and the nascent phages are released (Riley 2009).

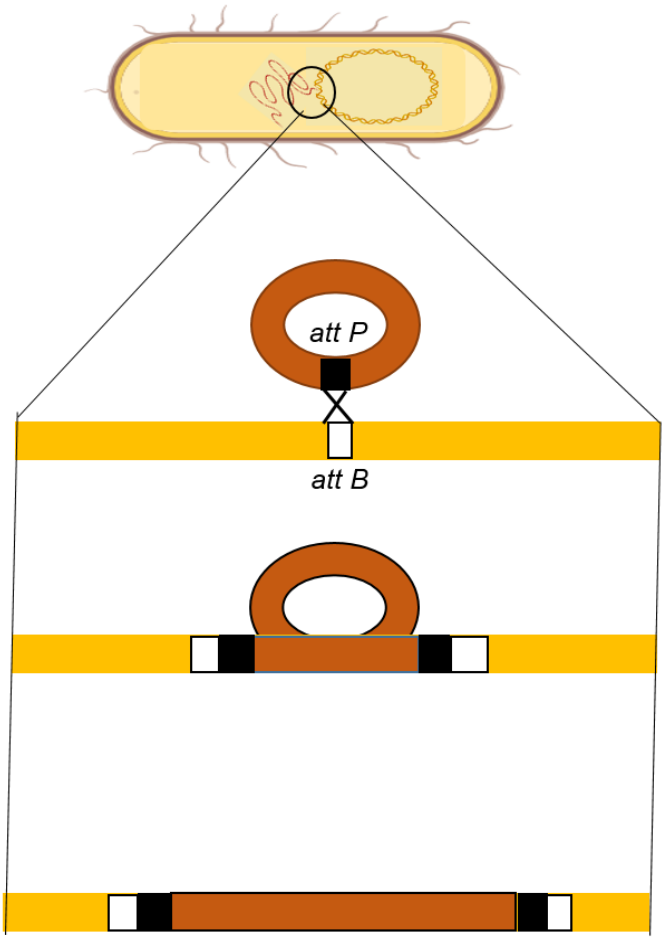

Figure 1. 6. The phage chromosome integrates into the host cell chromosome.

In Lambda phage λ the expression of *int* gene (encodes the enzyme integrase) that is located in recombination region is responsible for integration of the phage genome into the bacterial host genome at distinct site-specific regions known as the phage attachment site (*att* P) and bacterial attachment site (*att* B). Upon integration occurs the phage DNA becomes known as a *prophage* and the host cell a *lysogen*. If an inducing signal is detected, the prophage can be induced to excise itself from the lysogen's genome, this excision results in two circular DNA molecules, the phage genome and the bacterial DNA molecule.

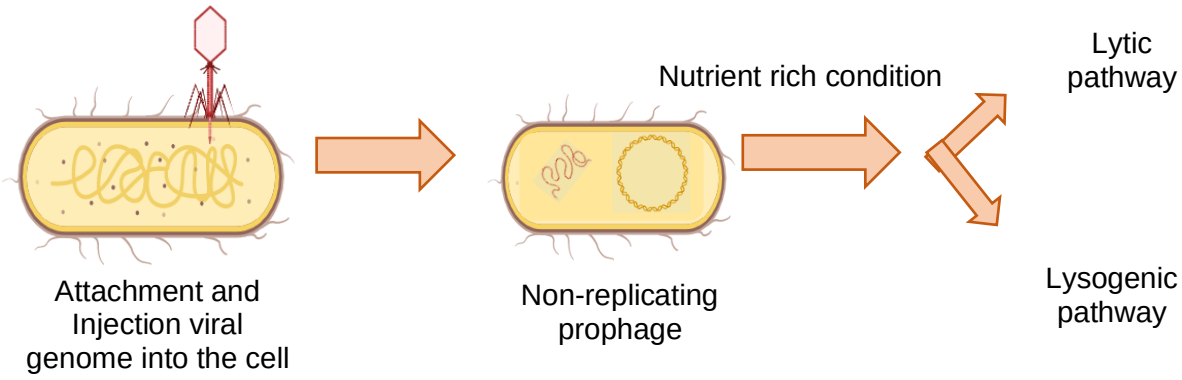

Figure 1. 7. The phage pseudolysogenic pathway.

Pseudolysogeny is an unstable status where the phage genome is unable to replicate (lytic pathway) or become as a prophage (lysogenic pathway). Pseudolysogeny happens during low nutrient conditions. Due to there poor conditions, the bacterial cells cannot support phage DNA replication or protein synthesis. Thus, the phage genome stays in a non-integrated, preprophage state. As the nutritional status of the bacterial is resolved, the phage has a second chance to enter either a lysogenic or a lytic replication pathway (Feiner et al., 2015).

connection inhibits transcription at both *p*L and *p*R, shutting off production of N and Cro and all the genes they activated with the exception of *cI* (Campbell, 1994). However, expression of *cI* remains active from *p*RM that can be turned off when CI levels rise to levels that allow it to occupy O_L3 and O_R3 binding regions. When this happens, CI becomes auto-regulatory and the prophage lies in wait for a future induction signal (Court et al., 2007)

1.3.3. Phage induction

Phage induction occurs when a prophage is stimulated to enter the lytic cycle. The prophage excises itself from the host cell's genome and begins replication of its own genome independently of the host as it enters the lytic replication cycle. Accumulated phage virions leads to lysate host cells and release new phage particles (Livny and Friedman, 2004a).

Induction occurrs in response to the prophage sensing DNA damage response within its lysogen. This DNA damage response is controlled by the host cell's SOS response, which detects and initiates a regulatory cascade to repair the damaged DNA through a protein called RecA. In the bacterial cell, RecA catalyses the auto-cleavage of the LexA repressor. The cleavage of Lex A enables the transcription of genes that are involved in the repair of DNA (D'Ari, 1985). However, when RecA is activated by the presence of damaged DNA, also catalyses the self-cleavage of CI, which shares a similar structure to LexA (Fig 1.11) (Koudelka et al., 2004a). Auto cleavage of CI causes it to let go of the binding regions within O_R and O_L, which leads to the depression of *p*R and *p*L (Fig. 1.8). The *int* and *xis* (excisionase gene) are needed for the excision of the phage DNA from the host genome and are transcribed from *p*L (Campbell, 1994) (Fig. 1.9). The *cro* gene is transcribed from *p*R and Cro links O_L and O_R binding regions (Fig. 1.8). The level of Q increases until able to act as an anti-terminator at tR' (Fig.1.9). As a result, the lytic cycle is underway and the host cell will be killed when the viral progeny are assembled and the lysis mechanism acts upon the cell envelope (Court et al., 2007).

Lysogens can be induced to any environmental stimuli that damage DNA *e.g.* UV radiation, fluoroquinolone drugs or mitomycin C, etc. (Łoś et al., 2009).

1.3.4. Stx phages

Converting phages are the phages that can change the phenotype of their host bacterial cell (Saunders et al., 2001). An example of converting phages is the Shiga

toxin-encoding bacteriophages (Stx phages). The first report of an Stx phages was *E. coli* strain H-19 expressed Shiga toxin that was encoded by a tailed phage with an icosahedral head in 1983 (Scotland et al., 1983). The *stx* genes have been encoded in various bacterial species such as EHEC and *Shigella* spp. (Smith, 2005). While in other bacteria the *stx* genes were found on a plasmid such as in *Aeromonas hydrophila* and *Aeromonas caviae* (Haque et al., 1996).

1.3.4.1. Phenotypic and genetic diversity of Stx phages

Stx phages are responsible for altering the pathogenic profile of the *E. coli* host by a mechanism called “lysogenic conversion”. (Feng et al., 1998, Riley et al., 1983, Pang et al., 2009). All currently characterised Shiga toxin phages (Stx) have been grouped within the lambdoid phages because they are temperate phages that share genomic organisation and context with the genome of bacteriophage lambda (λ) (Recktenwald and Schmidt, 2002, Allison et al., 2003). Stx phages like other lambdoid phages, possess a high degree of genetic mosaicism (Smith et al., 2012b). However, the genome of Stx phages are generally larger than the (λ) genome by approximately 20-25 kb (Smith et al., 2012b), or put in another way, Stx phage genome are generally 50% larger than the genome of λ (Allison, 2007), so it has long been postulated that Stx phages must confer additional phenotypes upon their host within this additional genetic material, as much of the additional genetic material is conserved (Allison, 2007).

The morphological features of Stx phages are varied. Their tails can be any shape from long contractile, long non-contractile, to short tails with or with decorations. Their capsids can be either elongated icosahedral heads or short, regular icosahedral heads (Recktenwald and Schmidt, 2002, Muniesa et al., 2004). Over 70% of Stx phages characterised so far possess a short-tailed phage morphotype. This tail has been shown to adsorb to an outer membrane protein in that is highly shared across the *Enterobacteriaceae*, named BamA (Smith et al., 2007a, McEwen, 2018). Many of the genes carried on a Stx phages which may share little sequence identity with a comparator Stx phage are conserved with respect to their type of function and their genomic context. In the Stx phage $\phi 24_B$, the *stx* genes encoding Shiga toxin are always located immediately downstream of the *Q* anti terminator gene (Fig.1.12) (Unkmeir and Schmidt, 2000) which is the main factor controlling Shiga toxin

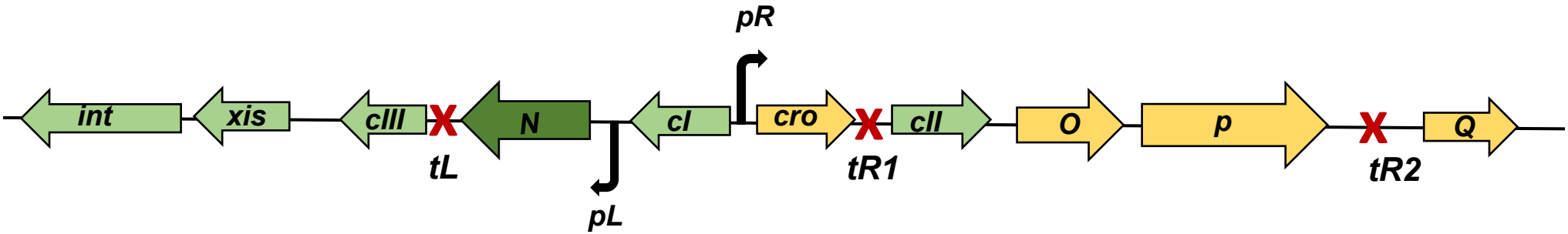

Figure 1. 8. The locations of the promoter *p*R and *p*L and terminators *t*R1 and *t*R2, and *t*L in the λ genome.
N is antitermination because the transcription from *p*R and *p*L can complete beyond *t*R1and *t*R2, and *t*L which leads to transcript essential genes for both lysis and lysogeny (Riley 2009).

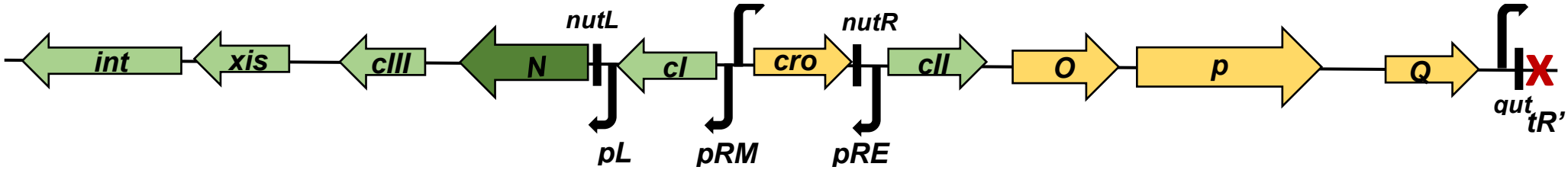

Figure 1. 9. Genes that are responsible for regulation of the lytic and lysogenic pathways in λ.
(Riley 2009).

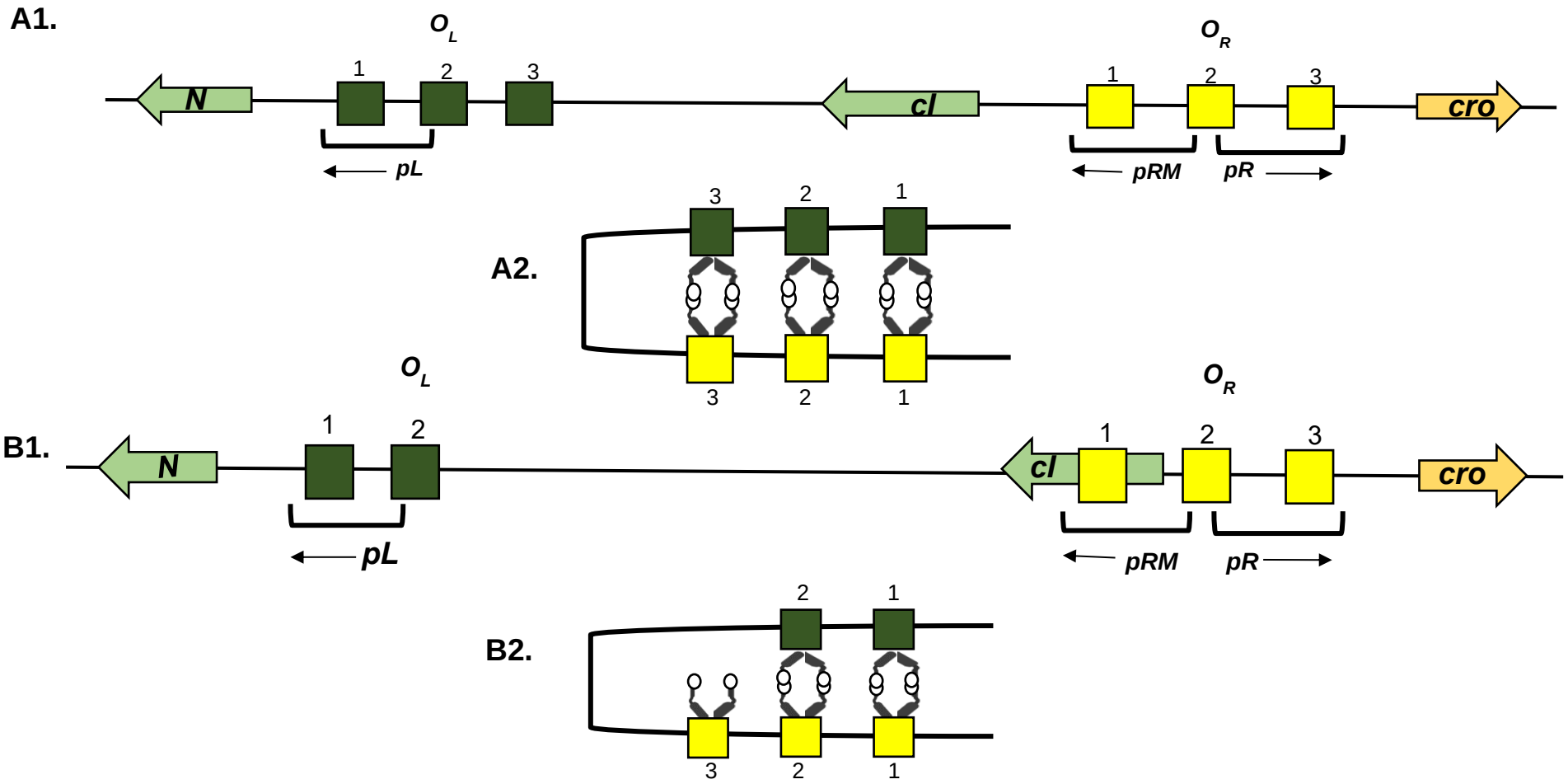

Figure 1. 10. The immunity sites of phage λ and ϕ24B.

A1. The immunity site of λ, presenting the position of the OL and OR regions in association with N, cI, and cro. A2. The figure describes how the cI repressor links co-operatively to the six operator regions. B1. The immunity site of Stx phage ϕ24B that has two left operator regions. B2. The figure describes how cI link co-operatively to OL1 and OL2, and OR1 and OR2, while cI linking to OR3 which is not connected to binding region at OL (Riley 2009).

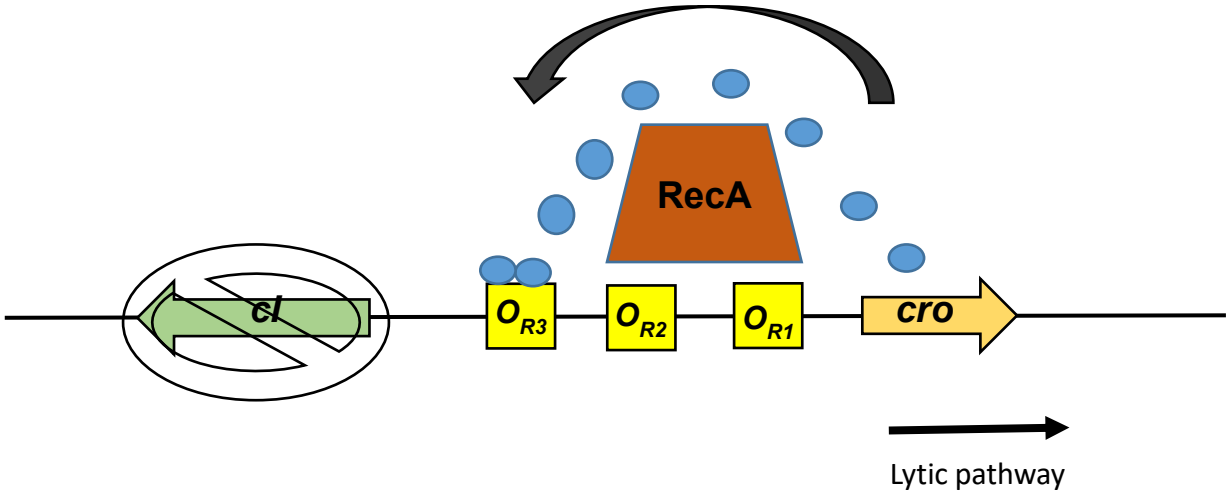

Figure 1. 11. Prophage induction to the lytic pathway by the SOS response system.
In prophage, host cell encodes protein RecA that raises CI self-cleavin, so there is no repressor covering in O_R1 and O_R2 that results inhibition the lysogenic promotors to transcribe, while the *cro* gene occupies the O_R3 and lytic promotor has started to transcribe.

production by *E. coli* lysogens (STEC). When Stx phages are induced into the lytic replication state, the *cI* repressor undergoes auto-cleavage a result of the function of activated RecA (Łoś et al., 2009, Little, 1984), leading to the production of *Q*, which enables production of all of the late transcripts (Łoś et al., 2009), following a similar paradigm to λ (1.3.3). Stx phages are not only acting to alter their bacterial host cell from one with a commensal background to one with a pathogenic profile, but Stx phages can also promote the production and release of novel recombinant phage mosaics through recombination between sequences of remnant prophage and resident inducible prophage in the infected host's genome (Smith et al., 2012b). However, if this combination carries a system like the λ-encoded Red recombinase system, the production of these phage novel mosaics will be even greater than predicted through the normal *E. coli* recombination system (Marinelli et al., 2012, Muniyappa and Radding, 1986, Wang et al., 2006). Moreover, many Stx phages carry genes that encode hypothetical proteins which are noticeable as accessory genes with activation other system such as *exo*, *bet*, and *gam* which are the three required genes of the λ-encoded Red recombinase (Allison, 2007). The site of recombination occurres in *situ* between prophages and various phages within an individual bacterial host cell. As a result, the bacterial lysogen becomes a site for recombination events which results producing a new mosaic phages (Allison et al., 2003, Johansen et al., 2001).

Stx phages as a group, are very heterogeneous; no two phages are totally identical. The only defining characteristic of an Stx phage genome is that it must carry the two gene operon that encodes one of the many variants of Shiga toxin. Outside this requirement there may be little or no genetic identify (Smith et al., 2012b), as evident from the genomic comparisons of the characterised Stx phages: $\phi 24_B$ (HM208303), Min 27 (EU311208), 933W (AF125520), VT2-Sakai (AP000363), Phi 27 (AJ298298), BP-4795 (AJ556162), YYZ-2008 (FJ184280), Stx2 converting phage I (AP004402), Stx2 converting phage II (AP005154), Stx2 converting phage 1717 (FJ188381) and Stx2 converting phage 86 (AB255436) (Smith et al., 2012b), against the archetypal non-Stx phage, λ (J02459). The genome analysis shows that the Stx phages $\phi 24_B$, Stx2 converting phage I, Stx2 converting phage II, 933W, VT2-Sakai, and Min 27 possess a *Podoviridae*-like morphology comprising of a short tail while λ and Phi27 are different from these phages and each other in their tail morphology (Fig. 1.13).

Stx phages possess genes similar to λ that are associated with the genetic decision in switching between the lytic or lysogenic relication pathways, *e.g. cIII, N, cI, cro, cII*, and *Q* (Smith et al., 2007b). The genome comparison of Stx phages (Fig.1.14) has shown the integrase gene that is possessed in $\phi 24_{B,}$ is similar to the integrase gene in the Stx2 converting phage 1717 and the Stx2 converting phage 86. While the *int* gene in phage λ is transcribed in the opposite direction to the previous mentioned phages. Moreover, the controlling of *int* in $\phi 24_B$ is done by its own promotor region that cannot be shut down by repression of *p*L and so is always expressed constitutively supporting high frequency superinfection events (Fogg et al., 2011). The antiterminator *N* gene, which is expressed in earliest stage of lambdoid phage infection, is not present in Phi 27 (the smallest genome of all characterised Stx phages), while it is present as one of three variants as listed N1 form in $\phi 24_B$, Min 27, 933W, Phi 27, BP-4795, Stx2 converting phage I, Stx2 converting phage II, and Stx2 converting phage 86; N2 form in VT2-Sakai, YYZ-2008, and Stx2 converting phage 1717; and N3 form in phage λ (Fig. 1.14).

1.3.4.2. Stx phage $\phi 24_B$

$\phi 24_B$ [GenBank: HM208303] is a short tail Stx phage, and is classified morphologically as a podovirus (Smith et al., 2007a). In order to work safely in a containment level 2 laboratory, a detoxified derivative, $\phi 24_B$::Kan, was created by replacing most of the *stx₂A* and *B* genes with the *aphA* gene of pUC4K conferring kanamycin resistance (James et al., 2001b). $\phi 24_B$ can multiply infect the single host cell via outer membrane protein Bam A (Smith et al., 2007; Smith et al., 2012), and integrate into many regions of chromosomal host cell (Fogg et al., 2011, Mohaisen et al., 2020).

The genome size of $\phi 24_B$ is 57.6 kb (Fig.1.12), and there are many important genes that encode for insertion, lysis, and lysogeny. Moreover, a few accessory genes carried by $\phi 24_B$ have known functions: *lom* and *bor* when expressed by *E. coli e.g.* promote lysogen adhesion to epithelial cells and aid the lysogen in resisting immune system attack, respectively (Barondess and Beckwfth, 1990, Vaca Pacheco et al., 1997). However, approximately three quarters of $\phi 24_B$ genes are hypothetical, having no readily predictable function, yet many are conserved across of variety of Stx and non-Stx phages, which hints to the idea that they play an as yet unknown role.

The Stx phage group at Liverpool has characterised $\phi 24_B$ with respect to its host range (James et al., 2001b), immunity profile (Allison et al., 2003), host recognition mechanism (Smith et al., 2007a), poly-lysogen (Fogg et al., 2007, Fogg et al., 2010), and its impact on the bacterial host (Riley et al., 2012b, Veses-Garcia et al., 2015b), so that it is now the most well characterised of all of the Stx phages.

1.3.4.2.1. Gene expression profiling of $\phi 24_B$

Approximately 30 kb of the genetic material in the $\phi 24_B$ genome is important for the lifestyle of $\phi 24_B$ phage (Allison et al., 2003). The genome of $\phi 24_B$ has been fully sequenced and annotated (GenBank: HM208303, Fig. 1.12, Table 1.2). Around 74% of the genes annotated in the genome of $\phi 24_B$ have not been assigned a probable function (Table 1.2), and most of hypothetical genes are located on the late site of the $\phi 24_B$ genome, which is downstream of the antiterminator *Q* (Smith et al., 2012b). The expression of hypothetical genes is likely to be associated with prophage induction or phage replication except if they are moron which refers to genes acquired horizontally with no action on the phage (Hendrix et al., 2000), they also have a high GC content and may be expressed independently by their own promoter (Hayashi et al., 2001b, Juhala et al., 2000). However, Morons are not important for phage replication but can benefit the bacterial host cell (Hendrix et al., 2000, Brüssow et al., 2004b). It is important to determine the function of the hypothetical genes to determine if they are beneficial for phage replication. This will enable the identification of the source of the gene whether it has been integrated in the genome via an *in situ* recombination event with no effect on the phage replication machinery or bacterial host, or these genes are retained in the genome because their expression is beneficial to the bacteria or the phage replication process (Smith et al., 2012b).

The $\phi 24_B$ gene expression profiles have been determined through RNA seq analysis of mRNA from the direct comparison of 4 culture conditions: norfloxacin-induction lysogen and naïve cultures compared to non-inducing conditions of lysogen and naïve cultures (Veses-Garcia et al., 2015b). It has been demonstrated that prophage-encoded gene expression can change the host cell phenotype such as adding virulence factors to host cell (Allison, 2007, Wang et al., 2010b, Arraiano et al., 2007). However, there are other prophage genes whose expression are not associated with viral replication, but appear to aid the host cell in surviving

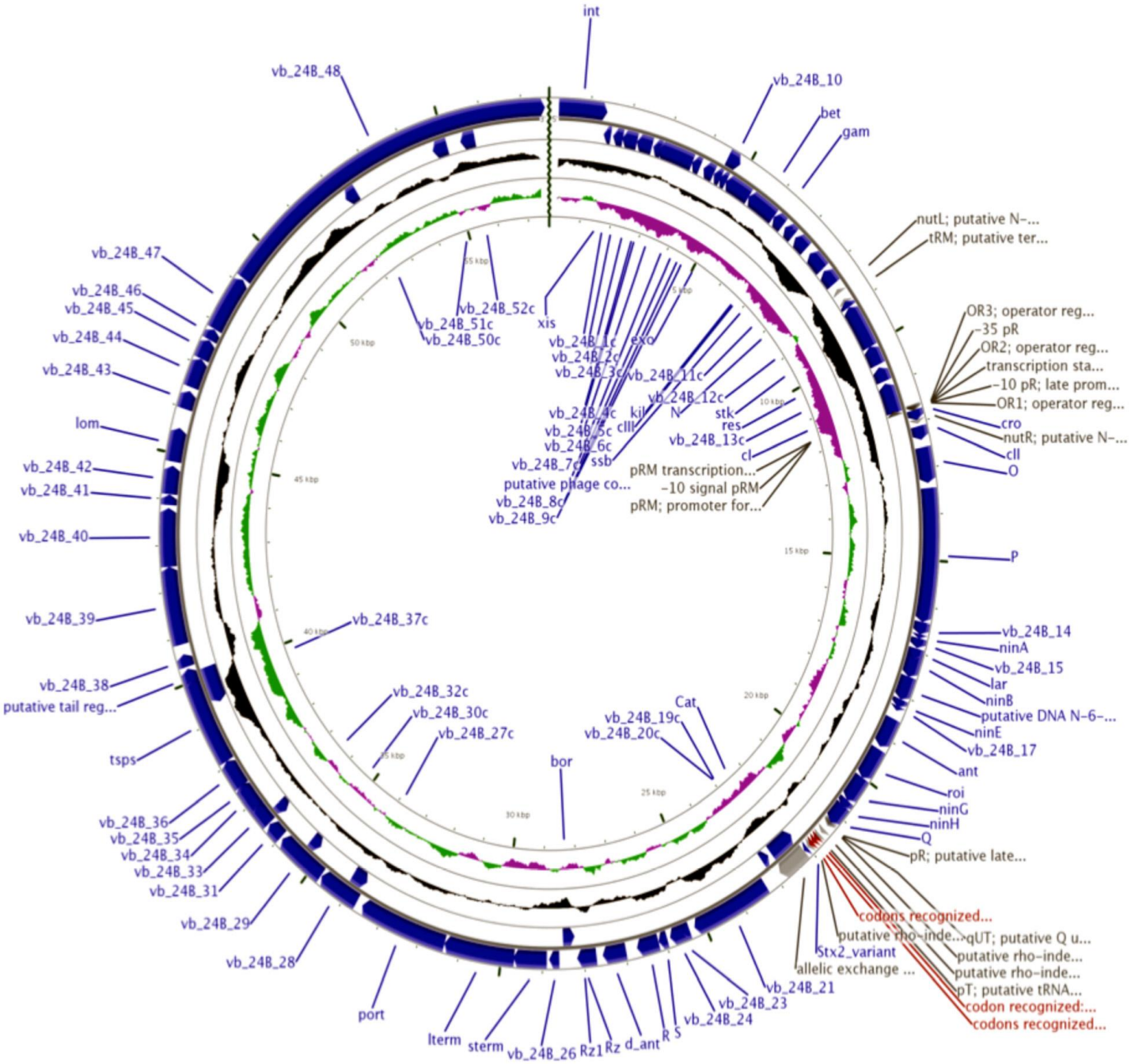

Figure 1. 12. CG view derived schematic of the $\phi 24_B$ genome.

The concentric rings include the annotation of 57,677 bp genome detected 88 putative coding regions, The external concentric ring presents the genes expression of profile of $\phi 24_B$ in the lytic and lysogenic pathways with location and direction of expression, open reading, promoters, and terminators. The blue arrows refer to CDS genes, the red arrows refer to tRNA genes, and gray arrow refers to non *stx* allelic exchange genes. The GC content blotting refers in black concentric ring. While the green color refers to GC skew +, and the purple color refers to GC skew -. The internal concentric ring presents the genes that are suffixed with 'c' that are expressed from the complimentary strand, and number of base pair in $\phi 24_B$ genome.This figure was taken from (Smith et al., 2012b).

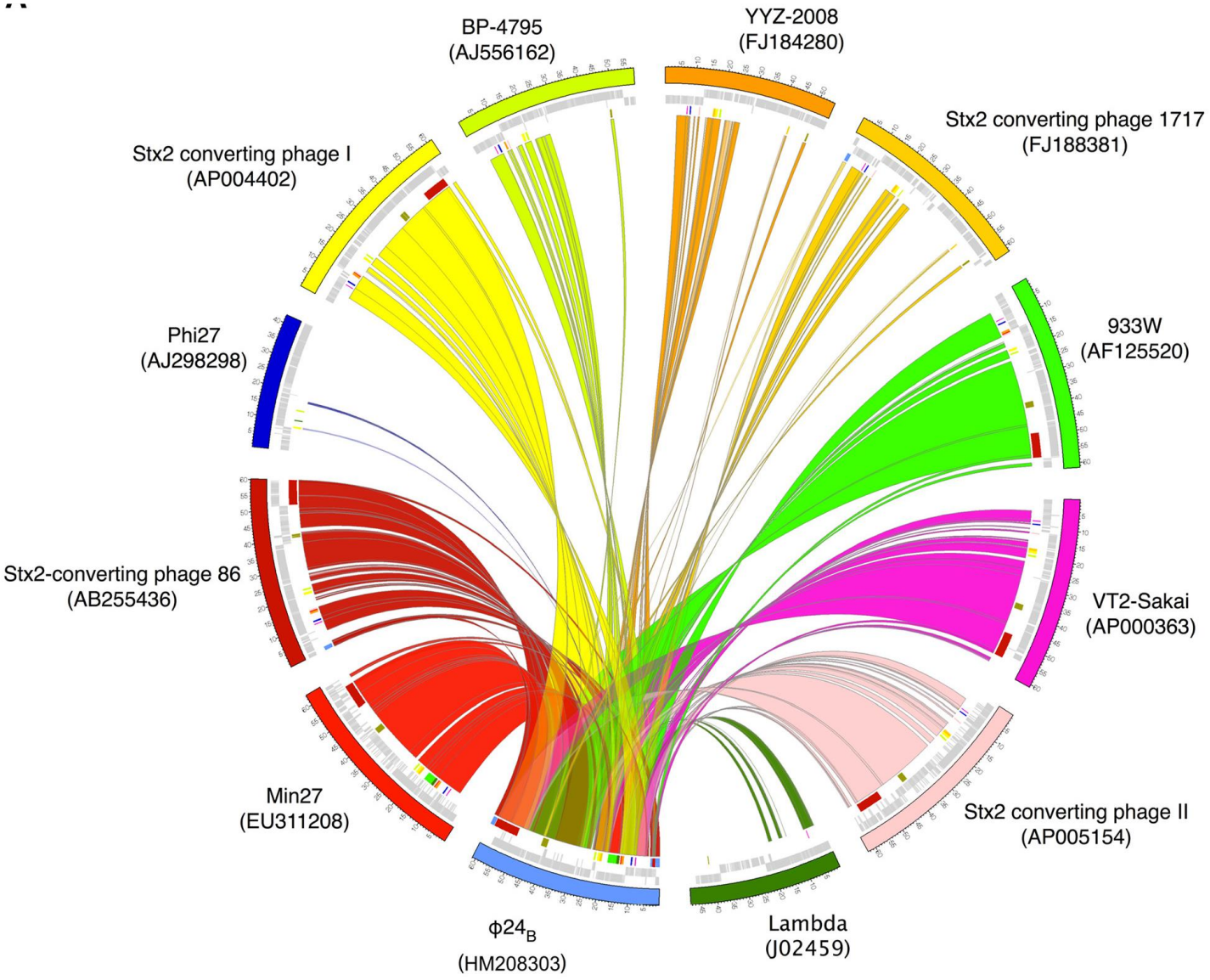

Figure 1. 13. Multi genome in a Circos Map of sequenced Stx phages, the archetypal lambdoid phage, Lambda and $\phi 24_B$.

Circos map describes the MuMer alignment that was produced with respect to Stx2 phage $\phi 24_B$. Every coloured segment presents a phage genome with the number on the external surface defining genome size in kb. Inside the genome ring are produced signs defining gene location and their respective coding strands. The inner circle is contained of coloured blocks that are definitive of gene conservation with $\phi 24_B$. The coloured swept arcs define sequence conservation and orientation of those sequence with respect $\phi 24_B$. This figure was taken from (Smith et al., 2012b).

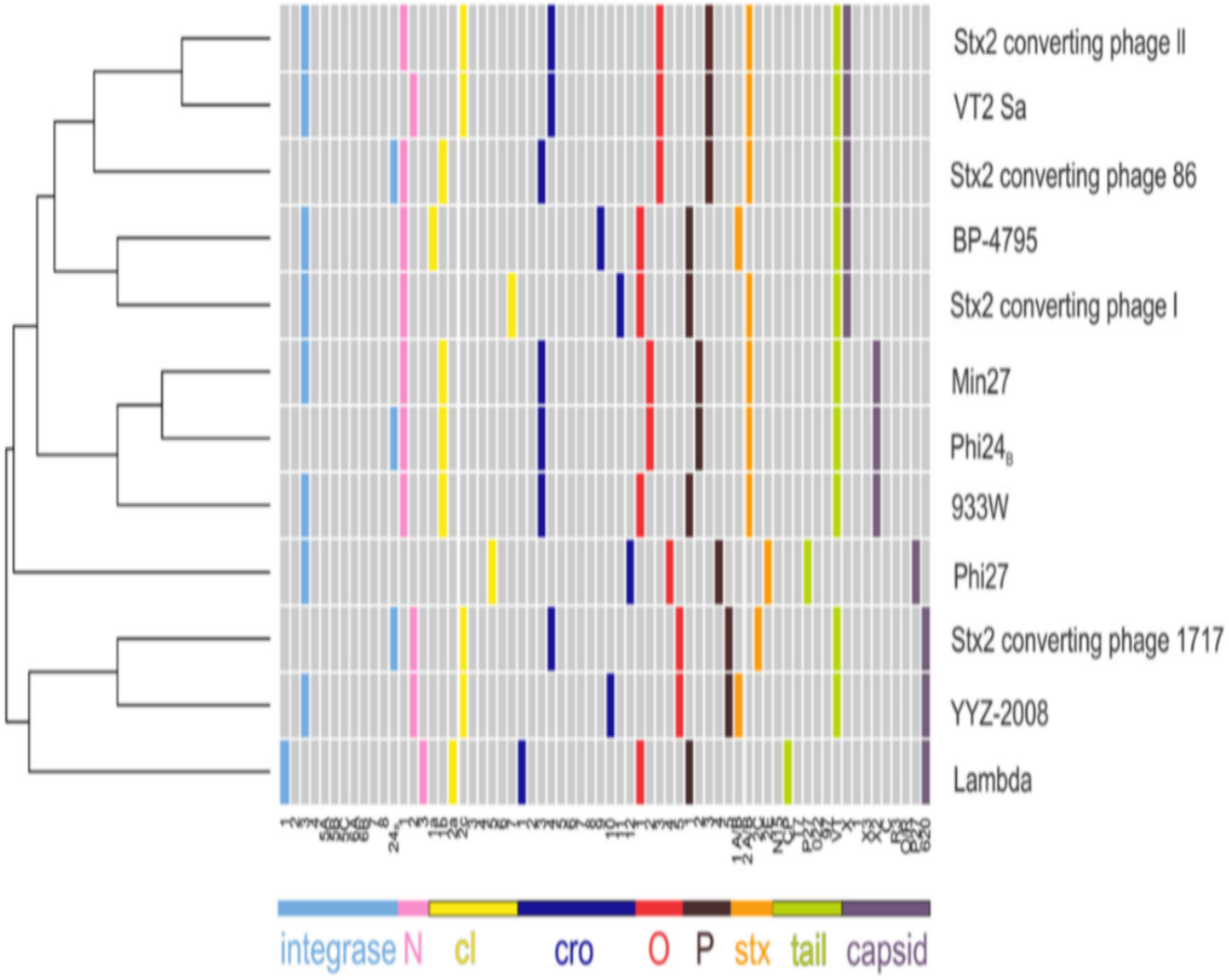

Figure 1. 14. Multi-loci comparison between different Stx bacteriophages and lambda phage.

11 Stx phages and phage λ have genomic were comprised in 9 various possessive genes. The comparison is based on gene presence, or variant form. It can notice that there is not all genome sequencing of Stx pages are similar. All lamboid phages which had mosaics features, share a genomic synteny and genomic loci but different level. This figure was taken from (Smith et al., 2012b).

environmental stresses such as polylysogeny, antibiotic resistance and acid tolerance (McGrath et al., 1999, Colomer-Lluch et al., 2011, Veses-Garcia et al., 2015b, Su et al., 2010, Vostrov et al., 1996a). A few accessory genes are carried by $\phi 24_B$ that have known functions: *lom* and *bor* when expressed by *E. coli*, promote lysogen adhesion to epithelial cells and aid the lysogen in resisting immune system attack, respectively (Barondess and Beckwfth, 1990, Vaca Pacheco et al., 1997).

However, λ and $\phi 24_B$ possess conserved region which is located between transcribed from the *pL* promoter and *exo* and *xis* genes, is named *exo-xis* region. The *exo-xis* fragments contain many open reading frames that assigns in phage revolution such as weakened lysogenization and risen up the efficient of phage DNA content in the *E.coli* host cells (Łoś et al., 2008). (Bloch et al., 2014) study showed a different expression manners of genes from this fragment which was in the prophage induction and bacterial host cell infection by phage condition and induction of prophage with environmental stimuli such as mitomycin C condition. For example, when the genes of exo-xis fragments of λ and $\phi 24_B$ were expressed in the infected host cell, the lytic development of $\phi 24_B$ was slower than λ. There were some of genes from the *exo-xis* fragments were similar to the N gene efficiency such as: *orf61*, *orf63* and *orf60a* in phage λ, and *ea22*, *orf73*, *orf60a* and *orf63* in phage $\phi 24_B$. Moreover, the genes that located upstream of the terminator λ were higher level of mRNA than downstream genes of the estimated terminator that were located between *orf601* and *orf73*. In contrast, bacterial host cells infected by the bacteriophage expression level of mRNA showed *orf61* was a little expressed, and *ea22* and *orf73* were high same as those for *orf63, orf61a* and *N.* The promoter *p1*_$\phi 24_B$ which was located upstream of *ea22* and *orf73*, was similar with analogous sequence of the promoter *p1*_ λ that was located upstream of the λ *orf73*.

The $\phi 24_B$ phage may find itself inside in chromosome of the host cell as an inducible prophage, or live inside the host cell long enough to facilitate recombination events that result in losing key prophage sequences that leave it as an uninducible remnant prophage (Hayashi et al., 2001a). Transduction is the process that *stx* genes transfer into lysogen. The *stx* genes that were encoded by Stx phages were more stable in the environment than inside a bacterial genome. As a result, lysogenized bacteria got advantage from transduction process in survival against ecological niches such as heat or high-pressure antimicrobial agents (Brabban et al., 2005). In (Nyambe

et al., 2016) study showed $\phi 24_B$ had recovered from water and soil was able to transduce and form lysogens with its bacterial host cell. Moreover, $\phi 24_B$ had extended period of surviving in four different types of water at 4°C, and 14 °C over 40 days period.

There is a small microRNA-size molecule which is size 20 nt, has been predicted in bacterial host cell after induction of $\phi 24_B$. It is called $\phi 24_B\_1$ which is located between *lom* and vb_$\phi 24_B$_43 (45711..45692), and may connect to two regions that are the first located upstream of *S* gene and another one located within the d_ant gene (Nejman-Faleńczyk et al., 2015). The (Nejman-Faleńczyk et al., 2015)study had predicted the functions of $\phi 24_B\_1$ which were minimizing the efficiency of lysogenization, increasing the prophage induction after stimulation the SOS response, rising up the efficiency of progeny phage outcomes during lytic pathway, and minimizing efficient adsorption on the *E.coli* host cell.

(Riley et al., 2012a) studied the phage genes expression in an *E. coli* lysogen carries $\phi 24_B$. The lysogen and naïve culture were subjected to both Change Mediated Antigen Technology (CMAT), and proteomic-based protein profile comparisons to detect proteins only expressed lysogeny. As a result, 26 genes from $\phi 24_B$ detected by either CMAT or 2D-PAGE, no genes were detected by both 2D-PAGE and CMAT and neither technique detected CI. qPCR profiling was done to identify the patterns of gene expression associated with $\phi 24_B$ genes expressed during lysogeny only or genes that expressed during the lytic cycle or genes that were uncoupled from regulation by the lytic and lysogenic regulatory cycles (Fig. 1.15). This was in part due to the fact that proteins expressed in the lysogen cultures could in fact be due to proteins produced by only a small subset of the lysogen population that were undergoing induction (Riley et al., 2012a). The expression levels of the induced genes though limited by cell number was actually very high by total number of mRNA molecules in the culture volume. The qPCR profiling (Fig. 1.15) enabled comparing of the shape of the expression data from lysogenic culture during the prophage induction status where the initial time point is prior to the addition of inducer (norfloxacin) (Fig.1.15). *cI* is lysogen restricted in its gene expression profile, so it is turned off after phage induction. Q, Cro, capsid and terminase are significantly increasing 50 minutes after adding norfloxacin because they are associated with late genes the lytic cycle through Cro and Q are seen first, being closest to *pR* (Fig.1.15A). The genes identified by CMAT and 2D-PAGE were assessed by qPCR profiling, as well. If the proteins link to genes

expressed by a small proportion of cells undergoing spontaneous induction, the expression levels would increase following induction status. (Fig.1.15C). Moreover, there are two genes that are detected by 2D-PAGE presented the same manner of cI that their levels of expression after adding induce is lower than level of expression before induction. According to genes that are detected by CMAT, there are five coding sequences (CDS) that choose for expression analysis. As result, four genes present manner as lytic pathway, while one gene presents manner as lysogenic expressed cultures (Fig.1.15B) (Riley et al., 2012a).

1.3.5. Fitness traits carried by prophages

The Stx phages have impacts on their bacterial host cells beyond conferring the ability to produce Shiga toxin, which does profoundly impact their pathogenic profile (Veses-Garcia et al., 2015a). There are prophage genes that are acquired fitness traits to host cell in adherence (Dziva et al., 2004), bacterial cell metabolism (Berger et al., 2019), polylysogen (Vostrov et al., 1996a), and be bacterial antipredator (Lainhart et al., 2009b).

The signature-tagged mutagenesis experiments of (Dziva et al., 2004) concluded that there were 59 genes involved in increasing gut adhesion of STEC in calves, 7 of these genes were carried by Stx prophage. For example, Stx1 in CP-933V encodes gene *z3341 (ecs2970)*, encoded between *stx$_1$AB* genes, was shown to reduce the subset of intraepithelial lymphocytes in a calf ligated ileal loop. As a result, it was postulated that this gene may modulate the mucosal immune response and increase the persistence of bacteria in intestine (Dziva et al., 2004). Moreover, (Berger et al., 2019) by microarray analysis that the Stx2 phage ΦO104, and Stx2 phage ΦPA8 lysogen on the *E. coli* MG1655, and naiive cells *E. coli* MG1655. The results showed that the Stx2 phage lysogens demonstrated reducing growth in minimal medium supplemented with single carbon sources *e.g.* Nacetylneuraminicacid, galactose, glucose, ribose maltose, and L-Lactate that in naive *E. coli* MG1655. Moreover, the Stx2 phage lysogens displayed decreasing in the cell respiration with gluconeogenic substrates *e.g.* nucleosides, carboxylic acids, dicarboxylic acids, amino acids that in naive *E. coli* MG1655, while the Stx2 phage lysogens displayed increasing respiration with many sugar components of the intestinal mucus such as N-acetyl-D-glucosamine, mannose, L-arabinose, and L-fucose. These data suggest that the Stx2 phage lysogens have ability to utilize substrates as a source of carbon. In addition,

Table 1.2. Genome annotation of $\phi 24_B$. (https://www.ncbi.nlm.nih.gov/nuccore/HM208303.1/)

Gene	Gene location	Product	Note	Protein ID
Int	236..1405	integrase	possesses P4 integrase conserved domain; site specific recombinase	ADN68388.1
Xis	1389..1571	excisionase	site-specific recombinase; direct factor	ADN68389.1
1c	1632..1883	hypothetical protein	identified in phages ED1a, Sf2a, P27, BP4795, and YYZ2008	ADN68390.1
2c	1871..2251	hypothetical protein	identified in phages VT2-Sa and Fels1	ADN68391.1
3c	2248..2646	hypothetical protein	similar to DUF1627 superfamily; identified in Stx-phage 86	ADN68392.1
4c	2682..2897	hypothetical protein	similar to DUF1382 superfamily	ADN68393.1
6c	2830..3735	hypothetical protein	possesses 2 conserved domains: DUF550 a conserved NH-terminal domain and DUF551 a conserved COOH domain similar to phosphodiesterase and chromosome segregation protein SMC (SMC_prok_B,TIGR02168)	ADN68394.1
5c	2840..2911	hypothetical protein		ADN68395.1
putative C4 zinc finger protein	3732..3953	putative C4 zinc finger protein	putative phage conjugal plasmid C-4 type zinc finger protein; TraR family; matches a sequence similar to protein families PF01258 and TIGR02419	ADN68396.1
7c	4052..4333	hypothetical protein	similar to ninL ORF61 of bacteriophage lambda and other Stx phages	ADN68397.1
8c	4344..4535	hypothetical protein	similar to DUF superfamily 07131	ADN68398.1
10	4487..4813	hypothetical protein	identified in Stx2 converting phages I, II and YYZ 2008	ADN68399.1
9c	4508..4696	hypothetical protein	similar to DUF superfamily 1317; also identified in Stx-phages 933W, Min27, Stx2 converting phages I and 2	ADN68400.1
Exo	4690..5367	exonuclease	possesses large core domain from the herpes alk_exo family, alkaline exonucleases, which plays an important role in herpes virus replication	ADN68401.1
Bet	5364..6149	Bet	possesses large RecT domain (RecT superfamily, pfam 03837); DNA single-stranded annealing proteins such as RecT, Red-beta, ERF and Rad52 function in RecA-dependent and RecA-independent DNA recombination pathways	ADN68402.1
Gam	6155..6451	Gam	host nuclease inhibitor protein; inhibits RecBCDnuclease and is asociated with both bacteria and bacteriophages; member of Gam superfamily; pfam 06064	ADN68403.1

Kil	6527..6796	Kil	host killing; lambda Kil superfamily; pfam 06301	ADN68404.1
cIII	6639..6803	CIII	regulatory protein CIII; stabilization of CII; member of lambda CIII superfamily; pfam 02061	ADN68405.1
Ssb	6876..7244	Ssb	putative single-stranded DNA binding protein	ADN68406.1
11c	7395..7865	hypothetical protein	identified in phages 933W, Stx2 phage 86, ED1a,Stx2 converting phage 1, HK97, H19B, BP4795; also identified with some similarity to Stx-phages VT2-Sa and Stx2 converting phages I and II	ADN68407.1
N	7924..8307	N	anti-terminator; functions in early gene expression	ADN68408.1
12c	8796..8960	hypothetical protein	identified in Stx-phages 933W, Stx2 converting I and 86 and Min27	ADN68409.1
Stk	8963..10009	Stk	putative protein kinase; contains domain Pkinase; belong to a very extensive family of proteins which share a conserved catalytic core common with both serine/threonine and tyrosine protein kinases; contain conserved regions: in N-terminal of the catalytic domain a glycine-rich stretch of residues in the vicinity of aysine residue has been shown to be involved in ATP binding; in the central part of the catalytic domain a conserved aspartic acid residue is important for the catalytic activity of the enzyme; member of clan PKinase (CL0016) which contains the following 13 members: ABC1, APH, APH_6_hur, Choline_kinase, DUF1679, DUF227, Fructosamin_kin, Kdo, Pkinase, Pkinase_Tyr, Pox_ser-thr_kin, RIO1, WaaY.	ADN68410.1
Res	10003..10464	resolvase	putative holliday junction resolvase; similar to RuvC resolvase superfamily cl00243; endonuclease	ADN68411.1
13c	10532..10873	hypothetical protein	identified in Salmonella phage SE1 and Stx2 phage 86; contains DUF superfamily 3024, pfam11225	ADN68412.1
cI	10934..11641	CI	repressor protein; contains helix-turn-helix-XRE DNA binding region superfamily; similar to S24 LexA/signal peptidase S24_S26 superfamily, pfam0071769	ADN68413.1
Cro	11720..11947	Cro	regulatory protein; transcriptional activator/repressor	ADN68414.1
cII	12086..12385	CII	transcriptional activator; establishment of lysogenic state; member of phage CII superfamily, pfam 05269	ADN68416.1
O	12548..13324	O	replication protein; DNA replication; contains a DNA binding motif and a PhnF trascriptional regulator region	ADN68416.1
P	13435..16341	P	replication protein; DNA replication; contains as Gp4D helicase region containing both Walker A, B and ATP binding motifs; similar to homing endonuclease, DNA Gprimase COG0358 and PRK0773 DNA helicase	ADN68417.1
14	16342..16611	hypothetical protein	identified in other bacteriophages including ES18,P22 and Sf6, bacteriophage 21, Lahn1, Lanh 2 and 3, Nil3,Salmonella phages	ADN68418.1
ninA	16608..16700	hypothetical protein		ADN68419.1

15	16697..16912	hypothetical protein	identified in Stx2 converting phages I and II,1717, VT2-Sa, VT1-Sa, Min27, 933W, Nil 3, Lahn2, YYZ2008 and Min27	ADN68420.1
Lar	16923..17159	Lar	putative restriction alleviation protein; similar to anti-R-lar family TIGR06355	ADN68421.1
ninB	17017..17562	NinB	recombination related; NinB operates in phage lambda with ninG and the E. coli RecF and RecBCD proteins in recombination events	ADN68422.1
phage_N6A_met	17559..18086	hypothetical DAM	putative DNA N-6-adenosine methyltransferase; similar to TIGR01712 and DAM superfamily, pfam 05869	ADN68423.1
nine	18083..18265	NinE	similar to TIGR01712 and DAM superfamily, pfam 05869	ADN68424.1
17	18262..18330	hypothetical protein		ADN68425.1
Roi	19286..20014	Roi	putative antirepressor protein; similar to phage regulatory protein pRHA superfamily, pfam 09669 and an antirepressor protein, a member of the Ant superfamily, pfam 03374	ADN68427.1
ninG	20014..20619	NinG	putative recombination endonuclease; NinG superfamily, pfam 05766	ADN68428.1
ninH	20616..20810	NinH	phage NinH superfamily, pfam06322; high levels of conservation in lambda and lambdoid like bacteriophages	ADN68429.1
Q	20764..21237	Q	antiterminator; phage antiterminator superfamily, pfam06530	ADN68430.1
stx	22021..22119	Stx		ADN68431.1
19c	22874..22999	hypothetical protein	similar to Shigella dysenteriae hypothetical protein in CAC05624.1 that also flanks the Stx genes	ADN68433.1
20c	22902..23069	hypothetical protein	identified in remnant bacteriophage in *E. coli* O157:H7 strain EDL 933, CP933O	ADN68434.1
21	23314..25251	hypothetical protein	Duf 1737 superfamily of unknown function, pfam 08410; similar to Duf superfamily03629; identified in VT2-Sa, 933W, Stx2 converting bacteriophage I and II, Min27, BP4795 and Stx phage 1717	ADN68435.1
23	25386..25565	hypothetical protein	identified in Stx phages VT2-Sa, Stx2 converting 1 and 2, Stx2 converting phage 86, Min27, BP4795	ADN68436.1
24	25432..25878	hypothetical protein	similar to Duf superfamily of unknown function Duf826	ADN68437.1
S	25955..26170	S	host cell lysis; part of lysis S superfamily	ADN68438.1
R	26175..26708	R	associated with endolysin_autolysin; similar to R of bacteriopahge Qin Lysozyme like superfamily, pfam cl00222; contains phage lysozyme domain (this family includes lambda phage lysozyme and E. coli endolysin)	ADN68439.1
Rz	27702..28166	Rz	host cell lysis; bacterial lysis protein superfamily, pfam 03245; similar to protein found in bacteriophages VT2-Sa, 933W, Stx converting I, II, 86, Min27 and BP4795	ADN68441.1

Rz1	27922..28107	Rz1	host cell lysis; bacterial lysis protein superfamily, pfam 06085. Rz1 is a proline-rich lipoprotein from bacteriophage lambda which is known to have fusogenic properties	ADN68442.1
bor	28198..28491	Bor	lambda bor superfamily pfam 06291; increases the resistance of *E. coli* to serum	ADN68443.1
26	28599..28844	hypothetical protein	identified in Stx phages VT2-Sa, 933W, Stx2 converting 1,2 and 86 and Min27	ADN68444.1
sterm	28900..29706	Sterm	putative small subunit terminase; idetified inVT2-Sa, 933W, Stx2 converting 1,2 and 86 and Min27	ADN68445.1
lterm	29687..31393	Lterm	putative large subunit terminase; identified in VT2-Sa, 933W, Stx2 converting 1,2 and 86 and Min27	ADN68446.1
port	31393..33537	Port	putative portal protein; identified in VT2-Sa, 933W, Stx2 converting 1,2 and 86 and Min27	ADN68447.1
27c	33689..34078	hypothetical protein	identified in Stx2 converting phage 1 and 2	ADN68448.1
28	33695..34702	hypothetical protein	identified in VT2-Sa, 933W, Stx2 converting 1,2 and 86 and Min27	ADN68449.1
29	34726..35940	hypothetical protein	possible phage structural protein; identified VT2-Sa, 933W, Stx2 converting phage 1,2, 86 and Min 27	ADN68450.1
30c	35116..35400	hypothetical protein	identified in Stx2 converting phages 1 and 2	ADN68451.1
31	35996..36385	hypothetical protein	identified in VT2-Sa, 933W, Stx2 converting phages 1, 2, 86, Min27	ADN68452.1
32c	36321..36593	hypothetical protein	identified in Stx1 converting phage, Stx2 converting phages 1, 2	ADN68453.1
33	36408..36896	hypothetical protein	identified in VT2-Sa, 933W, Stx2 converting phages 1, 2, 86, Min27	ADN68454.1
34	36772..37443	hypothetical protein	identified in VT2-Sa, 933W, Stx2 converting phages 1, 2, 86, Min27	ADN68455.1
35	37196..37492	hypothetical protein	identified in VT2-Sa, 933W, Stx2 converting phages 1, 2, 86, Min27	ADN68456.1
36	37443..38093	hypothetical protein	identified in VT2-Sa, 933W, Stx2 converting phages 1, 2, 86, Min27	ADN68457.1
tsps	38090..40027	Tail spike protein	contains 4 pfam superfamilies: phage tail N superfamily, pfam08400; collagen superfamily pfam 01391; phage fiber repeat superfamily, pfam 03406; phage fiber C terminus superfamily pfam 06820; conserved tail spiken protein in 933W, VT2-Sa, Stx1, Stx2 converting phages 1,2	ADN68458.1

37c	39335..40189	hypothetical protein	identified in Stx2 converting I; similar to the hypothetical protein enterobacteria phage cdt1	ADN68459.1
hypothetical tail fiber protein	39909..40298	hypothetical tail fiber protein	putative tail region; phage fiber C superfamily; contains a RLGP motif similar to the phage side tail fiber	ADN68460.1
38	40345..40626	hypothetical protein	identified in 933W and Enterobacteria phage P-EibD	ADN68461.1
39	40843..42546	hypothetical protein	identified in VT2-Sa, 933W, Stx2 converting phages 1, 2, 86, Min27	ADN68462.1
40	42543..43811	hypothetical protein	similar to putative tip tail fiber in Stx2 converting phage 86; identified in Min27, 933W, VT2-Sa, Stx2 converting phage 1and 2, Stx1 converting phage and Vibrio cholera phage RC586	ADN68463.1
41	43877..44104	hypothetical protein	possesses putative outer membrane protein region;identified in VT2-Sa, 933W, Stx2 converting phage	ADN68464.1
42	44110..44727	hypothetical protein	identified in VT2-Sa, 933W, Stx2 converting phages 1, 2, 86, Min27	ADN68465.1
lom	44818..45552	Lom	outer membrane protein of the enterobacterial Ail/Lom family	ADN68466.1
43	45981..46382	hypothetical protein	identified in VT2-Sa, 933W, Stx2 converting phages 1, 2, 86, Min27	ADN68467.1
44	46475..47131	hypothetical protein	identified in VT2-Sa, 933W, Stx2 converting phages 1, 2, 86, Min27	ADN68468.1
45	47134..47580	hypothetical protein	identified in VT2-Sa, 933W, Stx2 converting phages 1, 2, 86, Min27	ADN68469.1
46	47590..47841	hypothetical protein	identified in VT2-Sa, 933W	ADN68470.1
47	47852..49117	hypothetical protein	similar to putative transcription initiation factorand seryl t-RNA synthetase; identified in VT2-Sa, 933W, Stx2 converting phages 1, 2 and 86, Min27	ADN68471.1
48	49148..57571	hypothetical protein	putative leader peptide sequence found using signalP-NN prediction (gram-networks); identified in VT2-Sa, 933W, Stx2 converting phages 1, 2 and 86, Min27	ADN68472.1
50c	52191..52514	hypothetical protein	similar ORF identified in Stx2 converting phages1,2 and Stx1 converting phage	ADN68473.1
51c	54666..55046	hypothetical protein	similar to metallophosphoesterase in ZP_01462790.1	ADN68474.1
52c	55397..55768	hypothetical protein	similar to ABC-type multi-drug transport system in ZP_01950625.1	ADN68475.1

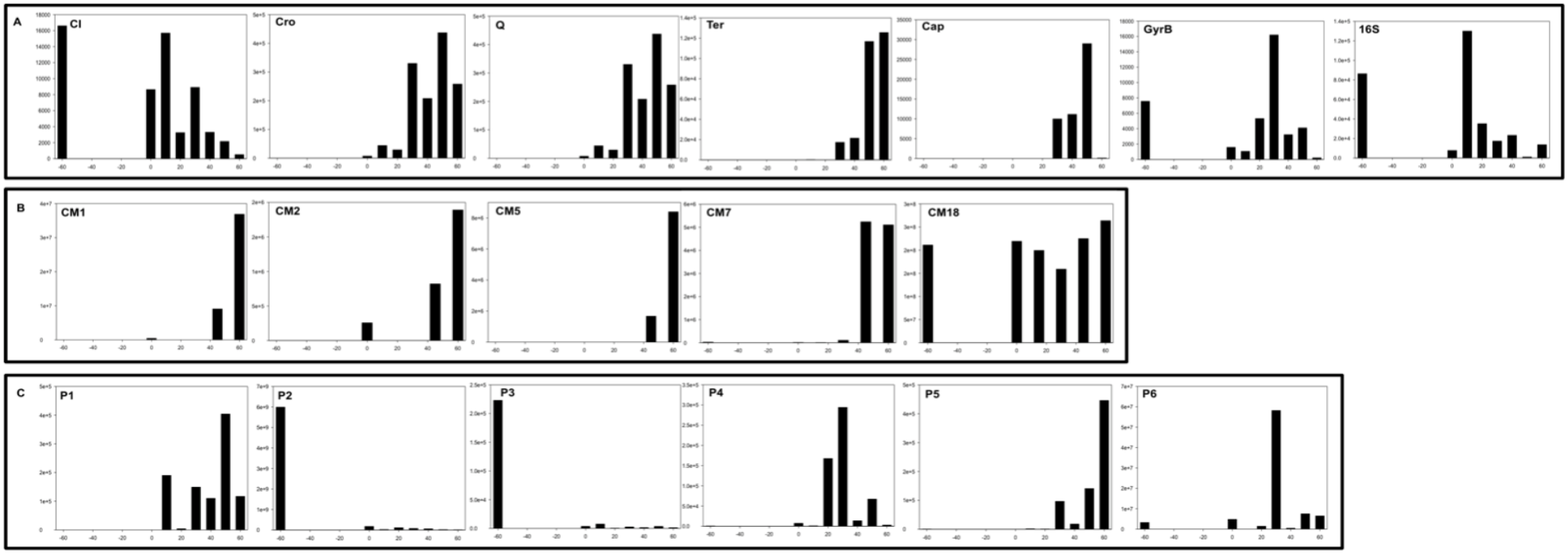

Figure 1. 15. qPCR profiling of lytic, lysogenic and uncoupled gene expression profiles from (Riley et al., 2012a) study.

Panel A: Control Genes. CI, marker gene for lysogeny-restricted expression; Cro and Q, marker genes for early induction response; Ter and Cap, marker genes for late gene expression; GyrB and 16S, marker genes for the cellular response. Panel B: Expression profiles of the prophage genes identified by CMAT. Panel C: Expression profiles of the genes identified by 2D-PAGE analyses of the lysogen. The Y axis represents gene copy number per 300 ng of RNA; the X axis represents time (min). Time -60 refers to the samples taken before induction and represents the lysogen population, Time 0 represents samples taken at the beginning of the recovery time, Time 10, 10 min after recovery, etc.This figure was taken from (Riley et al, 2012).

Coliphages N15 and ϕ80 encode the *cor* gene that express the Cor protein whose molecular mass 8 kDa (MALININ et al., 1993). The Cor protein can form a transmembrane helix that facilitates protein integration with host cell membrane, so increasing the polylysognic status (Vostrov et al., 1996a), and interact with membrane receptors in Coliphages N15 and ϕ80. Such as; FhuA which is an outer membrane receptor of *E.coli* for adsorption function, is required in Coliphages N15 and ϕ80 to uptake iron that needs ToB inner membrane protein to produce energy for transporting iron products through outer membrane, and TonB that acts as energy transmitter in inner membrane, and interacts with FhuA that causes a conformational change that permits producing of the bound ligand from FhuA through the periplasmic space. In contrast, The Cor protein showed direct interaction with FhuA and indirect interaction via TonB protein that indicated in ϕ80 Cor^+ lysogen Δ *fhuA* phenotypes no adsorbing on *fhuA* and growing on tonB cells. So, Cro protein as the FhuA protein target (Vostrov et al., 1996b). Finally, the Stx phages carry *stx* genes (Lainhart et al., 2009b) suggest that can be act as a bacterial antipredator. When (Lainhart et al., 2009b) study compared between EDL933 bacterial carring a Stx encoding temperate phage and EDL933Δ*stx* which is the variant carring a deletion all the *stx* genes in coculture with *Tetrahymena thermophlia* (Lainhart et al., 2009b) results demonstrated that the number of cell count of bacterial cells that encodes *stx* genes was higher than the bacterial cells that does not encode *stx* genes. Moreover, when *Tetrahymena thermophlia* cocultured with bacterial cells that encodes *stx* genes, the number of protozoa cell count was lower than number of protozoa cell count that cocultured with bacterial cells that does not encode *stx* genes.

1.3.6. Fitness traits carried by $\varphi 24_B$

1.3.6.1. Acid resistance

The $\phi 24_B$ prophage confers a significant acid resistance phenotype on the bacterial host cell that is caused by upregulating genes of the glutamic acid decarboxylase (GAD) operon, through the action of the $\phi 24_B$ encoded transcriptional regulator CII (Veses-Garcia et al., 2015a). RNA seq analysis (Veses-Garcia et al., 2015a) resulted increasing expression level of around 3- to 5-fold of the genes in the GAD system responsible for controlling acid resistance in *E. coli*. The genes of GAD operon are *gadA* and *gadB* whose function are glutamate decarboxylase, and

comprising the structure of GAD operon with *gadC*, while *gadE* whose function is transcriptional activator*, gadX gadW* regulators of the operon (Ma et al., 2003, Hommais et al., 2004, Kailasan Vanaja et al., 2009).

The lysogen that carried $\phi 24_B$ and naïve cell were compared in acid resistance assays in (Veses-Garcia et al., 2015a). As a result, the lysogen cells demonstrated in *vitro* higher rate of surviving than naïve cells under acidic cultural condition pH 2.5 for 2h at 37°C. Moreover, the lysogen and *E. coli* naïve cells compared to naïve cells harbouring an arabinose-inducible expression plasmid with the *cI* gene, the *cII* gene or both the *cII* and *cIII* genes to define the effect of these phage regulators on the expression of the genes GAD system and on acid resistance. It was demonstrated that CII controlled expression of the GAD genes and was capable of activating a significant arabinose inducible acid resistance in the absence of the rest of the prophage (Veses-Garcia et al., 2015a).

1.3.6.2. Cell proliferation

The $\phi 24_B$ integrates into host cell's chromosome at an integration site which is 250 bp upstream of the *intS* gene (Fogg et al., 2007). As a result, the lysogen requires the host cell to use uridine-2-monophosphate (U-2-P) instead to use D-allose for respiration because the prophage integration stops the function of the genes *alsB*, *alsA*, and *alsC* in *E. coli* that are associated with the utilisation of D-allose (Kim et al., 1997).

This study (Holt et al., 2017a) had compared the lysogen and naïve cells respiration under (U-2-P) conditions using bacterial phenotypic microarrays from (BIOLOG, United States). As a result, the $\phi 24_B$ lysogen showed significantly high ability to grow and respire U-2-P when that was compared to the naiive cells. However, U-2-P is associated with some cellular metabolism processes such as nucleotide metabolism, pyrimidine catabolism, and biotin metabolism (Kanehisa and Goto, 2000). Moreover, the 5-methyluridine intensity was decreased in the $\phi 24_B$ lysogen that increased pyrimidine catabolism (Holt et al., 2017a).

1.3.6.3. Metabolic profile

The $\phi 24_B$ lysogen presents a noticable differences in metabolic profile when compared to naïve *E. coli* under normal cultural condition that is analysed by using partial least discriminant analysis (PLS-DA). There are 6 specific metabolites that are

strongly identities from retention times, low accurate mass error (PPM), and fragmentation patterns (Holt et al., 2017a). The 6 metabolites are: FAPy-Adenine, sphinganine, hexadecanoic acid, ophthalmic acid, 5-Methyluridine, and pimelic acid. Altering of metabolic profile of lysogen in early growth revels to positive impact on bacterial host cell metabolic profile that can subvert the biotin pathway, so $\phi 24_B$ lysogen can be able to tolerate chloroxylenol and 8-hydroxyquinoline antimicrobials antimicrobials such as during early and mid-exponential growth phase (Holt et al., 2017a).

1.3.6.4. Antimicrobial tolerance

The $\phi 24_B$ prophage gained the host cell a tolerance of antimicrobial by controlling of the *E. coli* biotin and synthesising fatty acid without impact of carried resistance genes. The metabolic profile of $\phi 24_B$ lysogen is altered that is caused by increasing levels of biotin concentration and fatty acid synthesis. As a result, it may alter growth and lipids that leads to reconstruct the cell surface which is responsible for promoting antimicrobial isolation to bind to bacterial host cell(Holt et al., 2017a).

In (Holt et al., 2017a) study has showed the impact of $\phi 24_B$ lysogen on the host cell in levels of biotin and fatty acid synthesis, and tolerance of lysogen in the presence of antimicrobial. The study compares between $\phi 24_B$ lysogen cells and naïve *E. coli* cells. The results demonstrated that $\phi 24_B$ prophage had a significant upregulatory effect on biotin which showed a ~3 fold higher than naïve cells in the level of biotin present per cell at mid-exponential growth phase. Moreover, the respiration curves of $\phi 24_B$ lysogen were higher in the naïve cells under antibiotics stress (chloroxylenol and 8-hydroxyquinoline) that were run by the biology bacterial phenotypic microarray. Also, the $\phi 24_B$ lysogen under antibiotic stress showed lower the sub-inhibitory concentration (SIB) than naïve cells in both antibiotics (chloroxylenol and 8-hydroxyquinoline).

1.4. Aims

This project will focus on determining the gene function of two conserved genes carried by $\phi 24_B$ [GenBank: HM 208303], whose gene expression profiles have been determined through RNA seq analysis of mRNA from the direct comparison of 4 culture conditions: norfloxacin-induced and uninduced naïve cultures, and norfloxacin-induced and uninduced $\phi 24_B$ lysogen cultures (Veses-Garcia et al., 2015b). It has been demonstrated that prophage-encoded gene expression can change the host cell phenotype such as adding virulence factors to host cell (Allison, 2007, Wang et al.,

2010b, Arraiano et al., 2007), but are other prophage genes whose expression is not associated with viral replication, but appear to aid the host cell in surviving environmental stresses such as polylysogeny, antibiotic resistance and acid tolerance (McGrath et al., 1999, Colomer-Lluch et al., 2011, Veses-Garcia et al., 2015b, Su et al., 2010, Vostrov et al., 1996a). Though a few accessory genes carried by $\phi 24_B$ have known functions: *lom* and *bor* when expressed by *E. coli* (1.3.4.2.1). Approximately three quarter of $\phi 24_B$ genes are hypothetical, having no readily predictable function, and many of these are conserved across of variety of Stx and non-Stx phages. This study will focus on two interesting genes which are carried by the detoxified variant of $\phi 24_B$, ϕ24B::Kan in which the *stx* operon has been replaced with a gene conferring resistance to kanamycin (James et al., 2001b). The first gene is vb_24_B_21 (*P21*) located from between nucleotides 23,314 and 25,251 in the $\phi 24_B$ prophage genome (Gene ID: 26040935, Protein ID: YP_009168140.1), and the second gene is vb_24_B_48 (gene *48*) located between nucleotides 49,148 to 57,571 $\phi 24_B$ prophage genome (Gene ID: 26040971, Protein ID: YP_009168177.1).

The aims of this project are to determine the roles of these proteins in the biology of the lysogen or phage by finding the answers to the following research questions. The question and the processes I followed to address these questions will comprise my three data chapters.

1. Does the expression of P21 impact phage replication and the lytic cycle?
2. Does P21 act at the level of peptidoglycan to impact phage replication**?**
3. Does protein 48 impact the biology of $\phi 24_B$ lysogen?

Each chapter goes beyond these initial questions to seek explanations behind how these proteins function and what this means for our understanding of phage host interactions.

CHAPTER 2:

GENERAL MATERIAL AND METHODS

2.1. Media, antibiotics and buffer recipes

Table 2.1. The compositions of all materials that were prepared to use in experiments

Material	Components
LB agar plates	3.7% (w/v) Luria Burtani Agar (Merck KGaA, Germany, #1.10283.500)
LB broth Media	2.5% (w/v) Luria Burtani Broth (Merck KGaA, Germany, #1.10285.0500)
LB Top agar	2.5% (w/v) Luria Burtani Broth (Merck KGaA, Germany, #1.10285.0500) + 0.5% Difco™ Agar, Granulated (Becton, Dickinson and Company, France, # 4156518+ 0.01 M $CaCl_2$ (BDH Laboratory Supplies, England, #TA940194 307)
SOB broth	0.5% (w/v) Yeast Extract (Merck KGaA, Germany, #1.03753.0500), 2% (w/v) Tryptone (acumedia LAB, United Kingdom, #MC005), 10 mM NaCl (Fisher Scientific, United Kingdom, #18600871), 2.5 mM KCl (Sigma-Aldrich, United States, #P9333), 10 mM $MgCl_2$ (BDH Laboratory Supplies, England, #A407233), 10 mM $MgSO_4$ KCl (Sigma-Aldrich, United States, #M7506)
Arabinose	20% (w/v), 15% (w/v), 10% (w/v), 5% (w/v) L-Arabinose (Sigma-Aldrich, United States, #A3256)
PBS	Phosphate buffered saline tablets (Melford, United Kingdom, #P32080)
TAE agarose gel	1% (w/v) agarose powder (BioLine, United States, # BIO-41025), 1x Tris-acetate-EDTA (TAE) Buffer (Thermo Fisher, United Kingdom, #B49), 0.1% (w/v) Midori Green (Nippon Genetics, Germany, # 654mg30089)
Transfer Buffer	1.4 % (w/v) glycine (Fisher Scientific, United Kingdom, #2059318), 0.3% (w/v) Tris (Fisher Scientific, United Kingdom, #1671855), 1% (w/v) SDS 10% (Fisher Scientific, United Kingdom, #1532314), 20 % (w/v) methanol (Fisher Scientific, United Kingdom, #2035657),
TBS Tween 20	50 mM Tris (Fisher Scientific, United Kingdom, #1671855) pH 7.5, 150 mM NaCl (Fisher Scientific, United Kingdom, #18600871), 0.1% Tween 20 (Sigma-Aldrich, United States, #P9416)
Blocking Buffer	5% (w/v) *Marvel* Original Dried Skimmed Milk in TBS tween
Running Buffer	25 mM Tris (Fisher Scientific, United Kingdom, #1671855), 192 mM Glycine (Fisher Scientific, United Kingdom, #2059318), 0.1% (w/v) SDS (Fisher Scientific, United Kingdom, #1532314)
Lysis Buffer	50 mM NaH_2PO_4 (BDH Laboratory Supplies, England, #10245), 300 mM NaCl (Fisher Scientific, United Kingdom,

	#18600871), 10 mM imidazole (Sigma-Aldrich, United States, #56750), pH 7.4
Wash Buffer 1	50 mM NaH_2PO_4 (BDH Laboratory Supplies, England, #10245), 300 mM NaCl (Fisher Scientific, United Kingdom, #18600871), 20 mM imidazole (Sigma-Aldrich, United States, #56750), pH 7.4
Wash Buffer 2	50 mM NaH_2PO_4 (BDH Laboratory Supplies, England, #10245), 300 mM NaCl (Fisher Scientific, United Kingdom, #18600871), 30 mM imidazole (Sigma-Aldrich, United States, #56750), pH 7.4
Wash Buffer 3	50 mM NaH_2PO_4 (BDH Laboratory Supplies, England, #10245), 300 mM NaCl (Fisher Scientific, United Kingdom, #18600871), 50 mM imidazole (Sigma-Aldrich, United States, #56750), pH 7.4
Elution Buffer	50 mM NaH_2PO_4 (BDH Laboratory Supplies, England, #10245), 300 mM NaCl (Fisher Scientific, United Kingdom, #18600871), 300 mM imidazole (Sigma-Aldrich, United States, #56750), pH 7.4
$NaPO_4$ Buffer	50 mM NaH_2PO_4 (BDH Laboratory Supplies, England, #10245), 300 mM NaCl (Fisher Scientific, United Kingdom, #18600871), pH 7.4
Tris/Glycine/SDS buffer 10X)	25 mM Tris, 192 mM glycine, and 0.1% (w/v) SDS, pH 8.3 (Bio RAD, United states, #1610772)
Coomassie Stain	5% (w/v) Coomassie blue (Thermo Fisher, United Kingdom, #G-250), 45% (v/v) Methanol (Fisher Scientific, United Kingdom, #2035657), 10% (v/v) Acetic acid (Fisher Scientific, United Kingdom, #1721413)
Coomassie Destain	5% (v/v) Methanol (Fisher Scientific, United Kingdom, #2035657), 7% (v/v) Acetic acid (Fisher Scientific, United Kingdom, #1721413)
10X MOPS Buffer	0.2 M MOPS (BDH Laboratory Supplies, England, #K35932091 626), 80 mM Sodium acetate (Geldenaaksebaa, Belgium, #27648.294), 10 mM EDTA (Fisher Scientific, United Kingdom, #16654046), pH 7.0
20X SSC Buffer	3 M NaCl, 300 mM Sodium Citrate (Sigma-Aldrich, United States, #71497), pH 7.0
Denaturing RNA gel	1x MOPS buffer, 1.2% (w/v) agarose powder (BioLine, United States, # BIO-41025) , 1.8% (v/v) Formaldehyde (BDH Laboratory Supplies, England, #29001), 0.1% (w/v) Midori Green (Nippon Genetics, Germany, # 654mg30089)
Rifampicin (Rif)	300 $\mu g\ mL^{-1}$ (Sigma-Aldrich, United States, #R3501)
Tetracycline (Tet)	10 $\mu g\ mL^{-1}$ (Sigma-Aldrich, United States, #T7660)
Kanamycin (Kan)	50 $\mu g\ mL^{-1}$ (Sigma-Aldrich, United States, #K1876)
Norfoxacin (Nor)	1 $\mu g\ mL^{-1}$ (Sigma-Aldrich, United States, #N9890)
Ampicillin (Amp)	100 $\mu g\ mL^{-1}$ (Sigma-Aldrich, United States, #A9518)
Chloramphenicol (Cat)	50 $\mu g\ mL^{-1}$ (Sigma-Aldrich, United States, #C3175)
Amoxicillin (Amox)	100 $\mu g\ mL^{-1}$ (Sigma-Aldrich, United States, #A8523)
Carbenicillin (Car)	100 $\mu g\ mL^{-1}$ (Sigma-Aldrich, United States, #C3416)

Cefoxitin (Cef)	100 μg mL^{-1} (Sigma-Aldrich, United States, #C7039)
8-hydroxyquinoline	100 μg mL^{-1} (Sigma-Aldrich, United States, #H6878)
Sanguinarine	100 μg mL^{-1} (Sigma-Aldrich, United States, #S5890)
Sodium metaborate	100 μg mL^{-1} (Sigma-Aldrich, United States, #S0251)

2.2. Bacterial strains, plasmids, phages and cultural condition

Most cultures in experiments were started from 3 to 4 colonies taken from an agar plate and used to inoculate LB broth with appropriate antibiotic selective pressure (dependent on strain). After overnight culture at 37°C with shaking at 200 r.p.m the cultures were routinely subcultured into fresh media (1:100 with appropriate antibiotic selective pressure) until the cells reached mid log phase of growth optical densities (OD_{600} 0.4 – 0.6). The following steps of culture were based on experiment.

Table 2.2. *E. coli* bacterial strains that were used in experiments.

***E. coli* Bacterial strains**	**Strain features**	**References**
MC1061	wild-type SOS response system	(James et al., 2001b)
TUV 93-0	Non toxigenic (1), Stx prophage deficient derivative of the O157:H7 outbreak strain EDL933 (2)	(Chong et al., 2007)[1], (Perna et al., 2001b)[2]
Solu BL 21	Expressed host, encoded T7 RNA polymerase via controlling the arabinose inducible *ara*BAD promotor	(Invitrogen, Paisley, U.K.)
TOP 10	Competent cells, propagated host for pBAD and pBAD P21	(Novagen, Notts, U.K.)
BL21 (DE3)	Self-transmissible, lack of outer membrane protease, mutation blocks ability to use galactose	(Invitrogen, Paisley, U.K.)
DM1187	Constitutively activated RecA protein (*recA 441*)	(James et al., 2001b)
$DM1187^{Rif}$	Resistant to Rifampicin, used in plaque assays where bacterial contaminants may interfere	(James et al., 2001b)

Table 2.3. Plasmids used in this study.

Plasmid	Strain features	References
pBAD	Resistant to ampicillin	(Invitrogen, 2012)
pEMT-11	Resistant to kanamycin	(Riley et al., 2012)
pGM190_3	Modelled from pBR322, harbours gene *48,* and resistant to ampicillin	(GeneMill, UoL, United Kingdom)
pGM304_1	Modelled from pBR322, harbours gene *48,* and resistant to tetracycline	(GeneMill, UoL, United Kingdom)

The phages $\phi 24_B$::Kan, and $\phi 24_B$::Cat were derived from an Stx phage that was induced from a clinical isolate of *E. coli* O157:H7 (James et al., 2001a, Allison et al., 2003). It was engineered to be non-toxigenic through a double recombination event in which the *stx* operon was exchanged with the *aphA* gene which confers kanamycin resistance in $\phi 24_B$::Kan, and confers chloramphenicol resistance in $\phi 24_B$::Cat (James et al., 2001a).

2.3. Prophage induction and phage stock production

Bacterial lysogen was cultured in 10 mL LB broth under antibiotic selective pressure overnight at 37°C with shaking at 200 r.p.m. On the next day, 100 µl of the overnight culture was subcultured into 10 mL sterile LB broth with appropriate antibiotic selective pressure. This subculture was incubated at 37°C with shaking at 200 r.p.m until the cells reached an OD_{600} = 0.4 – 0.6. At this point the SOS inducing fluoroquinilone antibiotic, norfloxacin (1 µg mL^{-1}) was added, and the culture was incubated for a further 1 h. The induced cells (1 mL) were allowed to recover in 10 mL fresh LB with 0.01 M $CaCl_2$ for 2 h at 37°C with shaking at 200 r.p.m and produce new phage. Finally, the culture was passed through a 0.45 µm filter to remove most of the cells and cellular debris. The filtered culture liquor was stored at 4°C along with a single drop of chloroform (CCl_3) to prevent bacterial growth.

2.4. Determination of colony forming units per mL

Cultures for cell enumeration were serially diluted from 10^{-3} to 10^{-8}. A sample (20 µl) from every serial dilution was dropped onto the surface of an LB agar plate (with appropriate antibiotics). The plates were incubated overnight at 37°C. The resultant colonies were counted the next day to determine c.f.u. ml^{-1} using the formula:

$$\text{c.f.u } mL^{-1} = \text{number of colonies} \times 50 \times \frac{1}{Dilution\ Factor}$$

2.5. Plaque assay

A plaque assay was used to enumerate phages from a liquid sample. Plaques were areas of clearing in a bacterial lawn due to bacterial growth inhibition mediated by phage infection. The four reagents necessary for plaque assay were agar plates, top agar (Table 2.1), a sample containing phages and an indicator bacterial host strain. The bacterial indicator host, usually *E. coli* strain DM1187 unless otherwise stated, was grown to mid-exponential phase in LB broth with 0.01 M $CaCl_2$ as determined by OD_{600} = 0.4-0.6. The phages were then serially diluted (10^{-1} to 10^{-6}) in LB with 0.01 M $CaCl_2$. The serial dilutions of phage (100 µl) were added to the mid-log indicator cells (100 µl), mixed and incubated at 37 °C for 25 min to allow phage to infect bacterial cells. Then, 5 mL of molten top agar (Table 2.1) cooled to 46 °C was mixed with the infection mix by vortex, and the sample was poured onto the top of an LB agar plate, allowed to set and incubated overnight at 37 °C. The next day, plaques on the plates were counted to determine the number of phages by p.f.u. ml^{-1} (Dimmock et al., 2015) using the formula:

$$\text{p.f.u } mL^{-1} = \text{number of plaques} \times 10 \times \frac{1}{Dilution\ Factor}$$

2.6. Phage propagation

After determining the p.f.u. mL^{-1} a phage stock and determining the necessary to obtain a semi-confluent plaque plate, further semi-confluent plaque plates were produced. Briefly, 100 µl of the appropriate phage dilution was mixed with 100 µl of mid log *E. coli* K-12 strain DM1187 optical densities (OD_{600} 0.4-0.6) cells. After incubation for 25 min at 37 °C the infection mix was added to 5 mL molten top agar (Table 2.1) 46 °C and poured onto an LB agar plate. This step was repeated 40 times.

After overnight incubation at 37°C, plaques were harvested and transferred to a sterile 50 mL tube a using sterile wire loop. The harvested material was subjected to centrifuge for 5 min at 4,284 x g. The supernatant was harvested, and was treated with a drop of chloroform (CCl_3) to destroy any bacteria and the harvested phages were stored at 4°C.

2.7. Lysogen production

A naïve culture *E. coli* K-12 strain (MC1061 or TUV93-0) was grown to mid-log phase in LB broth supplemented with 0.01 M $CaCl_2$. Then these cells were infected with phage that was determined as an MOI number which is a ratio of phage number to cell numbers, and then they were incubated for 1 h at 37°C with shaking at 200 r.p.m. Then, cells were plated on LB agar with appropriate antibiotic selective pressure and incubated overnight at 37°C.

2.8. Production of cell lysates

Colonies (3-4) of bacterial *E. coli* cells were inoculated in 10 mL LB broth with 1:1000 appropriate antibiotic selective pressure overnight at 37°C with shaking at 200 r.p.m. On the next day, overnight culture cells were added to sterilized LB broth (1:100) with (1:1000) appropriate antibiotic selective pressure at 37°C with shaking at 200 r.p.m. As the cells growth level reached optical densities OD_{600} = 0.4 – 0.6, (1:1000) 0.1 mM of protein inducer (basd on plasmid promoter *e.g.* arabinose) was added and the culture incubated for 3 h. After that, cells were harvested by centrifugation at 15,191 x g for 30 min. The supernatant was discarded, and the cell pellet was prepared for lysis or stored at -20°C. The frozen cells were suspended in 5 mL lysis buffer (50 mM NaH_2PO_4, 300 mM NaCl, 10 mM imidazole), and 50 µl protease inhibitors (Sigma-Aldrich, United States, # P8849). The cells were disrupted by sonication at 15-18 µm for 6 × 10 bursts. Following lysis, the sample was centrifuged at 20,833 x g for 30 min. Finally, the supernatant was transferred to sterilized tube.

2.9. Immobilized Ni^{+2} affinity chromatography

Recombinant proteins from cell lysates were purified using immobilized metal affinity chromatography (IMAC) techniques, using the ability of a string of histidine residues (known as a tag) to bind to immobilized Ni ions. The Ni^{+2} media was held in 5 mL polypropylene column (QIAGEN, Germany, #34964). The principle of purification

is that the Ni^{+2} binds to an agarose bead by chelation using nitroloacetic acid beads. The protein binds to the Ni^{+2} on the media 1 mL NiNTA Agarose (QIAGEN, Germany, #30210) when they were mixed overnight (Hengen, 1995) and then were poured the next day into a gravity fed polypropylene column. The target protein binds tightly to the metal ions. Other proteins were removed from the column using washing buffers from low concentrations to higher concentrations of imidazole (Table 2.1). The Recombinant Histidine tagged protein was finally eluted with 3 x 1 mL washes of a high concentration of imidazole solution (50 mM NaH_2PO_4, 300 mM NaCl, 300 mM imidazole).

2.10. Sodium dodecyl-sulfate-polyacrylamide electrophoresis (SDS-PAGE)

Sodium Dodecyl Sulfate (SDS) electrophoresis is a method used for analysing proteins. Samples were run in 4-15% Mini-PROTEIN TGX gels (Bio RAD, United States, #4561084) that contained both separating and stacking gels that allowed proteins to be separated to a high resolution. The gel was placed in the appropriate Bio Rad apparatus which was then filled with electrophoresis running buffer (1x Tris/Glycine/SDS buffer) (Bio RAD, United states, #1610772). The gels were run at 120 V for 60 min. To determine the position of proteins after electrophoresis, the SDS gels were placed in Coomassie blue stain (Table 2.1) at room temperature for 30 min with gentle agitation. The gel was destined by Coomassie blue distain solution (Table 2.1) that was refreshed every 15 min at room temperature with gentle agitation until bands were visible.

2.11. Production of rabbit anti-P21 sera

Recombinant P21 was collected by producing cell lysate *E. coli* Top10 cells carrying pBAD *P21* (2.8), and then the lysate was run in an immobilizing chromatography (2.9). Followed by the P21 recombinant was run in Sodium Dodecyl Sulfate (SDS) electrophoresis (2.10), and the piece of P21 recombinant was cut from the gel and sent to the (Gemini Biosciences Ltd, United Kingdoms). Personal contact with the company that provide the protocol of polyclonal antibody production in rabbit that was adding Freund's adjuvant to the P21 at a ratio 1:1 to immunisation. 100 µg of P21 was used per immunisation. (Table 2.4) describes the production schedule of antisera. However, the antisera was tested after the 2^{nd} and 3^{rd} antigen injections by using dot-blotting to confirm the presence of antigen specific antibody.

Table 2.4. Production schedule that was in rabbit polyclonal antibody protocol (Gemini Biosciences Ltd, United Kingdoms).

Time	Action
Week 0	Collection of pre immune or 1st bleed
Week 2	First immunisation
Week 4	Second booster of antigen
Week 6	Collection of 2nd bleed
Week 7	Third booster of antigen
Week 9	Collection of 3rd bleed

2.12. Western Blotting

Bacterial whole cell lysates and Ni-affinity purified recombinant protein sample were subjected to SDS-PAGE electrophoresis at 120 v for 60 min. One of these gels was placed in coomassie blue stain, while the other gels were soaked in transfer buffer (Table 2.1). A transfer sandwich was prepared that contained soaked filter papers and nitrocellulose membrane in transfer buffer. After the sandwich was set up, it was placed in electrophoretic transfer apparatus at 125 mA for 1 h at 4°C. As the protein transferred onto the nitrocellulose membrane which could be visualised by the prestained marker leader transfer onto the nitrocellulose membrane. The membrane was blocked using 5% Marvel overnight at 4°C with gentle agitation. On the second day, the membrane had placed in anti-P21 sera as a primary antibody solution (1: 20,000 in TBS Tween 20 (Table 2.1)) for 2 h at room temperature with gentle agitation, and one of nitrocellulose membrane was kept in 5% Marvel without adding the primary antibody as a control sample to be treated with secondary antibody only. Both membranes were then washed with TBS Tween 20 3x for 10 min. The membranes were then incubated with secondary antibody solution (Horse Radish Peroxidase [HRP] conjugated anti-Rabbit IgG (Sigma-Aldrich, United States, #RABHRP1) in 1:10,000 TBS Tween 20 for 1 h at room temperature with gentle agitation, followed by washing the membrane with TBS Tween 20 3x for 10 min. Finally, chemiluminescent detection (ECL prime western blotting detection kit [GE Healthcare, Sweden, #28980926]) was used to detect where the secondary antibody was bound. Luminol solution mL and 1 mL peroxide solution were poured onto the nitrocellulose membrane

for 1 min. Then, the membrane was drained. Finally, chemiluminescent detection film ImageQuant LAS 4000 (Healthcare).

2.13. Romaval of cross-reacting antibodies for rabbit anti-P21 sera

E. coli TOP10-pBAD was inoculated in two cultures of 100 mL LB broth with (Ampicillin 100 µg mL^{-1}) overnight at 37°C with shaking at 200 r.p.m. The next day, the cells were centrifuged at 15,191 x g for 30 min. The first bacterial pellet was suspended in 5 mL PBS and treated with 50 µl protease inhibitors (Sigma-Aldrich, United States, # P8849). The cells were disrupted by sonication (15-18 µm for 6 × -18 µm. 10 second for 6 x 10 burst). Followed by sample was centrifuged at 15,191 x g for 30 min. Finally, the supernatant was transferred to sterilized tube as a cytoplasm protein. The second bacterial pellet was washed by 100 mL PBS and the cells recovered by centrifugation at 15,191 x g for 30 minutes. Followed by very well mixed the pellet with 5 mL rabbit anti-P21 sera (2.11) that was incubated for 40 min at room temperature. Then, the second sample was centrifuged at 15,191 x g for 30 min. The 5 mL antisera supernatant was sufficient for immunoblot analysis and against the cytoplasm protein. Turning to incubate the cytoplasm protein with a nitrocellulose membrane for 15 min with gently inverted shaking at room temperature. As the cytoplasm protein transferred on nitrocellulose membrane, the nitrocellulose membrane was blocked by blocking buffer (Table 2.1) for 30 min with gently inverted shaking at room temperature. Then, washing the nitrocellulose membrane by TBS Tween 20 buffer (Table 2.1). Finally, rabbit anti-P21 sera was incubated with nitrocellulose membrane for 45 min with gently inverted shaking at room temperature. The rabbit anti-P21 sera was collected and used as a primary antibody in western blotting technique (2.12).

2.14. RNA extraction

RNeasy® Mini Kit (QIAGEN, Germany, #74106) was used to extract RNA from 200 mL bacterial cultures. First, cells were harvested by centrifugation at 15,191 x g for 30 min at 4°C. The pellets were suspended with 700 µl buffer RLT that contained 1:100 β-mercaptoethanol (Sigma-Aldrich, United States, #SHBB2632V). Then, the sample was transferred to a 2 mL safe lock tube that contained 50 mg acid washed, glass beads, (Sigma-Aldrich, United States, #G8772) to disrupt the cells in a

PowerLyzer™ 24 (MO BIO, United States) at a speed of 2000 rpm for 5 min at 23°C. After that sample was centrifuged at maximum speed for 10 sec, and the supernatant, containing the RNA, was transferred to a new tube. An equal volume of ethanol (70%) was added mixed well, and the contents were transferred to an RNeasy spin column that was centrifuged at 10,000 rpm for 15 sec. The column was washed 2x with 700 µl buffer RW1 and centrifuged at 10,000 rpm for 15 sec. Then the column was washed 3x with 500 µl of buffer RPE and centrifuged at 10,000 rpm for 15 sec. The column was placed in a new 2 mL collection tube and centrifuged at 10,000 rpm for 2 min. The sample was recovered in 30-50 µl of ddH_2O by centrifugation at 10,000 rpm for 1 min.

2.14.1. RNA clean up

RNeasy® MinElute Cleanup Kit (QIAGEN, Germany, #74204) was used to increase the quality of the RNA obtained from the extraction detailed 2.13. The collected sample of RNA was incubated with 6.2 µl DNase buffer (Invitrogen, United Kingdom, #00530339), and 1 µl turbo DNase (Invitrogen, United Kingdom, #00539292) at 37°C for 30 min. RLT buffer (350 µl) containing 1:100 β-mercaptoethanol (Sigma-Aldrich, United States, #SHBB2632V) and 250 µl 100% ethanol were then added to the sample and mixed. The mixture was transferred to a RNeasy MinElute Cleanup column and centrifuged at 10,000 rpm for 15 sec. The column was then washed with 500 µl RPE buffer and centrifuged at 10,000 rpm for 15 sec. The column was washed with 500 µl 80% ethanol and centrifuged again at 10,000 rpm for 2 min. The column was then placed in a new 2 mL collection tube and centrifuged at 10,000 rpm for 5 min. The sample was recovered in 20 µl of ddH_2O following a centrifugation step at 10,000 rpm for 1 min. RNA quantification was measured using NanoDrop spectrophotometry The RNA sample was stored at -80°C.

2.15. DNA extraction

Bacterial cells from an overnight culture (1 mL) were harvested by centrifugation at 1500 x g for 10 min. Then, using Genomic DNA to extract DNeasy Blood & Tissue Kit (Qiagen, Hilden, Germany, #163032580) 25 µl proteinase K and 200 µl AL buffer were added to lyse the cells. This mixture was incubated at 56°C for 30 min. After incubation, 200 µl of 100% ethanol was added, vortexed to mix and the solution transferred into a DNeasy Mini spin column. The column was centrifuged for 1 min at 6,000 x g. The column was placed in new 2 mL collection tube for washing steps that were done using 500 µl of AW1 buffer followed by centrifugation at 6000 x

g for 1 min, and then adding 500 µl of AW2 buffer followed by centrifugation at 17,000 x g for 3 min prior to elute DNA with 100 µl of ddH_2O. DNA quantification was done by NanoDrop spectrophotometry. DNA was stored at -20°C.

2.16. Plasmid isolation

The ISOLATE II Plasmid Mini Kit (BioLine, United States, #BIO-52057) was used to extract plasmid DNA from bacterial cultures. Overnight cultures (10 mL) of bacteria carrying plasmids of interest were harvested by centrifuging at 11,000 x g for 15 min. The pellets were resuspended in 500 µl of buffer P1 by pipetting up and down. Lysis buffer P2 (500 µl) was added to the sample and mixed gently by inverting 6 to 8 times and incubated at room temperature for 5 min. Neutralization buffer (P3, 600 µl) was added and mixed thoroughly by inverting 6 to 8 times. The sample was centrifuged at 11,000 x g for 20 min. The supernatant was loaded onto ISOLATE II Plasmid Mini Spin Column in placed within a 2 mL collection tube, and the column was centrifuged at 11,000 x g for 1 min. Washing buffer (PW1, 500 µl) was added to the column which was then centrifuged at 11,000 x g for 1 min. Followed by adding PW2 (600 µl) followed by another centrifugation step at 11,000 x g for 1 min. The silica membrane was then dried by centrifugation of the column at 11,000 x g for 2 min. The plasmid was recovered in 25 µl of ddH_2O. The plasmid was quantified by NanoDrop spectrophotometry. Plasmid DNA was stored at -20°C.

2.17. Oligonucleotides primers

Primers were designed for experimentation (Table 2.5 [Eurofine Genomic, Germany]).

2.18. Polymerase chain reaction (PCR)

PCR experiments were run in thermal cycle (labcycler, Geneflow). The thermal cycle programme was set up with an initial denaturation for 5 min at 94°C, followed by 35 cycles of denaturation at 94°C for 30 sec, the annealing temperature was optimised based on the selected primers' annealing temperature for 30 sec (Table 2.5), and an extension period at 72°C for 30 sec. The reaction was ended in final extension cycle at 72°C for 7 min. PCR product components of one reaction (50 µl) were: 20 µl of 2x BioMix Red (BioLine, United States, BIO-25006), 2 µl of 10mM Forward primer, 2 µl of 10mM Reverse primer, 2 µl DNA template, and 24 µl ddH_2O. In negative control

sample 2 µl DNA template was replaced by 2 µl ddH_2O. PCR products were separated by agarose gel electrophoresis.

2.19. Agarose gel electrophoresis

DNA samples were run by TAE agarose (Table 2.1) electrophoresis on 1% agarose gel, at 100 V for 45 min. 5 µl of DNA sample of each reaction and 3 µl of 1 kb DNA ladder (NEB, United Kingdom, #H1-819 101A) were separated on the gel. Finally, the gel image was visualised under UV transillumination at wavelength of 302 nm and the image was captured by GeneSnap software.

2.20. PCR product clean up

DNA fragments were extracted from TAE agarose gels using ISOLATE II PCR and Gel Kit (BioLine, United States, #BIO-52060). The first step was solubilisation of the gel by the addition of 200 µl Binding Buffer (CB) per 100 mg gel. This reaction was incubated at 50°C for 10 min with intermitant vortexing. This sample was then loaded onto an ISOLATE II PCR and Gel column. The column was centrifuged at 11,000 x g for 30 sec. The silica membrane was washed 2x using 700 µl CW Buffer followed by centrifugation at 11,000 x g for 30 sec. The silica membrane was then dried by centrifuging the column at 11,000 x g for 1 min. DNA was recovered in 20 µl of ddH_2O. The DNA quantification was performed by NanoDrop spectrophotometry. DNA was stored in -20°C.

2.21. Cloning

Genes were cloned by first amplifying the target by PCR (2.18). DNA of product of PCR was purified (2.20); and at the same time, a plasmid that was to be the vector for this clone was prepared (2.16) and purified (2.20). In order to get these two products to fit together the next three steps were followed: restriction enzymes digestion (2.21.1), ligation of the DNA fragment (2.21.2), and transformation of the recombinant product (2.22.3).

Table 2.5. The oligonucleotide primers that were designed in experiments

Primer	Sequence (5' – 3')	Information	T_{Aneal}
NB *P21* F	TTCGACAGCCCTGATCCAC	Forward primer to amlify 270 bp of *P21* for labelling PCR DIG probe in northern blotting (23617.. 23887)	58.8°C
NB *P21* R	TGAACCACCACGACAGCAC	Reverse primer to amlify 270 bp of *P21* for labelling PCR DIG probe in northern blotting (23617.. 23887)	58.8°C
NB *R* F	TGCGCCTGAAATCCTCGAC	Forward primer to amlify 294 bp of *R* for labelling PCR DIG probe in northern blotting (26240.. 26534)	58.8°C
NB *R* R	GGGAAACACTTACCGGGAC	Reverse primer to amlify 294 bp of *R* for labelling PCR DIG probe in northern blotting (26240.. 26534)	58.8°C
NB *S* F	TGTGTCATACACCACGTCAG	Forward primer to amlify 187 bp of *S* for labelling PCR DIG probe in northern blotting (25985.. 26172)	57.3°C
NB *S* R	TTACTCTCCCCGTGCCGCCT	Reverse primer to amlify 187 bp of *S* for labelling PCR DIG probe in northern blotting (25985.. 26172)	57.3°C
NB Rz F	GCTGCGCTCGATGCAAAATAC	Forward primer to amlify 200 bp of *Rz* for labelling PCR DIG probe in northern blotting (27886.. 28086)	60°C
NB Rz R	TAATCCCGTTCAGCGGTGTCTG	Reverse primer to amlify 200 bp of *Rz* for labelling PCR DIG probe in northern blotting (27886.. 28086)	60°C
NB $Rz1$ F	TAAGCGCCTGCGGATCAAC	Forward primer to amlify 137 bp of *Rz1* for labelling PCR DIG probe in northern blotting (27972.. 28109)	58.8°C

NB *R_{Z1}* R	TCAGCCTCTCTCTGAGGATG	Reverse primer to amlify 137 bp of *Rz1* for labelling PCR DIG probe in northern blotting (27972.. 28109)	59°C
SP 1	CTCGCGTCACTGTATGTGCC	P21 specific primer that is required to transcribe the $\phi 24_B$ mRNA into first strand cDNA (23908 .. to transcription start site of *P21*) for 5' race experiment.	60°C
SP 2	GCTGAACCACCACGACAGC	Nested primer that is located upstream of SP1 (23870 .. to transcription start site of *P21*) for 5' race experiment	60°C
SP 3	CAGCAGAATGCCCGCATTCG	Nested primer that is located upstream of SP2 (23843 .. to transcription start site of *P21*) for 5' race experiment	60°C
Start *48* F	ATGCCCGGCCATTGTGCCG	Forward primer to amlify fisrt 1200 bp of *48* from (49148.. 50348)	60°C
Start *48* R	GCCCTCCCATGGCGATACATCCA	Reverse primer to amlify fisrt 1200 bp of *48* from (49148.. 50348)	60°C
Middle *48* F	TCCGCGTCGTCAGGCTGATT	Forward primer to amlify middle 1200 bp of *48* from (52766..53966)	60°C
Middle *48* R	CCATGCCGCCACGAATTTATTCGG	Reverse primer to amlify middle 1200 bp of *48* from (52766..53966)	60°C
End *48* F	CCAGCAGGCGGCGTCTCTTG	Forward primer to amlify last 1200 bp of *48* from (56371.. 57571)	60°C
End *48* R	CCCGCTCAACCGATTTCACC	Reverse primer to amlify last 1200 bp of *48* from (56371.. 57571)	60°C

48 st qPCR F	ATGCCCGGCCATTGTGCCG	Forward primer to amlify first 200 bp of *48* from for qPCR (49148 .. 49348)	60°C
48 st qPCR R	GCGATTCGGATCAGAGAAAA	Reverse primer to amlify first 200 bp of *48* from for qPCR (49148 .. 49348)	60°C
48 en qPCR F	ACCGGTGCAGAAAGAACGG	Forward primer to amlify last 200 bp of *48* from for qPCR (57371 .. 57571)	60°C
48 en qPCR R	CCCGCTCAACCGATTTCACC	Reverse primer to amlify last 200 bp of *48* from for qPCR (57371 .. 57571)	60°C
pdxA F	GTACGGAAGAGATAGACACCAT	Forward primer of housekeeping gene for qPCR	58°C
pdxA R	GCGTTATCAAGATATTTCGGCTG	Reverse primer of housekeeping gene for qPCR	58°C

2.21.1. Restriction endonuclease digestion

The desired gene and plasmid were separately digested with matching enzymes. The restriction enzymes digestions reactions contained 2-8 units of restriction enzyme per 1 µg of gene DNA, 5 µl cut smart buffer, and ddH_2O up to 50 µl. While the reaction of plasmid restriction enzymes contained 2-8 units of restriction enzyme per 2 µg of plasmid DNA, 5 µl cut smart buffer, and ddH_2O up to 50 µl. Restriction endonuclease digestion reactions were incubated at 37°C for 60 min. The digested reactions were confirmed by gel electrophoresis (2.19), and cleaned up from the gel (2.20).

2.21.2. Ligation of DNA fragment

The molar ratio between the DNA to be cloned and the plasmid vector DNA was optimised to get a successful ligation. The total volume of the ligation reaction was 8 µl and incubated with 1 µl T4 DNA ligase (5 U/ µl) (Thermo Fisher, United Kingdom, #00800476) and 1 µl 10x T4 DNA ligase buffer (Thermo Fisher, United Kingdom, #00776968) at 4°C for 18 h.

2.21.3. Transformation

3 to 4 colonies of overnight *E. coli* Solu BL 21 strain were inoculated in 20 mL SoB broth (Table 2.1) and incubated at 37°C with shaking at 200 r.p.m until the cells reached an optical density OD_{600} = 0.4–0.6. The cells were harvested by centrifugation at 4000 x g for 10 min at 4°C, the pellet was resuspened in cooled 20 mL 1 M $CaCl_2$ and then incubated on ice for 30 min. The cells were then recovered by centrifgation at 4000 x g for 10 min at 4°C and resuspended in a final volume of 1 mL 1 M $CaCl_2$. The cells were aliquoted into 200 µl units to which 10 µl ligation of a ligation reaction was added, mixed and incubated on ice for 30 min. The sample was heat shocked at 42°C for 45 sec and sample was placed directly back on ice for 3 min. Cold SoB broth (800 µl) of was incubated with the cells and the mixture was incubated at 37°C with shaking at 200 r.p.m. for 1 h. Cells (500 µl, 250 µl, 150 µl 50 µl and 10 µl) were plated onto LB agar with appropriate selective pressure and incubated overnight at 37°C.

2.22. Sequencing analysis

The DNA samples were sequenced by (Eurofine Genomic, Germany) by the Sanger method. The concentrations of sequenced DNA were 80-100 ng/µl in plasmid DNA, 2 ng/µl in purified PCR product whose length 150-300 bp, 12 ng/µl in purified PCR product whose length 300-1000 bp, or 25 ng/µl in purified PCR product whose length 1000-3000 bp. A premix of template DNA and primer contained 5 µl of template DNA and 5 µl of primer at concentration 5pmol/5 µl. The Blast programs on the NCBI website and GenBank database (https://blast.ncbi.nlm.nih.gov/Blast.cgi) were used to confirm the identities of the products sequenced.

2.23. Statistical analysis

The statistical tests perfromed during this work are as follows. A two-way analysis of variance (ANOVA) was applied in measuring the growth impact on naïve cells and different lysogen phenotypes, comparing the binding of P21 to peptidoglycan in the presence of competitors assay, the flow cytometry experiment, and the antibiotic resistance assay, and the drug tolerance assay, the two-way ANOVA and t test used the GraphPad Prism 7 software (GraphPad Software, United States).

CHAPTER 3:

DRIVING RESEARCH QUESTION: WHAT IS THE FUNCTION OF A CONSERVED HYPOTHETICAL GENE, 21, ENCODED BY MANY STX PHAGE THAT ALWAYS LIES NEXT TO THE LYSIS CASSETTE, BUT LOOKS LIKE "*nanS*, THE GENE ENCODING N-ACETYLNEUAMINATE ESTERASE?"

3.1. Background

3.1.1. Gene 21 is located and expressed with the phage lysis gene region

The vb_24$_B$_21 gene (which encodes P21) is one of the genes that are expressed in the late gene region of the ϕ24$_B$ based on previous phage analysis studies (1.3.4.2.1) (Veses-Garcia et al., 2015a), and ϕ24$_B$ genome sequence annotation (Table 1.2) (Smith et al., 2012a). The *P21* gene is currently annotated as a hypothetical gene. It is located downstream from the *stx* operon that encodes the shiga toxin and upstream of the holin, lysozyme, and spanin proteins of the lysis cassette (*S*, *R*, *Rz* and *Rz1* genes) (Fig. 1.12) that encode proteins that puncture the bacterial cell envelope and destroy the peptidoglycan cell wall (Holt et al., 2019). P21 is expressed as part of the lysis transcript (Veses-Garcia et al., 2015a), and is presently linked to phage replication unless it is moron, meaning that it was acquired by the phage through horizontal gene transfer (Smith et al., 2012a). However, it is the most highly conserved gene across all the Stx phages (Fig. 3.1), and there is no *P21* gene homolog associated with lambda phage (Christie et al., 2012).

The size of the *P21* gene is 1938 bp, and it lies between nucleotides 23,314 and 25,252 in the prophage genome. P21 is 645 amino acids long and is comprised of three domains which are homologes to DUF1737, esterase domain, jelly roll domain (Fig. 3.2) (Franke, Veses-Garcia et al. 2020). The first domain is comprised of DUF1737 which is an unknown function domain set in N- terminus of viral and bacterial hypothetical proteins (https://pfam.xfam.org/family/PF08410), located between amino acid 1 to 72, the second domain is an esterase domain which is homolog of NanS (PDB code 3PT5), located between amino acid 73 to 392, and the third domain is a jelly roll domain in C- terminus which located between amino acid 423 to 640 which

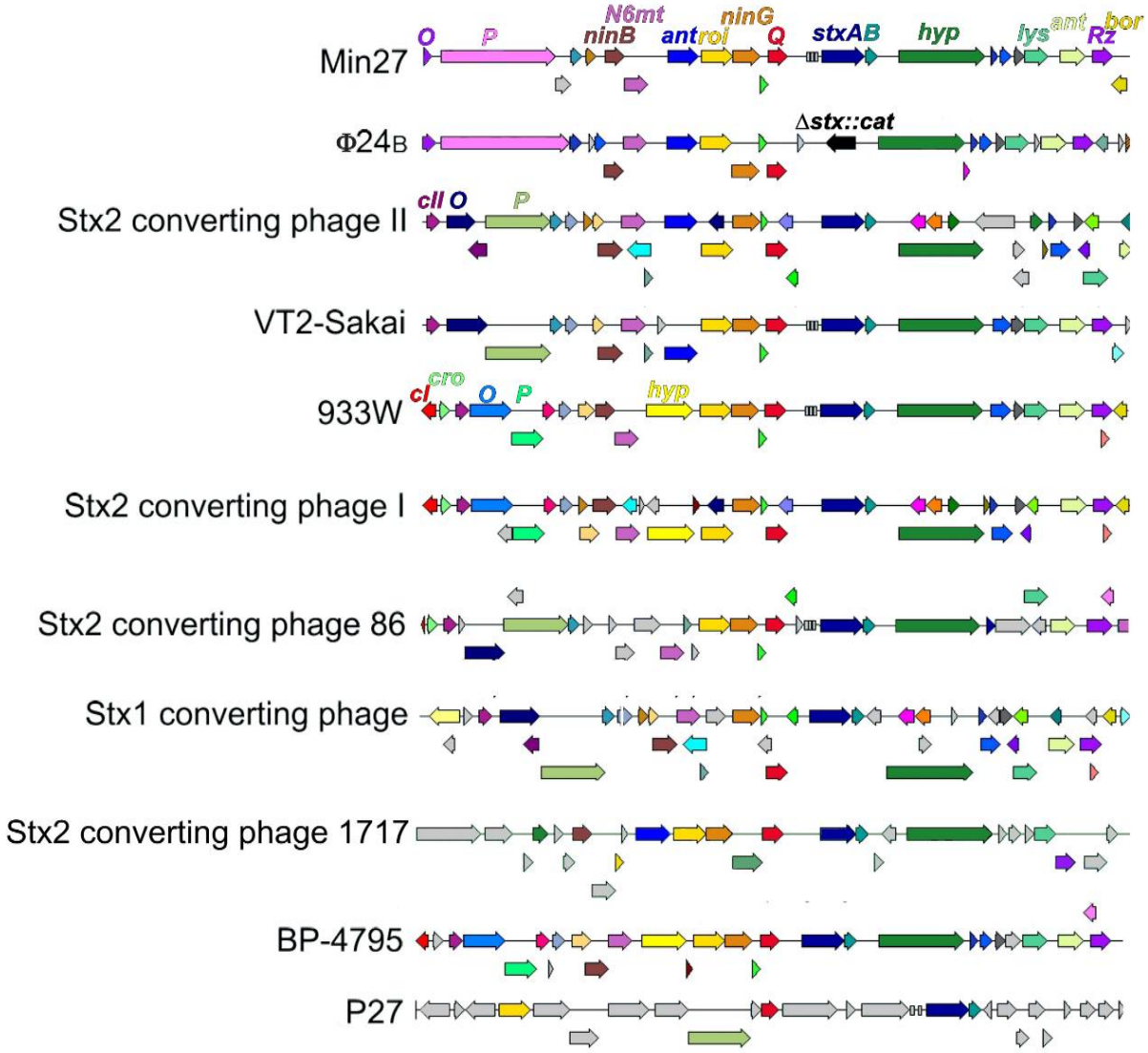

Figure 3. 1. Stx phage comparisons in the RAST annotation server.

This comparison asked what the most conserved gene was across the Stx phage genomes shown. The gene annotations can be found above their respective gene in the upper most line in the maps above where they first appear. The hypothetical gene *P21* from $\phi 24_B$ is indicated in dark green arrow is the most highly conserved gene across all the Stx phages. The light green arrows refer to lysis gene (*R* gene), the purple arrows refer to *Rz* gene that encodes spanin, the dark blue arrows refer to *stxA*, and the grey arrows *stxB*. In $\phi 24_B$ the stx_2AB in black arrow had replaced through allelic exchange chloramphenicol (cat) resistance gene from pLysS *(Smith et al., 2012b)*. Figure was taken from (Christie et al., 2012)

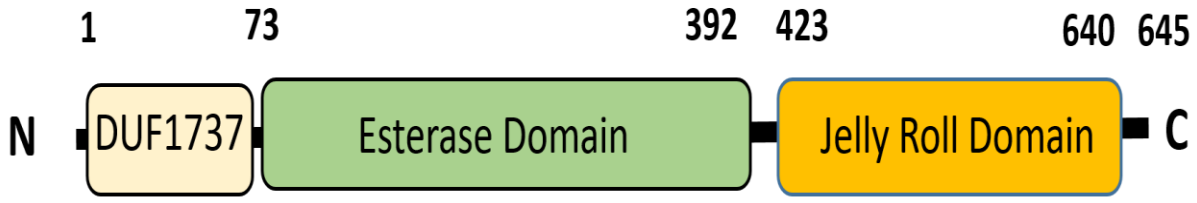

Figure 3. 2. Domain's structure of P21.

645 amino acids of P21 sequence displays three domains: the first domain is DUF1737 located at the N-terminus from residues 1 to 72, the second domain is an Esterase domain from residues 73 to 392, and the third domain is a jelly roll domain in C- terminus that from residues 423 to 640.

has undergone X-ray crystallographic analysis, its structure interpreted and it appears to be a carbohydrate binding domain (Fig. 3.2) (Franke et al., 2020a).

3.1.2. Gene homology within the *E. coil* chromosome

Homologs to *P21* found in $\phi 24_B$ have been called NanS-p (933Wp42) (Nübling et al., 2014) in the phage 933W. NanS-p denotes that is a phage encoded derivative the chromosomally encoded *nanS* (N-acetylneuraminate esterase), which is a much *E. coli* smaller protein.The chromosomal *nanS* gene is a highly homologous to the genome of open reading frames (ORFs) prophage in *E.coli* O157:H7 strain EDL933 (Saile et al., 2018a). The *nanS* is located between the antiterminator Q and upstream of the lysis genes in *E. coli* O157:H7, the *nanS* gene also is part of nanCMS operon (Rangarajan et al., 2011, Steenbergen et al., 2009) which encoded esterase that is involved in monodeacetylation of 5-*N*-acetyl-9-*O*-acetyl neuraminic acid (Saile et al., 2018a). The function of encoded Nans is cleaving acetyl residues of bovine submaxillary gland mucin and 5-N-acetyl-9-O-acetyl neuraminic acid (Neu5,9Ac2), as a result of cleaving, Neu5,9Ac2 is metabolized to N-acetyl neuraminic acid (Neu5Ac) (Nübling et al., 2014, Saile et al., 2016a). The bacterial host cell is up taken the N-acetyl neuraminic acid for utilizing sialic acid as energy source (Saile et al., 2018a).

The structure of the esterase domain was found to be partially homologuos to the endogenous NanS esterase of *E. coli* (57% seq. id., 68% conservation). Because the result of high conservation, the structural features of NanS is calculated as a homology model for the esterase domain of P21 (Fig. 3.3A) (Franke et al., 2020a). The Carbohydrate-Active Enzyme (CAZy) database (http://www.cazy.org) classify carbohydrate esterase enzymes in 16 defined families. Although, NanS recently ranks in a non-classified group of this data base, NanS shares homologies with the overall structure of SNGH carbohydrates esterase, but lacks the typical catalytic region (Rangarajan et al., 2011). The SGNH fold which is found in the three-dimensional structure of this carbohydrate esterase family, has four important residues (Gly and Asn residues that cause the oxyanion hole and catalytic Ser, His residues) (Mølgaard et al., 2000).

(Rangarajan et al., 2011) differentiated between two esterase groups they termed “the canonical group I”, and an “atypical group II” in which NanS falls. The four typical motifs in group I are: 1) a GDS motif that is responsible for hosting the catalytic Ser to act as nucleophile as well as proton donor to the oxyanion hole. 2) a conserved

Gly that is responsible for contributing the oxyanion hole. 3) a GXN in some asparagine forms in oxyanion hole. 4) a DXXH including the two remaining catalytic residues of the triad, an aspartic acid and a histidine. The Ser-His catalytic dyad results in the absence of aspartate (Lo et al., 2003, Nakamura et al., 2017). While for NanS in the atypical group II, there is a large GQSN motif that carries the catalytic Ser and an adjacent glutamine that participates in the oxyanion hole. The asparagine is replaced in the canonical GXN (motif 3) with a longer motif QGEXD, which stabilises the orientation of the glutamine in the GQSN motif. However, the aspartate in the DXXH (motif 4 of group 1) is absent and only the histidine residue of the motif presents in NanS that results a Ser-His catalytic dyad (Franke et al., 2020a). It can see that in P21 from $\phi 24_B$ (Fig. 3.3) atypical structure of NanS is strictly conserved for the oxyanion hole and the Ser-His catalytic dyad. As a result, P21 in $\Phi 24_B$ has been classified as an atypical deacetyl esterase of type II (Franke et al., 2020a).

3.1.3. Hypothesis for P21 mode of action

The hypothesis is based on genome context, structure functional study and expression of *P21*. Many papers propose that P21 is involved in mucin metabolism, like the chromosomal *nanS* gene (Saile et al., 2018b, Saile et al., 2016b). The homology of *P21* gene show possesses an esterase domain which is annotated and featured as a NanS esterase of *E. coli* (3.1.2). However, The protein P21 has been shown *in vitro* to be capable of deacetylating several compounds: 4-methylumbelliferyl-acetate (4-MUFAc); triacetin; synthetic mono-, di-, and tri-O-acetylated derivatives of Neu5Ac and N glycolylneuraminic acid; and 5-N-acetyl-9-O-acetyl neuraminic acid (Neu5,9Ac2; the most abundant neuraminic acid derivative in humans) (Saile et al., 2016a, Nübling et al., 2014). The gene encoding P21 is located immediately upstream of the genes that involved in hydrolysis the peptidoglycan of host cell (Fig. 3.4) which is involved in releasing newly assembled phages and is only expressed in the lysis cassette during the lytic replication cycle, but by the prophage (Veses-Garcia et al., 2015a).

The lysis cassette genes (*S*, *R*, *Rz* and *Rz1*) that are expressed in lysis transcript, involved in lysis bacterial cell envelope that includes the inner membrane, peptidoglycan cell wall, and lipopolysaccharide (LPS) outer membrane. The lysis starts when *S* gene encodes protein called holin that form a micron scale holes in inner membrane (Young, 2013, Young et al., 2000). As a result, these huge nonspecific

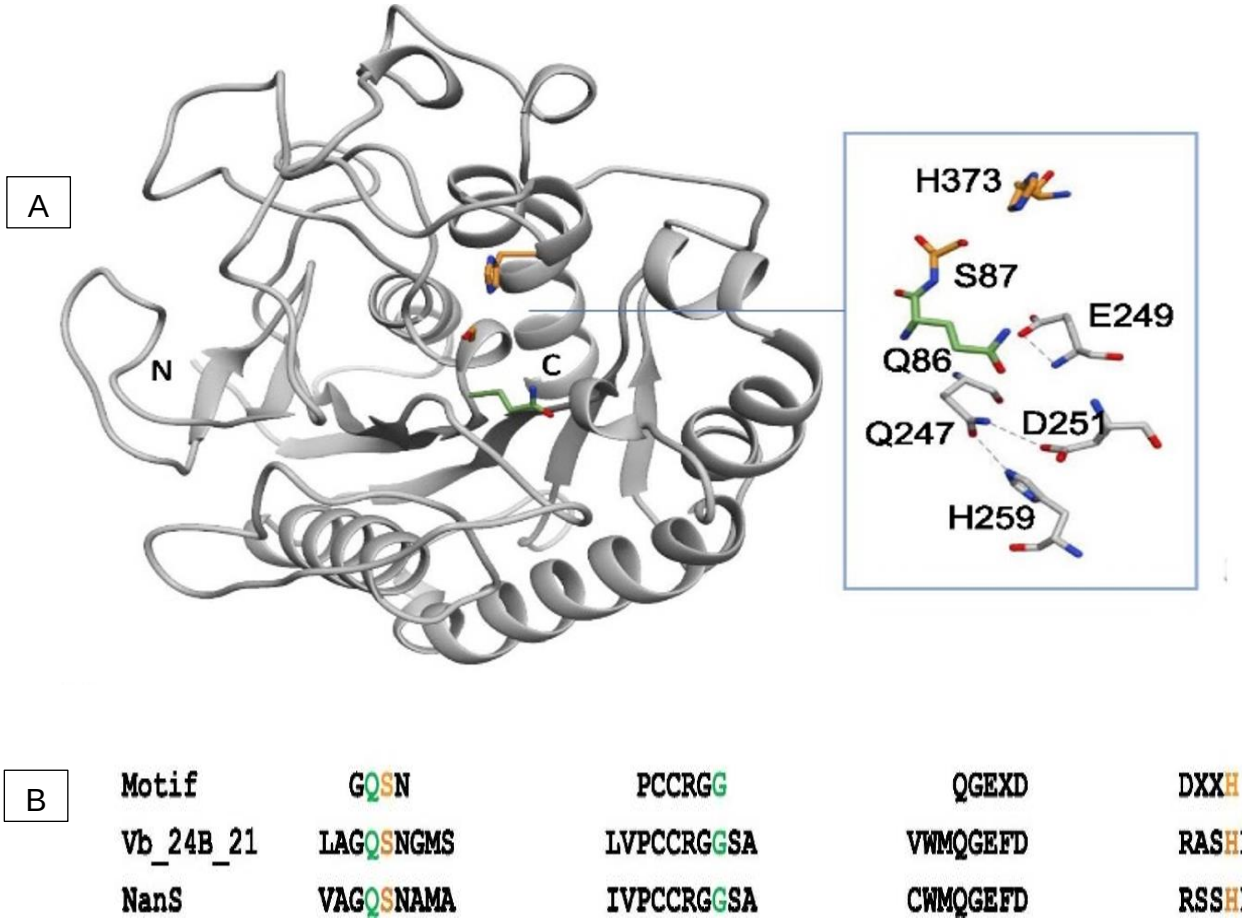

Figure 3. 3. The three dimensional structural homology model of the P21 esterase domain from $\Phi 24_B$ and the defined functional motifs.

Panel A) Inset to the right highlights the residues that in NanS form the atypical **oxyanion hole, and the catalytic dyad.** The ribbon structure provides the structure of the esterase domain of P21 from $\Phi 24_B$.

Panle B) The four motifs from P21 of $\Phi 24_B$ and NanS from the *E. coli* chromosome aligned under the motifs of the canonical Group I esterases. In the DXXH motif only the histidine in NanS are conserved. Figure was taken from (Franke et al., 2020a).

holes permit the endolysin that is encoded from *R* gene to move from cytoplasm to periplasm for attacking the peptidoglycan (Young et al., 2000). The spanin genes *Rz* and *Rz1* encode subunits of complex which join the inner membrane and outer membrane by forming a complex of a heterotetramer formed by C-terminal interaction of the periplasmic domain (Berry et al., 2013, Cahill et al., 2017). Resulting in destruction of peptidoglycan by endolysin, as a result, the killing of the bacterial host cell and liberation of the progeny phage (Berry et al., 2013, Cahill et al., 2017).

The hypothesis is testing if *P21* may have an impact on lytic phage replication by increasing the phage releasing as lysis cassette genes function that encodes proteins for hydrolysis or it may benefit the host cell by removing of ester based chemical modification in peptidoglycan in acting de-O-acylation or de-N-acylation which helps the host cell for growth and re-biosynthesis its peptidoglycan, so effecting on number of phage releasing and viral genome replication.

3.1.4. Aims

A detoxified variant of $\phi 24_B$, $\phi 24_B$::Kan, in which the *stx* operon has been replaced through allelic exchange with a gene conferring resistance to kanamycin, was further mutated by exchanging the gene encoding P21 with a gene that confers resistance to tetracycline from pBR322 to produce the recombinant phage $\phi 24_B$::KanΔP21::Tet (this phage was created previously by Marta Veses-Garcia (personal communication Dr. H.E. Allison). Previous work has already identified that the gene encoding P21 is directly linked to the expression of the lysis-associated genes *S*, *R*, *Rz* and *Rz1* (Veses-Garcia et al., 2015a). In this chapter, we aimed to:

1. Determine if P21 has an impact on plaque formation
2. Determine if ths impact on plaque formation is due to the impact on phage replication of on phage release
3. Confirm that *P21* is part of the lysis cassette
4. Try to identify where P21 is located in the cell

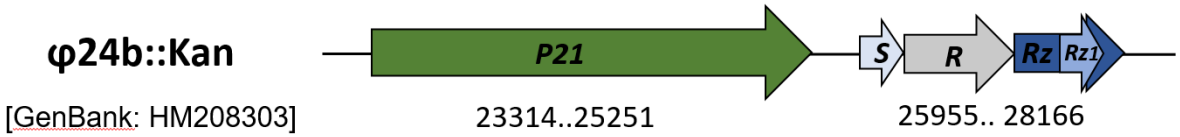

Figure 3. 4. *P21* location at the genetic construct of ϕ24$_B$

P21 gene in green arrow is located upstream of the genes that are repsponsible to break down the peptidoglycan of host cell which are *s* gene in light grey arrow that endoces holin, *R* in dark grey arrow that encodes endolysin, and spanin genes *Rz* in dark blue arrow, and Rz1 in light blue arrow.

3.2. Specific Methods

3.2.1. Lysogen creation

To produce the required lysogens naïve cultures of *E. coli* K-12 strain MC1061 or *E. coli* O157:H7 strain TUV93-0 were grown to mid-log phase (Optical Densities $O.D._{600}$ = 0.4 - 0.6) in LB broth with 0.01 M $CaCl_2$. These cells were singly infected with each phages (Table 3.1), and lysogens were screened for on appropriate selective LB agar plates (Table 3.2).

Table 3.1. The titres of $\phi 24_B$::Kan and $\phi 24_B$::KanΔP21::Tet induced from the MC1061 lysogens.

Phage	Titre in p.f.u. mL^{-1}
$\phi 24_B$::Kan	2.1×10^8
$\phi 24_B$::KanΔP21::Tet	2.3×10^8

Table 3.2. Infections used to produce *E. coli* lysogens.

Bacterial cell (~ 1 x 10^7)	Number of phages	Selective media
MC1061	$\phi 24_B$::Kan -2.1×10^8 p.f.u	LB + Kan (50 μg m^{-1})
MC1061	$\phi 24_B$::KanΔP21::Tet -2.3×10^8 p.f.u	LB + Kan (50 μg ml^{-1}) + Tet (10 μg ml^{-1})
TUV93-0	$\phi 24_B$::Kan -2.1×10^8 p.f.u	LB + Kan (50 μg ml^{-1})
TUV93-0	$\phi 24_B$::KanΔP21::Tet -2.3×10^8 p.f.u	LB + Kan (50 μg ml^{-1}) + Tet (10 μg ml^{-1})

3.2.2. One-step growth curve with and without cell lysis

The experiment compared and assayed four lysogens types. The wild type lysogens, those carrying the *P21* gene were MC1061/ $\phi 24_B$::Kan and TUV93-0/ $\phi 24_B$::Kan, while the mutant lysogens lacking *P21* were MC1061/ $\phi 24_B$::KanΔP21::Tet and TUV93-0/ $\phi 24_B$::KanΔP21::Tet. 3 to 4 colonies of each strain were inoculated in different 10 mL LB broth cultures under antibiotic selective pressure overnight at 37°C with shaking at 200 r.p.m. On the next day, 100 µl of each overnight cultures were inoculated into fresh 10 mL sterile LB broth with 0.01M $CaCl_2$ with appropriate antibiotic selective pressure. These subcultures were incubated at 37°C with shaking at 200 r.p.m until the cells reached an optical densities OD_{600} 0.4 – 0.6 (Mid-log phase).

Then, the lysogens were induced by adding the SOS inducing antibiotic norfloxacin (1 µg mL^{-1}) for a further 1 h. Next,1 mL of these induced cells, were added to 100 mL LB with 0.01M $CaCl_2$. Samples from all four cultures were taken every 20 min for 8 h and serially diluted from 10^{-3} to 10^{-6} to determine both the c.f.u mL^{-1} and p.f.u mL^{-1}. Samples (2x) were treated with one drop of chloroform to lyse the cells in the sample, and 2 were untreated. To determine c.f.u. mL^{-1}, a sample (20 µl) from every serial dilution was dropped onto the surface of an LB agar plate (with appropriate antibiotics). The plates were incubated for overnight at 37°C. To determine p.f.u mL^{-1}, 100 µl of every appropriate phage dilution from 10^{-3} to 10^{-6} was mixed with a 100 µl of mid log *E. coli* strain $DM1187^{Rif}$ (OD_{600} 0.4-0.6) cells. Followed by adding the infection mix to 5 mL molten top agar (46 °C) containing rifampicin (300µg mL^{-1}), which was poured onto LB agar plate and incubated for overnight at 37°C.

3.2.3. P21 immunolabeling fluorescence

Naïve MC1061 cells and $\phi 24_B$::Kan/MC1061 lysogen cells were cultured in separate 10 mL LB broth cultures under antibiotic selective pressure overnight at 37°C with shaking at 200 r.p.m. On the next day, 100 µl of each overnight cultures were inoculated into fresh 10 mL sterile LB broth with 0.01M $CaCl_2$ with appropriate antibiotic selective pressure. These subcultures were incubated at 37°C with shaking at 200 r.p.m until the cells reached an optical densities OD_{600} 0.4 – 0.6 (Mid-log phase). Then, the lysogens were induced by adding the SOS inducing antibiotic norfloxacin (1 µg mL^{-1}) for a further 1 h. Next,1 mL of these induced cells, were added to 100 mL LB with 0.01M $CaCl_2$, and the subculture was incubated for 260 min, which was the time of point in which the $\phi 24_B$::Kan/MC1061l ysogen has been repeatedly shown to release the fewest number of phages upon induction when compared to the P21 mutant or direct Choloform (CCl_3) lysis. The cells were were then fixed in 2.8% formaldehyde and 0.04% glutaraldehyde by incubating 12.2 mL of cell culture with 1 mL 37% formaldehyde and 21 µl 25% glutaraldehyde for 15 min at room temperature. The cells were recovered by centrifugation at 4000 x g for 10 min, and then washed in an equal volume PBS followed by centrifugation again at 4000 x g for 10 min. The cells were resuspended two times in 150 µl PBS and each time recovered by centrifugation at 4500 x g for 5 min. Then, the cells were incubated for 45 min in 15 µl Triton X-100 with 135 µl PBS and then were centrifuged at 4500 x g for 5 min that

were followed by washing three times in 150 µl PBS with centrifuging at 4500 x g for 5 min. After that, the cells were incubated in 150 µl PBS that contained 100 µg/mL lysozyme and 5 mM EDTA for 45 min at room temperature, followed by washing three times in 150 µl PBS and recovered by centrifugation at 4500 x g for 5 min. Non-specific binding sites were blocked by incubating the cells in 150 µl blocking buffer (Table 2.1) for 30 min at 37°C with shaking at 200 r.p.m. Then, the cells were washed three times in 150 µl PBS and 0.05% Tween 20. The cells were then placed in anti-P21 sera (2.11) as a primary antibody solution (1: 10 diluted in TBS Tween 20 (Table 2.1)) for 2 hours at 37°C with gentle agitation. Then, the cells were washed three times in 150 µl PBS and 0.05% Tween 20. Cells had incubated with secondary antibody solution (Goat Anti-Rabbit IgG (H+L) Secondary antibody, FITC) (Invitrogen, United Kingdom, #31579) (1: 600 diluted in TBS Tween 20) for 1 h at 37°C with gentle agitation. Followed by cells washing with 150 µl PBS and 0.05% Tween 20 and centrifuging at 4500 x g for 5 min. Then, the cells were washed once in only 150 µl PBS with centrifuging at 4500 x g for 5 min. Finally, the cells were resuspened in 100 µl PBS. Samples were examined under the fluorescent microscope.

3.2.4. Northern Blot Analysis

Total RNA was extracted from induced lysogen MC1061/ ϕ24_B::Kan. The bacterial lysogen was induced as described in section 2.3 and total RNA was extracted and cleaned as described in section (2.14), and (2.14.1), respectively.

3.2.4.1. RNA separation by denaturing gel

The RNA molecules were separated by size on a denaturing agarose gel (Table 2.1), which was poured in a fume cupboard until solidified. The gel was immersed in running buffer (1x MOPS buffer, and 7% formaldehyde). The induced MC1061/ ϕ24_B::Kan lysogen RNA sample (15 µg) was mixed with equal volume of 2x NorthernMax™ Formaldehyde loading Dye (Thermo Fisher, United Kingdom, #AM8552). Millennium™ RNA Markers (3 µg) (Thermo Fisher, United Kingdom, #AM7150) were diluted in the same volume of 2x NorthernMax™ Formaldehyde loading dye as the lysogen RNA sample. The two samples were denatured at 65°C for 15 min, loaded into separate wells in the gel and subjected to electrophoresis at 125 V for 75 min.

3.2.4.2. Transfer of RNA to nylon membrane

The separated RNA samples were transferred to a positively charge nylon membrane (Roche, Switzerland, #11 209 272 001), which was soaked in 20x SCC buffer (Table 2.1) along with required filter papers. The northern blotting sandwich order was as follows: 1) a wet piece of filter paper was placed on a glass stand that also acted as a wick, 2) the denaturing RNA gel, 3) the Nylon membrane, 4) a wet piece of filter paper, 5) dry pieces of filter paper, 6) a stack of paper towels were put above of the northern blotting sandwich, 7) a glass plate was balanced upon which a weight (200-500 g) was placed. This blotting process ran overnight. On the second day, the RNA samples were fixed to the membrane by UV cross linker (CL-1000 UV-crosslinker) which was set up at 360,000 $\mu J/cm^2$. After that, the membrane was kept wet in 2x SSC unitil the hybridization step.

3.2.4.3. Probe labelling

The forward and reverse primers of genes (*P21*, *S*, *R*, *Rz*, and *Rz1*) to be probed were designed (Table 2.5) and used to create DIG-labelledprobes via the PCR DIG Probe Synthesis Kit (Roche, Switzerland, #11 636 090 910). The reactions utilised: 5 µl PCR buffer with $MgCl_2$, 5 µl PCR DIG probe synthesis mix, 5 µl of 10 mM Forward primer, 5 µl of 10 mM Reverse primer, enzyme mix 0.75 µl, 5 µl of $\phi 24_B$ DNA, made up to a total of 50 µl with ddH_2O. The unlabelled control probe reaction contained: 5 µl PCR buffer with $MgCl_2$, 5 µl dNTP stock solution, 5 µl of 10 mM Forward primer, 5 µl of 10 mM Reverse primer, enzyme mix 0.75 µl, 5 µl of $\phi 24_B$ DNA, and ddH_2O was added up to 50 µl. The samples were run on the PCR thermal cycle (2.18), and 5 µl of every sample was analysed by agarose gel electrophoresis (2.19) to confirm the amplification.

3.2.4.4. Hybridization and washing the membrane

The wet nylon membrane was placed in a sterilised glass hybridisation tube (Stuart, #SI30H). DIG Easy Hyb Hybridization buffer (5 mL) was added (Roche, Switzerland, #11 796 895 001) and the tube containing the membrane tube was placed in the hybridization oven at 68°C for 60 min. After that, the DIG Easy Hyb Hybridization buffer was discarded. Fresh DIG Easy Hyb Hybridization buffer (5 mL) was added to the tube along with 5 µl of one of the PCR DIG probe synthesis mixes that had been

denatured by heating to 95°C for 15 min. The glass tube and membrane were placed back into hybridization oven for the probes to hybridize overnight at 42°C. The next day the hybridization buffer was discarded and the membrane was washed 2x in the glass tube at room temperature on a roller mixer in 10 mL wash buffer 1 (2X SSC with 0.1% SDS) for 5 min, and then the membrane was washed 2x in 10 mL wash buffer 2 (0.1X SSC with 0.1% SDS) for 15 min. In order to detect the Dig-labelled probe, the blot was then prepared using the DIG Wash and Block Buffer kit (Roche, Switzerland, #11 585 762 001). The membrane was washed using 10 mL washing buffer according to the manufacturer's instructions for 5 min, and then the membrane was blocked using 5 mL of the manufacturer's bespoke 1% blocking buffer for 30 min at room temperature on a roller mixer. The blocking buffer was discarded, and the membrane was incubated for 30 min at room temperature on a roller mixer with 5 mL anti-Dig Antibody solution (Anti digoxigenin-AP conjugate, Fab frag (Roche, Switzerland, # 11 093 274 910) diluted 1:10000 in 1% blocking buffer. This solution was then discarded, and the membrane was washed in 1 mL washing buffer (as per Instructions in the kit) 2x for 15 min. Then, the membrane was incubated with 5 mL of the detection buffer at room temperature on the roller mixer.

3.2.4.5. Exposing and analysing the northern blot

The excess of liquid nylon was drained from the membrane, which was then covered with drops of CDP-Star™ substrate (Roche, Switzerland, # 12 041 677 001). The membrane was incubated for 5 min in the dark. After that, the membrane was drained and placed in a plastic bag. Chemiluminescent Detection Film ImageQuant LAS 4000 (Healthcare) was exposed to the membrane in the dark.

3.2.5. LIVE/DEAD® BacLight™ Bacterial Viability

Various strains (3 to 4 colonies of each strain tested) were inoculated in different vials of LB broth (10 mL) under appropriate antibiotic selective pressure overnight at 37°C with shaking at 200 r.p.m. On the next day, 100 µl of each overnight culture was used to inoculate 10 mL of sterile LB broth containing 0.01 M $CaCl_2$ and appropriate antibiotic selective pressure. These subcultures were incubated at 37°C with shaking at 200 r.p.m until the cells reached an optical densities OD_{600} = 0.4 – 0.6. The lysogens were then induced by adding the SOS inducing antibiotic norfloxacin (1 µg mL^{-1}) and the cultures incubated for a further 1 h. The induced cells (4 mL) of were then subcultured into 400 mL sterile LB broth with 0.01M $CaCl_2$. These subcultures

were incubated at 37°C with shaking at 200 r.p.m and sampled at indicated times post induction (Table. 3.3). The cells from the subcultures were harvested by centrifugation at 10,000 x g for 10 min in 4°C. The cells were resuspended in 2 mL 0.85% NaCl washing buffer. Then, the cells were diluted 1:20 in 0.85% NaCl and incubated at room temperature for 1 h whilst being mixed every 15 min. The cells were then recovered by centrifugation at 10,000 x g for 10 min at 4°C and the cells resuspend in 20 mL 0.85% NaCl. In the bacterial staining step, LIVE/DEAD® BacLight™ kit (Thermo Fisher, United Kingdom, #L7012) stains which were used, were SYTO® 9 and propidium iodide were combined in similar volumes. The dye mixture (3 µl) was added to 1 mL of the cell suspension that was incubated at room temperature in the dark for 15 min. Samples were examined under the fluorescent microscope.

Table. 3.3. The type of wild type and mutant lysogenic cultures that were collected for LIVE/DEAD® BacLight™ bacterial viability experiment.

Lysogen culture	Time point
MC1061/ ϕ24$_B$::Kan	180 min
MC1061/ ϕ24 $_B$::KanΔP21::Tet	180 min
MC1061/ ϕ24$_B$::Kan	240 min
MC1061/ ϕ24 $_B$::KanΔP21::Tet	240 min
MC1061/ ϕ24$_B$::Kan	300 min
MC1061/ ϕ24 $_B$::KanΔP21::Tet	300 min
TUV93-0/ ϕ24 $_B$::Kan	180 min
TUV93-0/ ϕ24 $_B$::KanΔP21::Tet	180 min
TUV93-0/ ϕ24 $_B$::Kan	240 min
TUV93-0/ ϕ24 $_B$::KanΔP21::Tet	240 min
TUV93-0/ ϕ24 $_B$::Kan	300 min
TUV93-0/ ϕ24 $_B$::KanΔP21::Tet	300 min

3.2.6. Fluorescence activated cell sorting (FACS)

There were two dyes that were used to stain the lysogen cells in this experiment: 1) SYBR™ Green I (ThermoFisher, United Kingdom, #S7563), which is highly sensitive and detects double-strand DNA; 2) carbocyanine dye 3,3'-dipropylthiadicarbocyanine iodide ($DiSC_3$ (5)) (ThermoFisher, United Kingdom,

#D306), a positively charged dye which accumulates on hyperpolarized membranes and is translocated across the lipid layers of gram positive and gram negative bacteria (Jindal et al., 2019).

Table. 3.4. The wild type and mutant lysogenic cultures examined by FACS.

Lysogenic culture	Time point
MC1061/ ϕ24$_B$::Kan	0 min
MC1061/ ϕ24 $_B$::KanΔP21::Tet	0 min
MC1061/ ϕ24$_B$::Kan	180 min
MC1061/ ϕ24 $_B$::KanΔP21::Tet	180 min
MC1061/ ϕ24$_B$::Kan	240 min
MC1061/ ϕ24 $_B$::KanΔP21::Tet	240 min

Every strain examined was used (3 to 4 colonies) to inoculate 10 mL LB broth under appropriate antibiotic selective pressure and cultured overnight at 37°C with shaking at 200 r.p.m. On the next day, 100 µl of each overnight culture was used to inoculate 10 mL sterile LB broth containing 0.01 M CaCl2 under appropriate antibiotic selective pressure. These subcultures were incubated at 37°C with shaking at 200 r.p.m until the cells reached an optical densities OD600 = 0.4 – 0.6. The lysogens were induced by adding the SOS inducing antibiotic Norfloxacin (1 µg mL-1) and incubated for a further 1 h. Then 4 mL of each induction was used to inoculate 400 mL sterile LB broth containing 0.01 M CaCl2. These subcultures were incubated at 37°C with shaking at 200 r.p.m until the determined time point (Table. 3.4). The lysogens were diluted in fresh LB at optical densities OD6oo = 0.001, and then 100 µl of each sample was transferred to a separate well in a 96-well plate and mixed with a final concentration of 3 µM SYBRTM Green I dye and 3 µM DiSC3 (5) stain. The 96-well plate was incubated in the dark at 37°C for 15 min. The samples were run in an iQue screener PLUS which had 3 excitation sources (405 nm, 488 nm, and 640 nm), and 7 fixed filter detectors with a midpoint in nm of (445/45, 530/30, 572/28, 585/40, 615/24, 675/30, and 780/60) that gave 13 fluorescence channels. The 488 nm excitation source obtained forward and side scatter, while the laser that was used (405 nm violet [VL], 488 nm blue [BL], and 640 nm red [RL]) referred to the detection channels (Jindal et al, 2019). In this experiment RL1 was set to detect DiSC3 (5), which programmed on the red laser and detected on 675/30 nm; BL1 was set to detect SYBRTM Green I,

which programmed on the blue laser and detected on 488/30 nm. The iQue Forecyt® Offline Analysis Edition 8.1 software, which was provided with the instruments, was used to analyse, and create visual outputs of the data.

3.2.7. 5’ race experiment

5’ race experiments were run to determine the locations of transcription start sites (TSS). The 5’/ 3’ RACE Kit, 2nd Generation (Roche, Switzerland, #03 353 621 001) was used in this experiment. There were 4 steps to the 5’ race experiment: 1) first strand cDNA synthesis, 2) degradation of the mRNA template, 3) tailing of first strand cDNA, and 4) amplification of the tailed cDNA (Fig. 3.5). The primers (SP1, SP2, and

SP3) were designed from three region of *P21* sequence (Table. 2.5) to use in this experiment.

3.2.7.1. First strand cDNA synthesis

The RNA sample which was used in first strand cDNA synthesis, was extracted from the lysogen MC1061/ $\phi 24_B$::Kan (3.2.3.1). The first strand cDNA synthesis reaction contained 4 µl cDNA synthesis buffer, 2 µl deoxynucleotide mixture, 1 µl cDNA synthesis primer (12.5 µM) SP1 (Table 2.5), 1 µl transcriptor reverse transcriptase (Roche, Switzerland, #03 531 317 001), 2 µg of $\phi 24_B$ RNA, and ddH_2O up to 20 µl. The reaction was incubated at 55°C for 60 min, after that the enzyme was inactivated by holding the sample at 85°C for 5 min.

3.2.7.2. Degradation of the mRNA template

High Pure PCR Product Purification Kit (Roche, Switzerland, #11 732 668 001) was used to degrade the mRNA template using the RNase activity of transcriptor reverse trancriptase. The 20 µl of first strand cDNA reaction was mixed with 100 µl binding buffer, and then the reaction mixer was added to the high pure filter tube and the collection tube. Following centrifugation at 8,000 x g for 30 sec, the column was washed with 500 µl washing buffer, centrifuged at 8,000 x g for 30 sec washed with 200 µl washing buffer, centrifuged at 13,000 x g for 2 min, and cDNA was recovered from the column in 20 µl of ddH_2O.

3.2.7.3. Tailing of first strand cDNA

A homopolymeric A-tail was added to the 3’ end of the first strand of cDNA using recombinant terminal transferase in the presence of dATP. The reaction

comprised of 19 µl purified cDNA, 2.5 µl 10 x reaction buffer, and 2.5 µl 2 mM dATP. The constituents were incubated at 94°C for 3 min, and then chilled on ice. Following this step, 1 µl terminal transferase was added and the reaction was mixed and incubated at 37°C for 30 min. The enzyme was then inactivated at 70°C for 10 min. The polydA-tailed cDNA was run in PCR reaction that contained 20 µl of 2x BioMix Red buffer (BioLine, United States, BIO-25006), 5 µl polydA-tailed cDNA, 2 µl Oligo dt-Anchor primer, (12.5 µM) 2 µl SP2 primer (Table 2.5), and ddH_2O up to 50 µl. The thermal cycles of PCR are described in (2.17). The PCR product was run in an agarose gel (2.18), and the PCR product was recovered (2.19).

3.2.7.4. Amplification of the tailed cDNA

The tailed cDNA was amplified in a PCR reaction that contained 20 µl of 2x BioMix Red buffer (BioLine, United States, BIO-25006), 2 µl cleaned up PCR production, 2 µl PCR anchor primer, 2 µl (12.5 µM) SP3 primer (Table 2.5), and ddH_2O up to 50 µl. The thermal cycles of PCR described in 2.17. The PCR product was run in an agarose gel (2.18), and the PCR product was recovered (2.19).

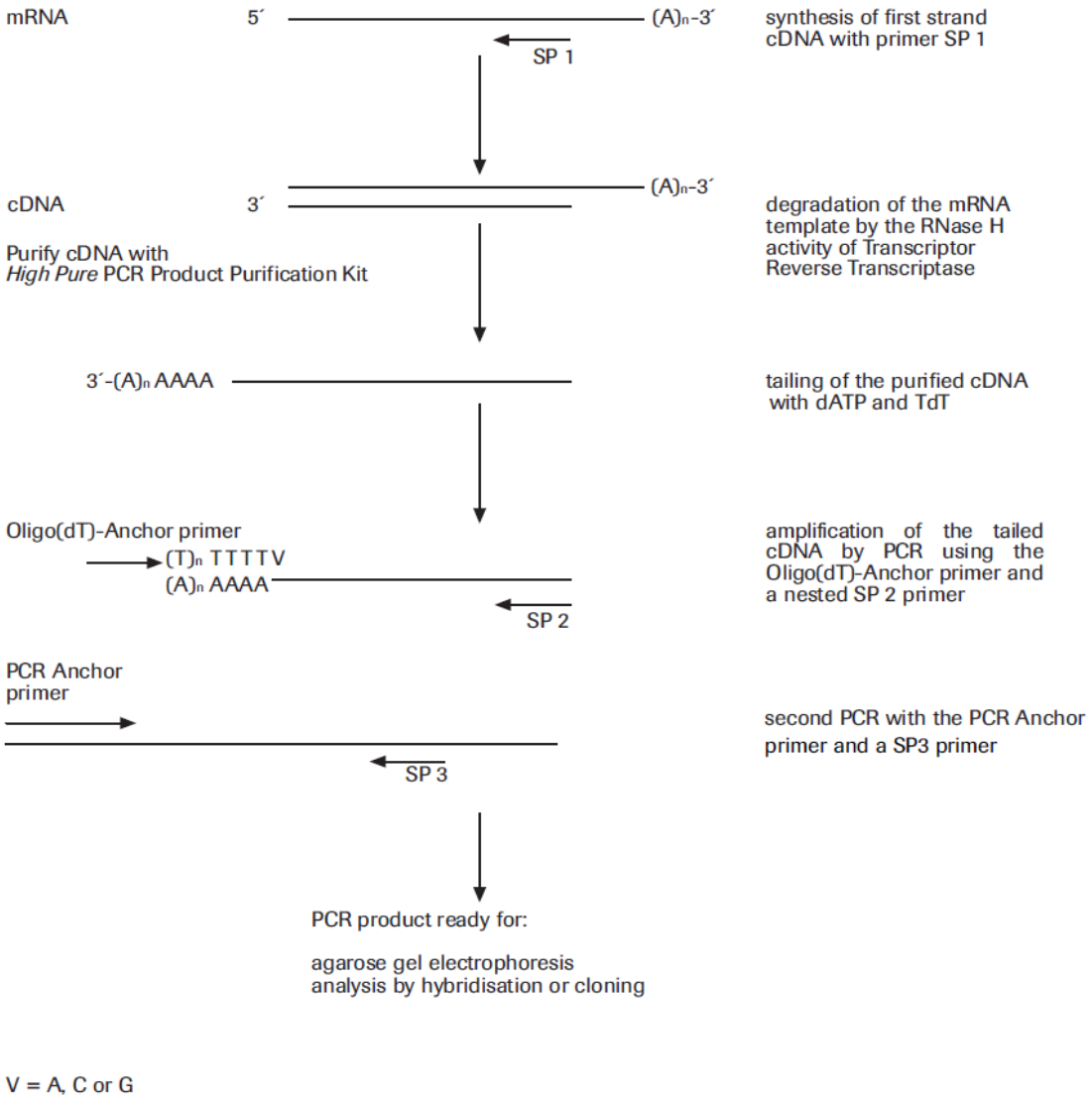

Figure 3. 5. 5' race experiment allowed to identify the promoter of *P21*.

There were 4 steps in the 5' race experiment which were: 1) first strand cDNA synthesis, 2) degradation of the mRNA template, 3) tailing of first strand cDNA, and 4) amplification of the tailed cDNA. Gene specific primers are: SP1 is needed to transcribe the mRNA into first strand cDNA, SP2 is a nested primer that is located upstream of SP1, and the last primer is SP3 is a nested primer that is located upstream of SP2. This figure was taken from (5'/ 3' RACE Kit, 2nd Generation manual version 14, 2018) (Roche, Switzerland, #03 353 621 001).

3.3. Results

The first step in trying to find a phenotype in plaque formation, plaque morphology or other general behaviour was to compare the ability of several different lysogens to grow, produce and release phage. These studies were run in two distinct *E. coli* backgrounds, a K-12 strain, specifically MC1061 with is nonpathogenic and easy to manipulate as well as a de-toxified *E. coli* O157:H7 strain, TUV93-0 which was created from a US outbreak strain EDL933 but lacks the 2 Stx phages that it once carried (Table 2.2). These *E. coli* strains were then used in their naïve state (not making phage) or carrying $\phi 24_B$::Kan (making phage and producing P21 [wild-type]) or carrying ϕ 24_B::Kan ΔP21::tet (making phage and not producing P21[mutant])

3.3.1. Comparison of the growth of wild type and mutant lysogens in K12 and O157:H7 host backgrounds

Before trying to compare the replication of phages on growing bacteria, the replication rates of the naïve and lysogen strains were first compared. Most Stx phages have a high spontaneous induction rate that results in the induction of prophages from lysogens with no apparant stimulus (Livny and Friedman, 2004b, Koudelka et al., 2004b) . To assess whether the growth of the naïve, wild type, and mutant lysogen were drastically impacted by prophage carriage. The results are expressed as mean ± standard error of mean (SEM) for three independent biological replicates, and the growth impact on different lysogen phenotypes were evaluated using a two-way analysis of variance (ANOVA). As a result, the growth rates measured during the exponential growth phase indicated that prophage carriage did not have an obvious impact on the growth rates of the lysogens cultures. (Fig. 3.6) illustrates the growth patterns of *E. coli* strain MC1061 as a naïve strain, a wild type lysogen (MC1061/$\phi 24_B$::Kan), and a mutant type lysogen (MC1061/$\phi 24_B$::Kan ΔP21::Tet). Moreover, (Fig. 3.7) illustrates the growth patterns of *E. coli* strain O157:H7 (TUV93-0) as a naïve strain, a wild type lysogen (TUV93-0/$\phi 24_B$::Kan), and a mutant type lysogen (TUV93-0/$\phi 24_B$::Kan ΔP21::Tet).

3.3.2. Identification of P21's impact on phage release from the host cell following prophage induction

To determine if P21 had an impact on plaque morphology or plaque production, the p.f.u mL^{-1} produced by a lysogen was examined over time (Figs 3.8 & 3.9). The p.f.u mL^{-1} production was examined in both a K12 backgraound (Fig. 3.8) and an

O157:H7 genetic background (Fig. 3.9) using a wild type phage ($\phi 24_B$::Kan) producing P21 and a mutant phage ($\phi 24_B$::KanΔP21::Tet) unable to produce P21. The results presented are mean ± standard error of mean (SEM) for three independent biological replicates. Following assessment for normality and equality of variances, statistical inferences on data were performed using a two-way analysis of variance (ANOVA) followed by an unpairwise comparisons treatment of the means using Bonferroni's multiple comparisons test (wild type prophage control vs mutant prophage). Differences are considered statistically significant when $p<0.01$. Statistical analyses were performed using (GraphPad Prism 7 Software Statistical Package, United States). As a result, the mutant lysogen that does not produce P21 (the E. coli strain carrying $\phi 24_B$::KanΔP21::Tet) has significantly enhanced plaque production compared to the wild-type lysogen that encodes P21 in a time-dependent fashion ($P < 0.01$; $P < 0.001$). It can be seen that the presence of P21 in an MC1061 genetic background results in fewer phages being released post induction after 260 min (Fig. 3.8). The presence of P21 in the TUV93-0 genetic background results in fewer phages being released post induction after 240 min (Fig. 3.9). It was clear that the number of plaques forming units visible was impacted by the expression of P21, but it was not clear why. Was P21 impacting the number phages being produced or was it impacting the release of phages. There is a well-established protocol for measuring the presence of fully assembled intracellular phages prior to release through the addition of chloroform CCl_3 (Hyman and Abedon, 2009) which chemically dissolves the cell envelope releasing fully formed phages before the phage encoded endolysin and holins can act (reviewed in section [3.1.3.]). The addition of CCl_3 to the samples taken over time prior to subjecting them to plaque assay (Figs. 3.8 & 3.9) demonstrate that the wild type lysogens produce the same number of plaques as the mutant. Therefore, these data that support the role of P21 in impacting the release of phages from the cell. However, these data do not support if this phenomenon is happening to every cell in the population, or to just a subset of cells.

3.3.3. Purification of P21 and production of rabbit anti-P21 sera

As P21 inhibits release of phages and it is linked to other cell envelope impacting effectors, tools and reagents that would enable cellular locations to be studied were needed. To this end, the production of anti-P21 sera was begun. The first step was to make a purified recombinant P21 protein. The gene encoding P21

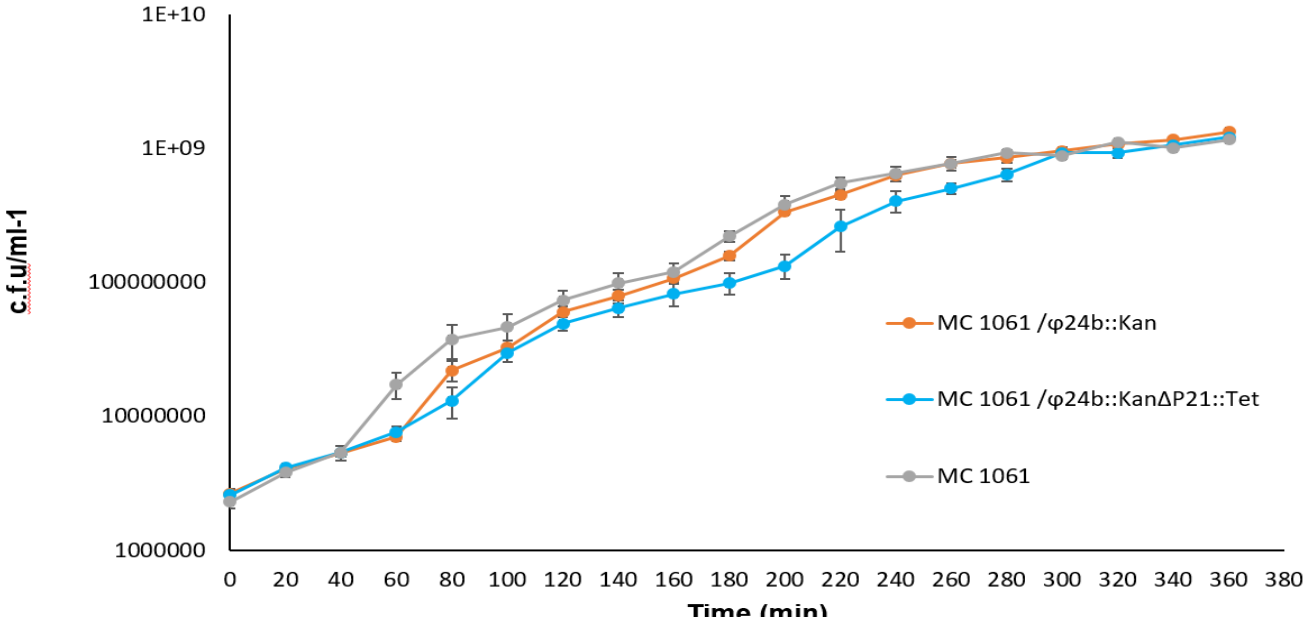

Figure 3. 6. Comparison of the growth of wild type and lysogens mutants in a K12 (MC1061) *Escherichia coli* host background.

Panel had represented growth patterns of *E. coli* strain MC1061 as a naïve strain, a lysogen of $\phi 24_B$::Kan *or* a lysogen of $\phi 24_B$::Kan ΔP21::Tet. The error bars represent standard error of the mean (n=3).

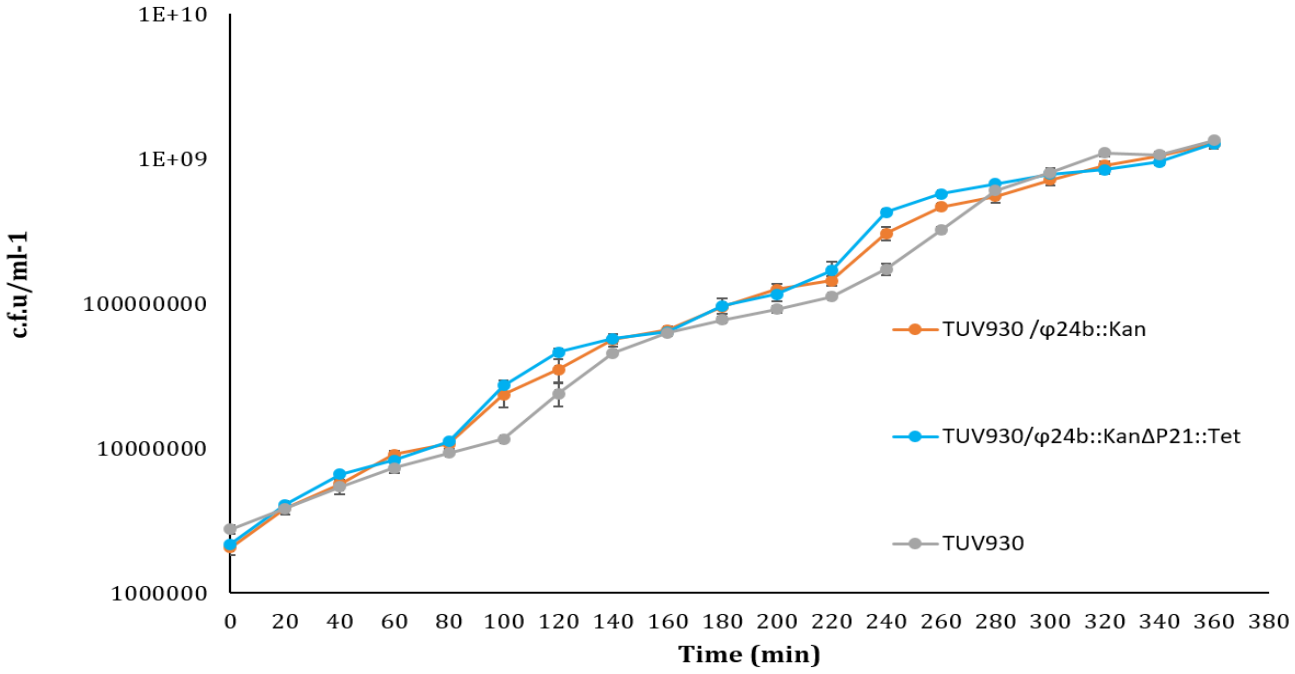

Figure 3. 7. Comparison of the growth of wild type and lysogens mutants in an O157:H7 (TUV93-0) *Escherichia coli* host backgound.

Panel had represented growth patterns of *E. coli* strains, TUV93-0 as a naïve strain, a lysogen of $\phi 24_B$::Kan or a lysogen of $\phi 24_B$::KanΔP21::Tet. The error bars represent standard error of the mean (n=3).

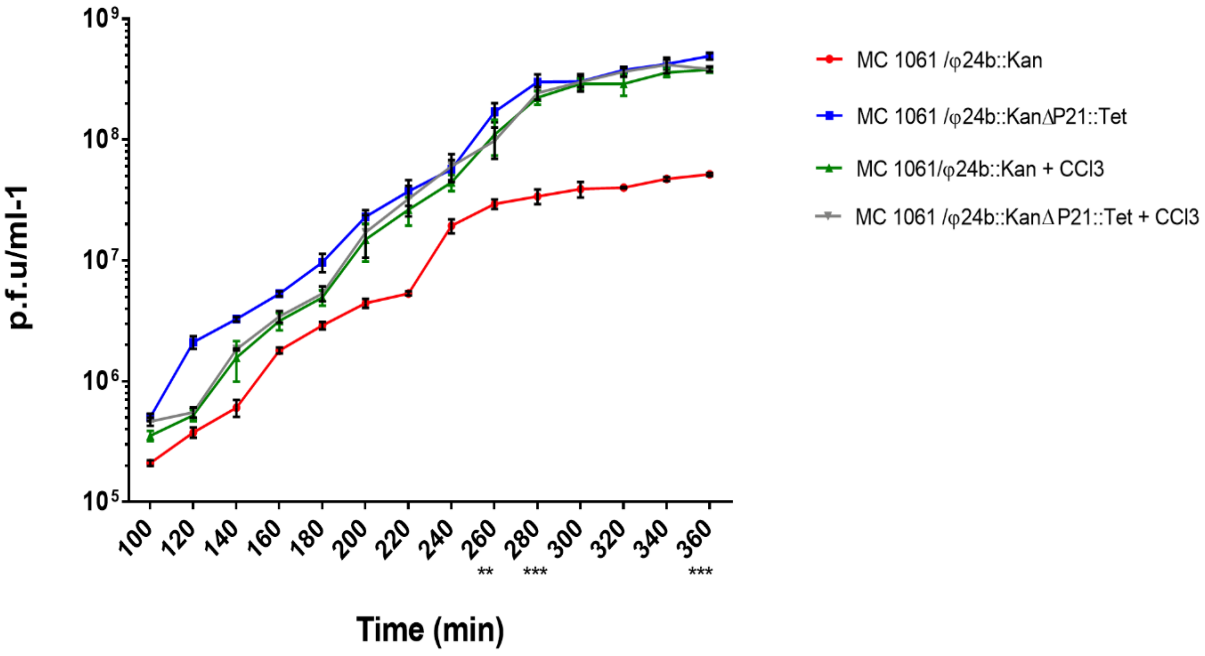

Figure 3. 8. The impact of P21 on phage release from the host cell following prophage induction. Phage release was measured by p.f.u mL^{-1} released during growth of the respective MC1061 (K12) lysogen cultures: $\phi 24_B$::Kan lysogen or $\phi 24_B$::KanΔP21::Tet lysogen, $\phi 24_B$::Kan lysogen lysed by CCl_3, and $\phi 24_B$::Kan ΔP21::Tet lysogen lysed by CCl_3. The presence of P21 in an MC1061 genetic background results in fewer phages being released post induction after 260 minutes comparing to another group samples. Significance was measured by two-way ANOVA and is indicated below the x axes (**P < 0.01; ***P < 0.001). The error bars represent standard error of the mean (n=3).

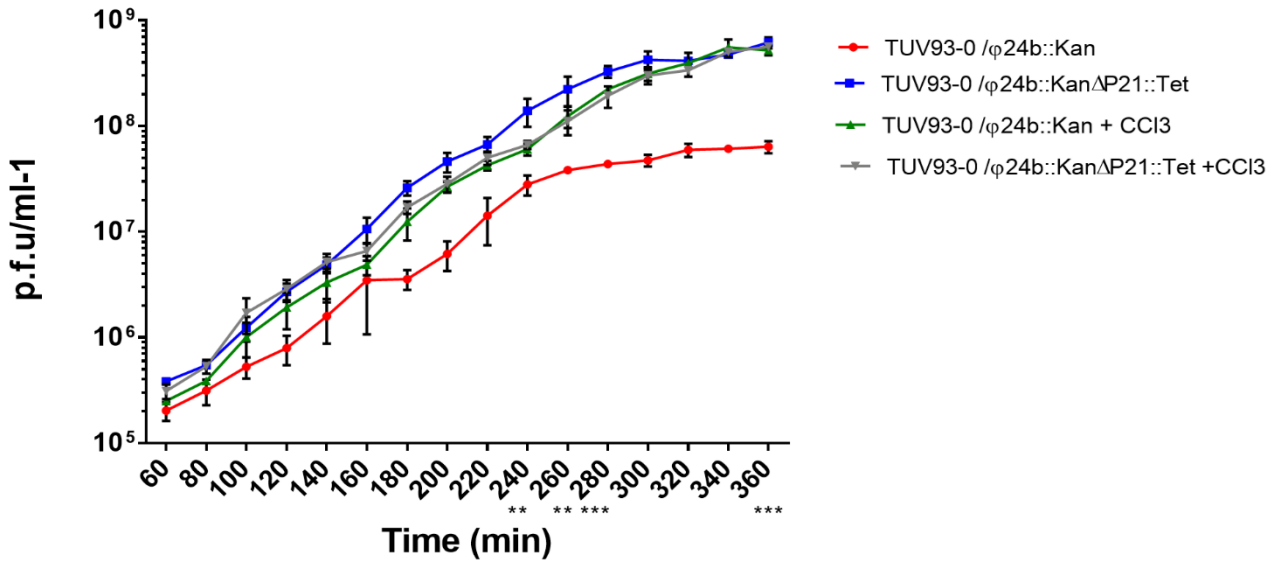

Figure 3. 9. The impact of P21 on phage release from the host cell following prophage induction.
Phage release was measured by p.f.u mL^{-1} released during growth of the respective TUV93-0 (O157:H7) lysogen cultures: $\phi 24_B$::Kan lysogen or $\phi 24_B$::Kan ΔP21::Tet lysogen, $\phi 24_B$::Kan lysogen lysed by CCl_3, and $\phi 24_B$::Kan ΔP21::Tet lysogen lysed by CCl_3. The presence of P21 in an TUV93-0 genetic background results in fewer phages being released post induction after 240 minutes comparing to another group samples. Significance was measured by two-way ANOVA and is indicated below the x axes (**P < 0.01; ***P < 0.001). The error bars represent standard error of the mean (n=3).

had previously been cloned into pBAD (Table 2.3) and transformed into *E. coli* Top10 cells (Franke et al., 2020b). The P21 protein from the cell lysate could be easily purified by using immobilized metal affinity chromatography (IMAC) based on a the ability of a string of histidine residues (known as a His-tag) to bind to an immobilized metal ion, in this case Nickle (Ni^{+2}) (QIAGEN, Hilden, Germany, #34964. The His-tag refers to six histidine amino acids located at the amino-terminal end of P21. The principle of purification is that the Ni^{+2} is bound to an agarose bead through chelation using nitroloacetic acid. The tagged protein binds to the Ni^{+2} on the column by mixing the sample with the beads (Hengen, 1995). In this case, the tagged P21 was bound to the Ni^{+2} and other no His-tagged porteins were washed off the column using buffers containing low concentrations of imidazole. The imidazole concentrations are slowly increased (washes 1 and 2) to remove contaminants until the protein of interest is finally released from the column (elution). The various fractions collected during these washes were then analysed on an SDS-PAGE gel (Fig. 3.10). A 68 kDa was purified to reasonable, but not complete homogeneity. Protein from this elution sample was given to Gemini Biosciences Ltd, Liverpool, UK and they produced rabbit poly-clonal antisera for us using 2 different rabbits.

Western blotting was used to demonstrate that the bespoke rabbit anti-P21 sera was specific to P21. The rabbit anti-P21 sera was washed three times (2.13) to get a purified specific antibody directed to P21 protein (Fig. 3.11). Lysates from *E. coli* Top10 cells carring pBAD *P21*, and IMAC purified His-tagged P21 were run in two SDS-PAGE gels. One gel was stained by coomassie stain to visualise the protein bands (Fig. 3.12A) and the second gel that was subjected to western blotting (Fig. 3.9B). The stained gel demonstrates the purified P21 band at the expected size of 68 kDa. The western blotting image was developed using the bespoke rabbit, anti-P21 sera as the primary antibody, Horse Radish Peroxidase [HRP] conjugated anti-Rabbit IgG (Sigma-Aldrich, United Kingdom, #RABHRP1) as the secondary antibody and a chemiluminescent substrate. The anti-sera enabled the detection of the 68 kDa protein as expected (Fig. 3.12B).

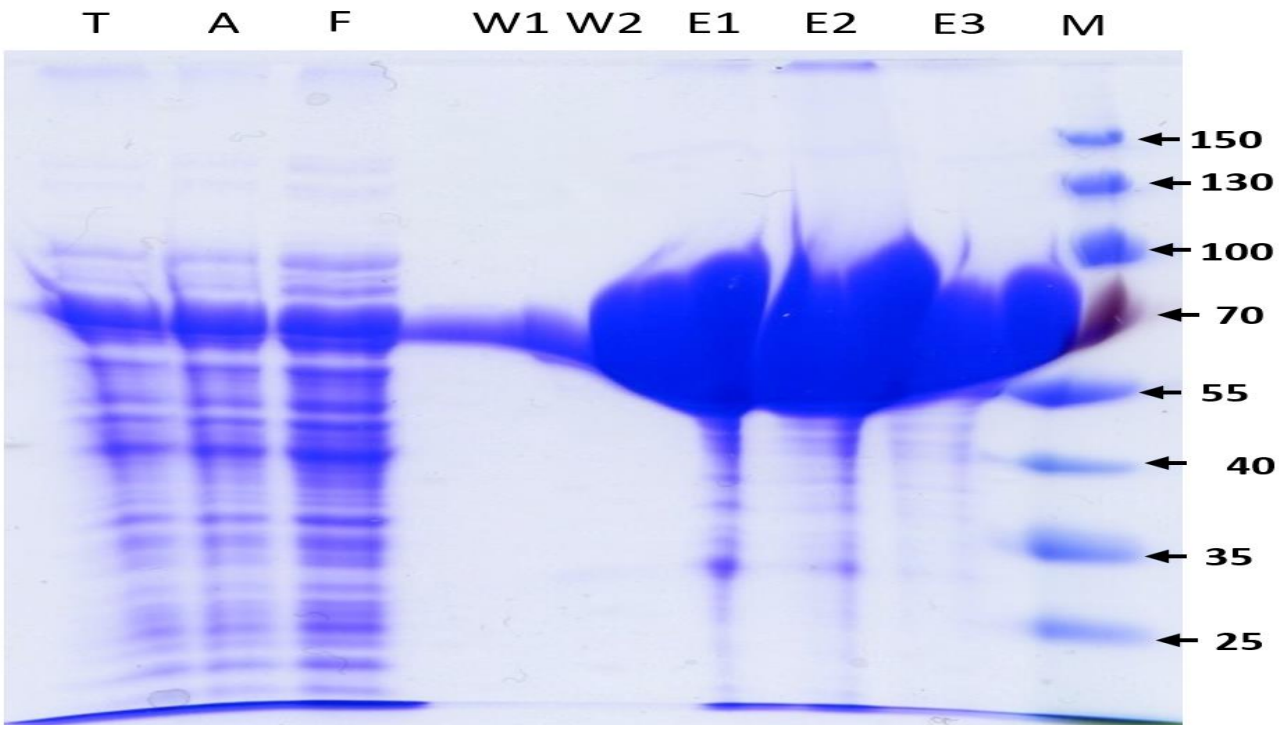

Figure 3. 10. Purification of recombinant P21.

Proteins produced by *E. coli* Top10 cells carrying pBAD *P21* clone. An SDS-PAGE shows the purification steps. **Lane Contents: T)** Whole cell lysate after sonication at 15-18 µm for 6 × 10 bursts. **A**) Proteins from cell supernatant (from cell lysate) after centrifugation at 20,833 x g for 30 minutes and before addition to Ni^{2+}-resin in column. **F**) Proteins unbound to the column after loading (50 mM NaH_2PO_4, 300 mM NaCl, 20 mM imidazole) and collected after opening the column but before washing,. **W1**) Cellular proteins washed from the column by (50 mM NaH_2PO_4, 300 mM NaCl pH 7.4 with 30 mM imidazole). **W2**) Cellular proteins washed from the column by (50 mM NaH_2PO_4, 300 mM NaCl pH7.4 with 50 mM imidazole). **E1**) Proteins collected after the first elution using (50 mM NaH_2PO_4, 300 mM NaCl pH 7.4 with 300 mM imidazole). **E2)** Protein collected after the second elution using (50 mM NaH_2PO_4, 300 mM NaCl pH 7.4 with 300 mM imidazole). **E3**) Protein collected after the third elution using (50 mM NaH_2PO_4, 300 mM NaCl pH 7.4 with 300 mM imidazole). **M**) Page Ruler Plus (ThermoFisher, United States, #00905335). The apparent molecular weight of the recombinant P21 is 68 kDa.

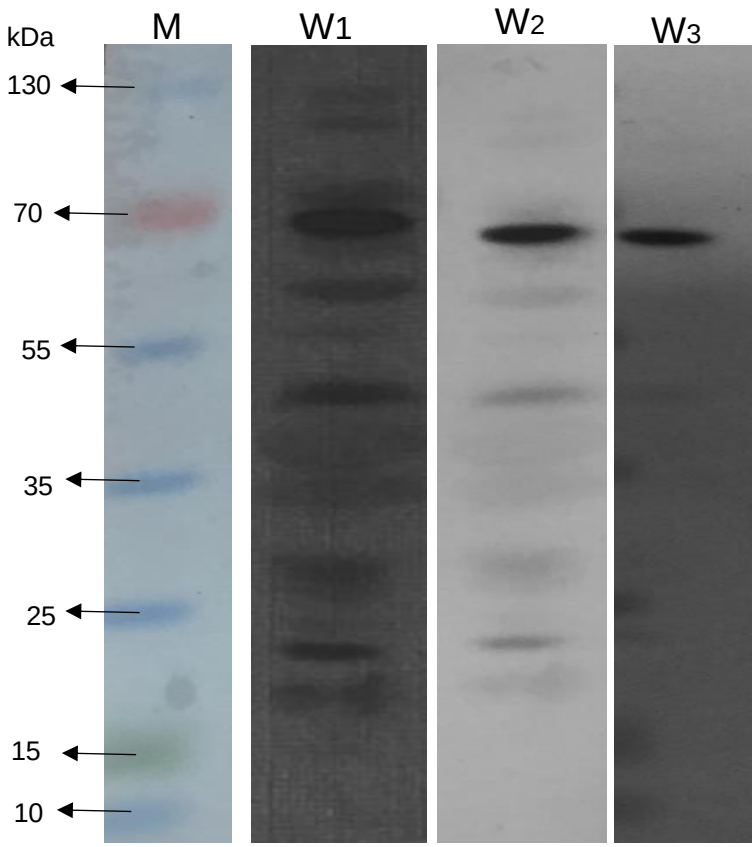

Figure 3. 11. Western blotting analysis of cleaned antisera against *E.coli* Top10 pBAD cytoplasm protein.

Lane Contents: **M**) Page Ruler Plus (ThermoFisher). **W1**) Western blot detection of recombinant P21 from whole cell lysate after first wash of antisera had presented there were general *E. coli* reactive antibodies. **W2**) Western blot detection of recombinant P21 from whole cell lysate after second wash of antisera had presented the general *E. coli* reactive antibodies were minimised than first wash. **W3**) Western blot detection of recombinant P21 from whole cell lysate after third wash had presented a single band at the expected size of 68 kDa of P21 protein which signifies the general *E. coli* reactive antibodies were removed from antisera.

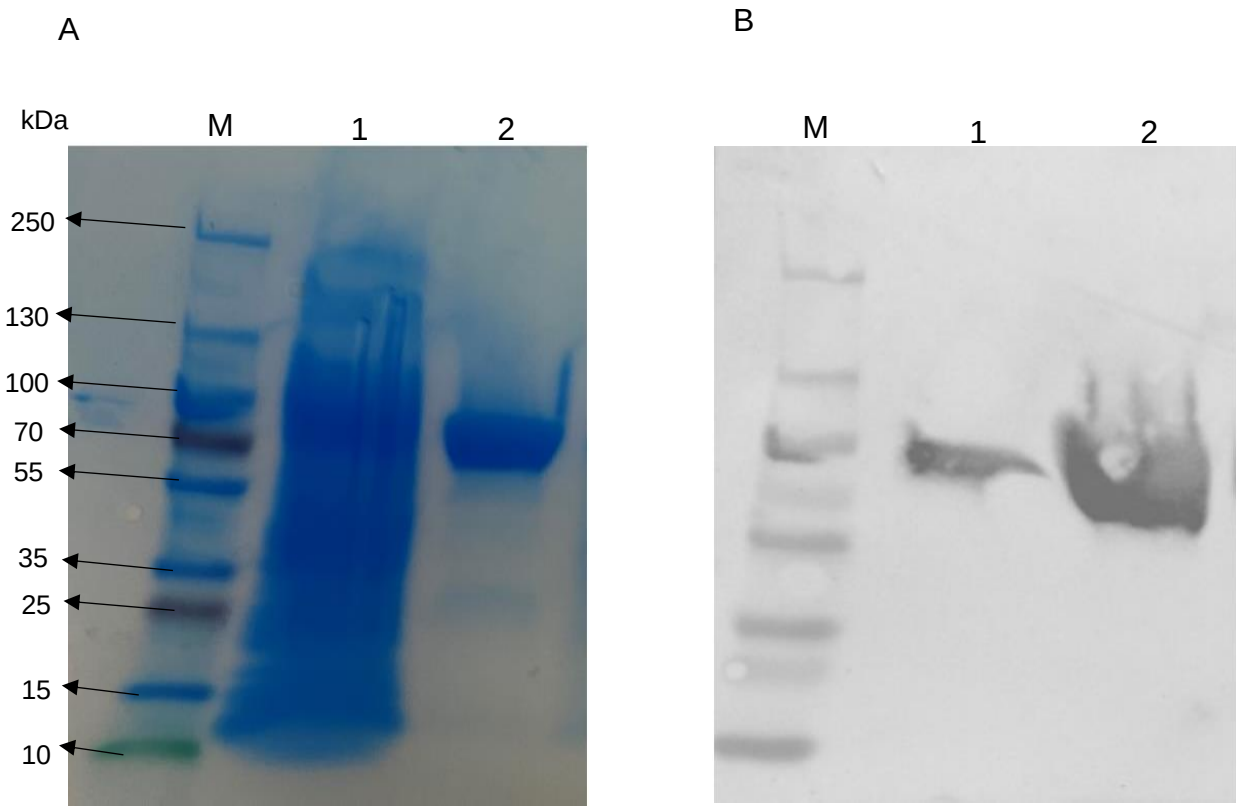

Figure 3. 12. Purification of P21, and production of polyclonal antisera.

Panel A) Coomassie blue stained SDS-PAGE gel showing whole cell lysate (lane 1) and Ni^{2+}-affinity purified recombinant P21(lane 2) at the expected size of 68 kDa. **Panel B)** Western blot detection of purified recombinant P21 (lane 2) bound with P21 antisera from a rabbit. Page Ruler Plus (Thermo Fisher, United Kingdoms, #B49) was used as a ladder (lane M).

3.3.4. Gene P21 expression in wild type phage

Having made the antibody as a tool for examining the cell localisation of P21 an attempt was set up. The main plan was to attempt immunogold labelling that would be visualised under high maginification transmission electron microscopy. However, the best way to ensure that this would work was to establish protocols for immunoflourescence labelling, as this is more sensitive and easier to troubleshoot (personal communication from the electron microscope facility that inform me that they have a technical issue in cryo-microtome). The immunofluorescence labelling experiments were run using wild type lysogen cells MC1061/ $\phi 24_B$::Kan (P21 +) and with naïve MC1061 cells (negative control (P21 -). A second group of control cells were also used. This group of cells were never exposed to the anti-P21 sera, they were only exposed to the conjugated secondary antibody solution (Goat Anti-Rabbit IgG H&L (FITC)). The samples were visualised at 260 min post recovery from norfloxacin treatment, which was the time when the wild type MC1061/$\phi 24_B$::Kan lysogen displays the most pronounced P21 phenotype (in fewer phages being released upon induction) (Fig. 3.8). The wild type lysogen that encodes *P21* shows fluoresces in (Fig. 3.13A) from fluorescence immunolabeling in the presence of the primary rabbit anti-P21 sera and the secondary Goat Anti-Rabbit IgG FITC (Invitrogen, United Kingdom, #31579. The negative control sample of *E. coli* naïve cells did not show any fluorescence detection because there was no antibody-antigen interaction between rabbit anti-P21 sera and naïve cells that did not carry the gene or encode the P21 (Fig. 3.13B). At the time of writing there was still hope that the immunogold labelling TEM microscopy might be done, but the impacts of COVID-19 on the availability of the facility have made this impractical. The plan had been to use the primary anti-sera at a 10x greater concentration for the immunogold labelling, due to the lower sensitivity of this technique.

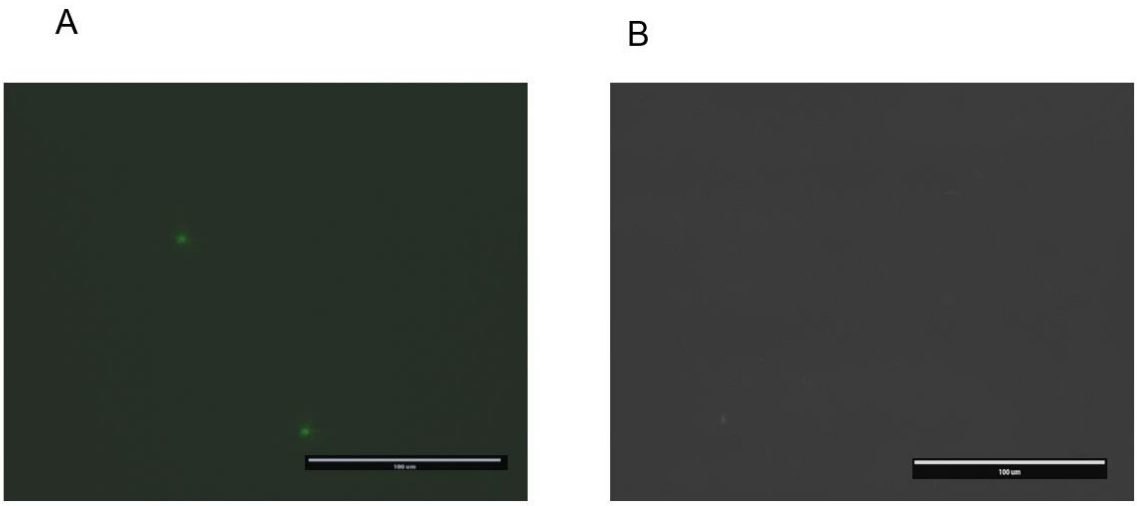

Figure 3. 13. Fluorescence microscopy of wild type lysogen cells and naïve K12 (MC1061) *E. coli* cells that were fluorescently immunolabelled.

Panel A) $\phi 24_B$::Kan in MC1061 *E. coli* in host background cells after 260 minutes post induction. **Panel B)** Naïve cells MC1061 *E. coli* cells after 260 minutes post induction. The fluorescent immunolabeling was Goat Anti-Rabbit IgG H&L (FITC).

3.3.5. P21 is expressed as a part of the lysis cassette transcript

RNASeq data indicated that P21 was likely to be expressed along with the rest of the lysis cassette as these genes are close together and appeared to be expressed at similar levels. However, transcription start sites were not deliberately mapped, so it is not possible to definitely state where transcripts begin and end and which genes share a transcript. Though the assumption has been made that P21 is likely to sit in the same transcript as the genes on the lysis cassette, experimental proof of this would help to logically apportion a role to this hypothetical protein.

Northern blot analysis would be a way of demonstrating that probes to specific genes were capable of binding to a transcript of the same, predicted size.The probes of the genes of interest were labelled using a PCR-based DIG labelling kit with the following results (Fig. 3.14). The labelled *P21* labelled probe and lysis cassette genes presents bands larger in size than their unlabelled control amplicons (*P21* gene (23617.. 23887) ; 270bp; *R* gene (26240.. 26534) 294bp; *S* gene (25985 .. 26172) 187bp; *Rz* gene (27886.. 28086) 200bp, and *Rz1* gene (27972 .. 28109) 137bp).

Total RNA was extracted from norfloxacin induced cultures of the MC1061/ $\phi 24_B$::Cat lysogen. The RNA was separated on denaturing agarose gel (Fig. 3.15A) where bands of 1.5 kn and 2.5 kn were readily visible. The RNA was then transferred to a nylon membrane that was stripped and prepared for every probe. The location of probe binding was detected by chemiluminescent signal (Fig. 3.13B). The nylon membrane shows after exposure to chemiluminescent two specific bands in size 1.5 kn and 2.5 kn (Fig. 3.15B) that were demonstrated from all DIG probes of *P21*, *S*, *R*, and *Rz* when hybridized with total RNA from the induced $\phi 24_B$::Cat. However, these bands represent rRNA, which is abundant in the cells and is more likely to represent probe trapping that specific binding. While, the expectation from this experiment is detecting mRNA whose size of long of transcript *P21* and lysis lysis cassette genes that present as a specific band in size 3 kn. It is likely that the rRNA would need to be hybridized out of the sample in a subtractive way to enable detection of the mRNA transcripts of interest or run alternative methods that prove P21 was expressed the rest of the lysis cassette genes such as 5' race experiment that prove the genes are expressed at the same promoter or reverse transcription polymerase chain reaction (RT-PCR).

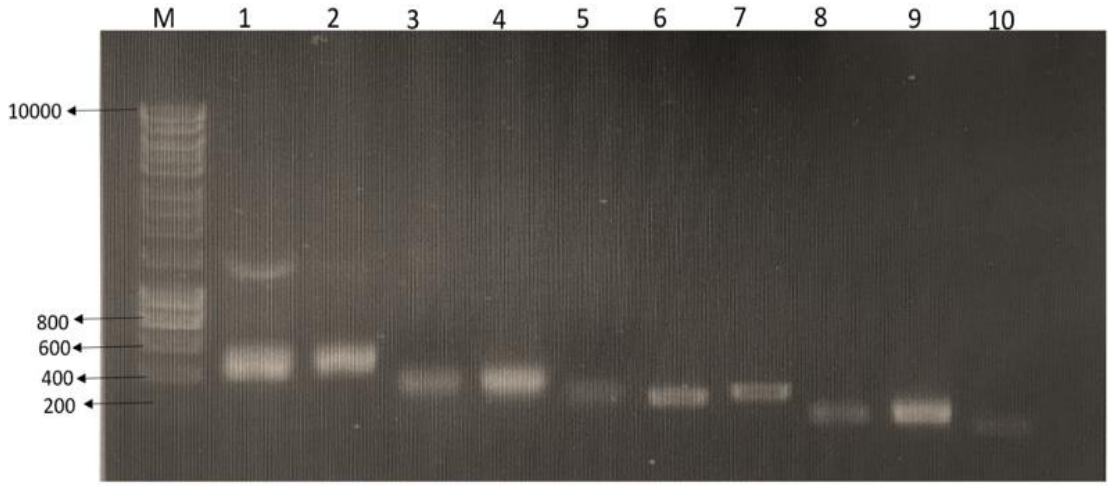

Figure 3. 14. Agarose gel electrophoresis proof of DIG labelling of probes for P21 and lysis cassette genes that were used in northern blot experiment.

Lane M: 1 kb DNA ladder (NEB, Herts, U.K.) with band size marker. **Lane 1)** *P21* labelled DIG probe. **Lane 2)** *R* labelled DIG probe. **Lane 3)** *S* labelled DIG probe. **Lane 4)** *Rz* labelled DIG probe. **Lane 5)** *Rz1* labelled DIG probe. **Lane 6)** PCR product of 270bp (23617.. 23887) of *P21* gene. **Lane 7)** PCR product of 294bp (26240.. 26534) of *R* gene. **Lane 8)** PCR product of 187bp (25985.. 26172) of *S* gene. **Lane 9)** PCR product of 200bp (27886.. 28086) of *Rz* gene. **Lane 10)** PCR product of 137bp (27972.. 28109) of *Rz1* gene.

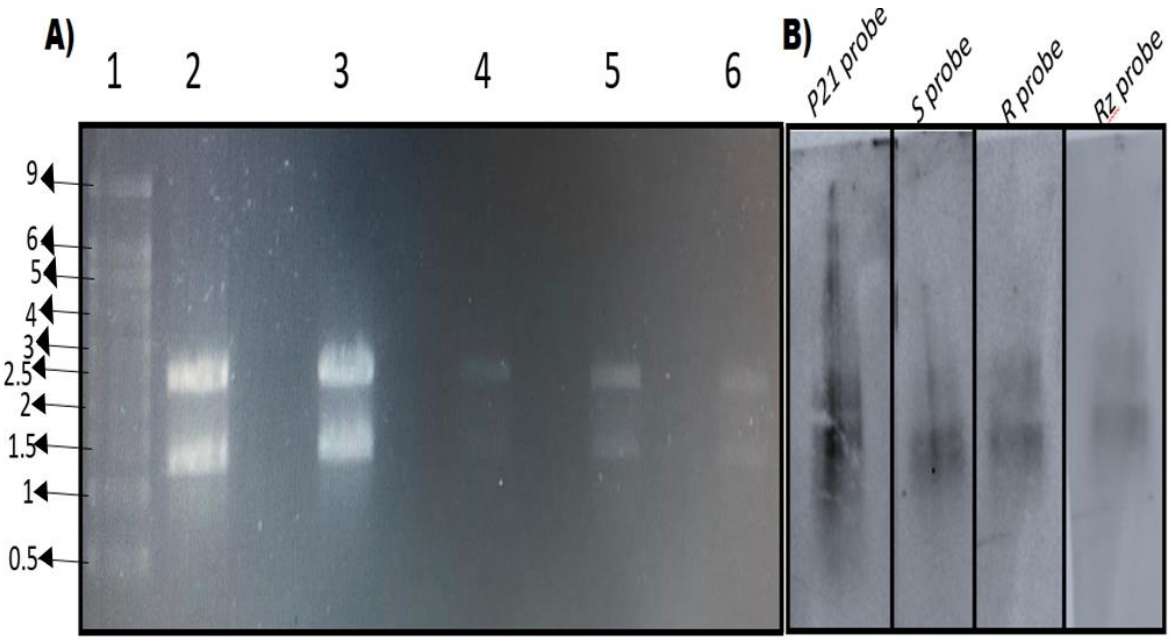

Figure 3. 15. Denaturing RNA gel and northern blotting exposure membrane.

Panel A) Denaturing agarose gel of multiple total RNA from the bacterial lysogen MC1061/ $\phi 24_B$. Lane 1) Millennium^{TM} RNA Markers (kn) (Thermo Fisher, United Kingdoms). Lanes 2,3,4,5, and 6) RNA extraction product from induced $\phi 24_B$::Cat lysogen. **Panel B)** Nylon membrane image of separated rRNAs from bacterial lysogen MC1061/ $\phi 24_B$::Cat were hybridized with DIG probe complementary labelled with targeted *P21*, *S*, *R*, and *Rz* sequence primers.

3.3.6. Determination of wild type and mutant lysogen viability

It is clear that expression of P21 limits the release of phage. It is not yet clear how P21 causes this limitation. The question of whether the cells release on average fewer phages or only some cells release phages has not yet been addressed. As phage release is associated with cell lysis, the latter scenario would make more sense, expression of P21 protects some cells from lysis. Therefore, the aim of this experiment was to identify if there is a difference in the viability of the lysogenic population as a function of the host cell membrane integrity between wild type and mutant lysogen LIVE/DEAD® BacLight™ Bacterial Viability kit (Thermo Fisher Scientific, United Kingdom, #L7012) was used in this experiment. The cultured cells with compromised membranes fluoresce red while the cultured cells with an intact membranes fluoresce green. The time points results that were examined were based on the number of phages released in previous experiments (Fig. 3.8, and Fig. 3.9). Again, the K12 (MC1061) and O157:H7 (TUV93-0) genetic backgrounds were tested carrying both the P21 produing ($\phi 24_B$::Kan) and P21 decificent prophages ($\phi 24_B$::Kan ΔP21::Tet). The lysogens were grown to mid log and the prophages were induced with norfloxacin for 1 h. The cultures were subcultured to enable the cells to recover and respond to the induction stimuli. Samples were stained with the LIVE/DEAD® BacLight™ Bacterial Viability kit at 180, 240, and 300 min post subculture. It is difficult to predict an obvious and marked differences between the wild type and mutant phage samples in both host back grounds at the three time points from the limited fluorescence microscope images that were sorted (Fig. 3.16). The work is an incompelete due Covid-19 situations which was a factor in limiting replication.

3.3.7. Cell sorting count in wild type and mutant lysogen

To try and obtain more quantitative data the same type of experiment was repeated but this time using fluorescence activated cell sorting (FACS) to determine number of living cell upon the induction in the bacterial lysogenic cultures in both types. Sony SH-800 was the instrument that used to run the samples and the iQue Forecyt® Offline Analysis Edition 8.1 software was used to analyse the data (the experiment was performed by Dr. Srijan Jindal from institute of integrative biology, University of Liverpool, United Kingdoms). The results are expressed as mean ± standard error of mean (SEM) for three dependent biological replicates, following assessment

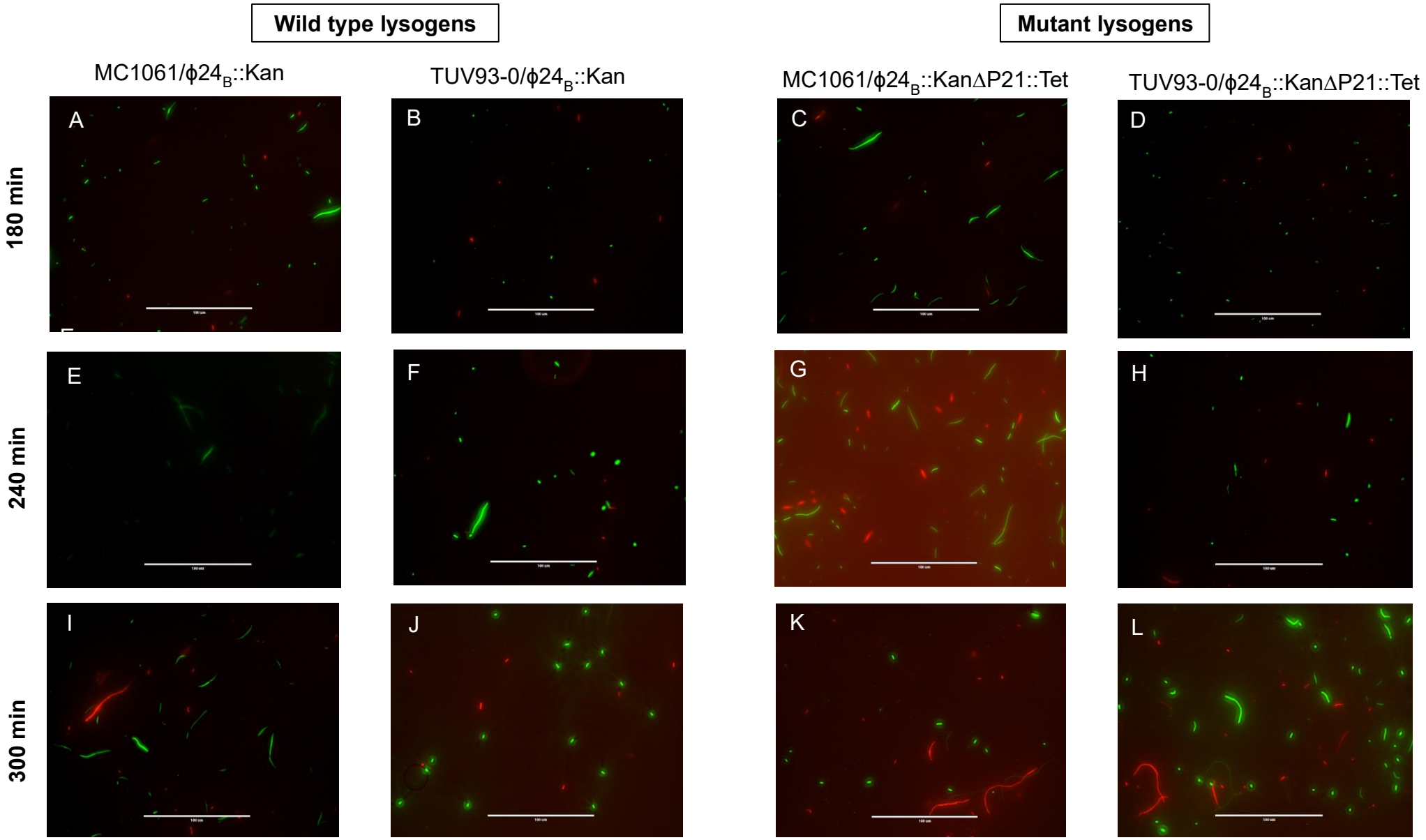

Figure 3. 16. Fluorescence microscopy of wild type and mutant lysogens in three different time points.

A) MC1061/ $\phi24_B$::Kan at 180 min. B) TUV93-0 / $\phi24_B$::Kan at 180 min. C) MC1061/ $\phi24_B$::Kan ΔP21::Tet at 180 min. D) TUV93-0 / $\phi24_B$::Kan ΔP21::Tet at 180 min. E) MC1061/ $\phi24_B$::Kan at 240 min. F) TUV93-0 / $\phi24_B$::Kan at 240 min. G) MC1061/ $\phi24_B$::Kan ΔP21::Tet at 240 min. H) TUV93-0/$\phi24_B$::Kan ΔP21::Tet at 240 min. I) MC1061/ $\phi24_B$::Kan at 300 min. J) TUV93-0 / $\phi24_B$::Kan at 300 min. K) MC1061/ $\phi24_B$::Kan ΔP21::Tet at 300 min. L) TUV93-0 / $\phi24_B$::Kan ΔP21::Tet at 300min. Live cells fluoresce green; dead cells fluoresce red (n=1).

for normality and equality of variances, statistical inferences on data were performed using two-way analysis of variance (ANOVA) followed by unpairwise comparisons of treatment means using Sidak's multiple comparission test (wild type cells control or vs. mutant lysogen used in the FACS study). Differences are considered statistically significant when $p<0.01$. Statistical analyses were performed using GraphPad Prism 7 Software Statistical Package, Unites States). As a result, the wild type lysogen in an MC1061 genetic background (MC1061/$\phi 24_B$::Kan) has significantly larger number of living cells that were stained by positively charged carbocyanine dye 3,3'-dipropylthiadicarbocyanine iodide ($DiSC_3$ (5)) (ThermoFisher, United Kingdom) dye in time-dependent fashion ($P < 0.01$) 240 min. after induction after than the mutant lysogen in an MC1061 genetic background (MC1061/$\phi 24_B$::Kan ΔP21::Tet) (Fig. 3.17). Moreover, the wild type lysogen in an MC1061 genetic background (MC1061/$\phi 24_B$::Kan) had a significantly greater number of intact cells that were stained by SYBR^{TM} Green I (ThermoFisher, United Kingdom) dye in time-dependent fashion ($P < 0.01$, $P < 0.001$) 180 min and 240 min after induction when compared to the mutant lysogen in an MC1061 genetic background (MC1061/ $\phi 24_B$::Kan ΔP21::Tet) (Fig. 3.18).

The full cytograms of forward and side scatters versus the RL1 channel which was set to detect $DiSC_3$, and the BL1 channel which was set to SYBR^{TM} Green I dye at three different after induction time are shown in (Fig. 3.19) at the starting point of entry into the recovery after norfloxacin treatment time point (0 min), (Fig. 3.20) in 180 min after induction, and (Fig. 3.21) in 240 min after induction. The gates were used to solely the wild type lysogen MC1061/ $\phi 24_B$::Kan samples. When the prophage induction, the wild type lysogen MC1061/ $\phi 24_B$::Kan cells present above 10^4 in RL1 channel (Fig. 3.19 (5A)), and the wild type lysogen MC1061/ $\phi 24_B$::Kan cells present above 10^5 in BL1 channel (Fig. 3.19 (5B)). While in post induction in 180 min, and 240 min, the wild type lysogen MC1061/ $\phi 24_B$::Kan cells present above 10^5 in RL1 channel (Fig. 3.20 (5A), and Fig. 3.21 (5A)), and the wild type lysogen MC1061/ $\phi 24_B$::Kan cells present above 10^6 in BL1 channel (Fig. 3.20 (5B), and Fig. 3.21(5B)).

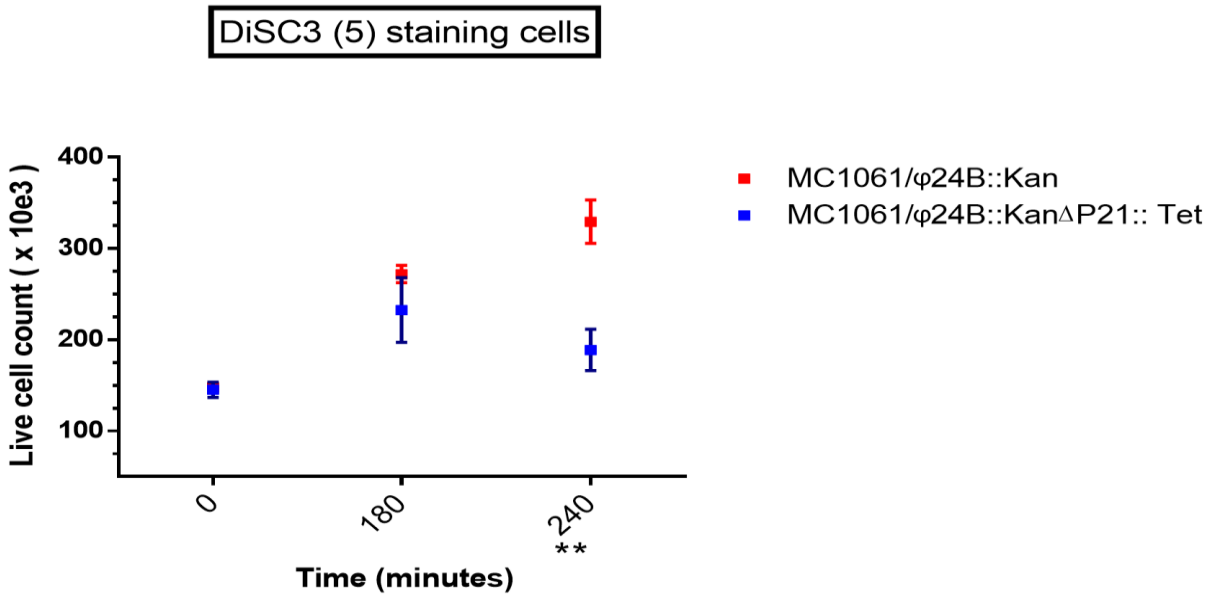

Figure 3. 17. Flow cytometric counting determines the live cells of both bacterial lysogens that were stained by 3,3'-dipropylthiadicarbocyanine iodide ($DiSC_3$ (5)) dye.

Panel had presented number of live cells count of the respective MC1061 (K12) lysogen cultures: $\phi 24_B$::Kan lysogen or $\phi 24_B$::Kan ΔP21::Tet lysogen. The presence of P21 in an MC1061 genetic background results in higher number of living cells than absent of P21 in an MC1061 genetic background post induction after 240 minutes. Significance was measured by two-way ANOVA, and is indicated below the x axes (**$P < 0.01$). The error bars represent standard error of the mean (n=3).

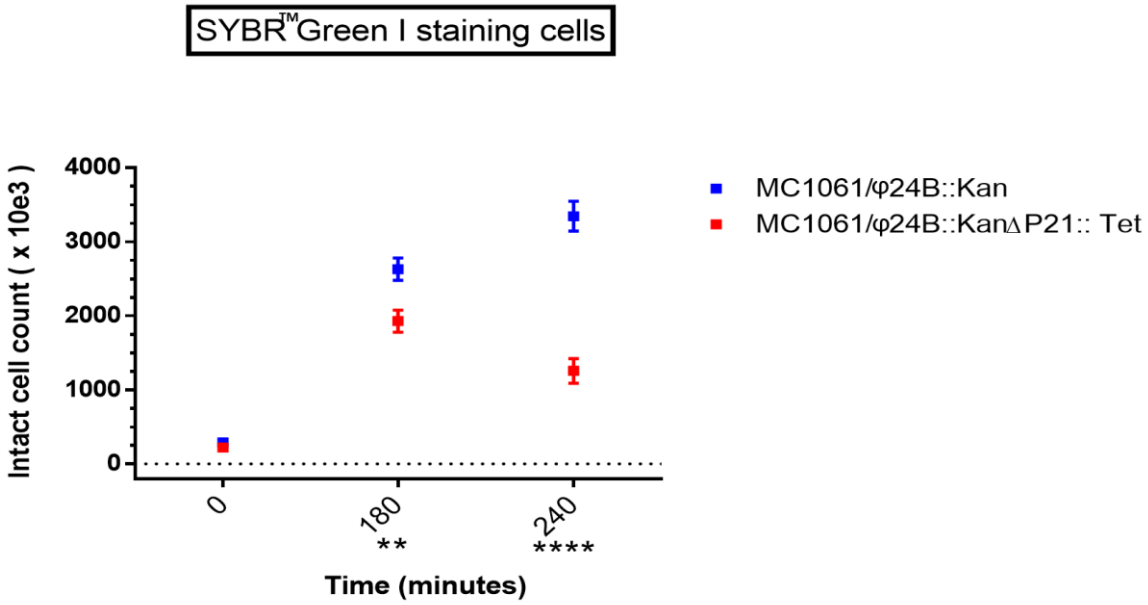

Figure 3. 18. Flow cytometric counting determines the intact cells of both bacterial lysogens that were stained by SYBR™ Green I dye.

Panel had presented number of intact cells count of the respective MC1061 (K12) lysogen cultures: $\phi 24_B$::Kan lysogen or $\phi 24_B$::Kan ΔP21::Tet lysogen. The presence of P21 in an MC1061 genetic background results in higher number of intact cells than absent of P21 in an MC1061 genetic background post induction after 180, and 240 minutes. Significance was measured by two-way ANOVA, and is indicated below the x axes (**P < 0.01; ***P < 0.001). The error bars represent standard error of the mean (n=3).

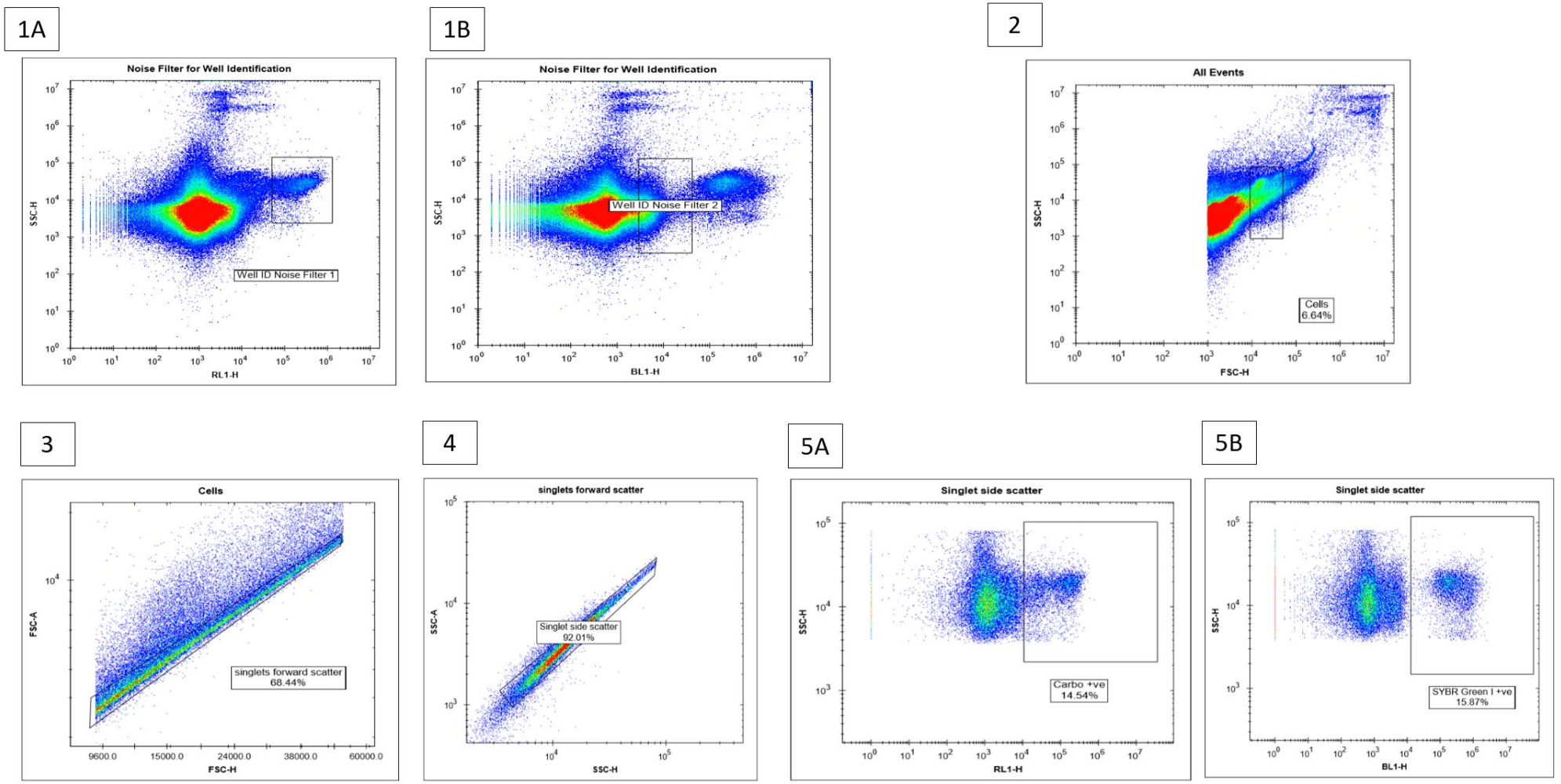

Figure 3. 19. Raw dot plots of the height of the forward and side scatters signal against RL1-H channel and BL1-H channels in the starting the prophage induction time point (0 minute).

From 1 (A&B) to 5 (A&B) were the gating strategies steps to get only wild type lysogen MC1061/ $\phi 24_B$::Kan singlet cells. 5A) The wild type lysogen MC1061/ $\phi 24_B$::Kan cells present above 10^4 in RL1-H channel which was set to detect $DiSC_3$ (5) dye. 5B) The wild type lysogen MC1061/ $\phi 24_B$::Kan present above 10^5 in BL1-H channel which was set to SYBR™ Green I dye. These figures were analysed by iQue Forecyt® Offline Analysis Edition 8.1 software.

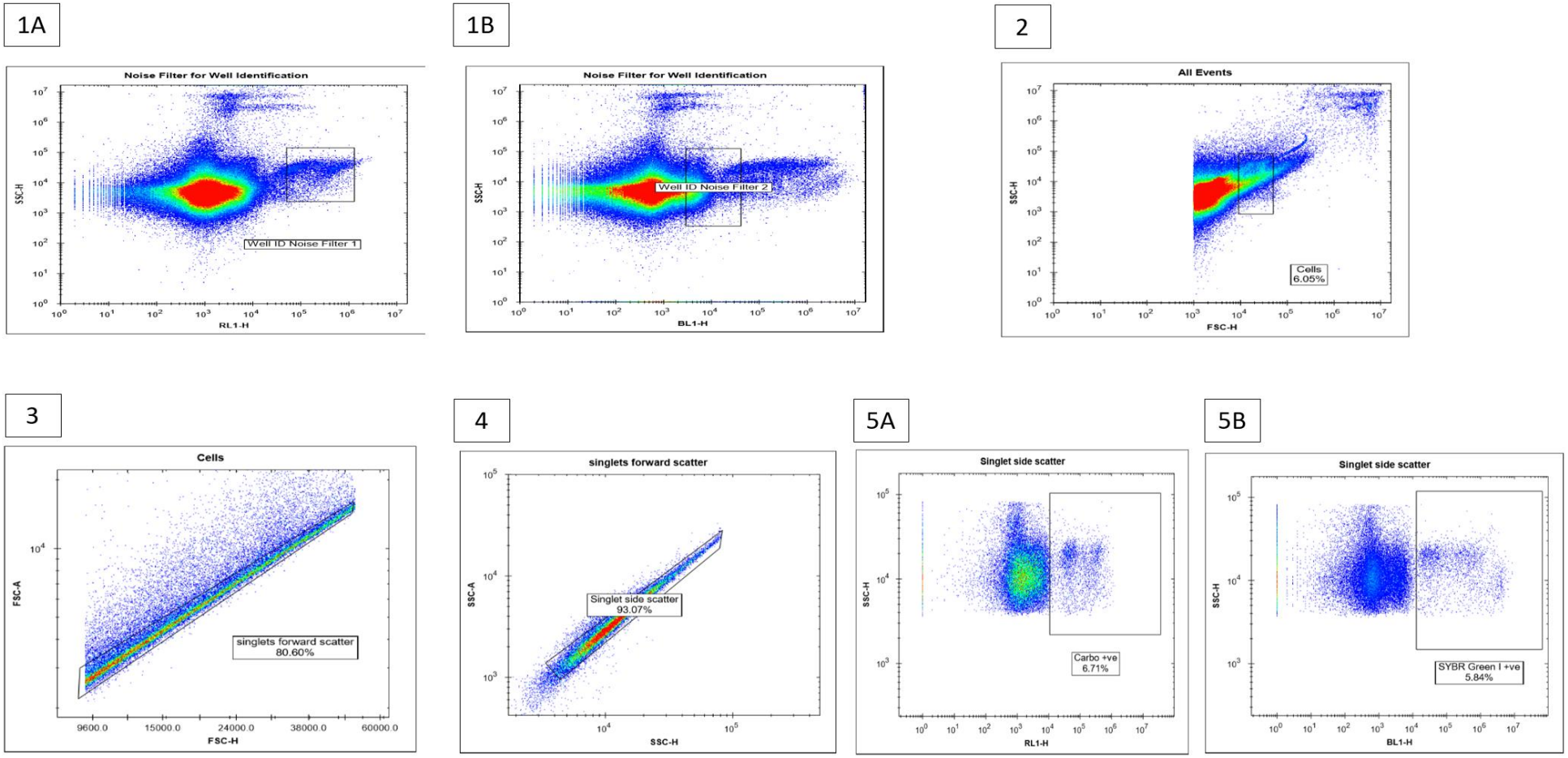

Figure 3. 20. Raw dot plots of the height of the forward and side scatters signal against RL1-H channel and BL1-H channels in the 180 minutes post induction.

From 1 (A&B) to 5 (A&B) were the gating strategies steps to get only wild type lysogen MC1061/ $\phi 24_B$::Kan cells. 5A) The wild type lysogen MC1061/ $\phi 24_B$::Kan cells present above 10^5 in RL1-H channel which was set to detect $DiSC_3$ (5) dye. 5B) The wild type lysogen MC1061/ $\phi 24_B$::Kan cells present above 10^6 in BL1-H channel which was set to SYBR™ Green I dye. These figures were analysed by iQue Forecyt® Offline Analysis Edition 8.1 software.

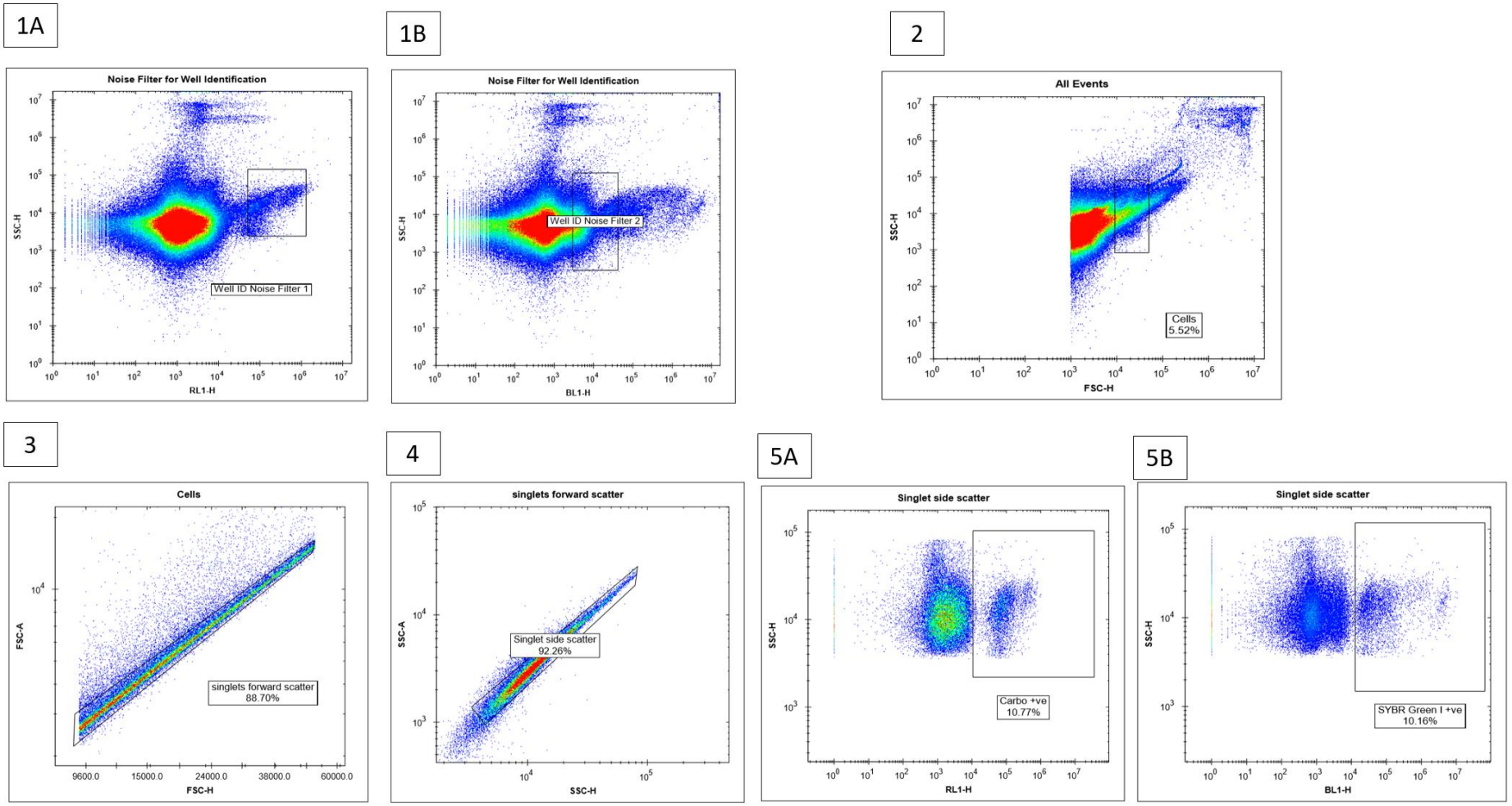

Figure 3. 21. Raw dot plots of the height of the forward and side scatters signal against RL1-H channel and BL1-H channels in the 240 minutes post induction.

From 1 (A&B) to 5 (A&B) were the gating strategies steps to get only wild type lysogen MC1061/ $\phi 24_B$::Kan singlet cells. 5A) The wild type lysogen MC1061/ $\phi 24_B$::Kan cells present above 10^5 in RL1-H channel which was set to detect $DiSC_3$ (5) dye. 5B) The wild type lysogen MC1061/ $\phi 24_B$::Kan cells present above 10^6 in BL1-H channel which was set to SYBR™ Green I dye. These figures were analysed by iQue Forecyt® Offline Analysis Edition 8.1 software.

3.3.8. P21 promoter's and length of transcript

The analysis of annonated ϕ24 $_B$ with CG view (Smith et al., 2012b) and RNA sequencing of ϕ24$_B$ (Veses Garcia, 2010, Veses-Garcia et al., 2015c) predict the P21 promoter's is pR putative late which is located downstream from the *Q* anti terminator gene. it was expected to have a sequence of P21 promoter's in around 2kbp size but the result of defining the P21 promotpr's by 5' race experiment demonstrates sequencing as not the expectation. The PCR product of amplifying tailing of first strand cDNA (3.2.7.3.) was around 200 bp (Fig 3.22). After that, this PCR product was cleaned up, the PCR product was used to amplify the tailed cDNA (3.2.7.4.). As a result, the PCR product was also around 200 bp (Fig 3.22). Then the PCR product was cleaned up and was sent to sequencing (2.22). The sequence query that was recived from (Eurofine Genomic, Germany), was searched in BLAST (https://blast.ncbi.nlm.nih.gov/Blast.cgi). As a result, the sequence was matched with ϕ24 $_B$ (HM_208303) in (215/221 bp) betwenn 23771 and 23550 which is located at the *P21* gene that lies between nucleotides 23,314 and 25,252 in ϕ24 $_B$ (Fig 3.23).

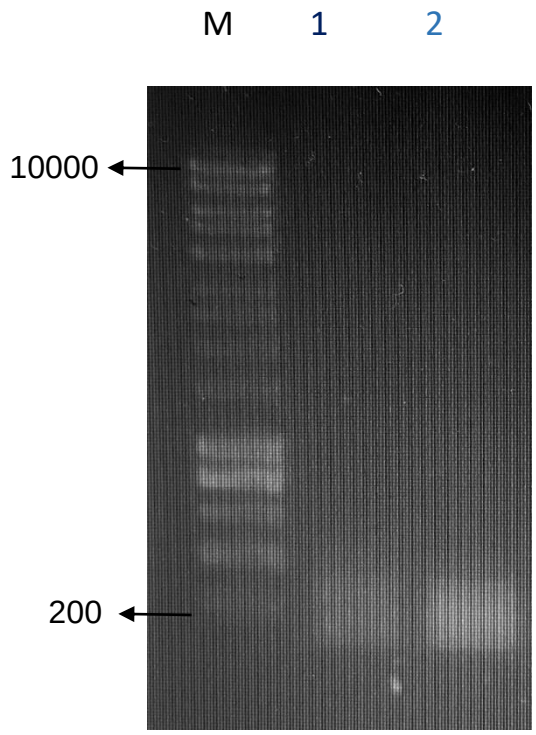

Figure 3. 22. Agarose gel electrophoresis of the amplification of cDNA to identify *p21* promoter

Lane M: 1 kb DNA ladder (NEB, Herts, U.K.), with band size marker. Lane 1: PCR product amplification of tailing of first strand cDNA by using SP2 reverse primer in reaction. Lane 2: PCR product amplification of tailing of first strand cDNA by using SP3 reverse primer in reaction.

A

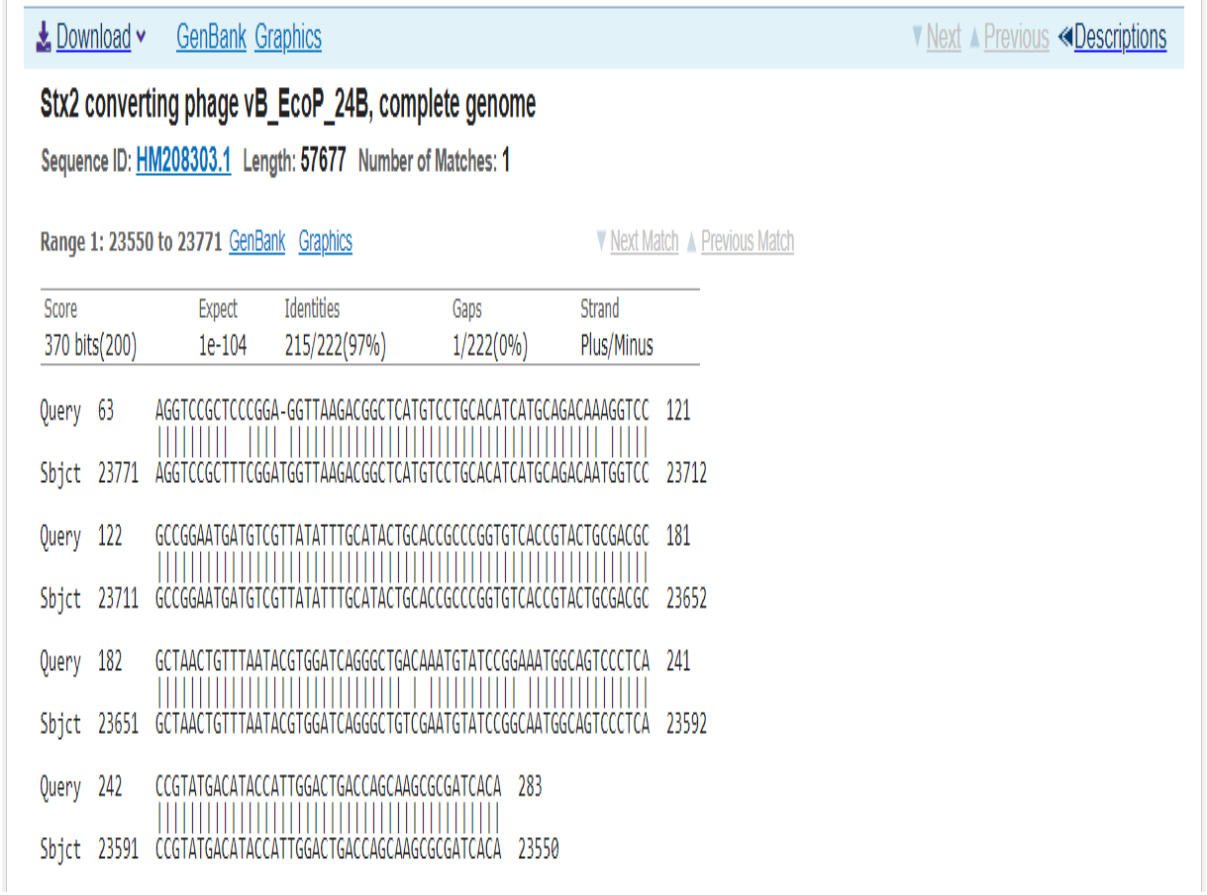

B

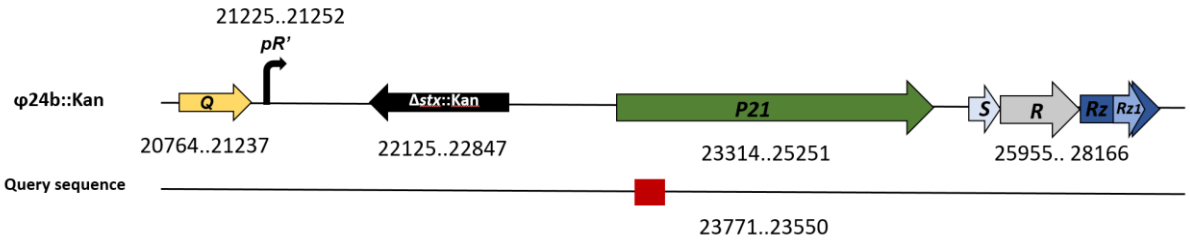

Figure 3. 23. Result of *P21* sequence which was amplified the tailed cDNA from SP3 site.

A) The query sequence was the result of cDNA of what was expected to be a promoter of P21. The result showed only 215bp of query sequence was identified with 222 bp of Stx converting phage Vb_EcoP_24B (97%). This result was searched by BLAST (https://blast.ncbi.nlm.nih.gov/Blast.cgi#alnHdr_307604077).

B) The query sequence location against the genome map of $\phi 24_B$::Kan that shows the genes that are transcript from pR putative late (*pR'*) promoter with their location (https://www.ncbi.nlm.nih.gov/nuccore/HM208303.1?report=graph).

3.4. Discussion

In previous studies, the annotated ϕ24$_B$ genome was analysed by CG view that resulted 32 genes, which are 75% of ϕ24$_B$ genome, are hypothetical. It is important to analyse the expression of these genes to define if they have been obtained by the phage through *situ* recombination events and have with no impact on the mechanisms of the phage or bacterial host's biology (a moron) or if they have been acquired and are now beneficial to the bacterial host or to the phage itself (Smith et al., 2012a). Moreover, both (Riley et al., 2012c), and (Veses-Garcia et al., 2015b) examined expression of ϕ24$_B$.(Riley et al., 2012c) displayed the genes expression analysis by using Change Mediated Antigen Technology (CMAT), and proteomic that were detected 26 genes and were assessed by qPCR. As a result, two genes were expressed as know lysogenic cycle promotor, four genes were expressed in lytic pathway, and one gene were expressed in the lysogen (1.3.4.2.1). (Veses-Garcia et al., 2015b) used RNA sequencing to study the transcriptomic analysis of ϕ24$_B$ and revealed that the ϕ24$_B$ prophage benefits the bacterial host cell to become more acid resistant (1.3.5.3.1).

One of these hypothetical genes is vb_24$_B$_21 gene (*P21*) which is located downstream from the *stx* operon that encode the Shiga toxins and upstream of the lysozyme protein of the lysis cassette genes (*S*, *R*, *Rz* and *Rz1*). In this chapter, the *P21* gene was studied to predict if the *P21* provided a phenotype to the host cell or replicating phage escpecially with availlabilty of lysogen structure that did not encode *P21*, so it is helpful to understand the phenotype of gene by comparing the induced ϕ24$_B$ lysogen in present or absent the expression of *P21* gene. Moreover, it can be seen if we could learn anything more about this hypothetical protein beyond its possession of an acetyl esterase domain (3.1.1) by studying the gene expression and long of transcript, determining the gene promoter, and recombinant of P21 protein for using in some experiment to understand the role of P21 inside the cellular.

(Veses-Garcia et al., 2015a) have studied the transcriptomic analysis of ϕ24$_B$ by RNA sequencing, as a result, the *P21* showed expression as part of the lysis transcript in the late gene region (Veses-Garcia et al., 2015a, Smith et al., 2012a). The northern blotting experiment with induced ϕ24$_B$ presented the *P21*, and the lysis cassette genes (*S*, *R*, and *Rz*) demonstrated bands that respresent rRNA (Fig. 3.15B) was an unexpected date that were looking to see the mRNA induced ϕ24$_B$ to prove

the expression *P21* and lysis cassette genes (*S*, *R*, *Rz*, and *Rz1*) at the same lysis transcript. RiboMinus™ Transcriptome Isolation Kit (Fisher Scientific, United Kingdom, #K155004) is one of suggestion that are used to solve the troubleshooting of rRNA by enrichment of mature polyadenylated mRNA and targeting depletion of rRNA. Then, the captured rRNA with complimentary oligos connect to paramagentic beads that follows by removing of band rRNA (Kraus et al., 2019). Moreover, 5' race experiment result did not predict the P21 promoter's because the size of band that was sorted in 5' race experiment (Fig.3.22) was totally small than an expected size of P21 promoter's in RNA sequencing of $\phi 24_B$ (Veses-Garcia et al., 2015a), and the sequence query was resulted sequence laying on the *P21* gene sequence (Fig.3.23). As a result, it can not be believing the 5' race experiment was succeeded due Covid-19 situations the time was run and the experiment need to repeat with designing new primers that are nested in *P21* and primers that are located on downstream of lysis cassette genes to identify the *P21* and lysis cassette genes have the same promoter of transcription. It could be trying a RT-PCR between *P21* and lysis cassette genes (*S*, *R*, and *Rz*) to see if these genes are on the same molecules. Otherwise, there were some studies revealed *R* gene was transcript in early stage such as *Streptococcus thermophiles* phage Sfi21 demonstrated *S* (encoded holin), and *R* (encoded endolysin) genes were transcript at the early stage that was determined by northern blotting experiment

The lysis cassette is possessed in many phages but in different aspects. The lysis cassette in $\phi 24_B$ is similar to the lysis cassette in Lambda phage λ which possed *S* gene that enoceds holin, *R* gene that endoces endolysin, and *Rz* and *Rz1* that encode two component spanin. The genes encoding proteins are similar in virulent podophage ϕKT of *E.coli* 4s but in different name which are *29* gene that enoceds holin, *27* gene that endoces endolysin, and *28* that encodes two component spanin. While in phage T1 possesses gene 13 that encodes pinholin, gene 12 that encodes signal arrest release (SAR) endolysin, and gene 11 that encodes unimolecular spanin (Holt et al., 2019). In general, the mechanism action of bacteriophage breaking down the host cell peptidoglycan and hydrolysis the bacterial cell wall is starting by *S* gene encodes the holin protein that forms a micron scale holes in inner membrane (Young, 2013, Young et al., 2000). These holes in the bacterial cytoplasmic membrane permit endolysin which is encoded by *R* gene to move to the periplasm by mechanism called passive diffusion (Park et al., 2007, Pang et al., 2010, Wang et al., 2008, Catalão et

al., 2011, White et al., 2011, Pang et al., 2013). While the holes that are made by pinholin are small and not enough size to pass the SAR endolysin which results a damaging of protons causing a membrane depolarization (Park et al., 2007, Pang et al., 2010, Pang et al., 2013). Endolysin breaks down the host cell peptidoglycan by hydrolysis of the glycoside bond of the MurNac-GlcNac (São-José et al., 2003). The spanin which is encoded by *Rz* and *Rz1*, forms a complex that encages the peptidoglycan network and fuses the outer and inner membrane, as a result, more progeny phages are liberated (Holt et al., 2019).

We suggest a phenotype of *P21* in the induced $\phi 24_B$ by comparing the wild type lysogen $\phi 24_B$::Kan that encodes *P21*, and the mutant type lysogen $\phi 24_B$::KanΔP21::Tet that dose not encodes *P21* in two genetic host *E.coli* background which were MC1061 *E.coli* strain (James et al., 2001a), and TUV 93-0 which is non toxigenic (Chong et al., 2007), Stx prophage deficient derivative of the O157:H7 outbreak strain EDL933 (Perna et al., 2001a). The P21 phenotype has proposed when the result of experiment demonstrates a difference between wild type lysogen and mutant type lysogen in plaques formation, and cell behaviour.

The first experiment was chloroform lysis intracellular phage results a significant difference between wild type phage that reduces a number of release a fewer phage than mutant type phage in both genetic host cell *E.coli* background after approximately 4 hours post induction (Fig. 3.8, Fig. 3.9). Chloroform was added in this experiment to release phage to prove intracellular assembly of phage before cell lysis. The second experiment was LIVE/DEAD® BacLight™ Bacterial Viability results a difference in cell morphology between wild type lysogen and mutant type lysogen by using a SYTO® 9 that was stained live bacteria with intact cell membrane with fluorescence green, and propidium iodide that was stained dead bacteria with compromised membrane fluorescence red in there time points which were 180, 240, and 300 min post induction. The fluorescence microscope images (Fig. 3.16) have limitations which are: there is only one time run this experiment with limited frames of images that make difficult to be qualitative and quantitative results. So, it is suggestion to repeat this experiment again. The third experiment was fluorescence activated cell sorting (FACS) results a difference in cell behaviour between wild type lysogen and mutant type lysogen by using SYBR™ Green I which was stained double-strand DNA of intact cells, and positively charged carbocyanine dye 3,3'dipropylthiadicarbocyanine

iodide ($DiSC_3$(5)) that was stained the live cell at there time points which were 0, 180, and 240 min post induction. The wild type lysogen in MC1061 host *E.coli* background presented a higher number of population of live cells and intact cells than mutant type lysogen in MC1061 host *E.coli* (Fig. 3.17, Fig. 3.18).

These preliminary data of *P21* suggest the way of benefit host cells which is opposite function of the lysis cassette action. *P21* may use structural features to benefit the host cell that may be by *P21* esterase domain or carbohydrate binding domain C-terminal of P21 causing modification host cell's peptidoglycan, as results, the host cell's peptidoglycan may go to the autolysin mechanism that results re-biosynthesis host peptidoglycan, and growth host cells. The C-terminal carbohydrate binding domain was found in lysin A *Mycobacterium* phage D29 (Pohane et al., 2014), *Bacillus anthracis* bacteriophage endolysins PlyL and PlyG (Mo et al., 2012), and *Listeria monocytogenes* phage endolysins Ply118 and Ply500 (Loessner et al., 2002)(Loessner et al., 2002) which their carbohydrate binding domain had interacted with the host cell wall, as a results, the endolysin held in lock status which minimizes the chances of hydrolysis host cell.

The P21 recombinant was collected, and P21 antisera was produced from polyclonal antibody. The P21 antisera was used in experiment of confirming the expression of P21 in wild type lysogen as a primary antibody. The P21 expression was shown in fluorescence microscope in wild type lysogen in MC1061 *E.coli* host background cells (Fig. 3.13).

CHAPTER 4:

CHARACTERISATION OF P21 AT THE HOST CELL ENVELOPE

4.1. Background

4.1.1. Peptidoglycan

The bacterial cell wall is mostly comprised of peptidoglycan. Peptidoglycan is important for keeping the shape, size and rigidity of the cell, especially at cell division (Cava and de Pedro, 2014). The polymeric structure of peptidoglycan also protects the cell from lysis by high osmotic pressure. Peptidoglycan structure is a complex of alternating *N*-acetylglucosamine (GlcNAc) and *N*- acetylmuramic acid (MurNAc) residues joined by β-(1-4)-glycosidic linkages (Vollmer et al., 2008, Hadi et al., 2011). There is a peptide chain that attaches to MurNAc residue that harbours a lactyl ether group on C-3 (Fig. 4.1) (Höltje, 1998). Peptidoglycan is often a target used to control many pathogenic bacteria within the host (Hadi et al., 2011). For example, the target of the *β*-lactam antibiotic penicillin is ultimately peptidoglycan. Penicillin works by irreversibly inhibiting the bacterial penicillin binding proteins which insert and crosslink the nascent peptidoglycan strands in the bacterial cell wall (Höltje, 1998). Peptidoglycan modification also plays an important role in the vitality of bacteria (Weadge and Clarke, 2006). For example, when bacterial cells invade tissues, the host cell releases lysozymes for defence which hydrolyse the glycosidic linkage that binds MurNAc to GlcNAc in peptidoglycan, as a result, the invaded bacteria creates methods of securing and covering its peptidoglycan via many covalent modifications (Clarke and Dupont, 1992).

4.1.2. Impacts of peptidoglycan modifications

Peptidoglycan can be modified and modulated to adapt to alterations in the external environment. Peptidoglycan modification is an essential ability for bacteria in surviving, responding to stress, and developing virulence. As a result, cell wall metabolism is a target of antibacterial studies to manipulate bacterial features, and bacterial invasion. There are many actions of peptidoglycan such as: peptidoglycan modification and morphogenesis, environmental modulation of peptidoglycan,

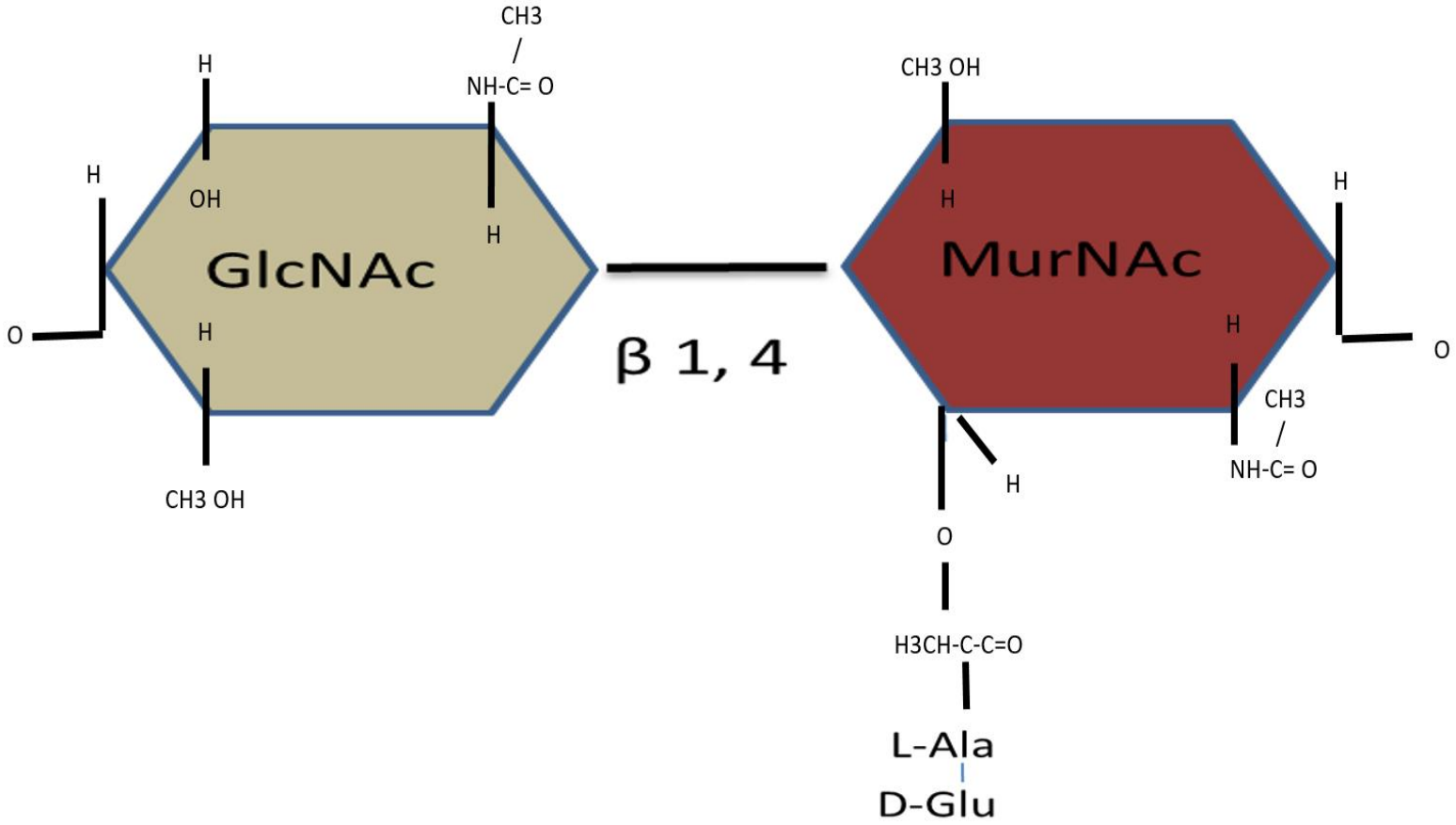

Figure 4. 1. Peptidoglycan structure.

Peptidoglycan, also known as murein, is a polymer consisting of sugars and amino acids that forms a mesh like layer outside the plasma membrane of most bacteria, forming the cell wall. The sugar component consists of alternating residues of β 1-4 linked N-acetylglucosamine and N-acetylmuramic acid residues. Attached to the N-acetylmuramic acid residues is a peptide chain.

interaction with host cells, and peptidoglycan modulation induced by the host cell (Cava and de Pedro, 2014).

4.1.2.1. Peptidoglycan modification and morphogenesis

Nutritional stress can stimulate bacteria to activate specific response mechanisms such as changing bacterial cell shape, size, and peptidoglycan composition (Pisabarro et al., 1985, Glauner et al., 1988, Young, 2006).The pathogenic bacterium *Helicobacter pylori* alters its morphology to coccoid shape subsequent with long term cultivation (Andersen and Rasmussen, 2009) that results in peptidoglycan rearrangment. of peptidoglycan. However, the peptidoglycan in coccoid shape was richer in diasaccharide dipeptide than peptidoglycan in spiral shape, and the peptidoglycan of the coccoid shaped cell has a reduction in cross-linking. Accumulation of dipeptide and promotion of coccoid shape depend on the activation of the amidase AmiA and improve escaping immune system recognitions (Chaput et al., 2006). There is a report on the behaviour of *Vibrio cholerae* and *Vibrio parahaemolyticus* under cold shock and carbon starvation conditions. These results show that the rod shaped cells, which have undergone reductive division, transform to a coccoid shape and are in a viable status. This transformed morphology is associated with a decline in the expression of some genes *e.g. mreB*, *ftsZ,* and *minE,* which rapidly return to normal as the bacterial cells recover (Krebs and Taylor, 2011, Chen et al., 2009). Although, there is no direct peptidoglycan modification in morphogenesis of *Vibrio* organisms, the mentioned genes are implicated with peptidoglycan regulation (Varma and Young, 2009, Potluri et al., 2012, Takacs et al., 2010). The pathogenic bacteria *Listeria monocytogenes*, when examined under osmotic pressure in different habitats, adapts in a temperature dependent manner. There are two genes, *lmo1215* and *lmo1216*, whose transcription is upregulated as part of a short term (50 minutes) adaptation under 6% salt stress at 7°C, to produce a modified peptidoglycan protein called carboxypeptidase (Bergholz et al., 2012).

4.1.2.2. Environmental modulation of peptidoglycan

Environmental response has a direct impact on the modulation of peptidoglycan metabolism in the bacterial cell wall. The presence of antibiotics is one example of an environmental toxin for bacteria. Peptidoglycan modification is involved in sensing and signalling to inhibit the antibiotic action (Cava and de Pedro, 2014). For example, *Staphylococcus aureus* and *Bacillus licheniformis* detected the presence of *β*-lactams

by membrane bound penicillin receptor (BlaR/MecR) that launched the cytoplasmic accumulated peptidoglycan that turn over derived dipeptides. This dipeptide causes inactivation of the BlaR/MecR repressor triggering the synthesis of *β*-lactams or decrease the target affinity (Amoroso et al., 2012). Vancomycin, VanB type, resistance in Gram positive bacteria is associated with peptidoglycan modification through the action of a two component signal transduction system that activates a set of enzymes: a ligase, dipeptidase, and dehydrogenase, which modify the peptidoglycan precursor lipid II that result in resistans to vancomycin (Courvalin, 2006).

4.1.2.3. Peptidoglycan interaction with host cell

Most infections are not caused by a single organism but are in fact the result of a polymicrobial assault. For example, *Pseudomonas aeruginosa* demonstrates increase in virulence when it is co-cultured with Gram-positive bacteria by using the peptidoglycan components shed as a signal of releasing harmful extracellular factors to eukaryotic and prokaryotic cells. It has been shown previously in Drosophila and murine infection models that peptidoglycan sensing leads to *Pseudomonas aeruginosa* induces displacement of Gram positive flora (Korgaonkar et al., 2013).

4.1.2.4. Peptidoglycan modulation induced by host cell

There is a modification that occurs to peptidoglycan (PG) by *O*-acetylation of the C-6 hydroxyl group on the MurNAc residues of peptidoglycan (Fig. 4.2A) in 53 bacterial species such as *Staphylococcus aureus*, *Neisseria gonorrhoeae,* and species of *Enterococcus* (Clarke et al., 2002, Vollmer et al., 2008). This modification inhibits the action of lysozyme on the peptidoglycan substrate by inhibiting binding, blocking lysozymal degradation. It also blocks the action of many bacterial autolysins, and lytic transglycosylase (LTs) (Scheurwater et al., 2008, Blackburn and Clarke, 2001a). However, autolysins and lytic transglycosylases need a free C-6 hydroxyl moiety to form the 1,6-anhydromuramoyl product (Blackburn and Clarke, 2001b). For example, The *ape1* gene in *Neisseria gonorrhoeae* encodes an O-Acetylpeptidoglycan esterase (Ape) enzyme that is responsible for removing the peptidoglycan O-acetyl and acetyl esterase enzyme adds balancing bacterial expression and activities of these enzymes (Fig. 4.2B), as a result, Ape can play role in cell growth and cell division (Weadge and Clarke, 2007, Weadge and Clarke, 2006).

4.1.3. Acetyl esterase activity

Peptidoglycan is not a constant structure; it is broken down repeatedly by autolysins to provide sites for the creation of new peptidoglycan for cell division and growth (Vollmer et al., 2008). To assure effectiveness, this process of damaging and re-growth in many organism includes the turnover and recycling of peptidoglycan metabolites, where released, 1,6-anhydromuropeptides are returned back into the cytoplasm for rework (Park and Uehara, 2008). Autolysins participate in the forming of septa, the site at which cells split at cell division; endospore formation; and germination (Smith et al., 2000). Maintaining cellular integrity against external stressors on the host cell membrane is one primary function of peptidoglycan. As a result, the space between the peptidoglycan strands and other cell membrane components must be tight (Scheurwater et al., 2008). Especially in Gram-negative bacteria, whose sacculus (an envelope with a rigid exoskeleton (Glauner, 1988)) is limited to as little as a signal complete layer of peptioglycan, so its O-acetylation can inhibit any subsequent cell wall metabolism (Weadge and Clarke, 2007). Most bacteria possess some mechanism to control their endogenous autolysins such as: modifying the chemical substrate, physically associated enzymes, the compartmentalization and/or production of specific proteinaceous inhibitors (Clarke et al., 2010).

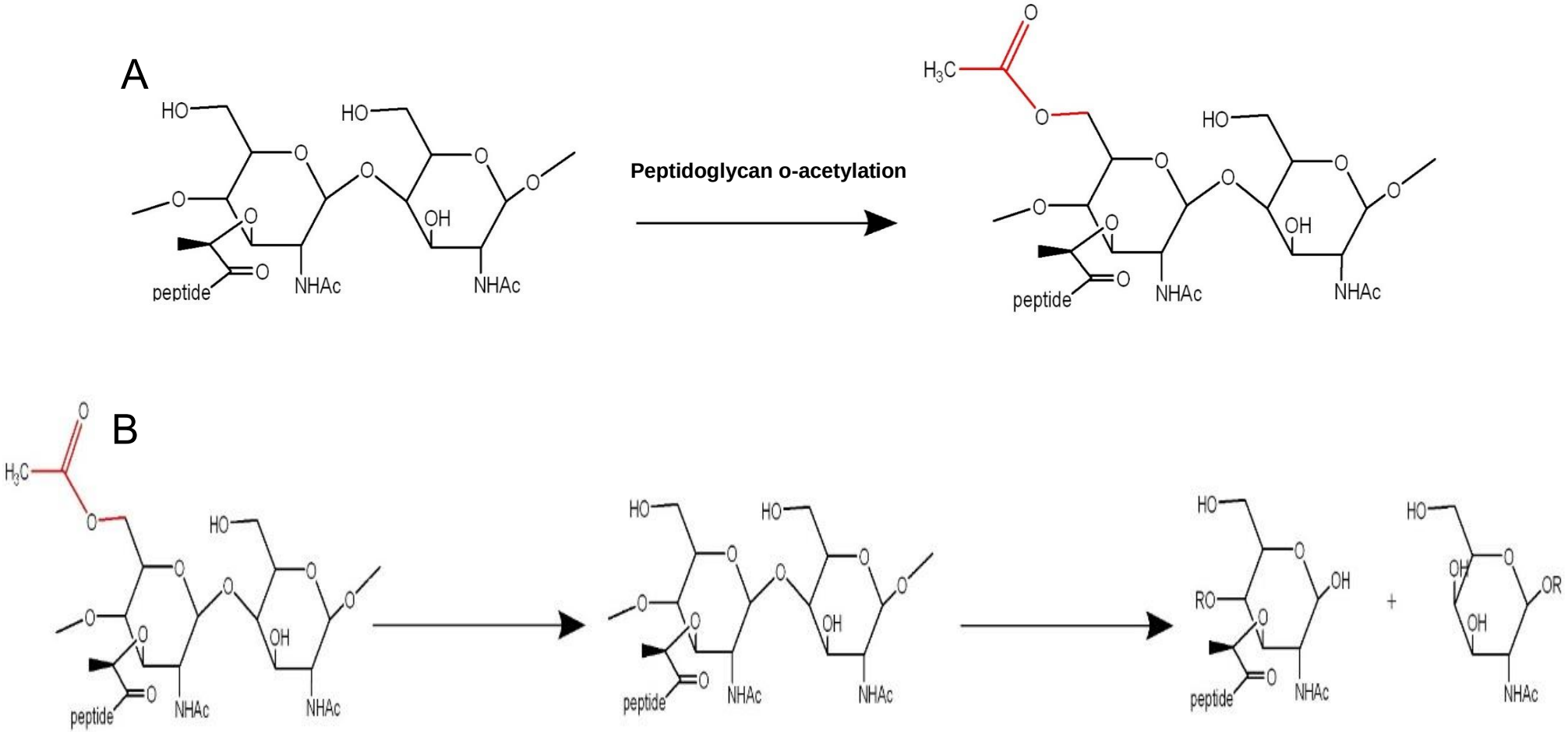

Figure 4. 2. Peptidoglycan structure in acetylation and acetylesterase modification action.

A) Peptidoglycan O-acetylation modification in some bacterial species has occurred at the C-6 hydroxyl group on the MurNAc residues of the peptidoglycan. B) The O-acetylpeptidoglycan esterase had removed this modification on peptidoglycan and then requires a lytic transglycosylase (LTs) that breaks the β-(1—4) linkages nonhydrolytictically to form 1,6-anhydromuramoyl residues.

4.1.4. X-ray crystallographic and bioinformatic analysis of P21

X-ray crystallography and bioinformatics analysis were used to understand the characterization of the P21 three-dimensional structure. The crystallization trials of the P21 production reveals that crystallisation was only possible with the C-terminal domain of P21 (Franke et al., 2020a). The C-terminal domain espouses the extended concanavalin-A-like jelly-roll fold exemplary of lectins (Loris et al., 1998, Brinda et al., 2005) (Fig. 4.3). The jelly-roll domain of P21 shows folding into 12 anti-parallel β –strands that are arrange into linked greek key motifs that formed a β-sandwich packing against each other. The β -sheet was comprised of seven short β –strands linked by prominent, long loops that form a groove on the concave side of the domain. While, a flatter β -sheet composed of five long β -strands connected by short connectors form the other side of the β –sandwich (Franke et al., 2020a).

The jelly-roll fold of the P21 C-terminus was analysed on the SCOP hierarchical database of protein domain structures, and the Pfam sequence database of families and domains, as a result, it is placed under the large superfamily b.29.1, (Concanavalin A-like lectins/glucanases), and clan CL0004 (Concanavalin) respectively. A carbohydrate-binding lectin protein is represented of concanavalin group proteins. Carbohydrate binding was the identified function by the classification on both database programs (Franke et al., 2020a). Although, domains whose concanvalin-like fold have either a catalytic role, and an noncatalytic carbohydrate binding function, the jelly-roll fold of P21 did not possess catalytic residues when it is examined in databases of catalytic site structural programs such as ProFunc (Laskowski et al., 2005), GASS (Moraes et al., 2017), and ASSAM (Nadzirin et al., 2012). Moreover, the three-dimensional structure of the jelly-roll fold of P21 was compared its three-dimensional structure present in the Protein Data Bank using DALI (Holm, 2019) to determine the homology with its structural neighbours. The results demonstrated that the nearest structural relatives share sequence identities of 16–10%. The closest neighbours with bound ligands are the N-terminal lectin domain of *Vibrio cholerae* sialidase, calreticulin of *Entamoeba histolytica*, arabinanase of *Geobacillus stearothermophilus*, a mammalian cargo receptor for the export of glycoproteins from the endoplasmic reticulum, and a canine transporter lectin for the secretion of mannose-rich glycoproteins (Fig. 4.4). The ligand for these structural

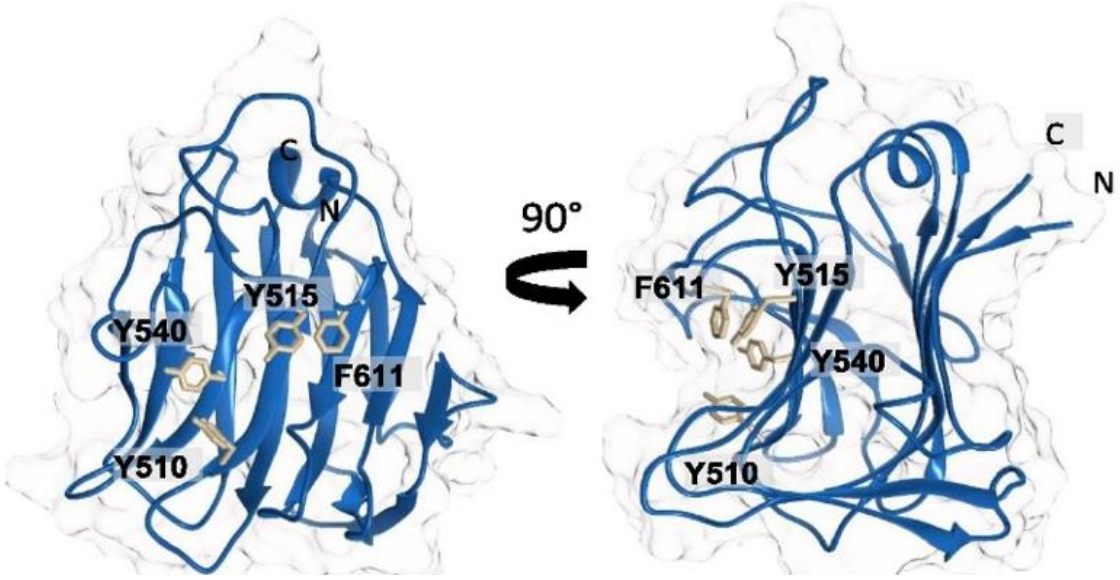

Figure 4. 3. The jelly-roll fold of P21 crystal structure.

The jelly-roll domain of P21 presents folding into 12 anti-parallel β –strands. The β -sheets is contained of seven short β –strands linked by prominent, long loops that form a groove on the concave side of the domain. While, a flatter β -sheet of five long β -strands connected by short connectors form the another side of the β –sandwich. In addition, the jelly-roll fold of P21 has residues in binding grove (F611, Y540, Y515, and Y510). This figure was taken from (Franke et al., 2020a).

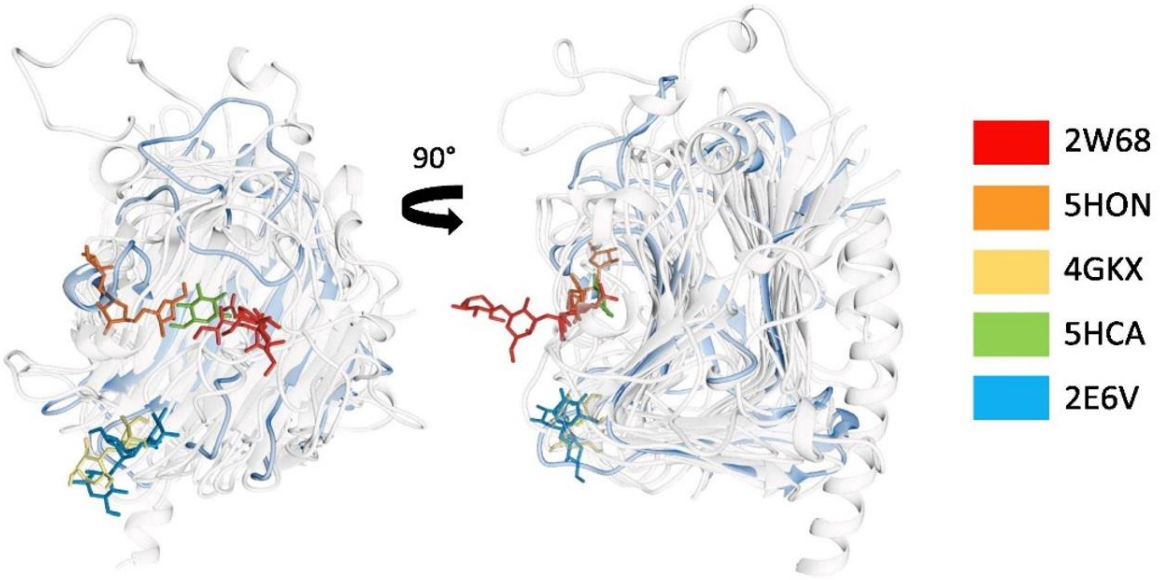

Figure 4. 4. Comparison of the jelly-roll fold of P21 and its structural neighbours.
The jelly-roll fold of P21 has identified the closet ligand bound structural neighbours by using DALI. The ligand bound structural neighbours are the N-terminal lectin domain of Vibrio cholerae sialidase (PDB code 2 W68; DALI Z-score 18.4), Entamoeba histolytica calreticulin (5HCA; Z-score 13.4), a mammalian cargo receptor for the export of glycoproteins from the endoplasmic reticulum (4GKX; Zscore13.5), Geobacillus stearothermophilus arabinanase (5HON; Z-score 13.0), and a canine transporter lectin for the secretion of mannose-rich glycoproteins (2E6V; Z-score 13.2). The jelly-roll fold of P21is presents in blue. This figure was taken from (Franke et al., 2020a).

relatives is a carbohydrate and binding occurs on the concave side of the jelly-roll fold in all neighbours which is seen in the pronounced groove of P21 (Fig. 4.3) (Franke et al., 2020a).

There are two distinct binding site regions for the jelly-roll fold: 1) a groove in the concave face of the β-sandwich, 2) a site within the variable loop cluster for interconnecting the β-strands at one end of the β-sandwich (Abbott and van Bueren, 2014). The structural neighbours of the jelly-roll fold of P21 present bound carbohydrate ligands in the same sites (Fig. 4.4). Crystal structure analysis for surface atom type propensities using STP (Mehio et al., 2010) surface topology in Profunc (Laskowski et al., 2005), and LISE (Xie et al., 2013) (Fig. 4.5A-C) were used to determine the ligand binding sites in the jelly-roll fold of P21. The jelly-roll fold of P21 includes residues in the proposed binding grove which are F611, Y540, Y515, and Y510 (Fig. 4.3). The three Tyr residues which were revealed during the analysis of sequence conservation using Consurf (Ashkenazy et al., 2010), are conserved though Y510 is often changed to a phenylalanine in other homologs (Fig. 4.5D). Moreover, there is a full length of groove that engages in carbohydrate binding (Fig. 4.5E) when the groove was analysed by the ISMBLab server in carbohydrate mode by using probability density distributions. It identified interacting atoms on protein surfaces (Tsai et al., 2012). As a result, the bioinformatics analysis demonstrates the C-terminal domain of P21 that is revealed a lectin like jelly roll β-sandwich fold is suggested to be a carbohydrate binding site without catalytic features (Franke et al., 2020b).

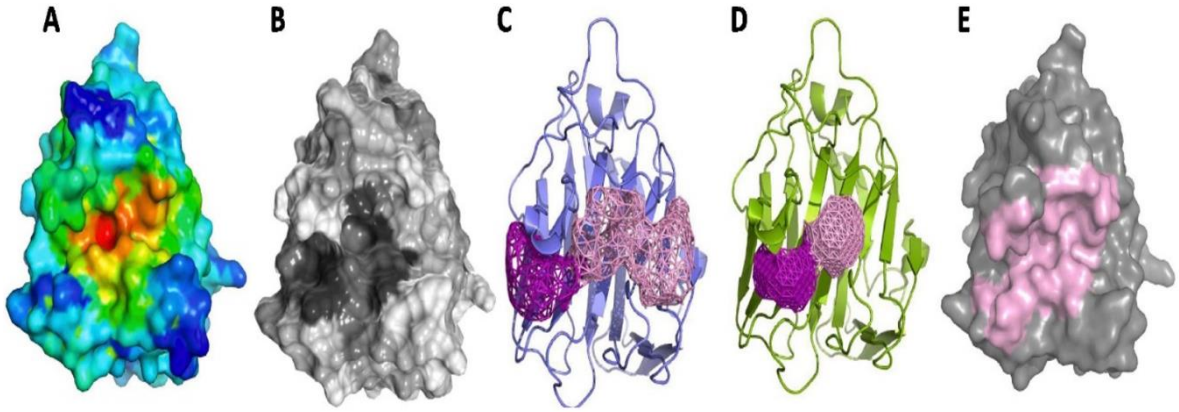

Figure 4. 5. The groove of the jelly-roll fold of P21 is an expected carbohydrate binding region.
A) STP (Mehio et al., 2010) calculation of protein ligand interactions is used to identify the triplets adjacent surface atomic groups. The probability ligand bin of the surface of the jelly-roll fold of P21 is degree coloured from red (highest) to blue (lowest). The highest probability in STP calculation is located around residues Y515 and Y540. B) ConSurf (Ashkenazy et al., 2010) sequence conservation mapping are coloured from white that refers to does not conserved to black that refers to conserve. C) ProFunc (Laskowski et al., 2005) calculation of cavities. The contiguous top cavity is coloured pink, and the second rank cavity is coloured purple that are presented like a wire mesh. D) LISE (Xie et al., 2013) calculation of static enriching at the ligand binding regions to detect of triplets of protein surface atoms. The contiguous top cavity is coloured pink, and the third rank cavity is coloured purple that are presented like a wire mesh. E) The cleft as carbohydrate binding is identified by the ISMBLab server (Tsai et al., 2012). The pink colour refers to all residues in the top-ranking patch. This figure was taken from (Franke et al., 2020a).

4.1.5. Aims

The data in chapter 3 support the hypothesis that P21 gene has an impact on phage release from the bacterial host. The *P21* gene is the most highly conserved gene across all the Stx phages and in genomic context is linked to the lysis cassette. P21 sequence based predictions shows the protein possesses an acetyl esterase domain. The esterase domain is located between the amino terminus that possesses DUF1737, and the carboxyl terminus of the protein has undergone X-ray crystallographic analysis. In this chapter, we:

- Confirm the P21 acetyl esterase activity in *vitro*.
- Determine the binding site of P21 to peptidoglycan of *E. coli*.
- Study the peptidoglycan structure in the wild type and mutant type lysogens.
- Study the P21 activity in peptidoglycan.

4.2. Specific Methods

4.2.1. Biological assay of P21 acetyl esterase activity

Purified recombinant P21 protein (10.9 mg/mL) (2.8) and (2.9) was mixed with three different concentrations (1µM, 3µM, and 10µM) of 4-Methylumbelliferyl acetate (4-MUFac) (Sigma-Aldrich, United States, #M0883). MUFac was dissolved in methanol. Reactions were set up as described (Table 4.1.) incubated at 37°C for 30 min. All samples analysed by Fluorescence spectroscopy (FLUOstar OPTIMA FL) (BMG Labtech, Germany) run at λ_{ex}=360 nm; λ_{em}=499 nm with a reading taken every minute for half hour. (4-MUFac) degradation rates was measured by fluorescence as consequence of product accumulation.

Table 4.1. The volume of materials that contained in every reaction in an acetyl esterase activity assay.

	P21 (1µM)	P21 (3µM)	P21 (10µM)	Control
$NaPO_4$ Buffer (Table. 2.1)	20 µl	20 µl	20 µl	20 µl
P21 protein	1.3 µl	4.2 µl	12.8 µl	_____
H_2O	78.7 µl	75.8 µl	67.2 µl	80 µl
4-MUFac 10 µM	100 µl	100 µl	100 µl	100 µl
Total volume	200µl	200µl	200µl	200µl

4.2.2. Peptidoglycan binding assay

The P21 binding assays were perfromed with purified *E. coli* peptidoglycan (4.2.3.1). Moreover, four competitors were added to the binding assay: N- acetyl glucosamine (Sigma-Aldrich, United Kingdom, # 7512-17-6), N- acetyl muramic acid (Sigma-Aldrich, United Kingdom, # 10597-89-4), bovine serum albumin (Sigma-Aldrich, United Kingdom, # 9048-46-8), and glucose (BDH laboratory supplies, United Kingdom, #K29108014 126). The assays were visualised in an SDS-PAGE gel (2.10), and western blotting by using anti-P21 serum (2.12).

4.2.2.1. P21 binding peptidoglycan assay

A 100 µl of 1 mg mL^{-1} purified peptidoglycan (PG) suspension from *E. coli* strain MC1061 (InvivoGen, United States, #tlrl-pgnek) was centrifuged at (22,000 x g,1h, at RT). The PG pellets were suspended depending upon the binding reaction to be tested. For the positive control sample containing only P21 and peptidoglycan, the

pellets were suspended in 100 µl binding buffer (10 mM Tris/Methylamine, 10 mM $MgCl_2$, 50 mM $NaCl_2$, pH 7.5) with 10 µg of P21 protein. While the negative control sample contained 100 µl binding buffer with 10 µg of P21 protein and no PG. For the samples examining P21 binding to PG in the presence of potential competitors, the pellets were suspended in binding buffer with 10 mg mL^{-1} of competitor in up to100 µl, and 10µg of P21 protein. The samples were centrifuged at (22,000 x g, 1h, at RT), after centrifugation the supernatants were collected (S). The pellets (PG) were washed with 200 µl binding buffer followed by centrifugation at 10,000 x g, 20 min at RT. The supernatants were collected (W). Finally, the pellets (PG) were incubated with 100 µl 2% SDS and stirred for 1h and then centrifuged at 10,000 x g, 20 min at RT and collected the supernatant (T). All the samples were run in an SDS-PAGE gel (2.10) and subjected to western blotting (2.12).

4.2.3. Examination of the interaction of P21 with purified peptidoglycan

Peptidoglycan structure modification in wild and mutant lysogens was examined at different time points in the presence or absence of the gene encoding P21 following prophage induction. The murein of each sample was purified and isolated from the cells and the peptidoglycan was isolated from sacculi and run on High Performance Liquid Chromotography (HPLC) in the lab of Waldemar Vollmer while I was a visiting scholar at the University of Newcastle.

4.2.3.1. Murein isolation and purification from cells

Colonies of every strain (3 to 4) were inoculated in different 10 mL LB broth bottles under antibiotic selective pressure and cultured overnight at 37°C with shaking at 200 r.p.m. The next day, 4 mL of the overnight culture was used to inoculate 400 mL sterile LB broth containing 0.01M $CaCl_2$, which was incubated at 37°C with shaking at 200 r.p.m until the determined time point (Table 4.2). The subcultures were cooled rapidly in ice for 10 min. The cells were harvested by centrifugation at 4225 x g for 30 min at 4°C. The cells were resuspended in 6 mL PBS. The cells suspension was dropped in 6 mL of boiling 8% (w/v) SDS with magnetic stirring for 30 min. The samples were cooled to room temperature. The sacculi of each lysogenic cultures were collected by ultracentrifugation at 90,000 r.p.m. for 45 min at RT. After a couple of SDS free water washings, the pellets were SDS free as determined by the Hayashi Test (335 µl, 7 µl 0.5% methylene blue, 170 µl 0.7 M sodium phosphate buffer pH 7.2 and 1 mL CCl_3). The pellets were suspended in 900 µl 10 mM Tris/HCl with 10 mM NaCl

pH 7.0 with 100 µl of 3.2 M imidazole pH 7. 30 µlα-amylase (10 mg mL^{-1}) was added and incubated for 2 h at 37°C. Then, 20 µl pronase E 10 mg mL^{-1} was added and incubated for 1 h at 60°C. This was followed by the addition of 1 mL of 8% SDS and boilling for 15 min in a heating block. The samples were washed to remove SDS by ultracentrifugation at 90,000 r.p.m. for 45 min at RT. After couple of washings, the pellets were determined to be SDS free by the Hayashi Test. The pelletes were resuspended gently in 400 µl 0.02% NaN_3 and stored in 4°C. The saccule were now isolated.

Table 4.2. The type of lysogenic cultures that were collected for purifying and isolating murein in certain time points.

Lysogenic culture	Time point
MC1061/ ϕ24$_B$::Kan	60 min
MC1061/ ϕ24 B::KanΔP21::Tet	60 min
MC1061/ ϕ24$_B$::Kan	260 min
MC1061/ ϕ24 B::KanΔP21::Tet	260 min
TUV93-0/ ϕ24 $_B$::Kan	60 min
TUV93-0/ ϕ24 $_B$::KanΔP21::Tet	60 min
TUV93-0/ ϕ24 $_B$::Kan	240 min
TUV93-0/ ϕ24 $_B$::KanΔP21::Tet	240 min

4.2.3.2. Peptidoglycan isolation from sacculi

Sacculi samples (150 µl) were mixed with 50 µl 4X buffer (80 mM $NaPO_4$, pH 4.8) along with 20 µl cellosyl (0.5 µg mL^{-1}) and the mixture was incubated at 37°C on a shaker for overnight. The next day, the samples were boiled at 100°C for 10 min in a dry block. Then, the samples were centrifuged at 14,000 r.p.m for 15 min. The supernatants were recovered and the volume reduced to 100 µl in the chilled speed vacuum at -150°C. After that, 100 µl 0.5 M sodium borate, pH 9.0 and a very small volume of solid sodium borohydrate were added and incubated for 30 min at RT followed by centrifugation at 1400 r.p.m. Finally, the samples were adjusted at pH 4.0 with 20% phosphoric acid and stored at -20°C.

4.2.3.3. Assay to monitor recombinant P21 interaction with *E. coli* peptidoglycan

The concentration of P21 was measured (10.9 mg/mL). P21 was assayed in two different buffers one with a pH of 7 (20 mM Mes, 100 mM Nacl pH 7.0), and the other with a pH of 5 (20 mM NaAcetate, 100 mM NaCl pH 5.0). The P21 protein (3.2 µl of 10µM stock) was mixed with 4 µl *E. coli* D456 peptidoglycan, in 10 µl buffer, and 22,8 µl ddH_2O. P21 was not added in a control sample. All samples were incubated overnight at 37°C with shaking at 900 r.p.m. On the second day, the reaction was stopped by boiling the samples at 100°C for 10 min. Followed by the addition of 30 µl 4X buffer (80 mM $NaPO_4$, pH 4.8) and 20 µl cellosyl (0.5 µg/mL) that were incubated at 37°C on a shaker overnight. Finally, the digestion of peptidoglycan was stopped by boiling the samples at 100°C for 10 min. The samples were subjected to centrifugation at 16,000 × g for 10 min, and the supernatants were recovered and reduced in volume to 100 µl in the chilled speed vacuum at -150°C. Then, 100 µl of 0.5 M sodium borate, pH 9.0 and a very small volume of solid sodium borohydrate were added and incubated for 30 min at RT followed by centrifugation at 1400 r.p.m. Finally, the samples were adjusted to pH 4.0 with 20% phosphoric acid and analysed by High Performance Liquid Chromatography (HPLC) using the Glauner method (Glauner, 1988) (4.2.3.4).

4.2.3.4. HPLC using the Glauner method

The principle of this HPLC analysis is based upon the separation of the digested muropeptides on the reserved phase chromatography. This technique uses sodium borohydride-reduced compounds, a reversed phase column (Prontosil 120-3-C18-AQ 3 µm, Bischoff, Germany), a linear gradient elution (solvent A: 50 mM sodium phosphate, pH 4.31 + sodium azide (10 µl of 10% NaN_3/L), and an organic modifier B: 75 mM sodium phosphate, pH 4.95 + 15% MeOH) on the 55ºC. The gradient and effected conditions (such as: pH, ionic strength and temperature) during the separation of the muropeptides form peaks based on retention times. The data were illustrated on Wang Model 700 computer software.

Table 4.3. The setting of percentage for solvent A to solvent B during the HPLC running in flow rate: 0.5ml/min.

Min	Flow rate	%A	%B
0	0.5	100	0
2	0.5	100	0
147	0.5	0	100
147.1	0.5	100	0
187	0.5	100	0

4.3 Results

Recombinant P21 has been shown to possess active acetyl esterase activity before (Veses Garcia, 2010, Franke et al., 2020b). However, in order to confirm that the recombinant protein purified during these studies maintained its enzymatic activity and was therefore likely to be folded in its proper conformation for other further studies; the acetyl esterase activity of P21 purified in this study was assayed.

4.3.1. P21 is an active acetyl esterase

Acetyl esterases are capable of cleaving the ester bond with acetate (Fig. 4.6) of (4-MUFac) that releases fluorescent complex 4-methylumbelliferone (4-MUF). When 4-MUF was mixed with increasing concentrations of P21 (1, 3 & 10 µM, Fig. 4.7). The accumulation of (4-MUF) was increased until the signal was saturated at 6500 µM (Fig. 4.7). It can be seen that (Fig. 4.7) when the concentration of P21 was 10 µM, the accumulation of (4-MUF) reached 6500 µM after 1 minute, and when the concentration of P21 were 3 µM and 1 µM, the accumulation of (4-MUF) reached 6500 µM in 6 min and 7 min respectively. While the control sample that did not have P21 in the reaction shows no accumulation of the fluorescent complex (4-MUF) which means there is no ester bond cleavage 4-MUFac. These data indicate that the purified recombinant P21 is enzymatically active and this activity is comparable to that identified by Marta Veses (Veses Garcia, 2010, Franke et al., 2020b).

Figure 4. 6. Chemical formats.

A) Acetyl group contains a methyl group **(CH_3)** that has a single bond to a carbonyl **(C=O)**. The carbonyl center of an acyl radical has one nonbonded electron with which it forms a chemical bond to the remainder of the molecule (R). B) ESTER Bond featured by carbon atom bounded with a double bond to an oxygen, a single bond to an oxygen, and a chemical bond to reminder of the molecule (R).

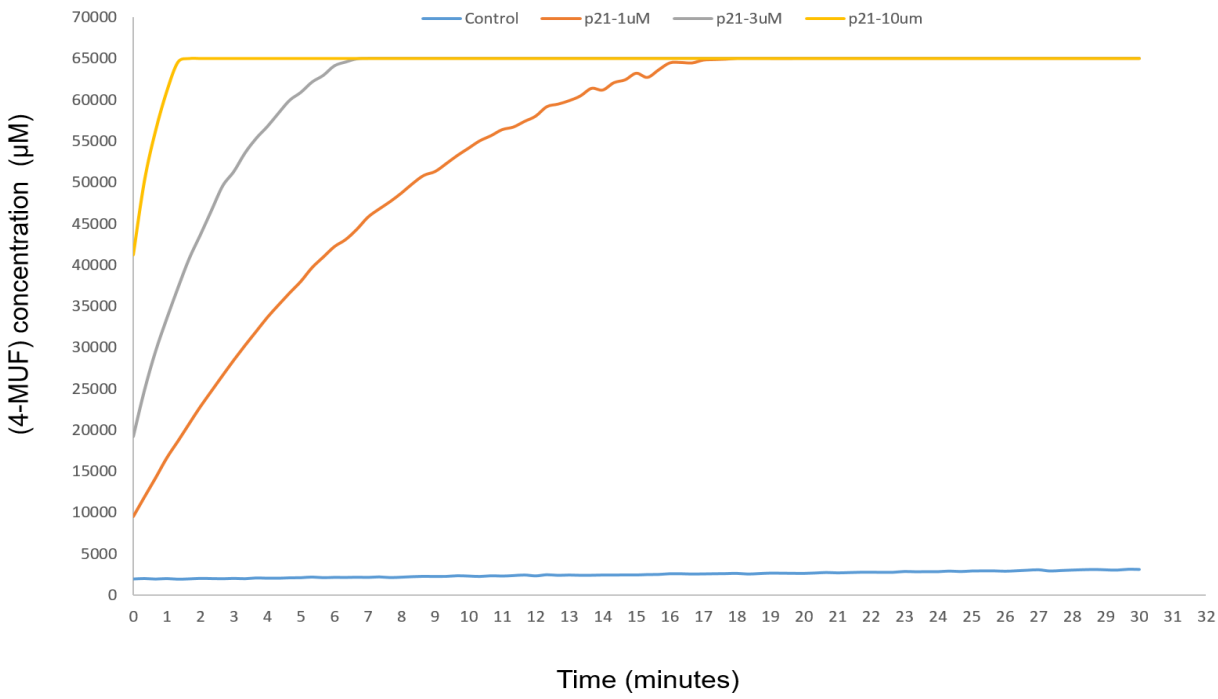

Figure 4. 7. Time analysis of the P21 acetyl esterase activity using 4-MUFac as a substrate.
P21 acetyl esterase activity at three different concentrations P21 (1µM), P21 (3µM), and P21 (10µM) using the 4-MUFac substrate to measure the accumulation of the fluorescent 4-MUF over time. The control reaction did not include P21. The samples were analysed by Fluorescence spectroscopy (FLUOstar OPTIMA FL) (n=1).

4.3.3. P21 binding and recognition to peptidoglycan

Having established in chapter 3 that P21 is linked to the lysis cassette of the Stx phage and that the phenotype of P21 expression is fewer phages released post prophage induction in the culture, which correlates to fewer lysogens actually dying in a culture after prophage induction. Adding to this the acetyl esterase activity of P21 and its likely ability to bind to sugars, its ability to bind directly to peptidoglycan seemed to be the next rational step to investigate. Recombinant P21 used in the peptidoglycan binding assays, was purified from the *E. coli* strain Solu BL21 carrying pETM11 with the cloned *P21* gene. The P21 was demonstrated to bind to peptidoglycan of *E. coli* in (Fig. 4.8) that demonstrates a band of P21 binding peptidoglycan sample (Fig. 4.8 (1P)) which was a collected supernatant after centrifugation (10000 x g, 20 min, RT), and incubation with 100 µl 2% SDS and stirred for 1h. While the negative control sample that does not contain peptidoglycan, there is no band (Fig. 4.8 (6P)). The band that shows in (Fig. 4.8 (6S)) refers to P21 recombinant. However, the P21 also bound to peptidoglycan with the presence the competitors at concentration (10 mg/mL) that were N- acetyl muramic acid (Fig. 4.8 (2P)), N- acetyl glucosamine (Fig. 4.8(3P)), bovine serum albumin (Fig. 4.8 (4P)), and glucose (Fig. 4.8 (5P)).

P21 binding to peptidoglycan in the presence of the 4 potentials competitors was repeated across a much greater range of potential inhibitor concentrations to better understand how P21 might recognise peptidoglycan whose complex structure contains *N*- acetylglucosamine (GlcNAc) and acid *N*- acetylmuramic acid (MurNAc). P21 bound to peptidoglycan with all competitors at all concentrations (5 mg/mL, 10 mg/mL, 20 mg/mL, and 100 mg/mL) (Fig. 4.9).

After the samples were run in the SDS-PAGE, they were transferred to nitrocellulose membrane for western blotting application. The P21 antisera production was used as a primary antibody and Horse Radish Peroxidase [HRP] conjugated anti-Rabbit IgG as a secondary antibody in western blotting. The results of western blotting shows in (Fig. 4.10) that present the bands which were a band of P21 recombinant only (Fig. 4.10 (A, 2)) was assumed as a control for western blotting, a band of P21 binding peptidoglycan of *E. coli* without adding any competitors (Fig. 4.10 (A, 1)), bands of P21 binding peptidoglycan with N- acetyl muramic acid at 4 different concentrations (5 mg/mL, 10 mg/mL, 20 mg/mL, and 100 mg/mL) (Fig. 4.10 (B)), bands of P21 binding peptidoglycan with N- acetyl glucosamine at 4 different

concentrations (5 mg/mL, 10 mg/mL, 20 mg/mL, and 100 mg/mL) (Fig. 4.10 (C)), bands of P21 binding peptidoglycan with glocuse acid at 4 different concentrations (5 mg/mL, 10 mg/mL, 20 mg/mL, and 100 mg/mL) (Fig. 4.10 (C)), and bands of P21 binding peptidoglycan with bovine serum albumin at 4 different concentrations (5 mg/mL, 10 mg/mL, 20 mg/mL, and 100 mg/mL) (Fig. 4.10 (D)). These bands were analysed by ImageJ (LOCI, University of Wisconsin, United States). The method of band analysis was measured the band intensity of P21 binding peptidoglycan by comparing its intensity to intensity of P21 recombinant band. Then, every band of P21 binding peptidoglycan with competitor at each concentration was separately measured by comparing its intensity to intensity of P21 binding peptidoglycan. Followed by statistical analysis that presented the results as mean ± standard error of mean (SEM) for three independent biological replicate, and statistical inferences on data were performed using t test followed by correct for multiple comparisons using the Holm-Sidak method (5 mg/mL concentration vs 100 mg/mL concentration).

However, as the concentration of N- acetyl muramic acid has increased, the band intensity percentage of P21 binding peptidoglycan western blotting is decreased. Differences are considered statistically significant when $p<0.001$ (Fig. 4.11). As a result, the P21 recognition of peptidoglycan is decreased with increasing volume of N-acetyl muramic acid. N- acetyl muramic acid has behaved as an inhibitor; it appears to block P21 from binding to peptidoglycan, which suggests that this might be all or part of the peptidoglycan cell wall component recognised by P21. In contrast as the concentration of N- acetyl glucosamine increased, the band intensity percentage of P21 binding peptidoglycan western blotting is increased. Differences are considered statistically significant $p<0.01$ when (5 mg/mL concentration vs 100 mg/mL concentration) (Fig. 4.12). As a result, the P21 recognition of peptidoglycan is increased with increasing volume of N- acetyl glucosamine. N- acetyl glucosamine has not behaved like an inhibitor, it has behaved more like a “glue” enhancing binding of P21 to peptidoglycan. Moreover, as the concentration of glucose has increased, the band intensity percentage of P21 binding peptidoglycan western blotting is increased, behaving similarly to N- acetyl glucosamine. Differences are considered statistically significant $p<0.001$ when (5 mg/mLconcentration vs 100 mg/mLconcentration) (Fig. 4.13). As a result, the P21 recognition of peptidoglycan is increased with increasing

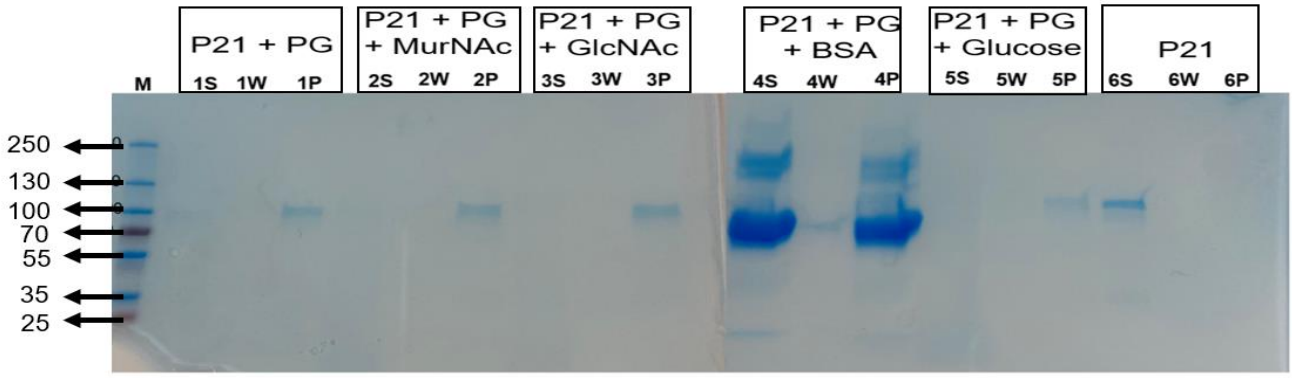

Figure 4. 8. SDS-PAGE gel of P21 binding peptidoglycan (PG) with 4 competitors.

The PG does not separate in the SDS-PAGE gel nor is the PG soluable in the reaction tubes during these assays. Only proteins that have bound to the PG can be seen in this assay. Lanes **M**) Page Ruler Plus (ThermoFisher). **1S**) Supernatant that was collected after centrifugation of samples that contains 1 mg/mL purified PG in binding buffer up to100 µl, and 10 µg of P21 protein. **1W**) Supernatant that was collected after centrifugation of washed samples by binding buffer. **1P**) Supernatant that was collected after centrifugation of samples that were incubated with 2% SDS and stirred for 1h. **2S**) Supernatant that was collected after centrifugation of samples that contains 1 mg/mL purified PG in binding buffer, and 10 mg/mLof N- acetyl muramic acid up to100 µl, and 10 µg of P21 protein. **2W**) Supernatant that was collected after centrifugation of washed samples by binding buffer. **2P**) Supernatant that was collected after centrifugation of samples that were incubated with 2% SDS and stirred for 1h. **3S**) supernatant that was collected after centrifugation of samples that contains 1 mg/mL purified PG in binding buffer, and 10 mg/mLof N- acetyl glucosamine up to100 µl, and 10µg of P21 protein. **3W**) Supernatant that was collected after centrifugation of washed samples by binding buffer. **3P**) Supernatant that was collected after centrifugation of samples that were incubated with 2% SDS and stirred for 1h. **4S**) Supernatant that was collected after centrifugation of samples that contains 1 mg/mL purified PG in binding buffer, and 10 mg/mL of BSA up to100 µl, and 10µg of P21 protein. **4W**) Supernatant that was collected after centrifugation of washed samples by binding buffer. **4P**) Supernatant that was collected after centrifugation of samples that were incubated with 2% SDS and stirred for 1h. **5S**) Supernatant that was collected after centrifugation of samples that contains 1 mg/mL purified PG in binding buffer, and 10 mg/mL of glucose up to100 µl, and 10µg of P21 protein. **5W**) Supernatant that was collected after centrifugation of washed samples by binding buffer. **5P**) Supernatant that was collected after centrifugation of samples that were incubated with 2% SDS and stirred for 1h. **6S**) Supernatant that was collected after centrifugation of samples that contains 10µg of P21 protein only in binding buffer up to100 µl, and. **6W**) Supernatant that was collected after centrifugation of washed samples by binding buffer. **6P**) Supernatant that was collected after centrifugation of samples that were incubated with 2% SDS and stirred for 1h.

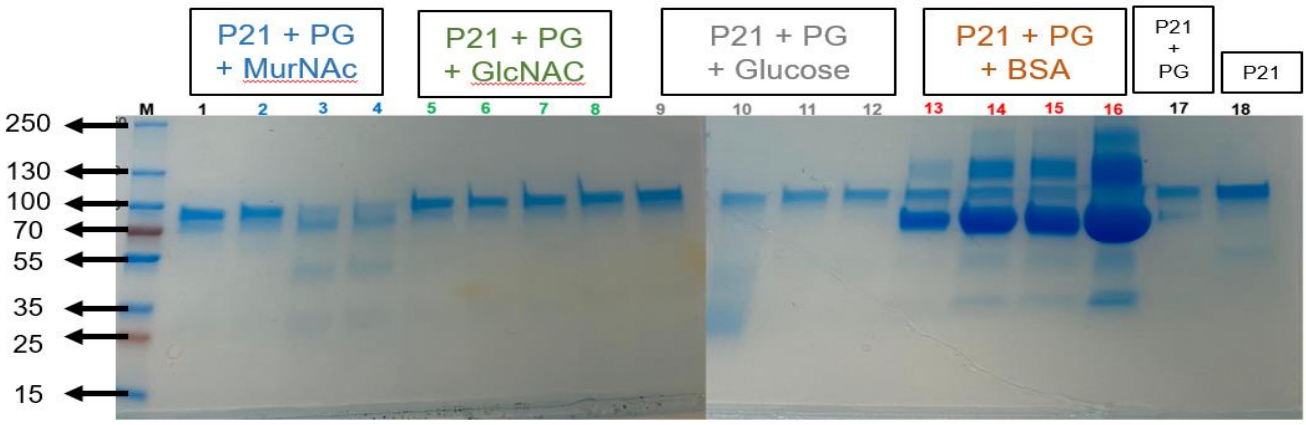

Figure 4. 9. SDS-PAGE gel of P21 binding peptidoglycan (PG) with and without 4 competitors at 4 different concentrations.

Lanes M) Page Ruler Plus (ThermoFisher). **1**) P21 binding PG with 5 mg/mL N- acetyl muramic acid. **2**) P21 binding PG with 10 mg/mL N- acetyl muramic acid. **3**) P21 binding PG with 20 mg/mL N- acetyl muramic acid. **4**) P21 binding PG with 100 mg/mL N- acetyl muramic acid. **5**) P21 binding PG with 5 mg/mL N- acetyl glucosamine. **6**) P21 binding PG with 10 mg/mL N- acetyl glucosamine. **7**) P21 binding PG with 20 mg/mL N- acetyl glucosamine. **8**) P21 binding PG with 100 mg/mL N- acetyl glucosamine. **9**) P21 binding PG with 5 mg/mL glucose. **10**) P21 binding PG with 10 mg/mL glucose. **11**) P21 binding PG with 20 mg/mL glucose. **12**) P21 binding PG with 100 mg/mL glucose. **13**) P21 binding PG with 5 mg/mL bovine serum albumin. **14**) P21 binding PG with 10 mg/mL bovine serum albumin. **15**) P21 binding PG with 20 mg/mL bovine serum albumin. Lane **16**) P21 binding PG with 100 mg/mL bovine serum albumin. **17**) P21 binding PG with no competitors adding. **18**) recombinant P21, only.

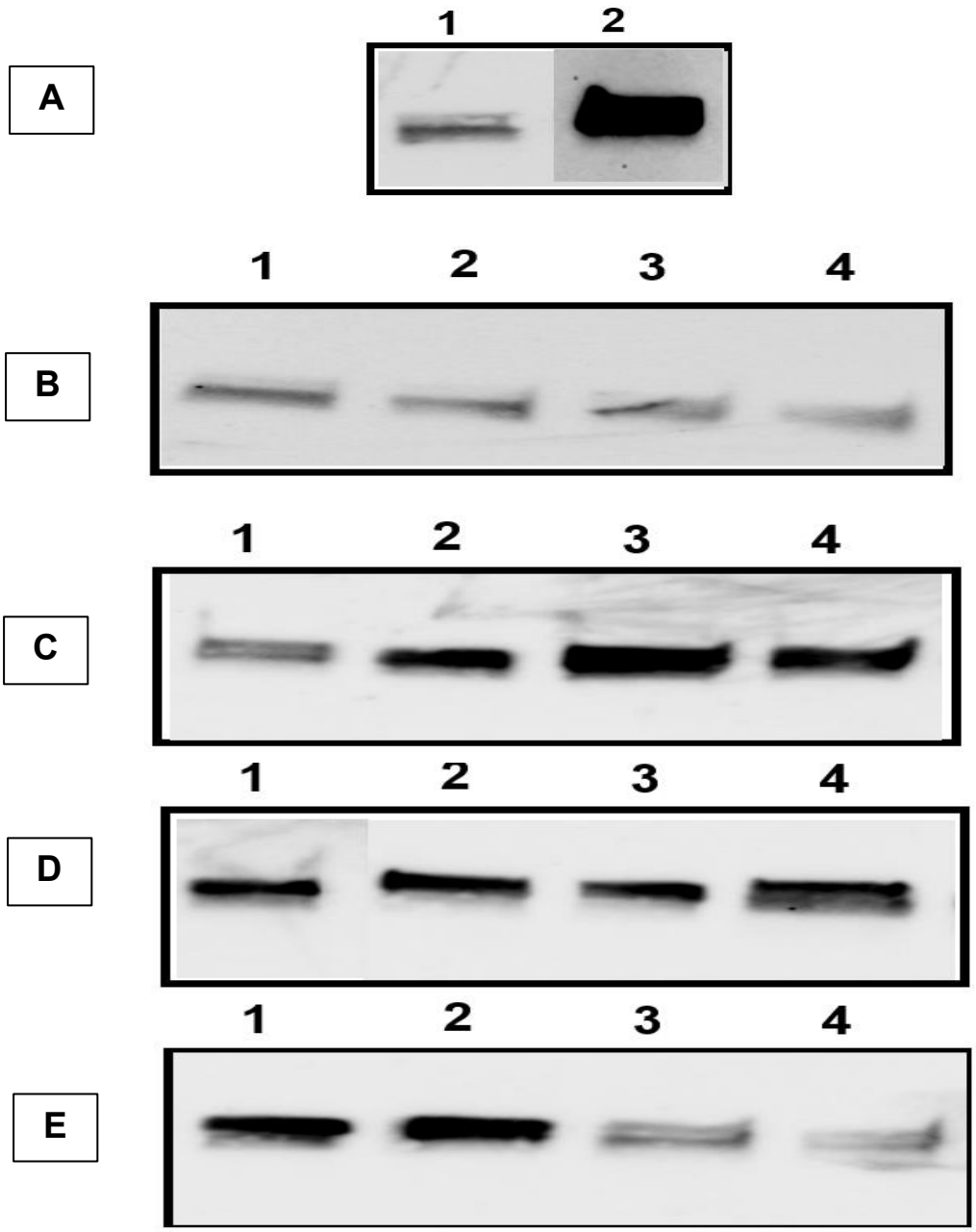

Figure 4. 10. Western blotting of P21 binding peptidoglycan (PG) and peptidoglycan with 4 competitors at 4 different concentrations of competitors.

A) P21 binding PG (lane 1), and P21 recombinant (lane 2). B) P21 binding PG with N- acetyl muramic acid at (5, 10, 20, and 100 mg/ml) from lane 1 to lane 4 respectively. C) P21 binding PG with N- acetyl glucosamine at (5, 10, 20, and 100 mg/ml) from lane 1 to lane 4 respectively. D) P21 binding PG with glucose at (5, 10, 20, and 100 mg/ml) from lane 1 to lane 4 respectively. E) P21 binding PG with bovine serum albumin at (5, 10, 20, and 100 mg/ml) from lane 1 to lane 4 respectively.

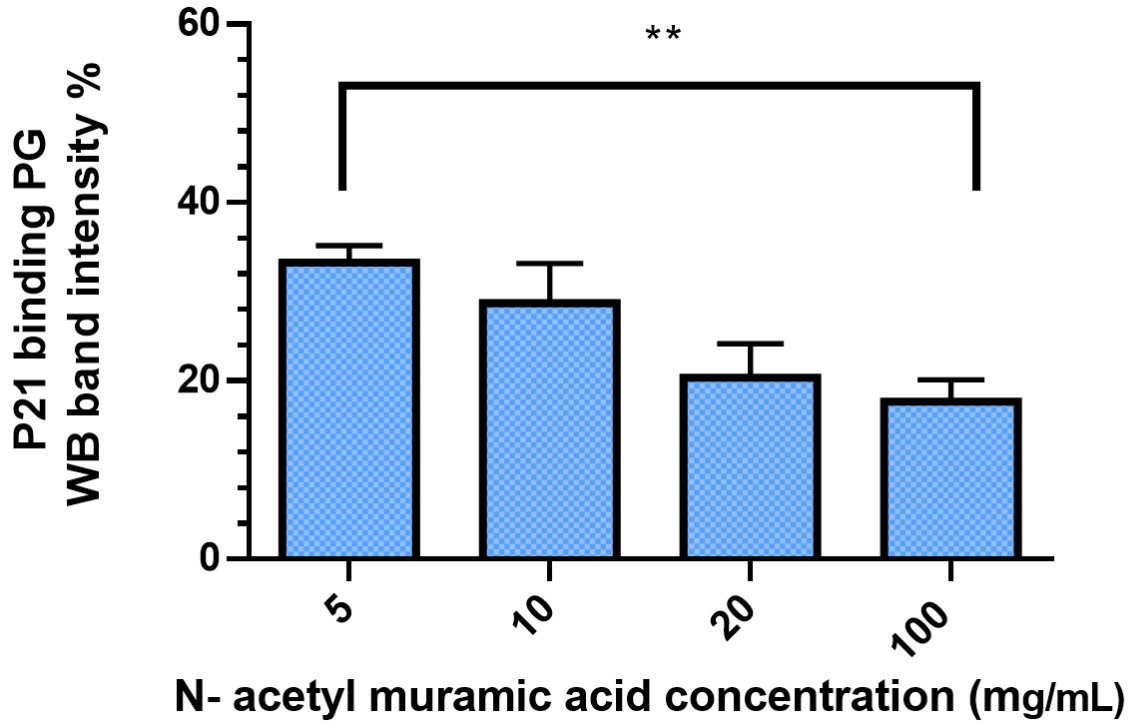

Figure 4. 11. Band intensity western blotting (WB) analysis of P21 binding peptidoglycan (PG) with N- acetyl muramic acid at 4 different concentrations.

The P21 bind to PG with that was compared in 4 different concentrations of N- acetyl muramic acid which were (5 mg/ml, 10 mg/ml, 20 mg/ml, and 100 mg/ml). After the samples were applied in western blotting, the bands intensity was analysed by ImageJ (LOCI, University of Wisconsin, United States). Significance was measured by t test and was indicated above the x axes (**P < 0.001). The error bars represent standard error of the mean (n=3).

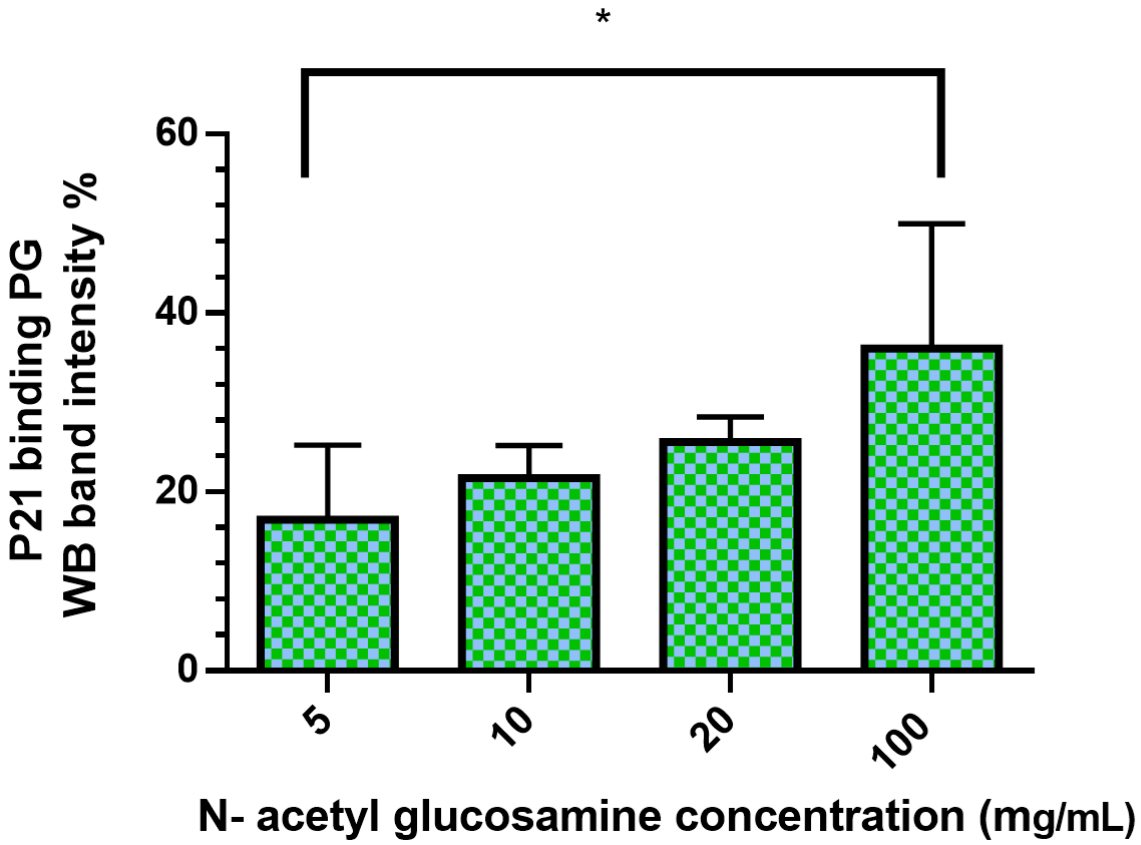

Figure 4. 12. Band intensity western blotting (WB) analysis of P21 binding peptidoglycan (PG) with N- acetyl glucosamine at 4 different concentrations.

The P21 bind to PG with that was compared in 4 different concentrations of N- acetyl glucosamine which were (5 mg/ml, 10 mg/ml, 20 mg/ml, and 100 mg/ml). After the samples were applied in western blotting, the bands intensity was analysed by ImageJ (LOCI, University of Wisconsin, United States). Significance was measured by t test and was indicated above the x axes (*P < 0.01). The error bars represent standard error of the mean (n=3).

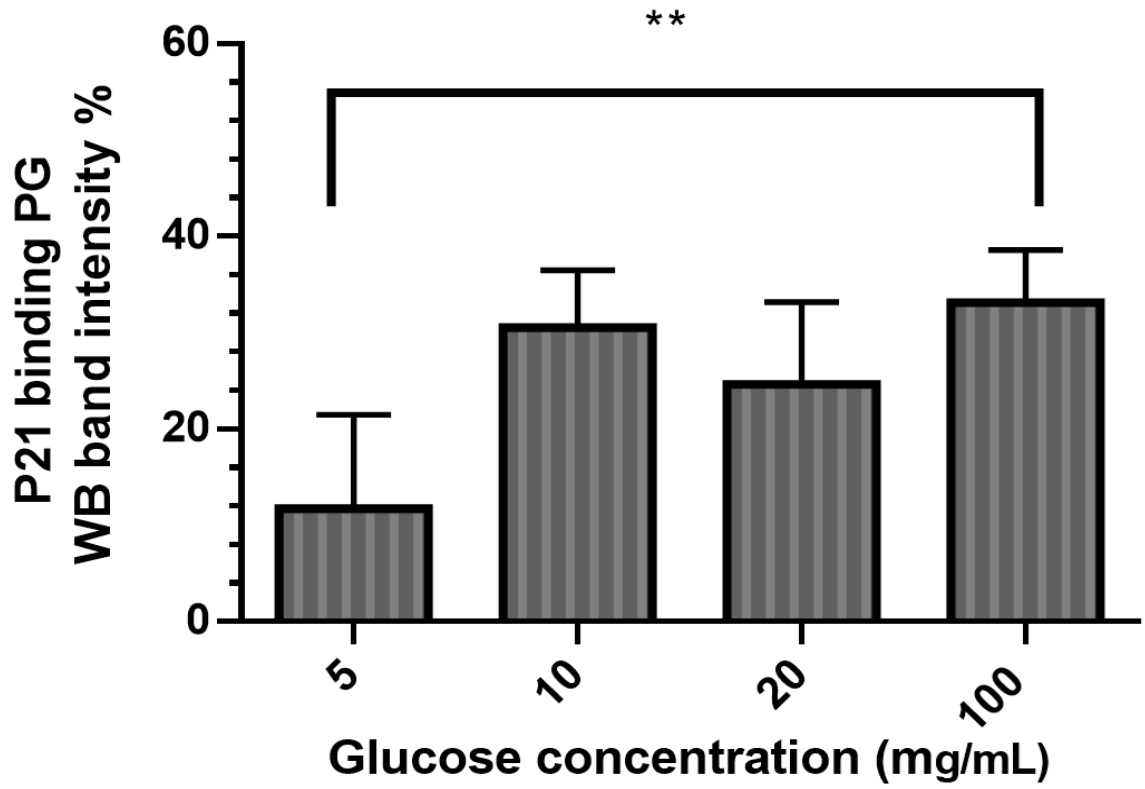

Figure 4. 13. Band intensity western blotting (WB) analysis of P21 binding peptidoglycan (PG) with glucose at 4 different concentrations.

The P21 bind to PG with that was compared in 4 different concentrations of glucose which were (5 mg/ml, 10 mg/ml, 20 mg/ml, and 100 mg/ml). After the samples were applied in western blotting, the bands intensity was analysed by ImageJ (LOCI, University of Wisconsin, United States). Significance was measured by t test and was indicated above the x axes (**P < 0.001. The error bars represent standard error of the mean (n=3).

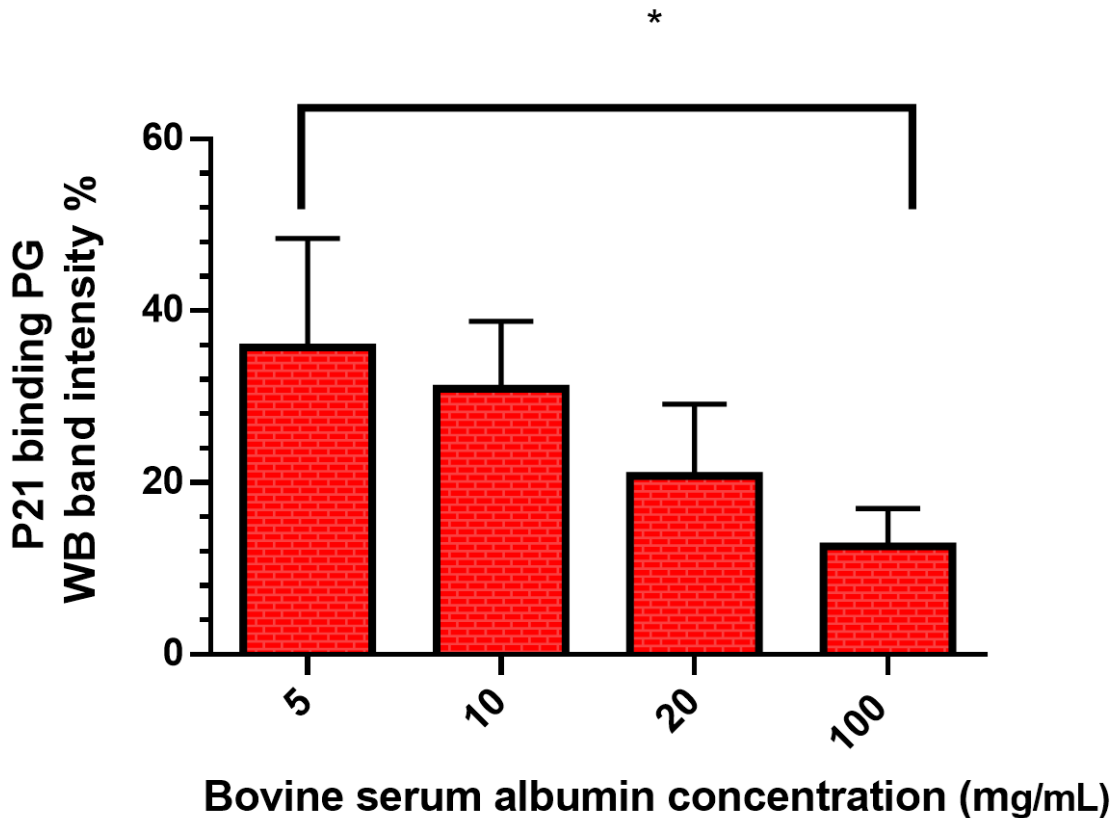

Figure 4. 14. Band intensity western blotting (WB) analysis of P21 binding peptidoglycan (PG) with bovine serum albumin at 4 different concentrations.

The P21 bind to PG with that was compared in 4 different concentrations of bovine serum albumin which were (5 mg/ml, 10 mg/ml, 20 mg/ml, and 100 mg/ml). After the samples were applied in western blotting, the bands intensity was analysed by ImageJ (LOCI, University of Wisconsin, United States). Significance was measured by t test and was indicated above the x axes (*P < 0.01). The error bars represent standard error of the mean (n=3).

volume of glucose. While as the concentration of bovine serum albumin has increased, the band intensity percentage of P21 binding peptidoglycan western blotting is decreased. Differences are considered statistically significant $p<0.01$ when (5 mg/mL concentration vs 100 mg/mL concentration) (Fig. 4.14). As a result, the P21 recognition of peptidoglycan is decreased with increasing volume of bovine serum albumin.

4.3.4. P21 HPLC analysis

The *P21* expression phenotype on the induced $\phi 24_B$ lysogen cells was suggested in previous experiments in chapter 3 that were demonstrated three differences (plaque formation, cell morphology, and cell population) than the induced $\phi 24_B$ lysogen cells that does not encode P21. These data let us to think for studying and understanding the structure of peptidoglycan lysogen in presence or absence encoding P21. The muropeptide analyses results of lysogen samples that were run on HPLC have not showed any modification in retention time of peaks but there is one difference that is observed which is an extra single peak that appears in the elution profile of muropeptides wild type lysogens MC1061/ $\phi 24_B$::Kan (Fig. 4.15 A and B), and TUV93-0/ $\phi 24_B$::Kan (Fig. 4.16 A and B) at both time points 60 and 240 min post induction, while the mutant type lysogens MC1061/ $\phi 24_B$::KanΔP21::Tet (Fig. 4.15 C and D), and TUV93-0/ $\phi 24_B$::KanΔP21::Tet (Fig. 4.16 C and D) at time points 60 and 240 min post induction. As a result, the composition of muropeptides in murein were the same and were not modified in the presence or absence of P21. However, The wild type lysogen MC1061/ $\phi 24_B$::Kan, 60 min post induction, was used an example to describe the muropeptides peaks visible after the separation method which was dependent on sodium borohydride reduction and reverse phase chromatography on C18 columns (Fig 4.17). The extra single peak that appears in wild type lysogen muropeptides is located in peak 16 which is unknown structure. Although, P21 has been shown to bind to the peptidoglycan of *E. coli*, there were no modifications to the peptidoglycan in the presence of P21 (Fig 4.17). The muropeptides structure of *E. coli* D456 did not show any change or modification in the presence P21 under either pH 5.0 or pH 7.0 conditions (Fig. 4.18).

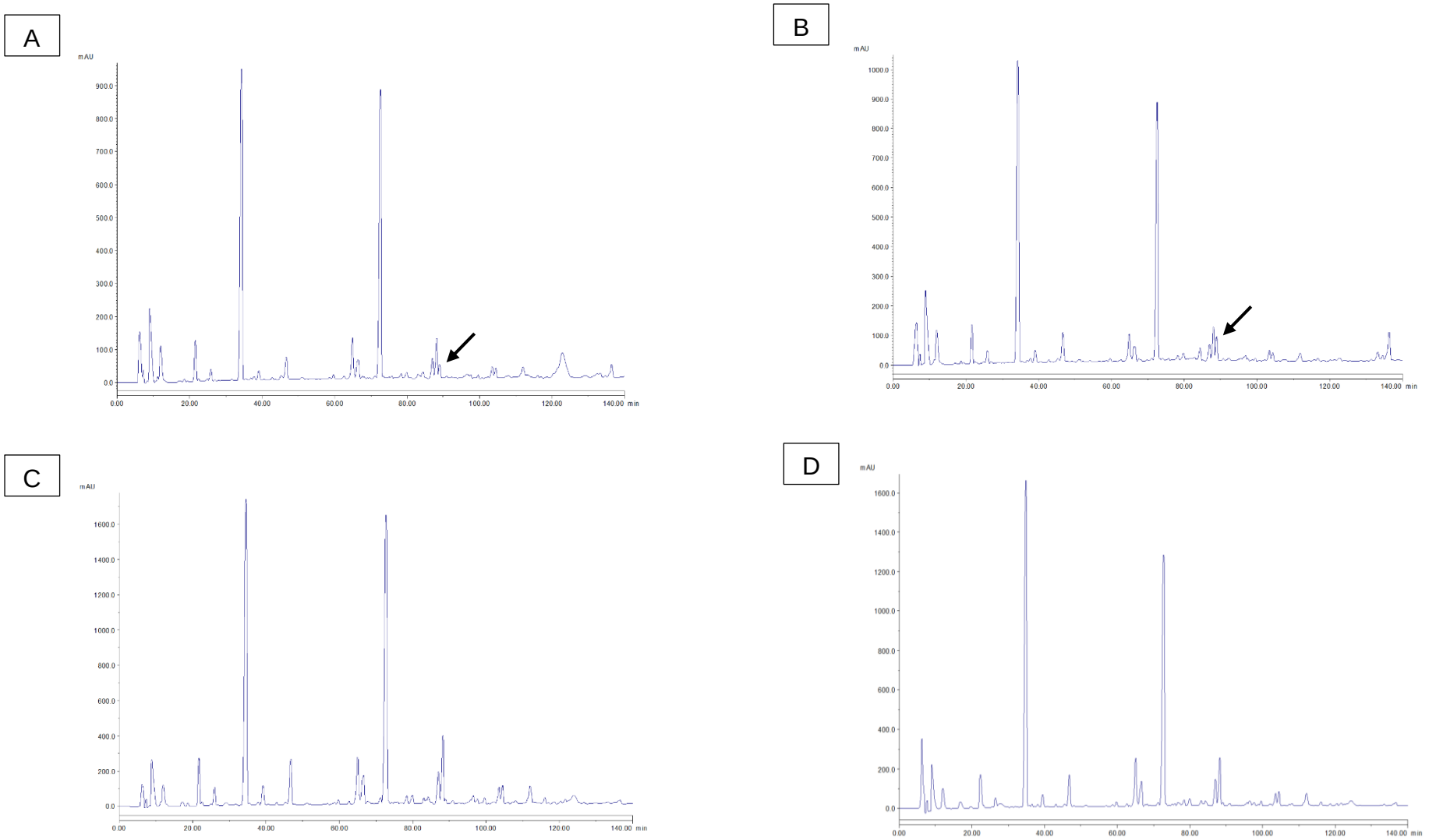

Figure 4. 15. Elution profile of muropeptides from wild type lysogen and mutant type lysogen in an MC1061 genetic background resulted by HPLC.
A) Muropeptides structure of wild type lysogen MC1061/ $\phi 24_B$::Kan in 60 min post induction. B) Muropeptides structure of wild type lysogen MC1061/ $\phi 2_B$::Kan in 240 min post induction. C) Muropeptides structure of mutant type lysogen MC1061/ $\phi 24_B$::KanΔP21::Tet in 60 min post induction. D) Muropeptides structure of mutant type lysogen MC1061/ $\phi 24_B$::KanΔP21::Tet in 240 min post induction. HPLC monitored the separation of the muropeptides were form peaks based on retention times. The black arrows in A and B refer to the extra single peak that presents in muropeptides structure of wild type lysogen in 60 and 240 min post induction. The data were illustrated on a Wang Model 700 software.

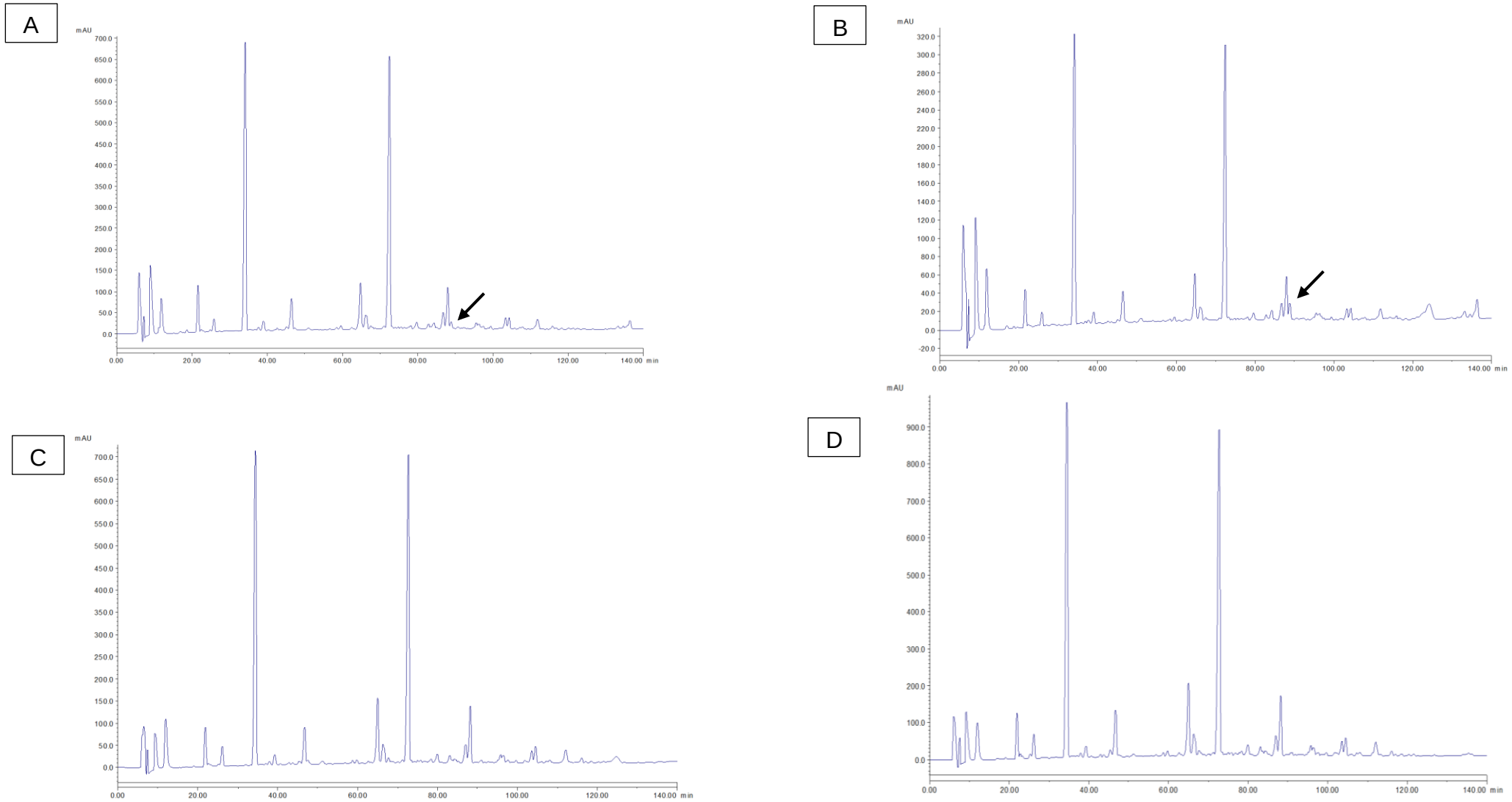

Figure 4. 16. Elution profile of muropeptides from wild type lysogen and mutant type lysogen in an TUV93-0 genetic background resulted by HPLC.
A) Muropeptides structure of wild type lysogen TUV93-0/ ϕ24$_B$::Kan in 60 min post induction. B) Muropeptides structure of wild type lysogen TUV93-0/ ϕ24$_B$::Kan in 240 min post induction. C) Muropeptides structure of mutant type lysogen TUV93-0/ ϕ24$_B$::KanΔP21::Tet in 60 min post induction. D) Muropeptides structure of mutant type lysogen TUV93-0/ ϕ24$_B$::KanΔP21::Tet in 240 min post induction. HPLC monitored the separation of the muropeptides were form peaks based on retention times. The black arrows in A and B refer to the extra single peak that presents in muropeptides structure of wild type lysogen in 60 and 240 min post induction. The data were illustrated on a Wang Model 700 software.

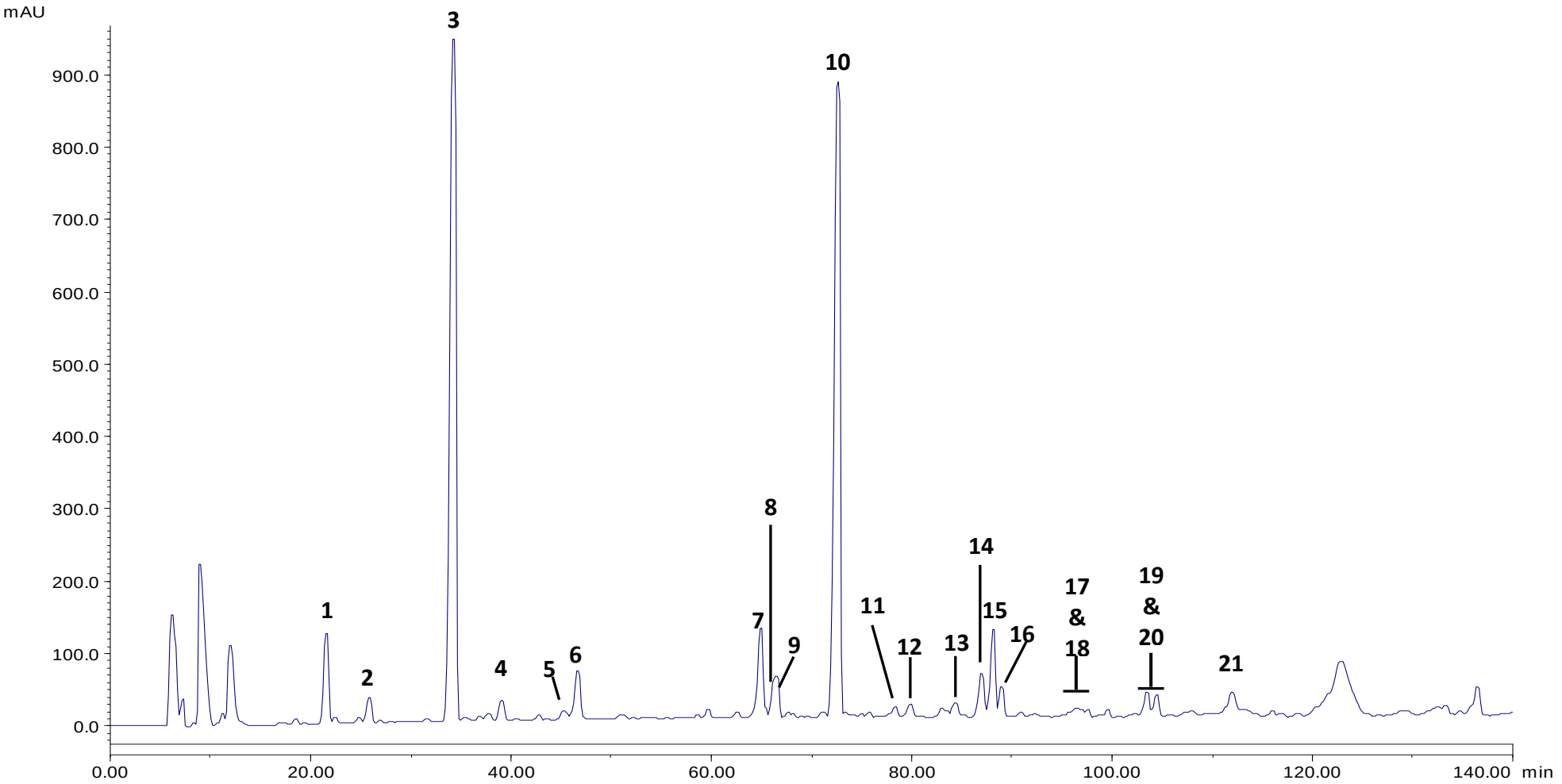

Figure 4. 17. Separation of wild type lysogen MC1061/ $\phi 24_B$::Kan in 60 minutes post induction muropeptides by HPLC.

Peaks were identified the muropeptide structure based on retention time. 1= Tri, 2= Tetra Gly4, 3=Tetra, 4= Di, 5= Penta, 6= Tri-LysArg, 7= TetraTri(Dap), 8= TetraTetraGly, 9= TetraTri, 10= TetraTetra, 11= TetraPenta, 12= TetraAnh, 13= TetraTetraTri, 14= TetraTri Lys Arg, 15= TetraTetraTetra, 16= Unknown, 17= TetraTri AnhI, 18= TetraTri AnhII, 19= TeraTetraAnh I, 20= TeraTetraAnh II and 21= TetraTetraTetra Anh. The samples were run on HPLC using Glauner method (run in column C18, temperature 55°C and flow rate 0.5ml/min for 120 minutes).

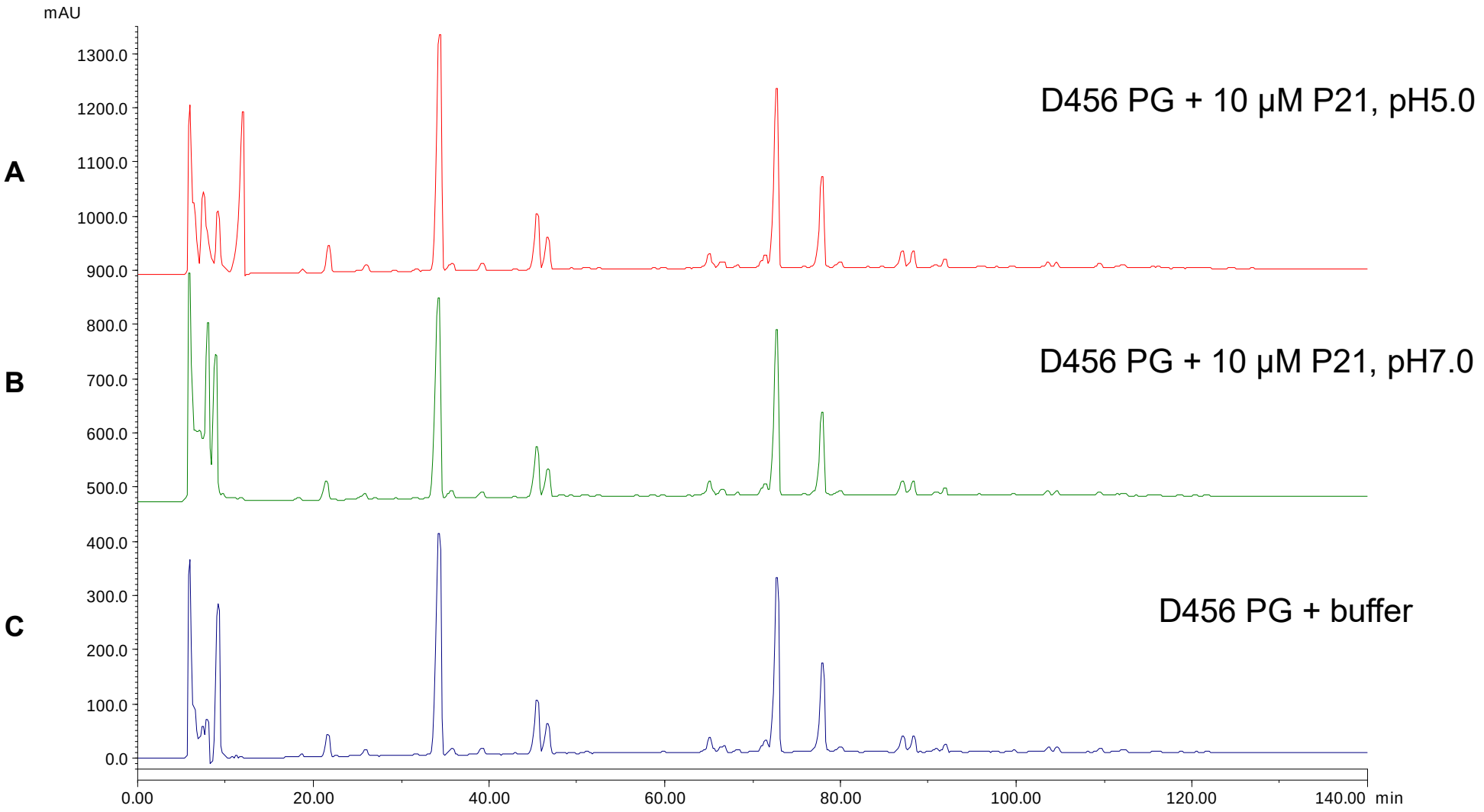

Figure 4. 18. Elution profile of muropeptides from *E. coli* D456 resulted by HPLC.

A) Muropeptides structure of *E. coli* D456 that were assayed and incubated with 10 µM P21 at pH 5.0. B) Muropeptides structure of *E. coli* D456 that were assayed and incubated with 10 µM P21 at pH 7.0.C) Muropeptides structure of *E. coli* D456 that was a control sample. HPLC monitored the separation of the muropeptides were form peaks based on retention times. The data were illustrated on a Wang Model 700 software.

4.4. Discussion

When the project started in 2017, the *P21* gene was the most highly conserved gene across all the Stx phages, but there was no *P21* gene homolog associated with lambda phage λ (Christie et al., 2012). Recently, the new Stx phages are discovered that lack *P21* on the *stx* regions such as Stx2d phage 2595 (Zuppi et al., 2020). The *P21* gene in $\phi 24_B$ size is 1938 bp. The structure of P21 was studied to try and aid prediction of its function. In this work the 645 amino acid protein was described as having three domains: 1) a domain unknown function (DUF1737) at the extreme N-terminus from residues 1 to 72, 2) an esterase domain from residues 73 to 392 and 3) a newly identified jelly roll domain at the C-terminus from residues 393 to 645, which was specifically identified by solving the its crystal structure (Franke et al., 2020a). Although, DUFs are often highly conserved across many viruses and bacteria, it may not be possible to assign function due to the lack of biochemical analyses of any known homologue predicting a biological function (Häuser et al., 2012). Others have minimal data supporting function. DUF 143 which is often found at the N-terminus of *E.coli* genes, is predicted to be a ribosomal silencing factor which inhibits the assembly of the ribosomal subunits and might block post-transcriptional expression (Häuser et al., 2012). So, it is possible that DUF1737 in *P21* may have an impact on the biological function of P21, which might be determined by making mutatns lacking this domain specifically.

Prior to this work, *P21* homologs were named NanS-p due to their partial sequence shared with the chromosomally encoded *nanS* gene and the fact that these genes were always associated with prophages (Franke et al., 2020a). The endogenous NanS esterase of *E. coli* was used as a homology model for the esterase domain of P21 because of its relative homology to P21 (57% seq. id., 68% conservation). NanS recently ranks as in the non-classified group of the Carbohydrate-Active Enzyme (CAZy) database. Moreover, the crystal structure of the P21 C-terminal domain showed a lectin-like, jelly-roll β-sandwich fold, and bioinformatic analysis of the P21 C-terminus presented a carbohydrate binding site with no any catalytic features (Franke et al., 2020a), so it might be expected that the esterase and the jellyroll domains work together to make a fully functional enzyme.

The chromosomal *NanS* gene is part of *nanCMS* operon (Rangarajan et al., 2011, Steenbergen et al., 2009) and the esterase it encodes is involved in the

monodeacetylation of 5-*N*-acetyl-9-*O*-acetyl neuraminic acid (Saile et al., 2018a). It has been demonstrated that a biological function of NanS is cleaving the acetyl residues from bovine submaxillary gland mucin and 5-N-acetyl-9-O-acetylneuraminic acid (Neu5,9Ac2). This results in Neu5,9Ac2 being metabolised to N-acetylneuraminic acid (Neu5Ac) (Nübling et al., 2014, Saile et al., 2016a). The bacterial host cell is then able to take up the N-acetylneuraminic acid and utilise this sialic acid as an energy source (Saile et al., 2018a). It has been proposed that this must be the same role that NanS-P plays in the lysogen (Saile et al., 2018a), though its genome context linking it behind the late gene regulator *Q* and it being linked to the Shiga toxin genes and the lysis gene cassette make little sense for it to lay an important role in metabolism when the cell is committed to death and about to die at the time of expression.

According to data and results that were sorted in chapter 3, which suggested the expression of P21 in induced $\phi 24_B$ had benefit to the host cells. in that it ensured that not as many cells died, although, the P21 was expression was likely to be part of the lysis transcript and located upstream of lysis cassette genes that control hydrolysis of the host cell's peptidoglycan and perforation of the host cell's membranes. To explain these results, the P21 esterase's features may benefit the host cell by removing an ester-based chemical modification in the peptidoglycan by acting as a de-O-acylation or de-N-acylation which means removal of acyl group from peptidoglycan which would occur via a specific deacetlases enzymes (Moynihan et al., 2014).

Firstly, starting to assure the recombinant P21 that was purified (2.8) and (2.9), had acetyl esterase activity. As a result, as the concentration of P21 protein had increased, as the degradation rates of 4-Methylumbelliferyl acetate (4-MUFac) to 4-methylumbelliferone (4-MUF) became faster (Fig. 4.7). Likewise, (Veses Garcia 2010) had been confirmed the acetyl esterase activity for P21 that proved the acetyl esterase breakes the ester bond with acetate that was released fluorescent compound (4-MUF), and the optimum pH for activity was determined in the range pH 6.0-7.5. It is suggestion to construct two different P21 structures which are P21 lacking the esterase domain from residues 73 to 392, and P21 with only the esterase domain from residues 73 to 392 structure using the pBAD plasmid cloning in vector to his-tag the P21 variants for expression in such Top 10 *E.coli* cells. These P21 variants would be assayed for the acetyl esterase activity to associate the activity of domain with a protein.

Secondly, P21 was assayed binding to peptidoglycan of *E.coli* MC1061 host cell. Moreover, the P21 was assayed binding to peptidoglycan in the presence of four potential competitors: N- acetyl glucosamine, N- acetyl muramic acid, bovine serum

albumin, and glucose in four different concentration (5 mg/ml, 10 mg/ml, 20 mg/ml and 100 mg/ml) to determine which component in peptidoglycan was likely to support P21 binding. The reason for choosing theses competitors is testing amino sugers for specific binding in N- acetyl glucosamine which is an amino sugar of GlcNAc part of peptidoglycan component N- acetyl muramic acid which is an amino sugar of MurNAc part of peptidoglycan component, bovine serum albumin for non-specific sticky protein, and glucose for non specific sugar. The result was P21 bound to peptidoglycan even in the presence of the competitors (Fig. 4.8), though much of this did disappear with increasing concentration of N- acetyl muramic acid. When comparing the amount of competitors with intensity of P21 binding to peptidoglycan, the results were as the N- acetyl muramic acid competitor inhibtor concentration was increased, the P21 intensity binding to peptidoglycan was decreased (Fig. 4.11). While, the N- acetyl glucosamine competitor inhibitor concentration was increased, the P21 intensity binding to peptidoglycan was increased (Fig. 4.12). The result of glucose competitor was not interrupted because it was fluctuated in concentration 10 mg/ml which was the P21 intensity binding to peptidoglycan was higher than concentration 20 mg/ml and lower than concentration 100 mg/ml (Fig. 4.13). While, the bovine serum albumin was sticky protein which was minimised the binding that presented as the concentration of bovine serum albumin was increased, the P21 intensity binding to peptidoglycan was decreased (Fig. 4.14). However, the carbohydrate binding sequence in C-terminus of P21 may suggest why P21 binds strongly to bind N- acetyl muramic acid part in peptidoglycan than the other competitors that can be more confirmation by testing function of all P21 domains. So, it is suggestion to create three structures which are: esterase domain of P21 from residues 73 to 392 construction, carbohydrate binding domain C-terminus of P21 from residues 393 to 645 construction, and P21Δ DUF1737 construction that DUF1737 may make P21 in an active state. For creation these structures, it is suggestion to use pBAD plasmid cloning vector to his-tag these various recombinant proteins for expression in Top10 E. coli cells and subsequent affinity chromatography purification. Then, the three constrctions going to run on P21 binding peptidoglycan assays (4.2.2.1). Moreover, one of suggestion is adding other competitor such as: peptide chains and optimising

more concentrations of competitors to exactly determine which concentration of competitor that inhibit P21 to bind peptidoglycan.

Thirdly, P21 was examined for its ability to modify the peptidoglycan of host cells. This study used HPLC analysis to identify the muropeptide structure of peptidoglycan of the wild type and mutant lysogens of both K12 and O157:H7 lysogens, and examine the impact of purified P21 on purified peptidoglycan of *E.coli*. The lysogens samples were prepared 60 min and 240 min post induction as this timing had been shown to highlight a pronounced phenotypic difference between strains producing or not producing P21. The results of HPLC did not see a significant modification to purified murein, but only saw alterations to murein when synthesied in a cell producing P21 (Fig. 4.15), and (Fig. 4.16) that were presented in very small peak that was numbered 16. There is no interpretation until now for the identity of peak 16 (Fig. 4.17). It is clear that the production of P21 is associated with producing peak 16, but it is a minor porduct. Is this sufficient to impact phage release? A way to address this question may be to control the production of P21 on an expression plasmid and monitor the size of peak 16 in relation to the induction signal for P21 expression. So, it is suggestion to indcuce P21 expression level to see if that impact of peak 16. In an *in vitro* assay, recombinant P21 was unable to modify the purified peptidoglycan from *E.coli* D456. As a result, there was no show any changes in muropeptide structure of naiive strain *E.coli* D456 in samples that were mixed with P21 recombination at pH 5.0 and pH 7.0, and show similar muropeptide structure of control sample that did not include P21 recombination in reaction (Fig. 4.18). It is interesting to speculate that this could be due to the activity of P21 on peptodooglycan while its being synthesized only, or possibly that the recombinant protein must be activated, may be the first DUF domain must be removed from the portein for full activity so P21 may be synthesised as a preprotein requiring activation in the lysogen.The expectation from studying the muropeptide structure of peptidoglycan of the wild type and the mutant lysogens is to find out a peptidoglycan modification such as de-O-acylation or de-N-acylation that may describe the reason different phenotype between wild type lysogen and mutant type lysogen results in chapter 3. While, the small peak 16 that was find in the muropeptide structure of peptidoglycan of the wild type lysogn at the both time point (60 min and 240 min) and P21 binds peptidoglycan with more specific in N- acetyl muramic acid part in peptidoglycan that can open prediction that there is a relationship

between P21and peptidoglycan of host cell. In contrast, there are many examples of de-O-acylation or de-N-acylation peptidoglycan modification in bacterium *e.g.* peptidoglycan deacetylase (PgdA) in *H.pylori* that deacetylyed the host cell peptidoglycan when the bacteria cells attacked by macrophages so the bacterial cells could resist the lysozyme (Wang et al., 2010a), and when the *Proteus mirabilis* decided to proceed the autolysin, it minimized the O-acetylation at the C-6 hydroxyl group of the N-acetylmuramic acid and rose up the anhydromuropeptides (Strating et al., 2012). The form of peptidoglycan modification of the lysogen by P21 may be a way to avoid escaping the phage encoded lysozyme and may explain the reduction number of cells that release phage (Fig. 3.8, and Fig. 3.9).

CHAPTER 5:

CHARACTERISATION THE IMPACT OF GENE 48 ON THE LYSOGEN

5.1. Background

5.1.1. Gene 48

The size of vb_24b_48 is 8.4 kbp. This is an enormously large gene, the largest bacteriophage gene identified so far. However, it is also conserved across many Stx phages such as 933W, Stx2 converting phage 86 and Min 27 (Smith et al., 2012b). It is located at the end of the integrated ϕ24B prophage and spans between bp 49,148 to 57,571. Additionally, gene 48 shares homology to a few other non-Stx prophages like the one carried by *Salmonella enterica* subsp. enterica serovar Kentucky isolate (ZP_0258689). The putative function of protein which is encoded by gene 48 cannot be adequately predicted bioinformatically (Emanuelsson et al., 2007a), but the protein 48 possesses a partial COG1483 domain between residues 345 and 1176 that is associated with the AAA+ superfamily of ATPase domains. However, the protein 48 has many of the conserved features of the bacterial "giant genes" that usually encode a surface protein associated in bacterial fitness (Reva and Tümmler, 2008), and it is know that the lysogen is resistant to several surface activing compounds that negatively impact the naïve cell (Smith et al., 2012b). A weak leader peptide sequence can be predicted in for the gene 48 product that suggests the gene 48 encodes a cell envelope protein. RNA-seq data has identified that this protein is expressed by the lysogen, so based on the fact that it is so large, yet conserved, it is likely to have an important role in the biology of the bacterial lysogens (Veses-Garcia et al., 2015b)

5.1.2. The antimicrobial tolerance of the lysogen $\phi24_B$

There are many studies that show the fitenss traits that carried by $\phi24_B$ lysogen (1.3.5.3) such as acid resistance (Veses-Garcia et al., 2015a), and antimicrobial tolerance (Holt et al., 2017b). However, $\phi24_B$ lysogen has shown an ability for tolerating many antimicrobial agents that have extracellular target *e.g.* amoxicillin, and cefoxitin, or intracellular target *e.g*. oxolinic acid, and 8-hydroxyquinoline (Holt et al., 2017b). The antimicrobial tolerance fitness trait that prophage $\phi24_B$ benefits the

bacterial host cell need to understand which genes that are accessory to the core biology of $\phi 24_B$, involve in tolerance bacterial host cell againt antimicrobial agents. One of suggestion of $\phi 24_B$ genes is gene *48* that is based on prediction sequence structure of gene (5.1.1).

5.1.3. Antibiotics

The word antibiotic refers to the metabolic production of organisms such as bacteria, and fungi that kill or inhibit bacterial growth. Antibiotic products, which have evolved within the natural environment and soil microorganisms, are concerned with facilitating a selective benefit for the producing organism in its competition for nutrients and space. However, the antibacterial agents that are used today in clinics are derived from fermentation of natural product and then are chemically modified that are called semi synthetic, or are completely artificial products *e.g.* quinolones and sulphonamide (Goering et al., 2012). Sir Alexander Fleming discovered penicillin production by the blueish-green nuisance mould (*Penicillium rubens*) in 1928 (Spellberg and Gilbert, 2014). Antibiotics were initially used to treat serious infections in the 1940s (Centers for Disease Control and Prevention, 2015). After penicillin successfully treated the bacterial infection of soldiers in World War II (Spellberg and Gilbert, 2014), the development of penicillin resistance began to be a clinical obstacle in the 1950s (Spellberg and Gilbert, 2014), which led to the discovery and development of new β-lactam antibiotics. In 1962, the first case of meticillin-resistant *Staphylococcus aureus* (MRSA) was recorded in the United Kingdom. Four years later, an MRSA case was recorded in the United States. This highly resistant organism was resistant to nearly all antibiotics. Vancomycin was produced in 1972 to treat methicillin resistance in both *Staphylococcus aureus* and coagulase-negative staphylococci. Unfortunately, the resistance of vancomycin was recorded in coagulase-negative staphylococci in 1979 and 1983 (Spellberg and Gilbert, 2014, Control and Prevention, 2013). The pharmaceutical factories produced many new antibiotics to solve the resistance problem during the decades (Spellberg and Gilbert, 2014).

The antibiotics are classified based upon whether they are bactericidal or bacteriostatic, and based on their target site. Bactericidal means the antibiotics kill the bacteria *e.g.* the aminoglycosides. While bacteriostatic drugs simply inhibit bacterial growth *e.g.* the tetracyclines. Although, bacteriostatic antibiotics successfully treat most infectious disease by preventing increasing bacterial growth, they rely on the

host's immunological mechanisms to clear the bacteria, so bacteriostatic antibiotics are less efficient in immunocompromised patients (Goering et al., 2012).

The classification of antibiotics based on the target site of action helps to understand the basic molecular action of the antibiotic, and conversely in the explanation of some of the synthetic processes in bacterial cell. There are five major target sites for antibiotic action: 1) The cell wall; drugs such as β-lactams that bind to penicillin binding protein, and glycopeptides that intervene with cell wall synthesis by binding to the peptide chains at terminal D-alanine-d-alanine, resulting in the inhibition of the transglycosylation reaction so new subunits cannot cooperate with cell wall growth (Goering et al., 2012). 2) Protein synthesis; drugs such as aminoglycosides that bind to formylmethionyl-transfer RNA forming complexes on the 70S ribosome, tetracyclines that bind a new aminoacyl transfer RNA to the acceptor site, or chloramphenicol that inhibits synthesis of peptide bond . The antibiotics that target protein synthesis lead to the translocation of peptidyl transfer RNA that exposes the terminator codon that releases and terminates the peptide chain (Goering et al., 2012). 3) Nucleic acid synthesis; drugs such as quinolones that intervene with replication of the bacterial chromosome through the inhibition of bacterial DNA gyrase and topoisomerase activities, and rifamycins that blocks mRNA synthesis by binding to DNA-dependent RNA polymerase (Goering et al., 2012). 4) Metabolic pathways, drugs such as sulphonamides that act as competitive inhibitors of the dihydropteroate synthetase which is involved in the synthesis tetrahydrofolic acid pathway, which is needed for nucleic acid synthesis in purine and pyrimidines synthesis (Goering et al., 2012). 5) The cell membrane; drugs such as lipopeptides that depolarize the cytoplasmic membrane of bacteria, by inserting themselves in a calcium-dependent matter, result in the inhibition of ATP synthesis and interfere the in uptake of nutrients, and polymyxins possess free amino groups which act as cationic detergents to disrupt the phospholipid structure of bacterial cell membrane (Goering et al., 2012).

5.1.3.1. β-lactams

β-lactam drugs are a group of broad-spectrum antibiotics that is categorized as having low toxicity (Georgopapadakou, 1993). The function of β-lactams is the inhibition of the cross-linking of peptidoglycan by preventing transpeptidation-dependent cross-linking of peptidoglycan polymers, weakening the cell wall of the bacteria making the cell more likely to lyse. Moreover, β-lactam acts as

pseudosubstrates and acylates the catalytic serine in the transpeptidase active site of the penicillin-binding proteins (Giesbrecht et al., 1998). The group of β-lactams are differential by the ring structure that attaches the β-lactam ring *e.g.* in penicillins possess a five membered ring, and cephalosporins possess a six membered ring and must be entire to possess antibacterial activity. The main classes of β-lactams are penicillins, carbapenems, monobactams, and cephalosporins (Goering et al., 2012). There are four generations of penicillin has been developed. The first generation are naturally ocurring penicillins; the second generation are β-lactamase- resistant penicillins *e.g.* cloxacillin, oxacillin; the third generation are amino penicillins *e.g.* amoxicillin and ampicillin; and the fourth generation are carboxy penicillins *e.g.* carbenicillin and ticarcillin or ureido penicillins *e.g.* mezlocillin (Lobanovska and Pilla, 2017). Cephalosporins, which possess a six membered ring, were invented for patients who are allergic to penicillin. There are also four generations of cephalosporins. First generation drugs are cefazolin, cephalexin, and cephradine. Second generation drugs cefoxitin, cefprozil, cefaclor. Third generation drugs are cefdinir, cefoperazone, and cefotaime. and fourth generations drugs are cefepime and cefpirome (Chang et al., 2012). Carbapenems are similar to penicillins in possessing a five membered ring but they do not possess a sulphur atom (Sykes et al., 1985). There are four cabapenems prescribed in the hospital environment which are ertapenem, meropenem, imipenem, and doripenem (Papp-Wallace et al., 2011).

5.1.3.2. Antibiotics resistance mechanisms

5.1.3.2.1. Antibiotic inactivation or alteration

Some bacterial pathogens such as *Staphylococcus aureus*, *Pseudomonas aeruginosa*, and *Klebsiella pneumoniae* produce enzymes that neutralize or damage the antibacterial agents (De Oliveira et al., 2020). Example of an enzyme that inactivates an antibiotic is a β-lactamase. β-lactamases are classified on their fundamental molecular structure (Ambler scheme) (Ambler, 1980), or hydrolytic combination and inhibiting function (Bush-Jacoby system) (Bush and Jacoby, 2010). The Ambler scheme class A enzymes such as cephalosporinases, extended-spectrum β-lactamases, and penicillinases are hydrolytic enzymes that are concentrated within the periplasm, so they that damage the β-lactam antibiotic before approaches the penicillin-binding protein (PBP) at the bacterial cell wall (Bush and Jacoby, 2010, De Oliveira et al., 2020, Bush and Bradford, 2019). While the Ambler scheme class B,

which is composed of metallo- β-lactamases, require a Zn^{+2} co-factor to hydrolyse most β-lactams agents such as carbapenems (Bush and Jacoby, 2010). Moreover, the Ambler scheme class C chromosomally encoded cephalosporinases which are found in *Enterobacter* spp, and *Pseudomonas aeruginosa (Jacoby, 2009)*, and the Ambler scheme class D enzymes include the oxacillin hydrolysing enzymes like those produced by *Klebsiella pneumoniae* and *Enterobacter* spp (Fig 5.1A) (Pitout et al., 2019).

Not all enzymes responsible for drug resistance act on β-lactam drugs. There are classes of enzymes that alter the target site interaction of aminoglycoside drugs by modifying the drug themselves, which reduces the activities of these modified antibiotics at the bacterial ribosome. There are three classes of aminoglycoside modifying enzymes: 1) aminoglycoside phosphotransferases 2) aminoglycoside nucleotidyltransferases 3) and aminoglycoside acetyltransferases (Shaw et al., 1993). Aminoglycoside phosphotransferases catalyse the ATP-dependent phosphorylation of hydroxyl groups of the antibacterial agents that results decreasing aminoglycoside binding affinity. Aminoglycoside nucleotidyltransferases decrease the toxic of aminoglycoside through the magnesium dependent transfer of a nucleotide monophosphate to hydroxyl group of the antibacterial agents. Aminoglycoside acetyltransferases catalyze the acetylation of the amino group of the antibiotic acceptor molecule (Fig 5.1A) (Ramirez and Tolmasky, 2010).

5.1.3.2.2. Biofilm and intracellular survival

Biofilm formation and lifestyle is one antibiotic resistance mechanism that facilitates to bacterial pathogen to avoid antibiotic impact. Biofilms are a structure that attach to a surface or to itself and cover the bacterial communities via extracellular matrix. As a result, antibacterial agents have limited access to cells and their impacts on cells are also minimised (Høiby et al., 2010, Hill et al., 2005, Nickel et al., 1985). Biofilms are associated with chronic infections such as those caused by *Pseudomonas aeruginosa* in the lung mucous of cystic fibrosis patients and staphylococci on indwelling medical device instruments (Høiby et al., 2010, Percival et al., 2015). There eight factors that increase the antibacterial resistance of biofilm: 1) the restriction of antibacterial drug penetration of the biofilm associated extracellular matrix, 2) the presence of antibacterial-modifying enzymes, 3) the presence of macromolecules in

the extracellular matrix, 4) the secretion of extracellular DNA, 5) the presence of filamentous bacteriophage that promote the formation and accumulation of liquid crystalline structures, 6) various metabolic activities & bacterial population persistence, 7) bacterial efflux pump upregulation, and 8) some bacterial species interact within a mixed-species biofilms (Fig 5.1B) (Hall and Mah, 2017, Secor et al., 2015). Additionally, some bacterial pathogens direct their invasion into host cells and are adapted to survive for periods of time inside a host cell. For example, *Klebsiella pneumoniae* and *Enterococcus faecalis* survive and persist inside intracellular vascular components (Cano et al., 2015, Zou and Shankar, 2016). Moreover, *Staphylococcus aureus* adhere to enter, and survive inside phagocytes such as macrophages and epithelial cells. (Fraunholz and Sinha, 2012, Lowy, 2000). While inside host cells some bacteria acquire a co-evolutinary interaction with phage that result in the conversion in to a lysogen, as a result, the prophages are created (1.3.1) which possessed genes accessory that may advance the bacteria in resistance antibiotic and tolerance antimicrobial. *e.g.* the shiga toxin encoding bacteriophage $\phi 24_B$ in *E.coli* MC1061 cells demonstrate increasing antimicrobial tolerance in chloroxylenol and 8-hydroxquinoline than *E.coli* MC1061 cells (Holt et al., 2017b)

5.1.3.2.3. Modification of target binding site

Bacterial pathogens cause modification in the antibacterial target site by some mechanisms such as target enzyme modification, alteration of bacterial cell wall precursor, and alteration the ribosomal target site. As a result, decreasing the affinity or inhibiting the molecular binding site of antibacterial agents (De Oliveira et al., 2020). Example of target enzyme modification in Meticillin-resistant *Staphylococcus aureus* (MRSA) that resists to methicillin and other β-lactams by expression *mecA* gene. The *mecA* gene production modifies penicillin-binding protein (PBP) with decreasing β-lactams affinity that results most β-lactam antibiotics do not active versus MRSA (Lakhundi and Zhang, 2018). Moreover, fluoroquinolones such as norfloxacin and ciprofloxacin are resistance in bacterial pathogens that spontaneous encode enzymes of bacterial DNA replication and repair such as DNA gyrase and topoisomerase IV (Hooper, 2001, Schmitz et al., 1998, Yoshida et al., 1991).

Alteration of the ribosomal target site occurs in macrolidelincosamide streptogramin B antibacterial resistance in *Staphylococcus aureus* and *Enterococcus* spp. via *erm*-encoded ribosomal RNA methyltransferases. The macrolide lincosamide

streptogramin B binding site is impaired by ribosomal RNA methyltransferases either mono- or dimethylate the A2058 that residue within the 23S ribosomal RNA of the bacterial 50S ribosomal subunit (Fig 5.1C) (Horinouchi and Weisblum, 1980, Weisblum, 1995).

Development of glycopeptide resistance is an example of alteration of bacterial cell wall precursor. Enterococci encodes *van* gene clusters that are responsible for the synthesis of modified peptidoglycan precursors that reduce glycopeptide binding, and producing D,D-carboxypeptidases that remove residual natural D-Ala–D-Ala precursors from the host cell (Fig 5.1C) (Arias and Murray, 2012, Kristich et al., 2014).

5.1.3.2.4. Reducing antibiotic accumulation

When the outer membrane channels (porins) are downregulated function and balance, and lost by mutation, the bacterial pathogens can resist the antibiotics. Some hydrophilic antibacterial agents such as fluoroquinolones and β-lactams depend on porins for penetrating the outer membrane barriers, while some resistance mechanisms such as broken enzymes and efflux pumps are enhanced in the mutations (Fig 5.1D) (Quinn et al., 1986, Hasdemir et al., 2004, Munita et al., 2016). For example, when the *Pseudomonas aeruginosa* OprD porin is lost or modified, carbapenem susceptibility reduces (Pages et al., 2008). In addition, the imipenem resists in *Acinetobacter baumannii* via losing or inactivation of CarO (Li et al., 2015). Bacterial pathogens use the efflux pumps to take antibiotics out the bacterial cell. There are six groups of efflux pumps have been featured which are multidrug and toxic compound extrusion, small multidrug resistance, proteobacterial antimicrobial compound efflux, resistance-nodulation-division, ATP-binding cassette, and major facilitator superfamily (Li et al., 2015, Hassan et al., 2015). For example, *Pseudomonas aeruginosa* chromosomally encodes MexAB-OprM efflux system that shows resistance β-lactams, fluoroquinolone, and aminoglycoside (Li et al., 2015). Likewise, in *Klebsiella pneumoniae* chromosomally encodes OqxAB efflux pump that reduces chloramphenicol and quinolone susceptibility (Ruiz, 2019, Wong et al., 2015).

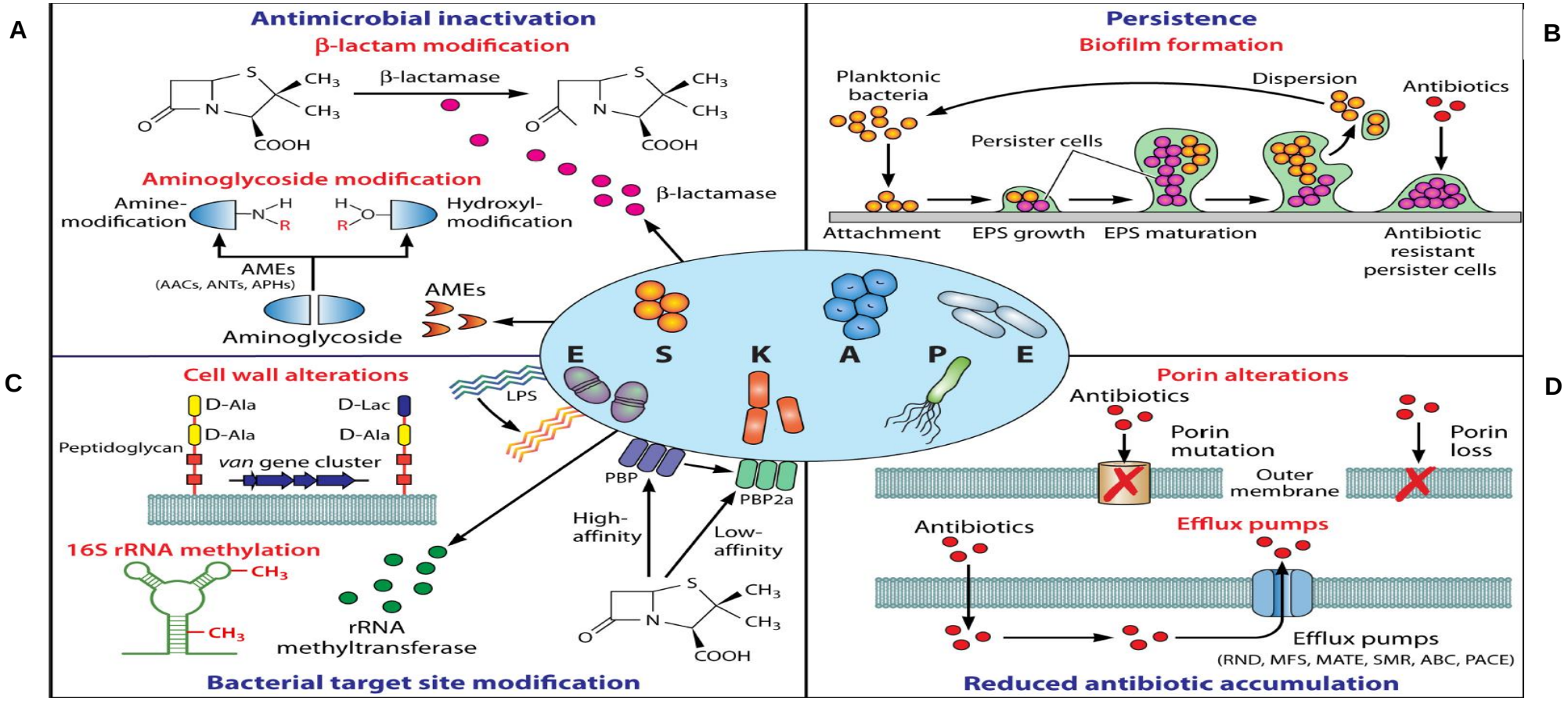

Figure 5. 1. Mechanisms of ESKAPE pathogen antibiotic resisteance.

ESKAPE pathogen refers to *Staphylococcus aureus*, *Klebsiella pneumoniae*, *Acinetobacter baumannii*, *Pseudomonas aeruginosa*, and *Enterobacter* species has four mechanisms to resist antibiotics which are: **A**) Antibiotic is inactivated by enzymes that damage the active antibiotic region such as β-lactam ring is hydrolytic cleavage by β-lactamases or the bacterial target site is hidden by covertly modifying to structural components of the antibiotic such as amino/hyroxyl group modifications are catalysed by aminoglycosidemodifying enzymes. **B**) Persistence of biofilm-embedded cells shows a strongly higher resistance to antibiotics than planktonic bacteria. **C**) Modification of target binding site decreases the affinity of the antibacterial molecule or inhabits the binding at the bacterial cell surface such as β-lactam affinity is reduced by protein binding penicillin 2a, and peptidoglycan modification via *van* gene cluster, or intracellularly such as 16S RNA methylation. **D**) Antibiotic accumulation is reduced by mutation or loss of outer membrane channels (porins) such as CarO in *Acinetobacter baumannii*, OmpK36 in *Klebsiella pneumoniae*, OprD in *Pseudomonas aeruginosa*, or expression of efflux systems to terminate antibiotics out of the cell. This figure was taken from (De Oliveira et al., 2020).

5.1.4. 8-hydroxyquinoline

8-Hydroxyquinoline has many derivatives, which are a broad spectrum in some biological activities (Dalecki et al., 2017). 8-Hydroxyquinoline is used for analysis and separation functions because it has strongly coordinating ability and perfect metal recognition features (Albrecht et al., 2008). However, metal ions are necessary in biological activities, so the metal homeostasis is demand to maintain the metal balance (Budimir, 2011, Crichton et al., 2008). Overloaded or deficiency metal are results of abnormal metal absorption or metabolism that can cause diseases (Vanparia et al., 2010). 8-Hydroxyquinoline has ability to form compounds with divalent metal ions via chelation, which can maintain the metal ion balance, so it can use as a treatment for metal associated diseases (Prachayasittikul et al., 2013). It has a wildly range of medicinal activities that can be anticancer, antimicrobial, anti-inflammatory, and antidiabetic (Prachayasittikul et al., 2013).

(Jeon et al., 2009) had studied the impact of 8-Hydroxyquinoline and its derivatives on the human gastrointestinal bacteria which are (*E. coli, Bifidobacterium longum*, *Lactobacillus acidophilus, Clostridium difficile*, *Clostridium perfringens,* and *Lactobacillus casei).* The paper disc agar diffusion method was used in this study. The results demonstrate 8-Hydroxyquinoline strongly inhibits the growth of *E. coli*, and *Clostridium difficile* in concentration of 0.5 mg/disc, and *Clostridium perfringens* in concentration of 0.1 mg/disc.

The antimicrobial activity mechanism of 8-Hydroxyquinoline is inhibition microbial enzymes (Prachayasittikul et al., 2013). 8-Hydroxyquinoline is a transcription inhibitor of RNA and can degrade RNA because it is featured as a heavy metal (Farrell Jr, 2009).

5.1.5. Sanguinarine

Sanguinarine, which is extracted from plants, is a benzophenanthridine under the group of benzylisoquinoline alkaloids (Kuete, 2014). Because alkaloid, sanguinarine has antimicrobial, antitumor, and anti-inflammatory features (Weerasinghe et al., 2013). It is prescribed as a treatment of gingivitis in mouthwash and toothpaste (Stiborová et al., 2002). It is involved in killing animal cells by its function on the Na^+-K^+-ATPase transmembrane protein (Pitts and Meyerson, 1981). Also, it has been reported that it has toxic side effects on the liver and skin (Kuete,

2014), as well as having a mutagenic effect by contributing to the DNA intercalating activity (Stiborová et al., 2002).

5.1.6. Sodium metaborate

Sodium metaborate is a compound includes sodium, boron, and oxygen and its chemical formula $NABO_2$. It is produced from sodium peroborate hydrolysis and is unstable because they possess boron-oxygen-oxygen bonds that react with H_2O (Becker, 2013). It has been used as bacteriostatic or antiseptic in many ways such as cosmetic productions, eyewashes, burn dressing, and mouthwashes (Becker, 2013, Seiler et al., 1990).

5.1.6. Aims

The gene *48* which is a numerous gene has conserved features of the bacterial "giant genes" that usually encode a surface protein associated in bacterial fitness (Reva and Tümmler, 2008), and the $\phi 24_B$ lysogen shows resistance to several surface activing compounds (Smith et al., 2012b). Plasmids harbouring gene 48 were constructed by GeneMill (University of Liverpool, United Kingdome). These plasmids were used to transform *E. coli* cells to use in biological sensitivity assays. The aim of this part of the thesis is to demonstrate whether gene 48 plays a role in delivering the observed resistance phenotypes that the prophage provides. In this chapter, we have:

- Designed a synthetic construction to express gene *48*.
- Confirmed the cloning of gene 48 in naïve *E. coli*.
- Demonstrated that the expression of gene *48* can be controlled.
- Compared the antibiotic resistance and drug tolerance of the $\phi 24_B$ lysogen the naiive cells and the cells carrying the cloned gene 48.

5.2. Specific Methods

5.2.1. Synthetic construction of recombinant gene 48

Plasmids pGM190_3 and pGM304_1 were constructed by GeneMill (University of Liverpool, United Kingdom). These plasmids, which harbour gene *48* of $\phi 24_B$ (vb_24B_48) (Fig 5.2 and Fig 5.3, respectively), were used to transform *E. coli* K-12 strain MC1061 cells.

5.2.1.1. Propagation of electrocompetent cells

Naïve *E. coli* K-12 strain MC1061 (3 to 4 colonies) was used to inoculate 10 mL of LB broth, which was cultured overnight at 37°C with shaking at 200 r.p.m. The next day, the overnight culture was used to inoculate in sterilized LB broth (1:100) that was incubated at 37°C with shaking at 200 r.p.m. When the culture reached an optical densities OD_{600} = 0.4 – 0.6, the cells were recovered by centrifugation at 4000 x g for 10 min at 4°C. The cells were washed twice with 1 mL ice cold ddH_2O and then recovered by a final centrifugation at 4000 x g for 10 min at 4°C. Finally, the pellets were resuspended in 1mL ice cold ddH_2O, ready for electroporation.

5.2.1.2. Transformation of electrocompetent cells

The proposed plasmid (pGM190_3 or pGM304_1) DNA (1 µl) from GeneMill was placed in a 2 mm electroporation cuvette. 100 µl of the electrocompetent cells (5.2.1.1) were mixed gently with the plasmid DNA in the electroporation cuvette and incubated for 1 min at RT. A negative control was also run which was contained of naïve cells without adding plasmid DNA to an elecrotroporation cuvette and treated the same as the sample to be transformed but with the absence of added DNA. The cells were electroporated at the following settings 2.50 mV, 200 Ω and 25 µF. Pre-warmed S.O.C. medium (1 mL) (Invitrogen, United Kingdom, #15544034) was added to each sample, and these were incubated at 37°C with shaking at 200 r.p.m. for 90 min. Samples from these reactions (500 µl, 250 µl, 150 µl 50 µl and 10 µl) were plated on LB agar with appropriate antibiotic selection and incubated overnight at 37°C.

5.2.2. Plasmid pGM190_3 and pGM304_1 extraction

Plasmids pGM190_3 or pGM304_1 that were used to transform into *E. coli* K-12 strain MC1061 (2.16) were extracted to confirm the presence and identity of the plasmids by restriction enzyme digest and amplification of gene *48*.

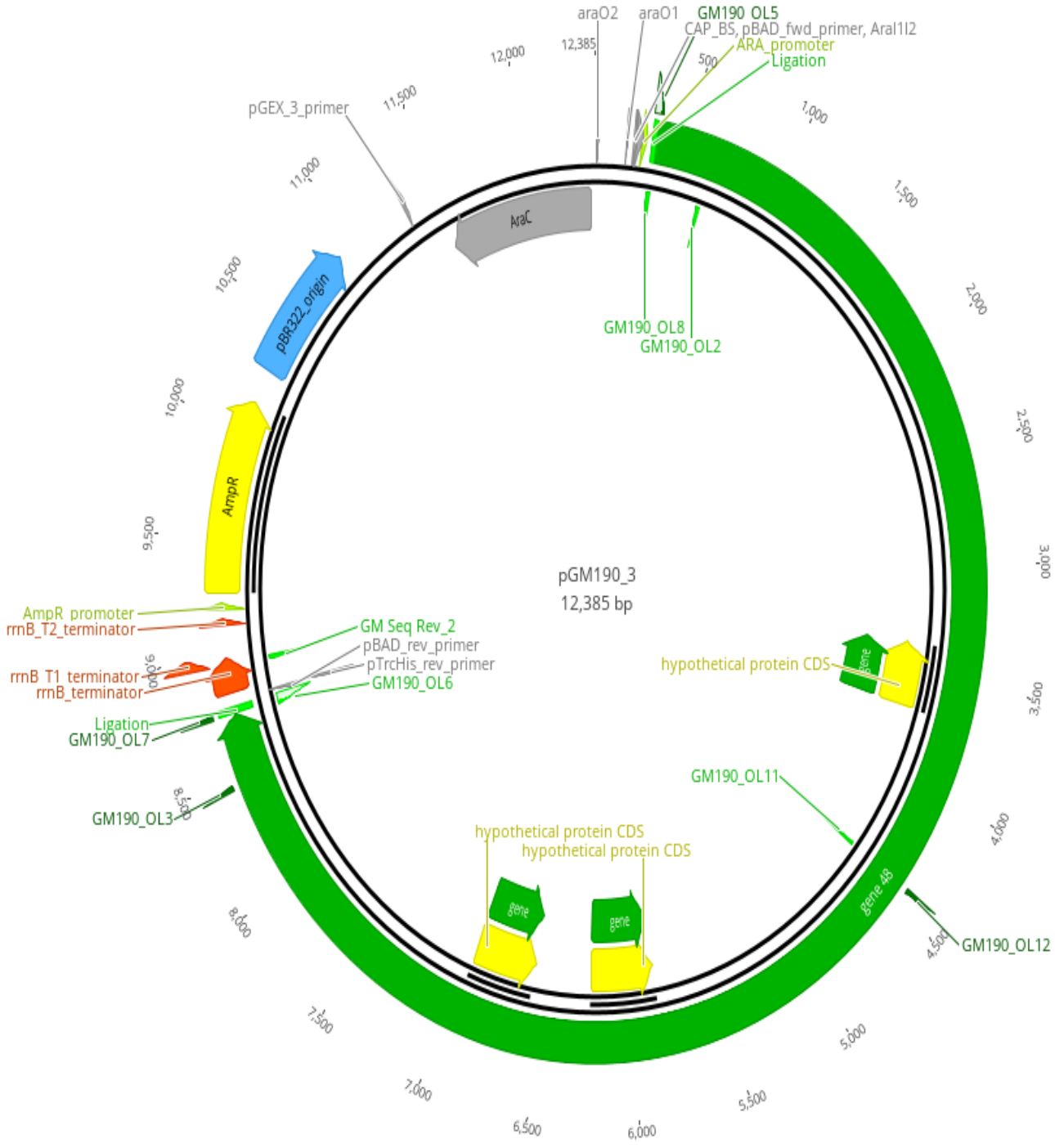

Figure 5. 2. Plasmid pGM190_3 genomic map.

The plasmid size is 12385 bp, pGM190_3 was modelled from pBR322 harbours gene *48* and **Ampicillin** resistance gene marker. Plasmid was constructed by GeneMill (University of Liverpool, United Kingdoms).

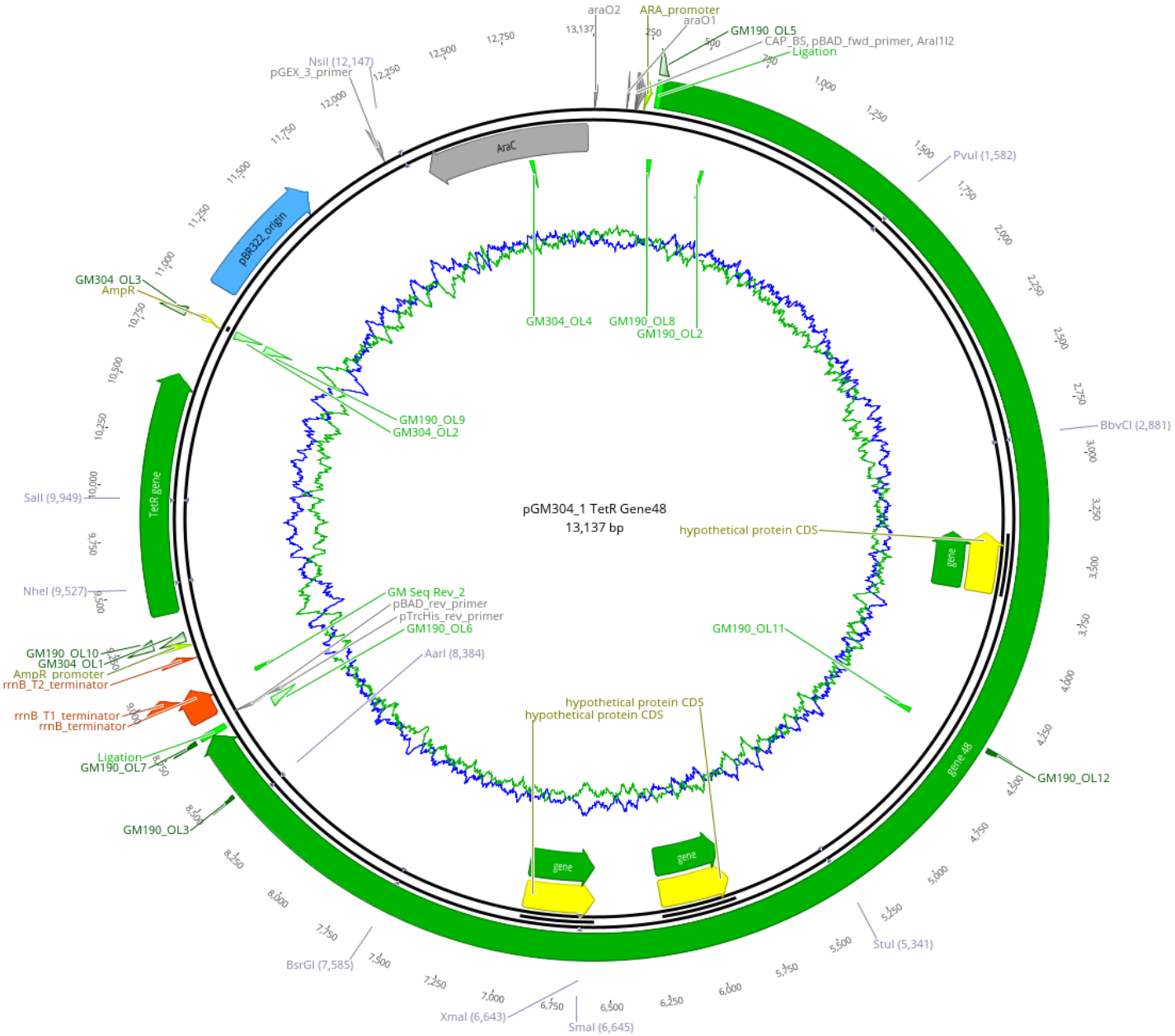

Figure 5. 3. Plasmid pGM 304_1 genomic map.

The plasmid size is 13137 bp, pGM 304_1 was modelled from pBR322 harbours gene *48* and **Tetracycline** resistance gene marker. Plasmid was constructed by GeneMill (University of Liverpool, United Kingdoms)

5.2.2.1. Restriction enzyme digest pGM190_3 and pGM304_1

Plasmid DNA (pGM190_3 or pGM304_1) (4 µl) was added to 2 µl *Hin*d III-HF® (NEB, United Kingdom, #R3104S), 2 µl cut smart buffer, and 12 µl ddH_2O that were incubated at 37°C for 1 h.

5.2.2.2. Gene 48 amplification

Gene *48* is 8.4 kb in size, so the amplification of gene *48* was done in three regions. The first region was the first 1200 bp of the gene *48*, the second region was from 3681 bp to 4880 bp (the middle of gene *48*) and third region was the last 1200 bp of the gene *48* (Table 2.5). The plasmids pGM190_3 or pGM304_1 used were used as template (2.17), and the PCR products were separated by agarose gel electrophoresis (2.18).

5.2.3. Real time PCR (RT-qPCR) of gene 48 expression with five concentrations of arabinose induction

To prove arabinose was capable of inducing the expression of gene *48*, qPCR was used to quantify the copy number of gene *48* expression at five different concentrations of arabinose induction. There are four steps for this experiment, which were culture of the bacterial cells under varied arabinose induction, extract RNA from the bacterial cells, generate cDNA (RT step), and perform qPCR.

5.2.3.1. Cultural bacterial cells with arabinose induction

E. coli K-12 strain MC1061 carried pGM190_3 (3 to 4 colonies) was used to start a 10 mL overnight culture with 100 µg mL^{-1} ampicillin at 37°C with shaking at 200 r.p.m. The next day, the overnight culture was used to inoculate LB broth (1:100) with 100 µg mL^{-1} ampicillin and this was incubated at 37°C with shaking at 200 r.p.m. until the culture reached an OD_{600} = 0.4 – 0.6. At this point the culture was divided into five different flasks. The expression of gene *48* was induced by adding 0.1 mM arabinose, to a final concentration of either 20% arabinose, 15% arabinose, 10% arabinose, 5% arabinose, or 0% arabinose. Each culture was allowed to continue growing for a further 3 h. Then, the cells from each culture were harvested by centrifugation at 15,191 x g for 30 min. at 4°C for RNA extraction.

5.2.3.2. RNA extraction

The RNA extraction of five bacterial cultures was done as described in (2.14), and (2.14.1).

5.2.3.3. cDNA generation

The Tetro cDNA Synthesis Kit (Bioline #BIO-65042) was used to generate cDNA from total RNA. The cDNA generation reaction included up to 5 µg total RNA, 1 µl Oligo $(dT)_{18}$ primer mix, 1 µl 10 mM dNTP mix, 4 µl 5x reverse transcriptase, 1 µl RiboSafe RNase inhibitor, 1 µl Tetro reverse transcriptase (200 u/ µl), and ddH_2O up to 20 µl. The reaction was mixed gently by pipetting, and the samples were incubated at 45°C for 30 min, then the enzyme was inactivated at 85°C for 5 min, following which it was chilled on ice. The cDNA samples were quantified by NanoDrop spectrophotometry, and stored at -20°C.

5.2.3.4. qPCR

qPCR was used to measure the gene 48 expression that was induced by the five different concentrations of arabinose. Two sets of primers were used to examine expression from the beginning and the end of gene 48. The first primer set were designed from start codon of gene *48*, and the second primers were designed with stop codon of gene *48*. The endogenous reference gene was *pdxA* (4-hydroxythreonine-4-phosphate dehydrogenase) because it has been shown to be a very stable gene in the lysogen and in the naïve cell regardless of prophage induction. Primers are described in Table 2.5. The qPCR reactions were run as follows: 10 µl SensiFAST SYBR HiMROX (Bioline #SF581), 0.5 µM forward primer, 0.5 µM reverse primer, 25 ng/µl cDNA, and ddH_2O up to 20 µl. The samples were run in the ABI StepOnePlus (ThermoFisher Scientific, United Kingdom). The run cycle setting was 95°C for 10 min, then 40 cycles of 95°C for 15 sec, 60°C for 1 min. The ABI StepOnePlus software was using to analyse the data.

5.2.4. Antimrobial agents resistance assays

These assays were run in two different ways. The first way was by comparing naïve *E. coli* K-12 (MC1061) cells to and lysogen (MC1061/$\phi 24_B$::Cat) cells in six antimicrobial resistance assays. The second way was inducing naïve MC1061 cells that carried pGM190_3 or pGM304_1 with 20% arabinose or 15% arabinose and comparing these responses to those from naïve MC1061 cells and lysogen (MC1061/ $\phi 24_B$::Cat) cells in six antimicrobial resistance assays. The antibiotics that were applied in resistance assay were amoxicillin, carbenicillin, and cefoxitin, and the antimicrobial agents that were applied in resistance assay were 8-hydroxyquinoline,

sanguinarine, and sodium metaborate. The original stocks of antibiotics and drugs were prepared at a concentration of 100 μg mL^{-1}.

The naïve and lysogen cells that were assayed, were cultured overnight in LB broth at 37°C with shaking at 200 r.p.m. On the next day, all comparable bacterial cells were diluted in fresh LB broth to OD_{600} = 0.05. The minimum inhibitory concentrations (MIC) of antibiotics and drugs in *E. coli* were determined, and then the desired concentration, which was prepared in LB broth, was 4x > MIC. The dilution of antibiotics and drugs were used in a traditional 2-fold serial broth dilution method in LB broth. The samples were placed in a 96 well plate, and every well contained 100 µl of bacterial cells was incubated with 100 µl of antibiotics or drugs mixed in broth at seven different concentrations. A positive control was included where only bacterial cells in 200 µl LB broth were present, and a negative control was included where no cells were added and the well contained only 200 µl LB broth. The 96 well plate was incubated at 37°C with shaking at 200 r.p.m. Finally, the optical densities OD_{600} was measured the next day in a FLU0starOmega (BAMGlabtech).

5.3. Results

5.3.1. Confirmation the presence pGM190_3 and pGM304_1

Over the years several project students have tried to clone gene 48 without success. To assure that this gene was cloned a synthetic construct was designed in collaboration with GeneMill (University of Liverpool) that would place gene 48 under control of the arabinose inducible promoter and put it on a mid-copy number plasmid. Plasmids pGM190_3 or pGM304_1 were produced by GeneMill and had to be introduced into *E. coli* for functional testing. The plasmids were transformed into *E. coli* by electroporation, but the identity of the transformants was confirmed by two tests: 1) restriction endonucealse digestion and 2) PCR and sequencing. First the plasmids were extracted and digested with the restriction endonuclease *HindIII*. The products of digestion were analysed on an agarose gel (Fig. 5.4). The uncut pGM190_3 resulted in a band whose size was larger than 10,000 bp. The plasmid pGM190_3 should be 12,385 bp. in size. There was only a single high intensity band following cutting with *HindIII* enzyme pGM190_3. When the plasmid pGM304_1, (Fig. 5.5) was purified and digested from MC1061 transformants, again a band lager than 10,000 bp was seen in the uncut lane (pGM304_1 is 13,137 bp) and two bands can be seen in the *HindIII* digest lane.

As little information other than the presence of a large plasmid was gathered from the extraction and digestion of the plasmids, PCR amplification of products across the entirety of gene 48 was performed. Using both plasmids that had been extracted from transformants (pGM190_3 or pGM304_1), 1.2 kb regions from the beginning, middle and end of gene 48 were amplified from each (Fig. 5.6) by PCR and analysed on an agarose gel. Both plasmids possessed all three regions of the correct size (Fig. 5.6 (1, 2, and 3) and (Fig. 5.6 (4, 5, and 6)).

5.3.2. Gene 48 expression is induced by arabinose

The synthetic contructs were designed to have gene 48 expression controlled by arabinose, but without a measurable phenotype, this needed to be confirmed before the hunt for a testable phenotype for gene 48 began. So instead of testing genes expression levels by protein function/phenotype, gene 48 expression levels were monitored by RT-qPCR in response to arabinose induction. The expression of gene

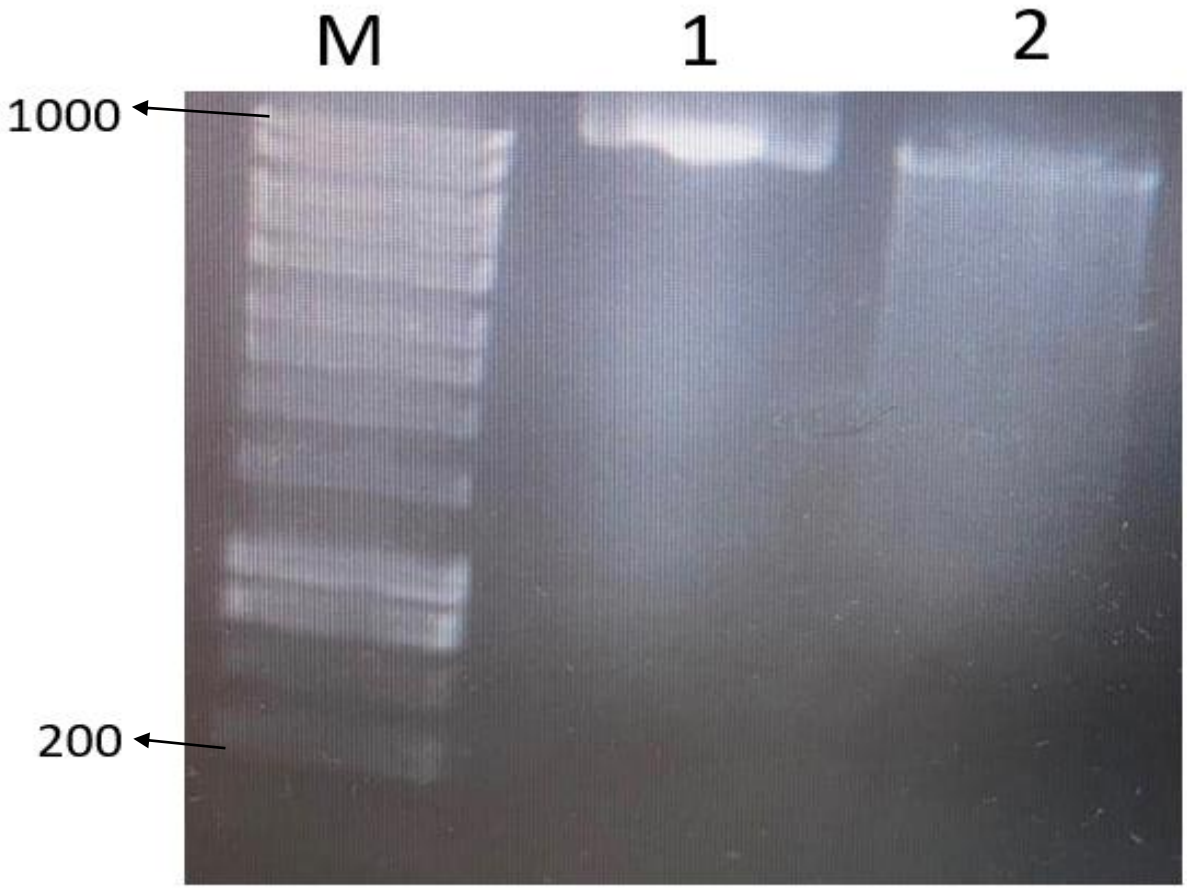

Figure 5. 4. Agarose gel electrophoresis confirmation of plasmid pGM190_3 presence and restriction enzyme digest.

Lanes M) 1 kb DNA ladder (NEB, Herts, U.K.), with band size marker. 1) Plasmid pGM190_3 was isolated from MC1061 carries pGM190_3, undigested 2) Plasmid pGM190_3 was digested by *Hin*d III enzyme.

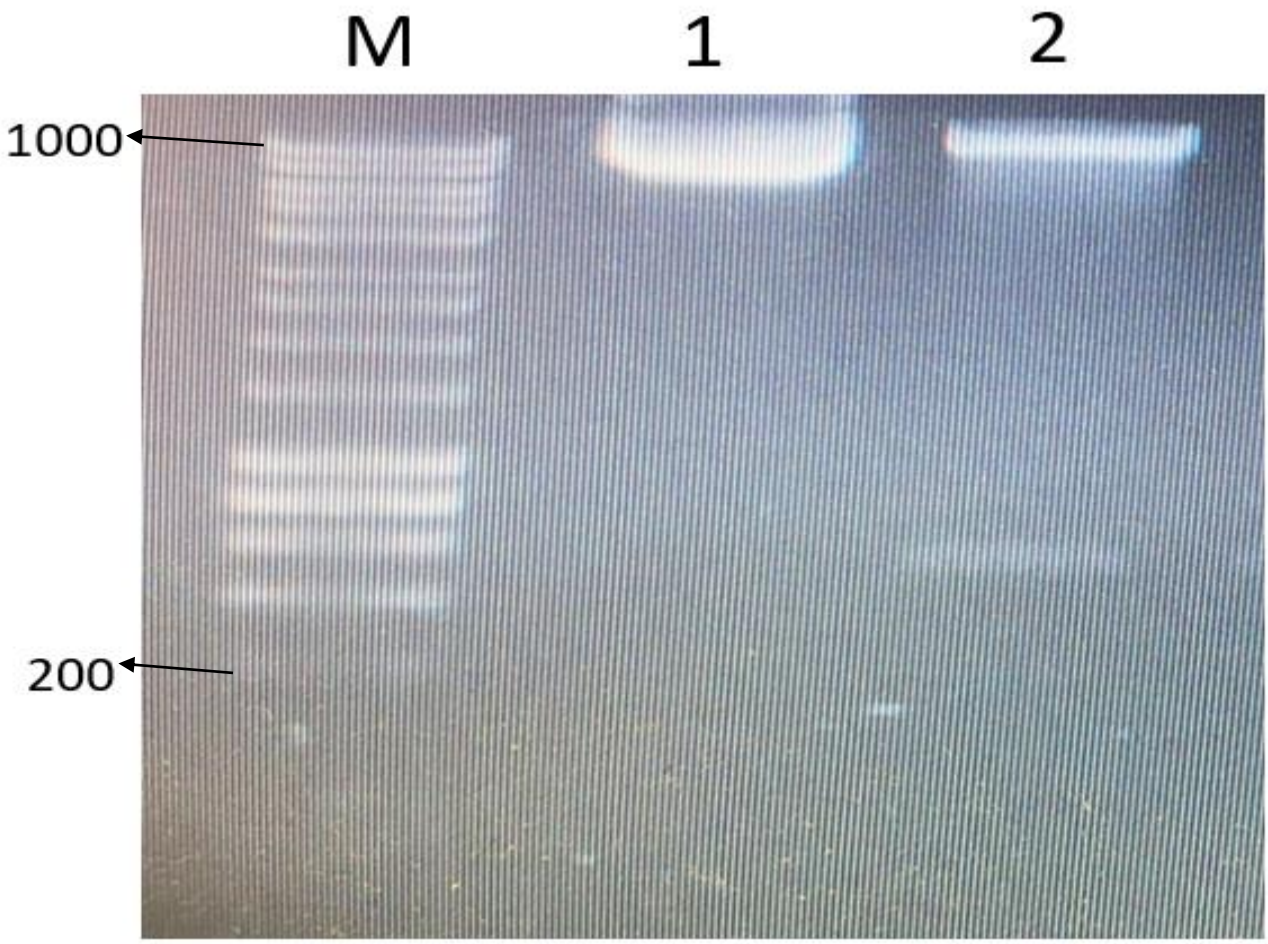

Figure 5. 5. Agarose gel electrophoresis confirmation of plasmid pGM304_1 presence and restriction enzyme digest.

Lanes M) 1 kb DNA ladder (NEB, Herts, U.K.), with band size marker. 1) Plasmid pGM304_1 was isolated from MC1061 carries pGM190_3. 2) Plasmid pGM304-1 was digested by *Hin*d III enzyme.

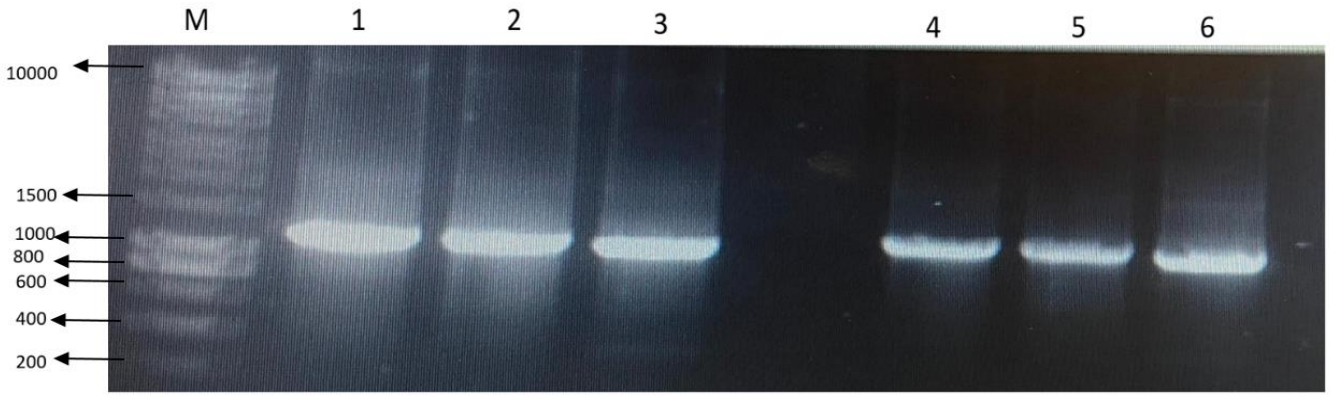

Figure 5. 6. PCR productions confirm constructed plasmids possess gene 48.

Lanes M) 1 kb DNA ladder (NEB, Herts, U.K.), with band size marker. 1) First 1200 bp of gene *48* in pGM190_3 DNA amplification. 2) 1200 bp from 3681 bp to 4880 bp gene *48* in pGM190_3 DNA amplification. 3) Last 1200 bp of gene *48* in pGM190_3 DNA amplification. 4) First 1200 bp of gene *48* in pGM304_1 DNA amplification. 5) 1200 bp from 3681 bp to 4880 bp gene *48* in 304_1 DNA amplification. 6) Last 1200 bp of gene *48* in 304_1 DNA amplification.

48 was induced by five different concentrations of arabinose: 0%, 5%, 10%, 15%, and 20%. The impact on expression was measured by relative quantification in RT-qPCR in two different ways: 1) at the beginning of the transcript and 2) and the end of the transcript. The rationale for this was based on the idea that this transcript was very long and it would be necessary to have a complete transcript to make a protein so it would be necessary to know not just what was happening at the start of the transcript but also was the transcription process going on all the way to the end of the gene to allow a functional protein to be made. These measurements where always made in comparison to a reference (housekeeping) gene transcript which was *pdxA*. This gene had been identified by Dr. Veses-Garcia during an RNASeq experiment with these lysogens and had been identified as one of the most stably expressed genes in the *E. coli* chromosome (Veses Garcia, 2010, Veses-Garcia et al., 2015c). Relative quantification depends on the levels of target gene expression against reference gene. Cycle threshold values (Ct) at a constant level of fluorescence was one of the many methods that determined the comparison of the distinct cycle to calculate the expression of a target gene (gene *48*) in association to an adequate housekeeping gene (*pdxA*).

The calculation of relative quantification is showing in (Fig. 5.7). The result demonstrates two groups of data. The first group is the cDNA generation of gene *48* that were induced by five concentrations of arabinose amplified in first 200 bp of gene *48*, and the second group is the cDNA generation of gene *48* that were induced by five concentrations of arabinose amplified in last 200 bp of gene *48*. In the first group, the highest expression of gene *48* which is induced by 20% arabinose at value of relative quantification 1348.36932. Otherwise, the expression of gene *48* that was not induced by arabinose presents higher value of relative quantification at 981.605825 than value of relative quantification of expression of gene *48* that was induced by 10% arabinose and expression of gene 48 that was induced by 15% arabinose at 759.023109, and 644.9305497, respectively. The expression of gene *48* that was induced by 5% arabinose results value of relative quantification at 1205.988137 (Fig. 5.7). In the second group, the results demonstrate the acceptation, which is increasing the expression of gene *48* associates with increase the concentration of arabinose induction. The value of relative quantification gradually increases from the expression of gene *48* that was not induced by arabinose to the expression of gene *48* which was

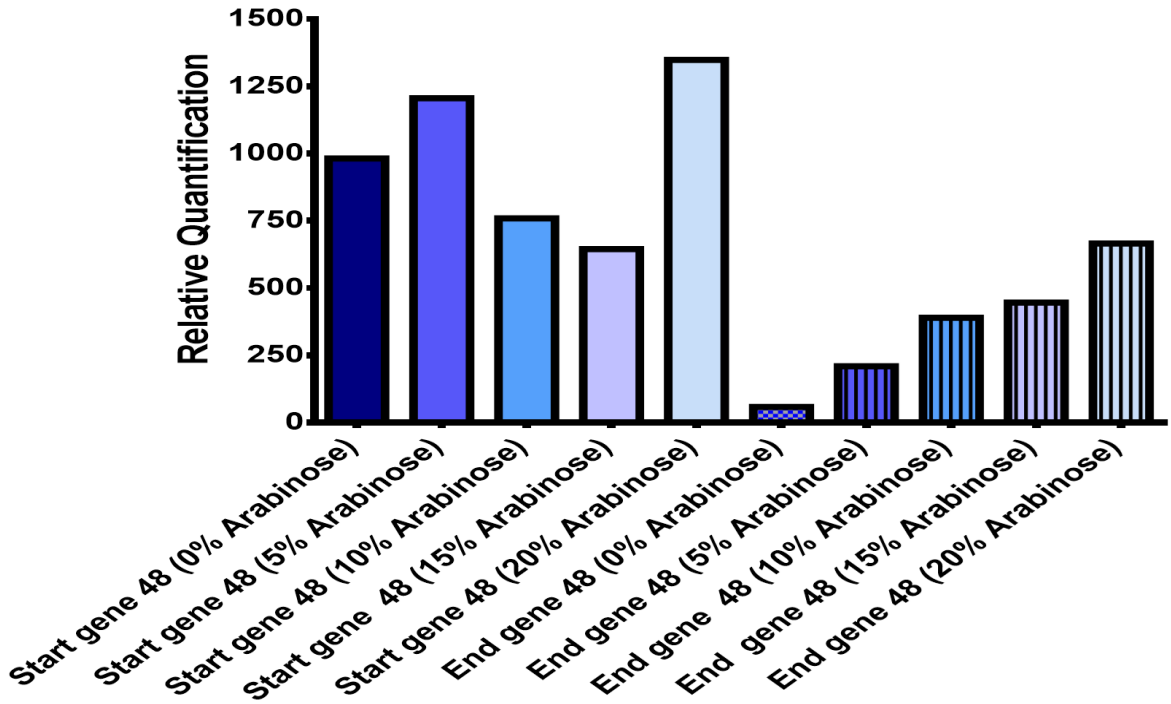

Figure 5. 7. RT-qPCR relative quantification of gene *48* that was induced by five different concertations arabinose in two different sites of gene.

The plain columns refer to the expression of the first 200bp gene *48* exposed to five different arabinose concentrations (0%, 5%, 10%, 15%, and 20%). The striped columns refer to the expression of the last 200bp of gene *48* in as a result of exposure to five different arabinose concentrations (0%, 5%, 10%, 15%, and 20%). The ABI StepOnePlus software was using to analyse these data in comparison to the *pdxA* gene (n=1).

induced by 20% arabinose. The values of relative quantification in the expression of gene 48 that were induced by 0%, 5%, 10%, 15%, and 20% arabinose are 58.32328196, 208.9479798, 389.3705608, 445.4130446, and 665.825355, respectively (Fig. 5.7).

5.3.3. $\phi 24_B$ lysogen has more antimicrobial resistance than naïve cells

There was a previous study (Holt et al., 2017b) demonstrated the $\phi 24_B$ integration altered resistance antimicrobials and rose *E. coli* MC1061 tolerance. In contrast, the experiments antibiotic resistance and drug tolerance assays (5.2.4) results show different susceptibility between naïve cells and lysogen that were assayed in amoxicillin, carbenicillin, cefoxitin, 8-hydroxyquinoline, sanguinarine, and sodium metaborate.

In the antibiotic resistance assay, the MC1061/$\phi 24_B$::Cat lysogen naive MC1061 cells were cultured overnight under amoxicillin (Fig. 5.8) , carbenicillin (Fig. 5.9) , or cefoxitin (Fig. 5.10), with both a positive control (cells, media, no antibiotic) and negative control (no cells, media, no antibiotic). The MIC of amoxicillin for *E. coli* is 5.2 µg/mL (Reimer et al., 1981), and the highest concentration tested here was 83.2 µg/mL, which was diluted traditionally in a 2-fold series 7 times with controls. The results are presented as mean ± standard error of mean (SEM) for two independent biological replicates (Fig. 5.8). Following assessment for normality and equality of variances, statistical inferences on data were performed using two-way analysis of variance (ANOVA) followed by unpairwise comparisons of treatment means using Sidak's multiple comparision test (naïve cells vs lysogen cells used in the amoxicillin resistance assay). Differences are considered statistically significant when $p<0.01$. Statistical analyses were performed using GraphPad Prism 7 Software Statistical Package, Unites States). As a result, (Fig. 5.8) shows the $\phi 24_B$::Cat lysogen in an MC1061 and naive cells *E. coli* strain MC1061 have approximately the same optical densities OD_{600} values in amoxicillin concentrations 0 µg/mL, 1.3 µg/mL, 2.6 µg/mL, 5.2 µg/mL, and 10.4 µg/mL. While the MC1061/$\phi 24_B$::Cat lysogen is more resistance than naive MC1061 cells at a concentration of 20.8 µg/mL amoxicillin ,****$P < 0.0001$. The MIC of carbenicillin for *E. coli* is 8 µg/mL (Mehra et al., 2019), and the highest concentration tested here was 128 µg/mL which was diluted traditionally in a 2-fold series 7 times with controls. The results are presented as mean ± standard error of mean (SEM) for two independent biological replicates (Fig. 5.9). Following

assessment for normality and equality of variances, statistical inferences on data were performed using two-way analysis of variance (ANOVA) followed by unpairwise comparisons of treatment means using Sidak's multiple comparission test (naïve cells vs lysogen cells used in the carbenicillin resistance assay). Differences are considered statistically significant when $p<0.01$. Statistical analyses were performed using GraphPad Prism 7 Software Statistical Package, Unites States). As a result, (Fig. 5.9) shows the MC1061/$\phi 24_B$::Cat lysogen and the naive MC1061 cells have approximately the same optical densities OD_{600} values in carbenicillin concentrations 0 µg/mL, 2 µg/mL, 4 µg/mL, and 8 µg/mL. However, the MC1061/$\phi 24_B$::Cat lysogen is more resistant to carbenicillin than naïve MC1061 in carbenicillin concentrations 16 µg/mL, and 32 µg/mL ($P < 0.0001$). The MIC of cefoxitin for *E. coli* is 3.6 µg/mL (Reimer et al., 1981), and the highest concentration tested was 57.6 µg/mL which was diluted traditionally in a 2-fold series 7 times with controls The results are presented as mean ± standard error of mean (SEM) for two independent biological replicate (Fig. 5.10). Following assessment for normality and equality of variances, statistical inferences on data were performed using two-way analysis of variance (ANOVA) followed by unpairwise comparisons of treatment means using Sidak's multiple comparission test (naïve cells vs lysogen cells used in the cefoxitin resistance assay). Differences are considered statistically significant when $p<0.01$. Statistical analyses were performed using GraphPad Prism 7 Software Statistical Package, Unites States). As a result, (Fig. 5.10) shows the MC1061/$\phi 24_B$::Cat lysogen and naive MC1061 cells have approximately the same optical densities OD_{600} values in cefoxitin concentrations 0 µg/mL, 0.9 µg/mL, and 1.8 µg/mL with no significant difference. While there is no growth of bacterial cells in lysogen and naïve cells in cefoxitin concentrations (3.6 µg/mL, 7.2 µg/mL, 14.4 µg/mL, 28.8 µg/mL, and 57.2 µg/mL).

In the antimicrobial agents resistance assays, the MC1061/$\phi 24_B$::Cat lysogen and naive MC1061 cells were cultured overnight under 8-hydroxyquinoline, sanguinarine, and sodium metaborate pressure in 7 different 2-fold serial dilution series, along with positive and negative controls as described earlier. The (MIC) of 8-hydroxyquinoline in *E. coli* is 32 µg/mL (Prachyasi et al., 2013), so the highest concentration tested was 512 µg/mL. The results are presented as mean ± standard error of mean (SEM) for two independent biological replicates. Following assessment for normality and equality of variances, statistical inferences on data were performed

using two-way analysis of variance (ANOVA) followed by unpairwise comparisons of treatment means using Sidak's multiple comparision test (naïve cells vs lysogen cells used in the 8-hydroxyquinoline tolerance assay). Differences are considered statistically significant when $p<0.01$. Statistical analyses were performed using GraphPad Prism 7 Software Statistical Package, Unites States). As a result, (Fig. 5.11) shows the MC1061/$\phi 24_B$::Cat lysogen and naive MC1061 cells have approximately the same OD_{600} values in 8-hydroxyquinoline concentrations 0 µg/mL - 16 µg/mL). While the MC1061/$\phi 24_B$::Cat lysogen has more resistance than naive MC1061 cells in 8-hydroxyquinoline concentrations of 32 µg/mL and 64 µg/mL ($P < 0.0001$). The MIC of sanguinarine in *E. coli* is (8 µg/mL) (Hamoud et al., 2014), and the higher concentration testing was (128 µg/mL) which was diluted traditional 2-fold serial broth method 7 times, and one bacterial culture did not include sanguinarine. However, the results are presented as mean ± standard error of mean (SEM) for two independent biological replicates. Following assessment for normality and equality of variances, statistical inferences on data were performed using two-way analysis of variance (ANOVA) followed by unpairwise comparisons of treatment means using Sidak's multiple comparision test (naïve cells vs lysogen cells used in the sanguinarine tolerance assay). As a result, (Fig. 5.12) shows the naive cells *E. coli* strain MC1061 demonstrate higher value of optical densities OD_{600} than $\phi 24_B$::Cat lysogen in an MC1061 in sanguinarine concentrations (0 µg/mL, 2 µg/mL, 4 µg/mL, 8 µg/mLand 16 µg/mL). Moreover, the naive cells *E. coli* strain MC1061 has more sanguinarine tolerance than $\phi 24_B$::Cat lysogen in an MC1061 in sanguinarine concentration (32 µg/mL) with a significant difference of optical densities OD_{600} which is (****$P < 0.0001$). There is no growth of bacterial cells in lysogen and naïve cells in sanguinarine concentrations (64 µg/mL, and 128 µg/mL). Finally, the (MIC) of sodium metaborate in *E. coli* is (400 µg/mL), and the higher concentration testing was (6400 µg/mL) which was diluted traditional 2-fold serial broth method 7 times, and one bacterial culture did not include sodium metaborate. However, the results are presented as mean ± standard error of mean (SEM) for two independent biological replicate. Following assessment for normality and equality of variances, statistical inferences on data were performed using two-way analysis of variance (ANOVA) followed by unpairwise comparisons of treatment means using Sidak's multiple comparision test (naïve cells vs lysogen cells used in the sanguinarine resistance assay). As a result, (Fig. 5.13)

shows the $\phi 24_B$::Cat lysogen in an MC1061 demonstrate slightly higher value of optical densites OD_{600} than naive cells *E. coli* strain MC1061 in sodium metaborate concentrations (0 µg/mL, 100 µg/mL, 200 µg/mL, 400 µg/mL, 800 µg/mL, 1600 µg/mL, 3200 µg/mLand 6400 µg/mL).

5.3.4. Comparing antimicrobial resistance assay between lysogen and naïve and naïve cells carries the plasmid encodes gene 48

Antimicrobial resistance assays were applied to investigate if gene *48* was involved in conferring any of the antibiotic resistance or drug tolerance phenotypes conferred by the $\phi 24_B$ prophage The bacterial cells that were compared under antibiotic or drug pressure were naïve MC1061 cells, MC1061/ $\phi 24_B$::Cat lysogen cells, naive MC1061 cells that carried either pGM190_3 or pGM304_1 (depending on selective pressure beng tested) that were induced with 0%, 15% or 20% arabinose. The plasmids (pGM190_3 or pGM304_1) possessed gene *48* and the arabinose induction increased the expression of gene *48*. In the antibiotic resistance assay, the MC1061 cells carried pGM304_1 which confers tetracycline resistance instead of carrying pGM190_3 which confers ampicillin resistance and would have interfered with the assays examining prophage and gene 48 based resistance to amoxicillin, carbenicillin, or cefoxitin.

As described preiously, in the antibiotic resistance assay, the comparable bacterial cells were cultured overnight under cefoxitin, amoxicillin, or carbenicillin pressure in 7 different 2-fold serial dilutions with positive and negative controls. All results are presented as mean ± standard error of mean (SEM) for two independent biological replicates. Following assessment for normality and equality of variances, statistical inferences on data were performed using two-way analysis of variance (ANOVA) followed by unpairwise comparisons of treatment means using Sidak's multiple comparision test. Differences are considered statistically significant when $p<0.01$. Statistical analyses were performed using GraphPad Prism 7 Software Statistical Package, Unites States). The highest concentration testest for cefoxitin resistance assay was 57.6 µg/mL which was serially diluted 7 times from there (Fig. 5.14). The five comparable bacterial cells have approximately the same OD_{600} values in cefoxitin concentrations (0 µg/mL, and 0.9 µg/mL) with no significant difference. While the MC1061 cells that carring pGM304_1 with 0%, 15% and 20% arabinose induction have more resistance than the MC1061/$\phi 24_B$::Cat lysogen or naive MC1061

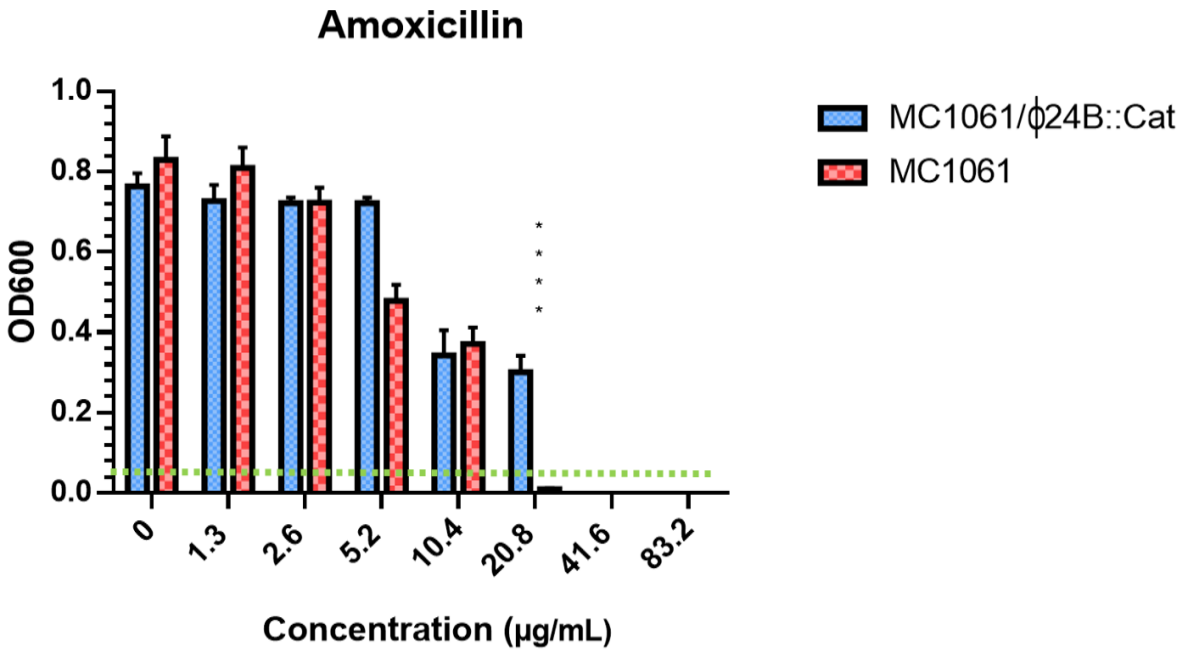

Figure 5. 8. Antibiotic resistance assay of $\phi 24_B$::Cat lysogen and *E. coli* strain MC1061 under amoxicillin pressure at 8 different concentrations.

MC1061/ $\phi 24_B$::Cat lysogen and naive MC1061 cells were cultured overnight under amoxicillin pressure under one of 7 different 2-fold dilutions. The dotted light green line indicates the bacterial inoculum density (OD_{600}= 0.05). The OD_{600} for samples were taken using a FLU0starOmega (BAMGlabtech). Significance was determined by two-way ANOVA and is indicated above the x axes (****P < 0.0001). The error bars represent standard error of the mean (n=2).

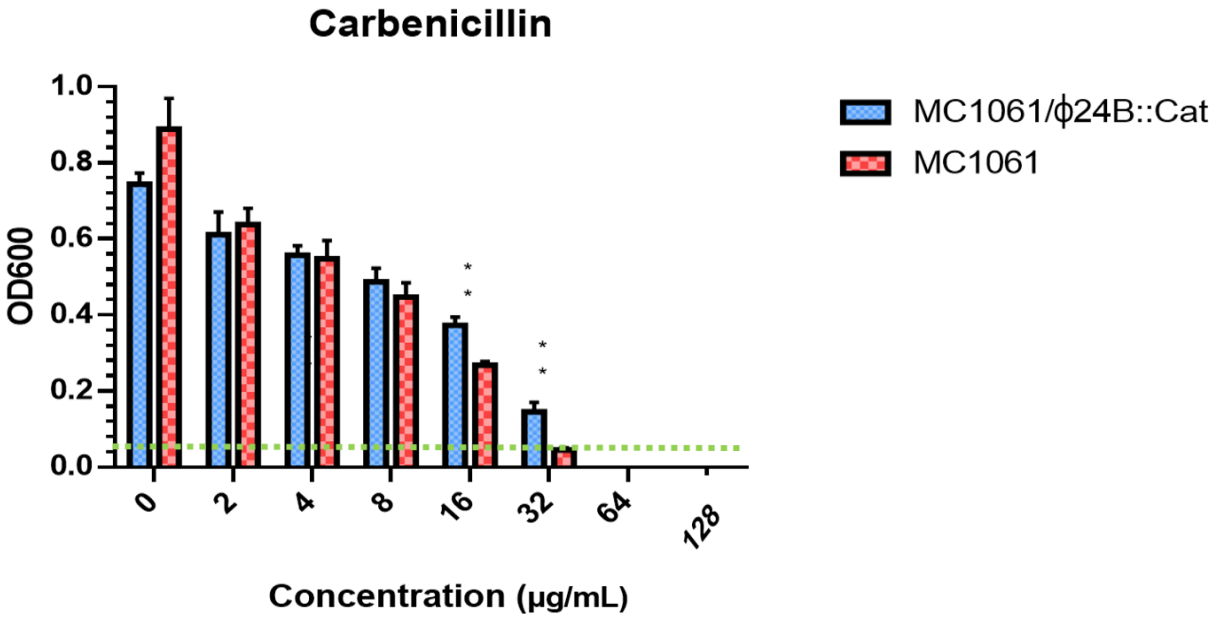

Figure 5. 9. Antibiotic resistance assay of $\phi 24_B$::Cat lysogen and *E. coli* strain MC1061 under carbenicillin pressure at 8 different concentrations.

MC1061/ $\phi 24_B$::Cat lysogen and naive MC1061 cells were cultured overnight under carbenicillin pressure under one of 7 different 2-fold dilutions. The dotted light green line indicates the bacterial inoculum density (OD_{600}= 0.05). The OD_{600} for samples were taken using a FLU0starOmega (BAMGlabtech). Significance was determined by two-way ANOVA and is indicated above the x axes (**P < 0.01). The error bars represent standard error of the mean (n=2).

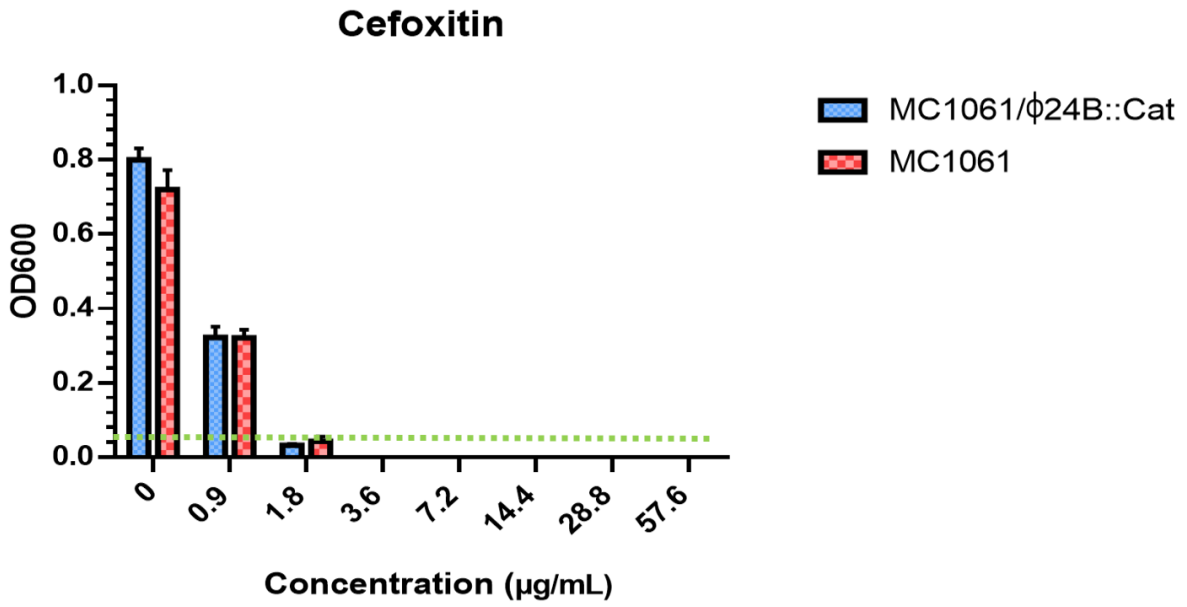

Figure 5. 10. Antibiotic resistance assay of $\phi 24_B$::Cat lysogen and *E. coli* strain MC1061 under cefoxitin pressure at 8 different concentrations.

MC1061/ $\phi 24_B$::Cat lysogen and naive MC1061 cells were cultured overnight under cefoxitin pressure under one of 7 different 2-fold dilutions. The dotted light green line indicates the bacterial inoculum density (OD_{600}= 0.05). The OD_{600} for samples were taken using a FLU0starOmega (BAMGlabtech). Significance was determined by two-way ANOVA. The error bars represent standard error of the mean (n=2).

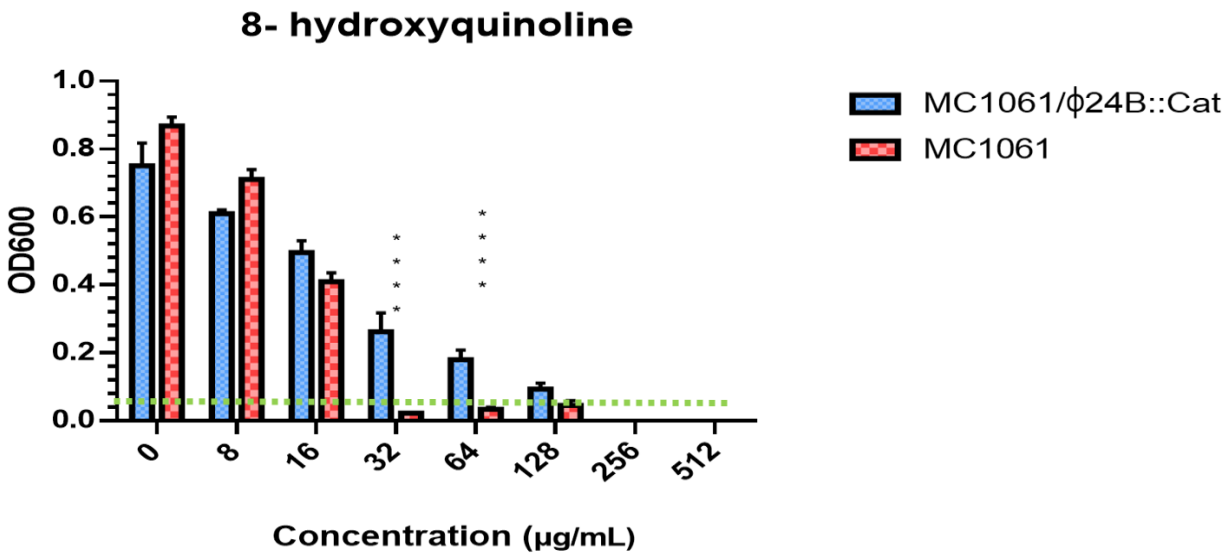

Figure 5. 11. 8-hydroxyquinoline resistance assay of $\phi 24_B$::Cat lysogen and *E. coli* strain MC1061 under 8-hydroxyquinoline pressure at 8 different concentrations.

MC1061/ $\phi 24_B$::Cat lysogen and naive MC1061 cells were cultured overnight under 8-hydroxyquinoline pressure under one of 7 different 2-fold dilutions. The dotted light green line indicates the bacterial inoculum density (OD_{600}= 0.05). The OD_{600} for samples were taken using a FLU0starOmega (BAMGlabtech). Significance was determined by two-way ANOVA and is indicated above the x axes (****P < 0.0001). The error bars represent standard error of the mean (n=2).

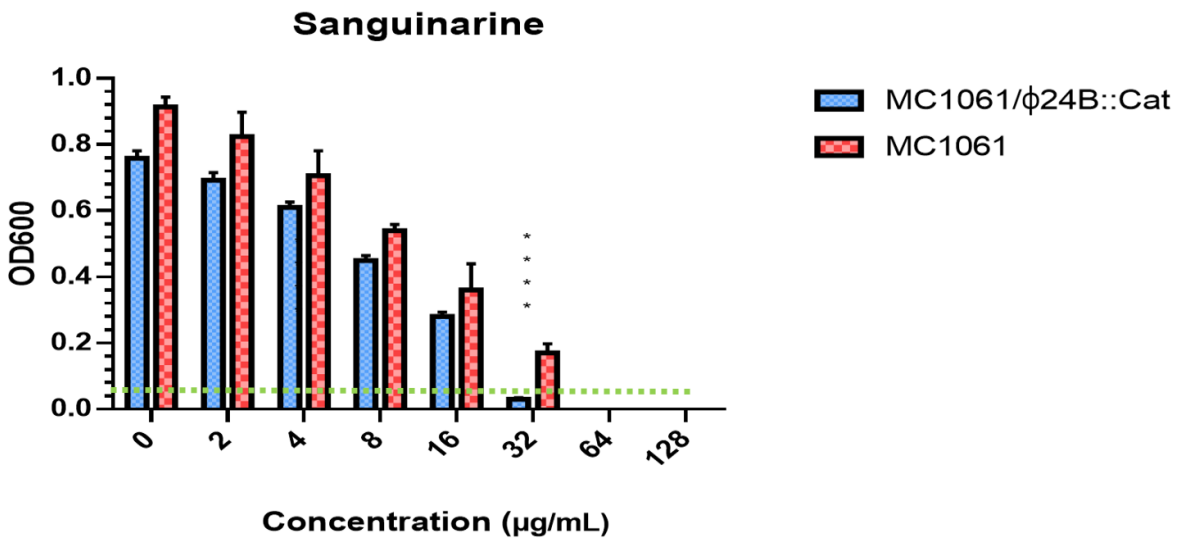

Figure 5. 12. Sanguinarine resistance assay of $\phi 24_B$::Cat lysogen and *E. coli* strain MC1061 under sanguinarine pressure at 8 different concentrations.

MC1061/ $\phi 24_B$::Cat lysogen and naive MC1061 cells were cultured overnight under sanguinarine pressure under one of 7 different 2-fold dilutions. The dotted light green line indicates the bacterial inoculum density (OD_{600}= 0.05). The OD_{600} for samples were taken using a FLU0starOmega (BAMGlabtech). Significance was determined by two-way ANOVA and is indicated above the x axes (****P < 0.0001). The error bars represent standard error of the mean (n=2).

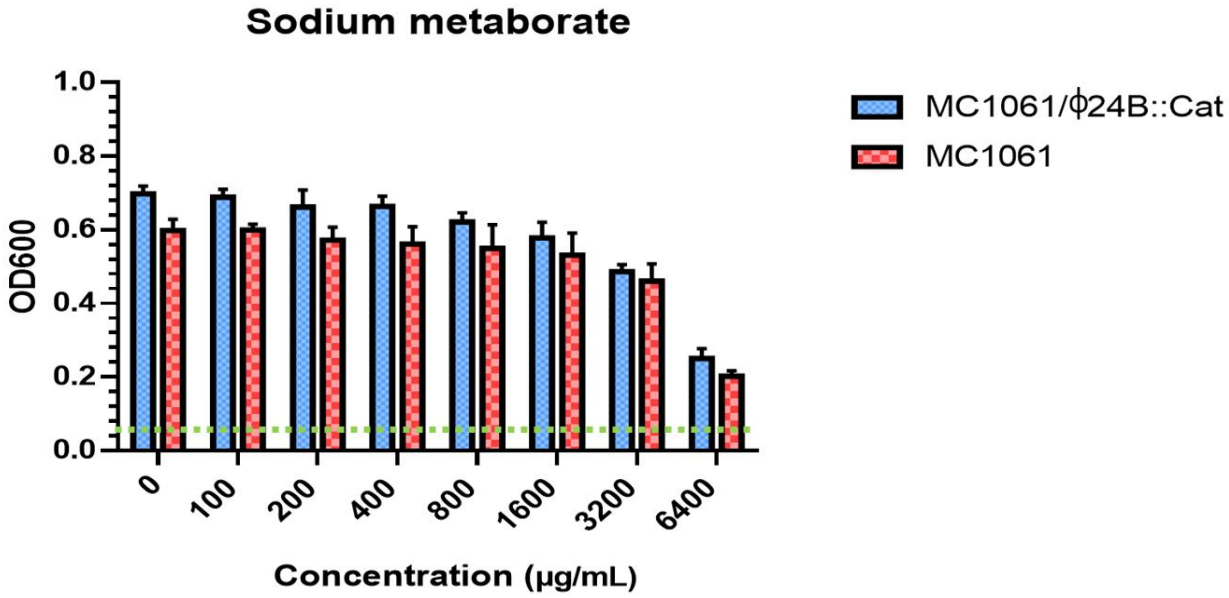

Figure 5. 13. Sodium metaborate assay of $\phi 24_B$::Cat lysogen and *E. coli* strain MC1061 under sodium metaborate pressure at 8 different concentrations.

MC1061/ $\phi 24_B$::Cat lysogen and naive MC1061 cells were cultured overnight under sodium metaborate pressure under one of 7 different 2-fold dilutions. The dotted light green line indicates the bacterial inoculum density (OD_{600}= 0.05). The OD_{600} for samples were taken using a FLU0starOmega (BAMGlabtech). Significance was measured by two-way ANOVA. The error bars represent standard error of the mean (n=2).

cells in cefoxitin concentration 1.8 µg/mL. The significant difference of optical densities OD_{600} in cefoxitin concentration 1.8 µg/mL is $P < 0.0001$. As gene 48 should not be expressed at 0% arabinose this resistance phenotyps has be put down to a vector effect and not to the function of gene 48. There is no growth of the five comparable bacterial cells in cefoxitin concentrations 3.6 µg/mL- 57.2 µg/mL). The highest concentration tested for amoxicillin resistance was 83.2 µg/mL which was serially diluted 7 times from there. The five comparable bacterial strains (Fig. 5.15) have approximately the same optical densities OD_{600} values in the amoxicillin concentrations 0 µg/mL, 1.3 µg/mL, and 2.6 µg/mL with no significant difference. However the MC1061/$\phi 24_B$::Cat lysogen is more resistance than naive MC1061cells, and MC1061 cells that carry pGM304_1 induced with 0%, 15% or 20% arabinose in 5.2 µg/mL, and 10.4 µg/mL cefoxitin ($P < 0.0001$). Moreover, the MC1061/24_B::Cat lysogen is the only bacterial cell that grew in the ampicillin at 20.8 µg/mL, so clearly gene 48 plays no role in ampicillin resistance, but the prophage does play a role in resistance. There is no growth of the five comparable bacterial strains at ampicillin concentrations of 41.6 µg/mL or 83.2 µg/mL. The highest concentration tested for carbenicillin resistance was 128 µg/mL, which was serially diluted 7 times from there. The five comparable bacterial strains (Fig. 5.16) have approximately the same OD_{600} values in carbenicillin the concentrations 0 µg/mL, 8 µg/mL with no significant difference. However, the MC1061/$\phi 24_B$::Cat lysogen and MC1061 cells that carry pGM304_1 with or without arabinose induction were more resistance than naive MC1061 cells at a carbenicillin concentration of 16 µg/mL ($P < 0.01$). Moreover, only the MC1061/$\phi 24_B$::Cat lysogen grew in carbenicillin at a concentration of 32 µg/mL. There was no growth in any of the five comparable bacterial strains in carbenicillin concentrations above 32 µg/mL. Taken together, gene 48 does not play a role in carbenicillin resistance, the prophage does not confer some resistance.

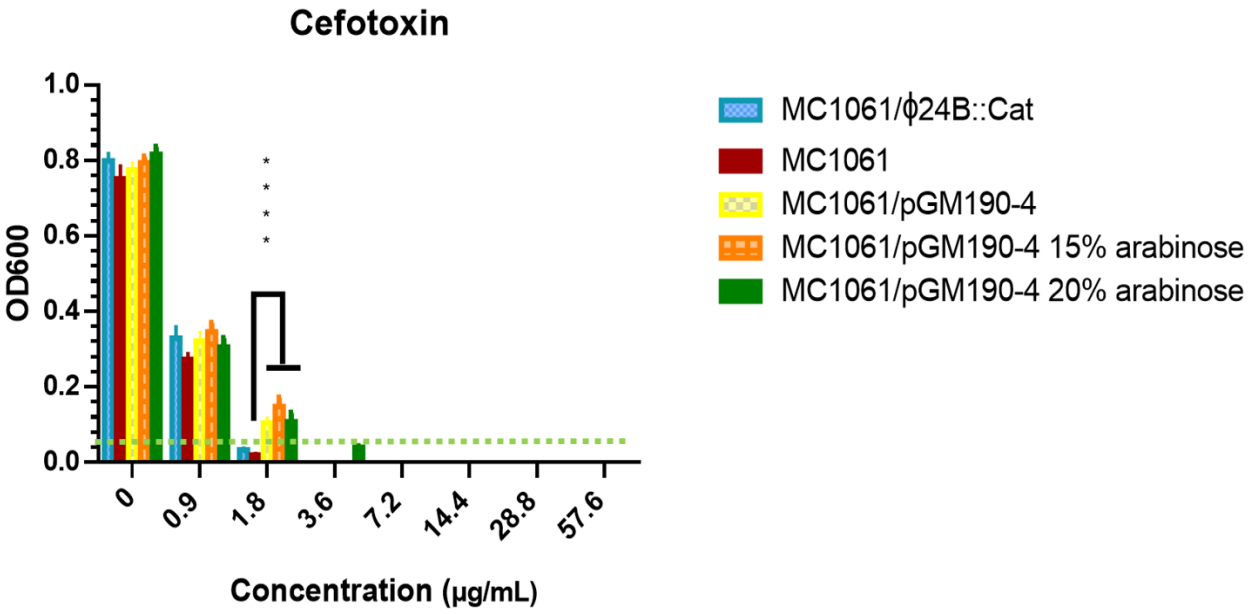

Figure 5. 14. Antibiotic resistance assay of MC1061/ϕ24$_B$::Cat lysogen , naïve MC1061, and MC1061 carrying pGM304_1 with three different concentrations of arabinose induction under cefoxitin pressure at 8 different concentrations.

The ϕ24$_B$::Cat lysogen in an MC1061 genetic background, naive cells *E. coli* strain MC1061, MC1061/pGM304_1, MC1061/pGM304_1 with 15% arabinose induction, and MC1061/pGM304_1 with 20% arabinose induction were overnight cultured under cefoxitin pressure under one of 7 different 2-fold dilutions, and positive control. The dotted light green line indicates the bacterial inoculum density (OD_{600}= 0.05). The OD_{600} for samples were taken by FLU0starOmega (BAMGlabtech). Significance was measured by two-way ANOVA and is indicated above the x axes (****P < 0.0001). The error bars represent standard error of the mean (n=2).

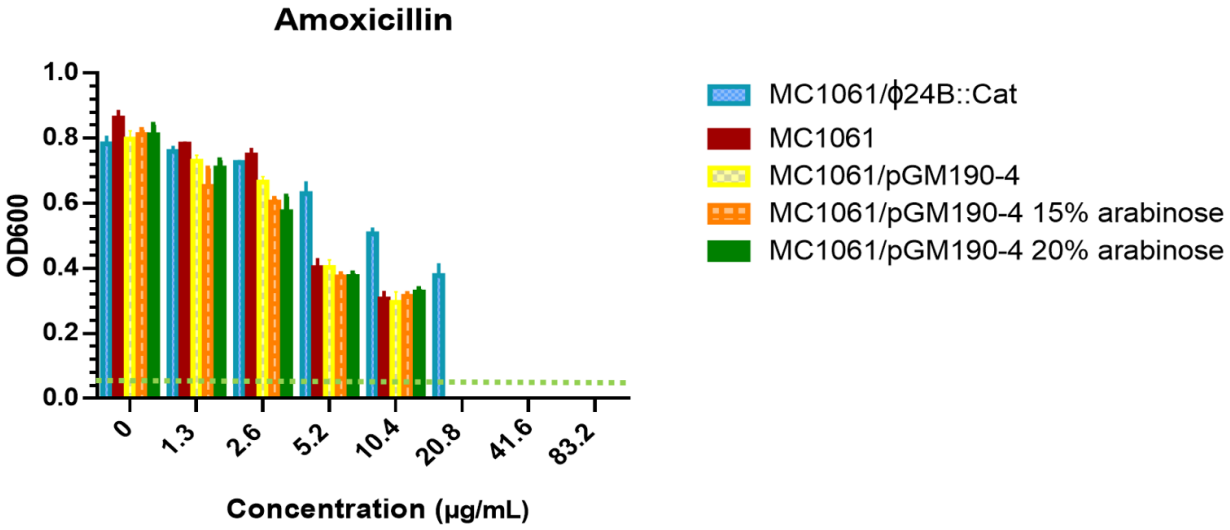

Figure 5. 15. Antibiotic resistance assay of MC1061/$\phi 24_B$::Cat lysogen , naive MC1061, and MC1061 carrying plasmid pGM304_1 with three different concentrations of arabinose induction under amoxicillin pressure at 8 different concentrations.

The $\phi 24_B$::Cat lysogen in an MC1061 genetic background, naive cells *E. coli* strain MC1061, MC1061/pGM304_1, MC1061/pGM304_1 with 15% arabinose induction, and MC1061/pGM304_1 with 20% arabinose induction were overnight cultured under amoxicillin pressure under one of 7 different 2-fold dilutions, and positive control. The dotted light green line indicates the bacterial inoculum density (OD_{600}= 0.05). The OD_{600} for samples were taken by FLU0starOmega (BAMGlabtech). Significance was measured by two-way ANOVA. The error bars represent standard error of the mean (n=2).

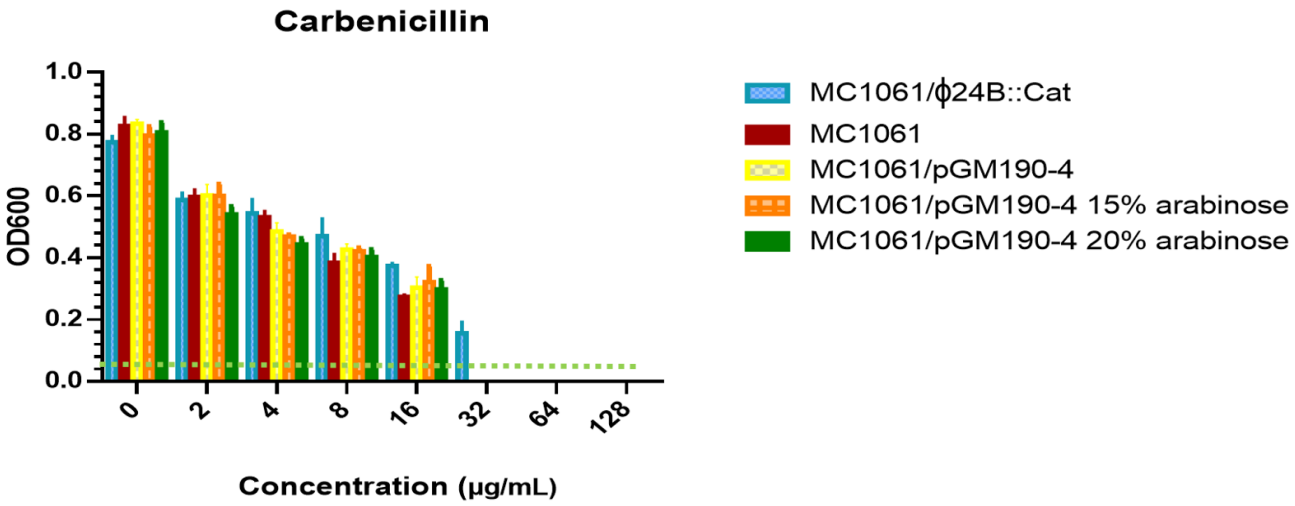

Figure 5. 16. Antibiotic resistance assay of MC1061/$\phi 24_B$::Cat lysogen , naïve MC1061, and MC1061 carrying plasmid pGM304_1 with three different concentrations of arabinose induction under carbenicillin pressure at 8 different concentrations.

The $\phi 24_B$::Cat lysogen in an MC1061 genetic background, naive cells *E. coli* strain MC1061, MC1061/pGM304_1, MC1061/pGM304_1 with 15% arabinose induction, and MC1061/pGM304_1 with 20% arabinose induction were overnight cultured under carbenicillin pressure under one of 7 different 2-fold dilutions, and positive control. The dotted light green line indicates the bacterial inoculum density (OD_{600}= 0.05). The OD_{600} for samples were taken by FLU0starOmega (BAMGlabtech). Significance was measured by two-way ANOVA. The error bars represent standard error of the mean (n=2).

In the antimicrobial agents resistance assay, the comparable bacterial cells were cultured overnight under 8-hydroxyquinoline, sanguinarine, and sodium metaborate pressure in 7 different 2-fold dilution concentration, and positive control. Firstly, the higher concentration testing which was applied in 8-hydroxyquinoline tolerance assay was (1024 µg/mL) that was diluted traditional 2-fold serial broth method 7 times, and one bacterial culture did not include 8-hydroxyquinoline. However, the results are presented as mean ± standard error of mean (SEM) for two independent biological replicates. Following assessment for normality and equality of variances, statistical inferences on data were performed using two-way analysis of variance (ANOVA) followed by unpairwise comparisons of treatment means using Sidak's multiple comparision test. Differences are considered statistically significant when $p<0.01$. Statistical analyses were performed using GraphPad Prism 7 Software Statistical Package, Unites States). As a result, (Fig. 5.17) shows the five comparable bacterial cells have approximately the same optical densities OD_{600} values in 8-hydroxyquinoline concentrations (0 µg/mL, and 16 µg/mL) with no significant difference. While the $\phi 24_B$::Cat lysogen in an MC1061, *E. coli* K-12 strain MC1061 cells that carry (pGM190_3) with 15% arabinose induction, and *E. coli* K-12 strain MC1061 cells that harbour (pGM190_3) with 20% arabinose induction have more resistance than naive cells *E. coli* strain MC1061, and *E. coli* K-12 strain MC1061 cells that carry (pGM190_3) that presents in 8-hydroxyquinoline concentrations (32 µg/mL, and 64 µg/mL). The significant difference of optical densities OD_{600} between *E. coli* K-12 strain MC1061 cells that carry (pGM190_3) with 15% arabinose induction, and *E. coli* K-12 strain MC1061 cells that harbour (pGM190_3) with 20% arabinose induction, and naive cells *E. coli* strain MC1061 in 8-hydroxyquinoline concentrations (32 µg/mL, and 64 µg/mL) is (****$P < 0.0001$). There is a slightly growth of five comparable bacterial cells in 8-hydroxyquinoline concentration (128 µg/mL), and there is no growth of the five comparable bacterial cells in 8-hydroxyquinoline concentrations (256 µg/mL, 512 µg/mL, and 1024 µg/mL). Secondly, the higher concentration testing which was applied in sanguinarine tolerance assay was (128 µg/mL) that was diluted traditional 2-fold serial broth method 7 times, and one bacterial culture did not include sanguinarine. However, the results are presented as mean ± standard error of mean (SEM) for two independent biological replicates. Following assessment for normality and equality of variances, statistical inferences on data were performed using two-way

analysis of variance (ANOVA) followed by unpairwise comparisons of treatment means using Sidak's multiple comparision test. Differences are considered statistically significant when $p<0.01$. Statistical analyses were performed using GraphPad Prism 7 Software Statistical Package, Unites States). As a result, (Fig. 5.18) shows the five comparable bacterial cells have approximately the same OD_{600} values in sanguinarine concentrations (0 µg/mL, 2 µg/mL, 4 µg/mL, 8 µg/mL, and 16 µg/mL) with no significant difference. While the naive cells *E. coli* strain MC1061, *E. coli* K-12 strain MC1061 cells that carry (pGM190_3), *E. coli* K-12 strain MC1061 cells that carry (pGM190_3) with 15% arabinose induction, and *E. coli* K-12 strain MC1061 cells that harbour (pGM190_3) with 20% arabinose induction have more resistance than $\phi24_B$::Cat lysogen in an MC1061 that presents in sanguinarine concentration (32 µg/mL). The significant difference of optical densities OD_{600} between naive cells *E. coli* strain MC1061, *E. coli* K-12 strain MC1061 cells that carry (pGM190_3), *E. coli* K-12 strain MC1061 cells that carry (pGM190_3) with 15% arabinose induction, and *E. coli* K-12 strain MC1061 cells that harbour (pGM190_3) with 20% arabinose induction, and $\phi24_B$::Cat lysogen in an MC1061 in sanguinarine concentration (32 µg/mL) is (****$P < 0.0001$). There is no growth of the five comparable bacterial cells in sanguinarine concentrations (64 µg/mL, and 128 µg/mL). Finally, the higher concentration testing which was applied in sodium metaborate tolerance assay was (6400 µg/mL) that was diluted traditional 2-fold serial broth method 7 times, and one bacterial culture did not include sodium metaborate. However, the results are presented as mean ± standard error of mean (SEM) for two independent biological replicates. Following assessment for normality and equality of variances, statistical inferences on data were performed using two-way analysis of variance (ANOVA) followed by unpairwise comparisons of treatment means using Sidak's multiple comparision test. Differences are considered statistically significant when $p<0.01$. Statistical analyses were performed using GraphPad Prism 7 Software Statistical Package, Unites States). As a result, (Fig. 5.19) shows the $\phi24_B$::Cat lysogen in an MC1061 demonstrate slightly higher value of OD_{600} than naive cells *E. coli* strain MC1061, *E. coli* K-12 strain MC1061 cells that carry (pGM190_3), *E. coli* K-12 strain MC1061 cells that carry (pGM190_3) with 15% arabinose induction, and *E. coli* K-12 strain MC1061 cells that harbour (pGM190_3)

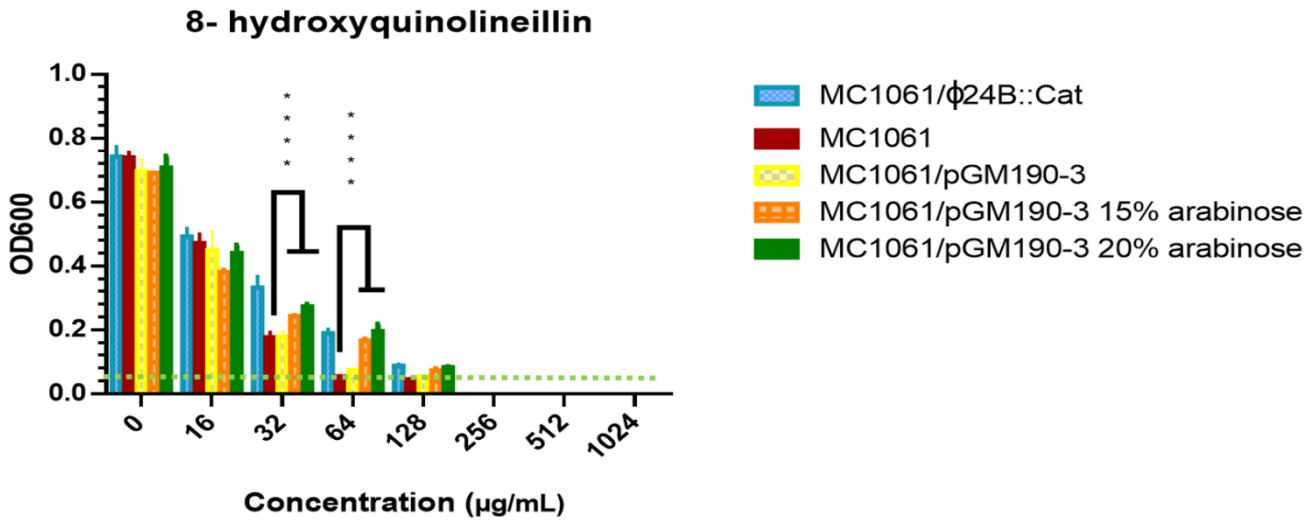

Figure 5. 17. 8-hydroxyquinoline resistance assay of $\phi 24_B$::Cat lysogen , *E. coli* strain MC1061, and *E. coli* strain MC1061 carries plasmid pGM190_3 with three different concentrations of arabinose induction under 8-hydroxyquinoline pressure at 8 different concentrations.

The $\phi 24_B$::Cat lysogen in an MC1061 genetic background, naive cells *E. coli* strain MC1061, MC1061/pGM190_3, MC1061/pGM190_3 with 15% arabinose induction, and MC1061/pGM190_3 with 20% arabinose induction were overnight cultured under 8-hydroxyquinoline pressure under one of 7 different 2-fold dilutions, and positive control. The dotted light green line indicates the bacterial inoculum density (OD_{600}= 0.05). The OD_{600} for samples were taken by FLU0starOmega (BAMGlabtech). Significance was measured by two-way ANOVA and was indicated above the x axes (****P < 0.0001). The error bars represent standard error of the mean (n=2).

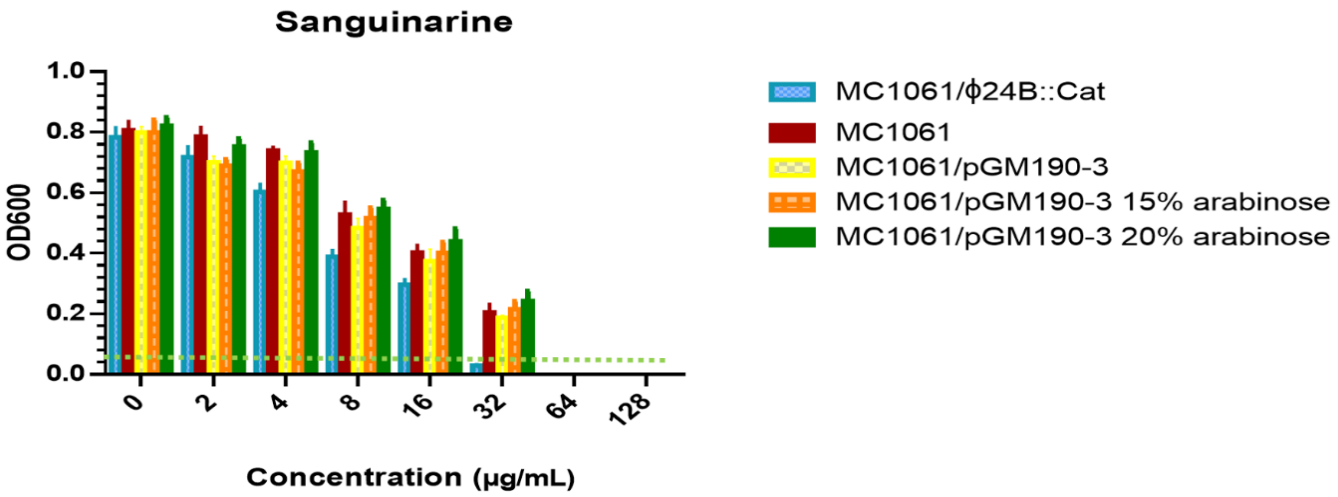

Figure 5. 18. Sanguinarine resistance assay of $\phi24_B$::Cat lysogen , *E. coli* strain MC1061, and *E. coli* strain MC1061 carries plasmid pGM190_3 with three different concentrations of arabinose induction under sanguinarine pressure at 8 different concentrations.

The $\phi24_B$::Cat lysogen in an MC1061 genetic background, naive cells *E. coli* strain MC1061, MC1061/pGM190_3, MC1061/pGM190_3 with 15% arabinose induction, and MC1061/pGM190_3 with 20% arabinose induction were overnight cultured under sanguinarine pressure under one of 7 different 2-fold dilutions, and positive control. The dotted light green line indicates the bacterial inoculum density (OD_{600}= 0.05). The OD_{600} for samples were taken by FLU0starOmega (BAMGlabtech). Significance was measured by two-way ANOVA. The error bars represent standard error of the mean (n=2).

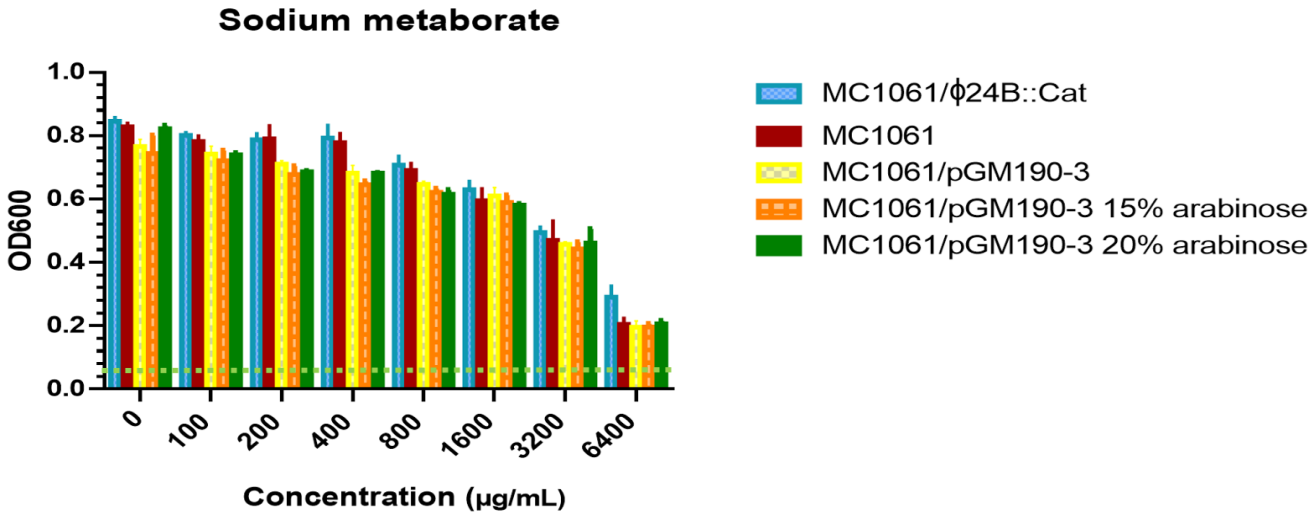

Figure 5. 19. Sodium metaborate resistance assay of $\phi 24_B$::Cat lysogen , *E. coli* strain MC1061, and *E. coli* strain MC1061 carries plasmid pGM190_3 with three different concentrations of arabinose induction under sodium metaborate pressure at 8 different concentrations.

The $\phi 24_B$::Cat lysogen in an MC1061 genetic background, naive cells *E. coli* strain MC1061, MC1061/pGM190_3, MC1061/pGM190_3 with 15% arabinose induction, and MC1061/pGM190_3 with 20% arabinose induction were overnight cultured under sodium metaborate pressure under one of 7 different 2-fold dilutions, and positive control. The dotted light green line indicates the bacterial inoculum density (OD_{600}= 0.05). The OD_{600} for samples were taken by FLU0starOmega (BAMGlabtech). Significance was measured by two-way ANOVA. The error bars represent standard error of the mean (n=2).

with 20% arabinose in sodium metaborate concentrations (0 µg/mL, 100 µg/mL, 200 µg/mL, 400 µg/mL, 800 µg/mL, 1600 µg/mL, 3200 µg/mLand 6400 µg/mL).

5.4. Discussion

The $\phi 24_B$ genome was visualised in CG view in 2012 (Smith et al., 2012a). The study concluded that three quarters of the phage genome was composed of hypothetical genes, which were located in late region, and their expression was associated with prophage induction. In addition, an enormous gene was recognised at the far right end of $\phi 24_B$ genome. The gene was vb_24_B_48 which encoded a 2088 amino acid protein. It is also conserved across many Stx phages such as VT2-Sa, 933W, Stx2 converting phage 86 and Min 27. A similar gene was annotated in a few other non-Stx prophages like the one carried by *Salmonella enterica* subsp. e*nterica* serovar Kentucky isolate (ZP_0258689) and shares 1128 of its 1611 amino acids residues. The protein 48 structure possesses an identifiable domain, a COG1483 domain, which is part of the AAA+ superfamily of ATPases and lies between residues 345 and 1176. The AAA + superfamily of ATPases proteins are related with various cellular activities such as extracting energy from ATP hydrolysis, involved in processes such as peroxisome biogenesis, DNA recombination, and protein unfolding and degradation, and included the molecular motor helicases and dynein that replicate and repair DNA (Snider et al., 2008). When the gene 48 sequence was analysed by SignalP, the results demonstrated there was a leader peptide sequence in the starting 15 nucleotides (Emanuelsson et al., 2007b). Additionally, analysis of the protein sequence of gene by TMPred resulted in the identification of membrane spaning domains (Hofmann, 1993). Moreover, the protein 48 had featured of giant genes which encoded surface proteins associated with bacterial fitness (Reva and Tümmler, 2008).

There were two plasmids (pGM190_3 or pGM304_1), which were constructed by GeneMill (University of Liverpool, United Kingdoms), harboured gene *48* from $\phi 24_B$. The reason for construction of pGM304_1 plasmid was that pGM190_3 harboured a β-lactamase gene which was replaced with a tetracycline resistance gene to avoid interference with the assays examing the lysogen and the role that gene *48* plays in resistance to β-lactam antibiotics. These plasmids were used to transform competent naïve *E. coli* K-12 MC1061 cells using electroporation. To confirm these plasmids were

transformed into the cells, the plasmids were extracted and digested from putative transformants (Fig. 5.4, and Fig 5.5). Additionally, the presence of gene *48* in the plasmid was confirmed through PCR amplification of three regions gene *48.* Three regions were amplified because of the huge size of this gene, which would make it difficult to amplify with one forward and reverse primer (Fig. 5.4). To demonstrate that gene 48 expression was controllable by arabinose levels in the absence of a known phenotype, the impact on expression of 5 different concentrations of arabinose was measured by RT-qPCR. Again, due to the length of the gene and the need of a full transcript to make a complete protein for a functional P48, two sets of primers were used in the RT-qPCR reactions. The first set amplified the transcript from the start codon site to the first 200 bp of the gene. The results of gene expression studies from these primers were unclear. The transcript measurements did not change proportionally to the concentraiton of arabinose. There is a leader peptide at the beginning of the full protein that extends for 15 residues from the first methionine (Smith et al., 2012a). Currently, there have been no studies on this large gene that is carried by many different phages. It is possible that our current annotations are not accurate. The annotation we currently reply on is based upon the identification of these standard leader peptide, and the presence of the large open reading frame. If our annotations are incorrect the lack of proportional expression of the 5'end of gene 48 with arabinose induction could be due to the presence of as of yet unidentified transcription signals cloned between the arabinose indicible promoter and the as of yet unidentified start of gene 48. It is suggestion to run 5' race experiment to identify the transcription start sites (TSS) that identifies where the gene translation begin, as a result, the starting of gene may known. The second set of primers amplied a sequence that also included the stop codon, and the results of gene expression were directly proportional to arabinose concentrations (Fig. 5.7), indicating that we could expect the protein product of gene 48 to be produced in a fully controllable arabinose inducible manner. These clones were used in the antimicrobial agents resistance assays.

When the MC1061/$\phi 24_B$ lysogen and naïve MC1061 cells were assayed for resistance to six antimicrobial agents across seven different concentrations, the results were the lysogen presented more resistance to antimicrobial agents such as amoxicillin, carbenicillin, and 8-hydroxyquinoline than naïve cells, while there was no

difference in antibiotic resistance between both types of cells under cefotoxin pressure. In contrast, (Holt et al., 2017a) had compared the respiration curve between the $\phi 24_B$ lysogen cells and naïve MC1061 cells under 29 different agents which were 22 antimicrobial agents and 7 salts by using the Biolog Phenotypic MicroArray for microbial cells. The respiration curve were calculated based on the $\phi 24_B$ lysogen's ability to tolerate the antimicrobial agents by the primary site 250bp upstream of *IntS* that prevents respiration utilising β-D-allose or limiting the cell repiration in an oxolinic acid avialabilty which is linked to phage induction (Matsushiro et al., 1999, Holt et al., 2017a). In the results presented here, the $\phi 24_B$ lysogen cells shows more resistance than naive host in amoxicillin, cefotoxin, and 8-hydroxyquinoline when assayed the $\phi 24_B$ lysogen and naiive cells under antimicrobial agents pressure in 8 different concentration. Likewise, these antimicrobial agents showed more tolerance in $\phi 24_B$ lysogen in (Holt et al., 2017a) study. However, it is recommended to repeat antimicrobial agents resistant assays one more time to confirm the result because there was not the time to completet the experiment due Covid-19 situations, and it is suggestion to run signature tagged mutagenesis that will help to identify which genes for phage and bacterial host cell that acquired for resistant amoxicillin, carbenicillin, and 8-hydroxyquinoline.

The results showed that the arabinose induced expression of gene 48 protected MC1061 only when under 8-hydroxyquinoline pressure, and this performed very similarly to the prophage itself. This is the first phenotype ever reported for gene 48. It is interesting to note that cells carrying the gene 48 plasmid constructs all demonstrated resistance to cefotoxin, this resistance was not controlled by arabinose induction, and so was therefore not likely to be expression of gene 48. There was no different on the arabinose inducted MC1061 whose carried plasmid possessing gene 48 behaviour in amoxicillin, and carbenicillin resistance, and sanguinarine, and sodium metaborate. The phenomenon of cells that encoded high expression of gene *48* having more resistance under 8-hydroxyquinoline pressure than naive cells that may happen from characteristics of protein 48 linked to those shared with bacterial giant genes (large genes of ~15 kb, with large repeated sequences that encode acidic, hydrophilic surface proteins with an abundance of serine and threonine residues and a dearth of cysteine) {(Reva and Tümmler, 2008)}. These surface proteins inhibit binding of cations and water, lack of any constraints by covalent disulphide bridges, and build micromilieu around the cell to save from threatening antimicrobial agents (Reva and

Tümmler, 2008). However, it is recommended to repeat 8-hydroxyquinoline resistant assay one more time to confirm the results because there was not the time to completet the experiment due Covid-19 situations, and it is suggestion to construct $\phi 24_B \Delta 48$ and use this construction in comparing with wild type phage that encode gene 48 to determine the phenotype of resistance under 8-hydroxyquinoline.

CHAPTER 6:

FINAL DISCUSSION AND FUTURE SUGGESTIONS

6.1. Final discussion and future suggestions

A bacteriophage, also known simply as a phage, is a virus that can infect bacteria. They were first identified in 1896 (Hankin, 1896b). Bacteriophages, as viruses, are obligate intercellular parasites that need a host cell in which to replicate. There are two aspects of phage life styles: 1) temperate phage that replicate following one of two pathways, lytic or lysogenic based on the host cell and its environment, or 2) virulent phage that follow a strictly lytic replication pathway. However, lytic or virulent phages always result in damaging their bacterial host cell following the production, assembly and release of progeny phages. Temperate phages can replicate like lytic phage or, under certain condition, they can direct the incorporation of their viral genome into the genome of the bacterial host in a mechanism called a recombination event. As a result, the phage becomes a prophage, and its bacterial host becomes a lysogen. All new generations from that lysogen cell will carry that prophage (Weinbauer, 2004). Prophages have been manifested to involve significant function in the diversification, virulence and evolution of bacteria (Canchaya et al., 2004, Ohnishi et al., 2001). Moreover, converting phages, a smaller group of temperate phages, so called because they can convert commensal bacteria and other non-pathogenic bacteria to virulent, pathogenic forms do so through the carriage of one or two genes that are expressed by their bacterial lysogens and are well known to drive the evolution of bacterial virulence (Allison, 2007, Bae et al., 2006).

An example of converting phage are the Shiga toxin-encoding bacteriophages (Stx phages). Stx phages are responsible for altering the pathogenic profile of the *E. coli* hosts by a mechanism called “lysogenic conversion “ (Feng et al., 1998, Riley et al., 1983, Pang et al., 2009, Strockbine et al., 1986). All *E. coli* carrying Stx phage are known as Shiga toxin-encoding *Escherichia coli* (STEC). STEC, particularly the more virulent subset of STEC known as EHEC, which colonise the human colonic epithelium through the production of A/E lesions, became a global challenge to food safety due to their carriage of an Stx prophage. EHEC were first really noticed during an outbreak of foodborne disease linked to undercooked ground beef in 1982 (Riley et al., 1983, Feng et al., 1998). The disease symptoms associated with EHEC can include bloody

diarrhoea and haemorrhagic colitis and life-threatening conditions such as thrombocytopenic purpura (TTP) and haemolytic uremic syndrome (HUS) (Allison, 2007). All currently characterised Shiga toxin phages (Stx) have been classified within the lambdoid phages because they behave as temperate phages and participate genomic organisation and context with the genome of bacteriophage lambda (λ) (Allison, 2007), but there is one recent Stx phage in last few months is revealed to be non lambdoid shiga toxin which is named Eru phage referring to *eru* genes. Eru phage does not encode replication proteins in lambda phage O and P instead of these proteins the Eru phage encodes erulA, erulB, and erulC that are suggested involving in phage replication (Llarena et al., 2021). However, Stx phages like other lambdoid phages, carry a high degree of genetic mosaicism (Smith et al., 2012a). Stx phage genome are bigger approximately twice than the genome of λ (Allison, 2007). Stx phages as a group are very heterogeneous but there are no two phages are identical (Smith et al., 2012a), as evident from the genomic comparisons of the characterised Stx phages: ϕ24B, Min 27, 933W, VT2-Sakai, Phi 27, BP-4795, YYZ-2008 and Stx2 converting phage 1717 (Smith et al., 2012a). The Stx phage group at Liverpool has characterised ϕ24B with respect to its host range (James et al., 2001a), immunity profile (Allison et al., 2003), host recognition mechanism (Smith et al., 2007a), poly-lysogency (Fogg et al., 2011, Fogg et al., 2007), and its impact on the bacterial host (Riley et al., 2012a, Veses-Garcia et al., 2015a) so that it is now the most well characterised of all of the Stx phages. However, like most of the other Stx phages, around 74% of the genes annotated in the genome of $\phi 24_B$ have not been assigned a probable function through bioinformatic analyses (Allison, 2007), even though many of the genes carried on Stx phages share sequence identity with other comparator Stx phages are conserved with respect to genomic context. The genes encoding Shiga toxin are always located immediately downstream of the Q anti terminator gene (Unkmeir and Schmidt, 2000), which is the main factor controlling Shiga toxin production by *E. coli* lysogens (STEC). When Stx phages are induced into the lytic replication state, the CI repressor undergoes autocleavage a result of the function of activated RecA (Łoś et al., 2009, Little, 1984), leading to the production of Q, which enables production of all of the late transcripts. RecA activation, which drives CI autocleavage can be induced *in vitro* by UV radiation or any compounds that lead to DNA damage, such as fluoroquinolone drugs (norfloxacin) or mitomycin C (Little, 1984, Łoś et al., 2009). This conserved genomic context has been proposed by Gerald

Koudelka to be important to the fitness of lysogens (Lainhart et al., 2009a). Reports of prophage loss upon passage in the lab, and the discovery of many remnant phage regions in bacterial genome sequences has led us to believe that phage genomes are inherently unstable (Murase et al., 1999, Bielaszewska et al., 2007). There are many reasons for genome differentiation and reduction, such as: miss-packaging progeny viral genome copies or miss excision as well as recombination of prophage sequences, which may lead to positive impact on the selection and survival of both the phages and host cell (Wang et al., 2010c, Gottesman et al., 1974). We assume that genes conserved in sequence and context across many phage genomes must be due to the provision of some benefit to the phage or its lysogen, though in many instances we have yet failed to identify the selective pressure.

Two hypothetical genes were studied in this thesis, one was expressed in the late stage of the lytic cycle of ϕ$24_{B,}$ (*P21*), and the other is expressed by the lysogen, vb_24_B_48 gene (*48*). The vb_24_B_21 gene appears to be part of the lysis cassette transcript that is controlled by the activation promoter R' (*p*R'). The expression of vb_24_B_48, gene *48,* as indicated by RNASeq, is controlled by it own promoter. The analyse of expression of these will help to understand the function of these genes if they are carried from *situ* recombination events with no impact from the mechanization of phage replication or bacterial host or they are holding their expression under control in the genome to do their function in advanced bacterial host or replication the phage (Smith et al., 2012a, Veses-Garcia et al., 2015a).

The first hypothetical gene is (*P21*) which is located downstream from the *stx* operon that encode the Shiga toxins and upstream of the lysis cassette genes (*S*, *R*, *Rz* and *Rz1*). As this project had strated in 2017, the researches showed that *P21* was the most highly conserved gene across all the Stx phages (Fig. 3.1) (Christie et al., 2012).Three years later, some Stx phages have discovered that show do not presence *P21* on the *stx* regions *e.g.* Stx2d phage 2595 (Zuppi et al., 2020). The lab experiment results that aims to prove the P21 is expressed as part of the lysis transcript is the same were not as expectation. The northern blotting experiment showed rRNA bands (Fig. 3.15B), while the aim was detectecting mRNA transcript of intresting genes *P21*, *S*, *R*, *Rz*, and *Rz1*. Beside this result the 5' race experiment also did not identify the promoter previously identified by RNASeq (Fig. 3.22) to identiy the transcription start site (TSS) sequence of P21 that is expected promotor *pR* putative late (Fig. 3.23)

(Smith et al., 2012a, Veses-Garcia et al., 2015a). It is suggestion to retry northern blotting experiment after subtracting rRNA from total RNA, and redesign the SP1, SP2, and SP3 primers in 5' race experiment, design the primers of *P21*, *S*, *R*, *Rz*, and *Rz1* to run RT-PCR for looking *S*, *R, Rz*, and *Rz1* on trscript with P21. The assigned function of P21 has proposed that may impact in lytic phage replication or benefit the host cell. Sorting a phenotype of induced $\phi 24_B$ cells in present expression P21 or absent will help to understand the function of hypothesis gene. So, the wild type phage that encodes P21 ($\phi 24_B$::Kan), and mutant phage that does not encode P21 ($\phi 24_B$::KanΔP21::Tet) were created in two different *E.coli* host background that had a highly development peptidoglycan structure to make sure P21 either or not impact on peptidoglycan in identical structure. There are three differences showing when the P21 expression in induced $\phi 24_B$ than absent P21 expression which are difference in plaques formation, and cell population. The first difference was in plaques formation, the wild type lysogen that encode P21 demonstrates reduce number of plaques than mutant type lysogen after approximately 4 h upon induction in both *E.coli* host background. It is thoughtful if the P21 was kept in fully produce phage inside the cell and prevent release that why the lysis agents chloroform that used to release phages to prove intracellular assembly of phage before lysis was added in both types of lysogens. As a result, the mutant lysogen had behaved as the lysogens in presence chloroform in both *E.coli* host background (Fig. 3.8, and Fig. 3.9). The second differences was in cell populations, when the both types of lysogen cells were stained by SYBR™ Green I and positively charged carbocyanine dye 3,3'-dipropylthiadicarbocyanine iodide ($DiSC_3$ (5)) and the both type lysogens were collected in three different time points post induction which were: 0 min, 180 min, and 240 min. As a results, the flowcytometry results presented the double number of cell survive of prophage production in present P21 expression than when the P21 expression was absent after 240 min post induction when the lysogen cells were stained by ($DiSC_3$ (5)) (Fig. 3.17). Moreover, the number of intact cells in present expression P21 approximately triple than the intact cells in absent P21 expression after 240 min post induction when the lysogen cells were stained by SYBR™ Green I (Fig. 3.18). These preliminary data suggest that P21 may function to benefit the lysogen which is opposite function to lysis cassette genes function that also can be more proven if the previous experiment run in the same protocol with bacterial cell

encode P21 had induced by arabinose that induces P21 experssion.To promote the P21 benefits the lysogen hypothesis, it is suggestion to run study similar to (Lainhart et al., 2009b) that predicts *stx* genes is act as a bacterial antipredator to the bacterial host cells againt *Tetrahymena thermophlia*. For future work running experiment to compare wild type lysogen and mutant type lysogen in the protozoal predation model to approach if the P21 expression alter the survival of the *E. coli* and the wildtype lysogen surive better beside producing Shiga toxin without dying. This work will begin in 2022 in collaboration with Gerald Koudelka's labroatroy at the University of Buffalo.

The homolog sequence of 645 amino acids long protein of P21 are showed DUF1737 in N-terminus that residues from 1 to 72, an esterase domain that residues from 73 to 392, and jelly roll domain in C-terminus that residues from 393 to 645 sequences. When the P21 was homologised within the *E.coli* chromosome, the results showed the homology structure of esterase domain was resulted relatively homology with the endogenous NanS esterase of *E.coli* (57% seq. id., 68% conservation). However, NanS deacetylates 5-N-acetyl-9-O-acetyl neuraminic acid and involved in muerin metabolism. The homology model for esterase domain of P21 is NanS which homology structure showed structural of SNGH carbohydrate esterase but without include the typical catalytic region (Franke et al., 2020a). Moreover, the C-terminus jelly roll domain of P21 crystal structure showed a groove surface which noticed on the concave side of the β –sandwich. However, when the jelly-roll fold of P21 C-terminus was run on the database programs, the results predicted a carbohydrate binding site (Franke et al., 2020a). The P21 recombinant was collected and was assayed the enzyme acetyl esterase in *vitro* to identify the P21 recombination has a highly enzymatic activity and the rest of protein domains behave well. As a result, the P21 recombinant demonstrated a high level of acetyl esterase activity that degraded the (4-MUFac) to (4-MUF) faster as the concentration of P21 had increased (Fig. 4.6). The P21 shows binding to peptidoglycan of *E.coli* and also the P21 binding to peptidoglycan in presence the competitors N- acetyl glucosamine , N- acetyl muramic acid, bovine serum albumin , and glucose (Fig. 4.8). The endolysin protein that is encoded by *R* gene, breaks down the peptidoglycan by hydrolysis the MurNac-GlcNac glycosidic bond (São-José et al., 2003). In contrast, the P21 binding peptidoglycan was assayed in four competitor inhibitors with four different concentrations to know which specific component of peptidoglycan has higher binding than other. These

reacted samples were run in SDS PAGE (Fig. 4.9), and western blotting using rabbit anti-P21 sera (Fig. 4.10). The bands of western blotting were measured and statistically analysis. As a result, P21 may recognise the peptidoglycan of host cell at the N- acetyl muramic acid that showed in as the N- acetyl muramic acid inhibitor was increased, the P21 binding peptidoglycan was decreased (Fig. 4.11), while as the N-acetyl glucosamine inhibitor was increased, the P21 binding peptidoglycan was increased (Fig. 4.12). The sticky protein bovine serum albumin inhibitor, the P21 binding peptidoglycan was decreased (Fig. 4.14). It is suggestion to clone the carbohydrate binding domain (CBD) in C-terminus that residues from 393 to 645 of P21 in pEMT11 plasmid (Table 2.3) (2.21), and then recombinant the protein (CBD P21) (2.8) and (2.9) to run in protein binding assay (4.2.2.1) to understand how if the P21 has useful this feature of cabohydrate binding in proposed role of P21 in host cell peptidoglycan. Moreover, it would be interesting to measure if the P21 expression has induced with arabinose, it can make peak 16 (Fig. 4.15, Fig. 4.16, and Fig. 4.17) get bigger rather than just looking at expression of P21 for a few minutes in the lysogen in HPLC: as well as having an impact on phage release in a lysogen population.

The second hypothetical gene is (*48*) which is located closing to the right end of phage genome. It is a large gene with size 8.4 kbp and encodes a 2088 amino acids protein. The gene annotation shares with *Salmonella enterica* subsp. e*nterica* serovar Kentucky isolate (ZP_0258689) in 1128 of the 1611 amino acids residues. In addition, the protein had traits of giant genes that encoded surface proteins which are characteristic acidity, hydrophilic, and lack threonine and serine, increased the bacterial fitness (Reva and Tümmler, 2008). Plasmids pGM190_3 and pGM304_1 were constructed to carry gene *48* of and then they were cloned in *E. coli* K-12 strain MC1061 naïve cell. Gene *48* shows increasing expression by arabinose induction (Fig. 5.7). When compare $\phi 24_B$::Cat lysogen in an MC1061 genetic background and naive cells *E. coli* strain MC1061in the antimicrobial agents resistance assays, the results were, the $\phi 24_B$ lysogen shows increasing antibiotic resistance than naïve cells MC1061 under amoxicillin, and carbenicillin, and increasing drug resistance than naïve cells MC1061under 8-hydroxyquinoline pressure. While the naïve cells MC1061 shows increasing drug resistance than $\phi 24_B$ lysogen under sanguinarine pressure. However, the cloned MC1061 that carried plasmid harboured gene *48* beside the same cells that were inducted by arabinose in two different concertation (15%

arabinose, and 20% arabinose) were added to compare with MC1061/ $\phi 24_B$::Cat lysogen and naive cells *E. coli* strain MC1061in the antimicrobial agents resistance assays. As a result, the arabinose inducted MC1061 whose carried plasmid harbouring gene *48* had more resistance under 8-hydroxyquinoline pressure, than $\phi 24_B$ lysogen cells and naïve MC1061 cells (Fig. 5.17). These results can initially suggest that gene *48* may play role in increased bacterial fitness. To strengthen this result, it needs to identify a phenotype of gene *48* by knocking out gene 48 in prophage that expected showing loss of resistance to antimicrobial, confer the resistance of 8-hydroxyquinolone by cheacking the absence of the plasmid that arabinose has no impact on 8-hydroxyquinolone resistance.

It is frustrating that the Covid-19 pandemic hit the UK so hard at the beginning of 2020 and impacted so much of the last two years I had to work on this project. The impact of this was that many experiments could only be run once instead of being replicated many times. I was unable to travel back to Newcastle to continue work with my collaborators at the University of Newcastle and here in Liverpool, access to equipment was severely impacted due to limited lab openings, shortened working hours and high demand and competition for usage for that equipment. Work has also been impacted by delays in getting consumables due is issues with Brexit, transportation and logistics. However, the end results of this project have produced functions for two previously uncharacterised genes and provided biological functions for both of them.

In conclusion, the two hypothetical genes (*P21* and *48*) that were encoded by $\phi 24_B$, showed some benefits to bacterial host in stabilise the lysogen, adding to the benefits of prophage carriage such as antimicrobial tolerance, acid resistance, and that may reveal in future modifying host cells peptidoglycan, and protozoan predation survival.

References

ABBOTT, D. W. & VAN BUEREN, A. L. 2014. Using structure to inform carbohydrate binding module function. *Current opinion in structural biology,* 28**,** 32-40.

ABU-MEDIAN, A.-B., VAN DIEMEN, P. M., DZIVA, F., VLISIDOU, I., WALLIS, T. S. & STEVENS, M. P. 2006. Functional analysis of lymphostatin homologues in enterohaemorrhagic Escherichia coli. *FEMS microbiology letters,* 258**,** 43-49.

ACHESON, D., MOORE, R., DE BREUCKER, S., LINCICOME, L., JACEWICZ, M., SKUTELSKY, E. & KEUSCH, G. 1996. Translocation of Shiga toxin across polarized intestinal cells in tissue culture. *Infection and immunity,* 64**,** 3294-3300.

ACKERMANN, H.-W. 1998. Tailed bacteriophages: the order Caudovirales. *Advances in virus research,* 51**,** 135-201.

ALBRECHT, M., FIEGE, M. & OSETSKA, O. 2008. 8-Hydroxyquinolines in metallosupramolecular chemistry. *Coordination Chemistry Reviews,* 252**,** 812-824.

ALDICK, T., BIELASZEWSKA, M., UHLIN, B. E., HUMPF, H. U., WAI, S. N. & KARCH, H. 2009. Vesicular stabilization and activity augmentation of enterohaemorrhagic Escherichia coli haemolysin. *Molecular microbiology,* 71**,** 1496-1508.

ALLISON, H. E. 2007. Stx-phages: drivers and mediators of the evolution of STEC and STEC-like pathogens.

ALLISON, H. E., SERGEANT, M. J., JAMES, C. E., SAUNDERS, J. R., SMITH, D. L., SHARP, R. J., MARKS, T. S. & MCCARTHY, A. J. 2003. Immunity profiles of wild-type and recombinant Shiga-like toxin-encoding bacteriophages and characterization of novel double lysogens. *Infection and immunity,* 71**,** 3409-3418.

AMBLER, R. 1980. The structure of ß-lactamases Phil. *Trans. R. Soc. Lond,* 289**,** 321-331.

AMOROSO, A., BOUDET, J., BERZIGOTTI, S., DUVAL, V., TELLER, N., MENGIN-LECREULX, D., LUXEN, A., SIMORRE, J.-P. & JORIS, B. 2012. A peptidoglycan fragment triggers β-lactam resistance in Bacillus licheniformis. *PLoS pathogens,* 8**,** e1002571.

ANDERSEN, L. P. & RASMUSSEN, L. 2009. Helicobacter pylori-coccoid forms and biofilm formation. *FEMS Immunology & Medical Microbiology,* 56**,** 112-115.

ARIAS, C. A. & MURRAY, B. E. 2012. The rise of the Enterococcus: beyond vancomycin resistance. *Nature Reviews Microbiology,* 10**,** 266-278.

ARRAIANO, C. M., BAMFORD, J., BRÜSSOW, H., CARPOUSIS, A. J., PELICIC, V., PFLÜGER, K., POLARD, P. & VOGEL, J. 2007. Recent advances in the expression, evolution, and dynamics of prokaryotic genomes. *Journal of bacteriology,* 189**,** 6093-6100.

ASHKENAZY, H., EREZ, E., MARTZ, E., PUPKO, T. & BEN-TAL, N. 2010. ConSurf 2010: calculating evolutionary conservation in sequence and structure of proteins and nucleic acids. *Nucleic acids research,* 38**,** W529-W533.

AZIZ, R. K., BARTELS, D., BEST, A. A., DEJONGH, M., DISZ, T., EDWARDS, R. A., FORMSMA, K., GERDES, S., GLASS, E. M. & KUBAL, M. 2008. The RAST Server: rapid annotations using subsystems technology. *BMC genomics,* 9**,** 1-15.

BACHMANN, B. J. J. B. R. 1972. Pedigrees of some mutant strains of Escherichia coli K-12. 36**,** 525-557.
BAE, T., BABA, T., HIRAMATSU, K. & SCHNEEWIND, O. 2006. Prophages of Staphylococcus aureus Newman and their contribution to virulence. *Molecular microbiology,* 62**,** 1035-1047.
BANDYOPADHYAY, P. & STEINMAN, H. M. 2000. Catalase-peroxidases of Legionella pneumophila: cloning of the katA gene and studies of KatA function. *Journal of Bacteriology,* 182**,** 6679-6686.
BARONDESS, J. J. & BECKWFTH, J. 1990. A bacterial virulence determinant encoded by lysogenic coliphage λ. *Nature,* 346**,** 871.
BARROSO, L., WANG, S., PHELPS, C., JOHNSON, J. & WILKINS, T. 1990. Nucleotide sequence of Clostridium difficile toxin B gene. *Nucleic Acids Research,* 18**,** 4004.
BAUER, M. E. & WELCH, R. A. 1996. Characterization of an RTX toxin from enterohemorrhagic Escherichia coli O157: H7. *Infection and immunity,* 64**,** 167-175.
BEAMAN, L. & BEAMAN, B. L. 1984. The role of oxygen and its derivatives in microbial pathogenesis and host defense. *Annual review of microbiology,* 38**,** 27-48.
BECKER, T. E. 2013. *Heat and B-10 enriched boric acid as recycled groundwater tracers for managed aquifer recharge*, University of California, Santa Barbara.
BERGER, P., KOUZEL, I. U., BERGER, M., HAARMANN, N., DOBRINDT, U., KOUDELKA, G. B. & MELLMANN, A. J. B. G. 2019. Carriage of Shiga toxin phage profoundly affects Escherichia coli gene expression and carbon source utilization. 20**,** 1-14.
BERGHOLZ, T. M., BOWEN, B., WIEDMANN, M. & BOOR, K. J. 2012. Listeria monocytogenes shows temperature-dependent and-independent responses to salt stress, including responses that induce cross-protection against other stresses. *Applied and environmental microbiology,* 78**,** 2602-2612.
BERGSTEN, G., SAMUELSSON, M., WULT, B., LEIJONHUFVUD, I., FISCHER, H. & SVANBORG, C. 2004. PapG-dependent adherence breaks mucosal inertia and triggers the innate host response. *The Journal of infectious diseases,* 189**,** 1734-1742.
BERNET-CAMARD, M.-F., COCONNIER, M.-H., HUDAULT, S. & SERVIN, A. L. 1996. Pathogenicity of the diffusely adhering strain Escherichia coli C1845: F1845 adhesin-decay accelerating factor interaction, brush border microvillus injury, and actin disassembly in cultured human intestinal epithelial cells. *Infection and immunity,* 64**,** 1918-1928.
BERRY, J. D., RAJAURE, M. & YOUNG, R. 2013. Spanin function requires subunit homodimerization through intermolecular disulfide bonds. *Molecular microbiology,* 88**,** 35-47.
BHARATI, K. & GANGULY, N. K. J. T. I. J. O. M. R. 2011. Cholera toxin: a paradigm of a multifunctional protein. 133**,** 179.
BIELASZEWSKA, M., PRAGER, R., KOCK, R., MELLMANN, A., ZHANG, W., TSCHÄPE, H., TARR, P. I. & KARCH, H. 2007. Shiga toxin gene loss and transfer in vitro and in vivo during enterohemorrhagic Escherichia coli O26 infection in humans. *Applied and environmental microbiology,* 73**,** 3144-3150.

BLACK, R. E., COUSENS, S., JOHNSON, H. L., LAWN, J. E., RUDAN, I., BASSANI, D. G., JHA, P., CAMPBELL, H., WALKER, C. F. & CIBULSKIS, R. 2010. Global, regional, and national causes of child mortality in 2008: a systematic analysis. *The lancet,* 375**,** 1969-1987.

BLACKBURN, N. T. & CLARKE, A. J. 2001a. Identification of four families of peptidoglycan lytic transglycosylases. *Journal of molecular evolution,* 52**,** 78-84.

BLACKBURN, N. T. & CLARKE, A. J. J. J. O. M. E. 2001b. Identification of four families of peptidoglycan lytic transglycosylases. 52**,** 78-84.

BLOCH, S., NEJMAN-FALEŃCZYK, B., DYDECKA, A., ŁOŚ, J. M., FELCZYKOWSKA, A., WĘGRZYN, A. & WĘGRZYN, G. 2014. Different expression patterns of genes from the exo-xis region of bacteriophage λ and Shiga toxin-converting bacteriophage Φ24B following infection or prophage induction in Escherichia coli. *PLoS One,* 9**,** e108233.

BOISEN, N., KROGFELT, K. A. & NATARO, J. P. 2013. *Escherichia coli: Chapter 8. Enteroaggregative Escherichia coli*, Elsevier Inc. Chapters.

BORTOLUSSI, R., VANDENBROUCKE-GRAULS, C., VAN ASBECK, B. & VERHOEF, J. 1987. Relationship of bacterial growth phase to killing of Listeria monocytogenes by oxidative agents generated by neutrophils and enzyme systems. *Infection and immunity,* 55**,** 3197-3203.

BOURRIAUD, C., AKOKA, S., GOUPRY, S., ROBINS, R., CHERBUT, C. & MICHEL, C. 2002. Butyrate production from lactate by human colonic microflora. *REPRODUCTION NUTRITION DEVELOPMENT,* 42**,** S55-S55.

BOUZARI, S. & VARGHESE, A. 1990. Cytolethal distending toxin (CLDT) production by enteropathogenic Eschrichia coli (EPEC). *FEMS microbiology letters,* 71**,** 193-198.

BOYD, B. & LINGWOOD, C. 1989. Verotoxin receptor glycolipid in human renal tissue. *Nephron,* 51**,** 207-210.

BOYD, E. F. 2012. Bacteriophage-encoded bacterial virulence factors and phage–pathogenicity island interactions. *Advances in virus research,* 82**,** 91-118.

BOYD, E. F. & BRÜSSOW, H. 2002. Common themes among bacteriophage-encoded virulence factors and diversity among the bacteriophages involved. *Trends in microbiology,* 10**,** 521-529.

BRABBAN, A., HITE, E. & CALLAWAY, T. 2005. Evolution of foodborne pathogens via temperate bacteriophage-mediated gene transfer. *Foodbourne Pathogens & Disease,* 2**,** 287-303.

BRENNER, D. 1981. Intrr~ duction to the family Enterobacteriaceae, in<< The prokaryotes, a handbook on habitat, isolatior, _ and identification of bacteria>>(MP Starr, F~. Stolp, HG Triiper, A. Balews & HG Schlegel)(pp. 1105-1127). Springer-Verlag, Berlin.

BRINDA, K., SUROLIA, A. & VISHVESHWARA, S. 2005. Insights into the quaternary association of proteins through structure graphs: a case study of lectins. *Biochemical journal,* 391**,** 1-15.

BRUNDER, W., SCHMIDT, H. & KARCH, H. 1997a. EspP, a novel extracellular serine protease of enterohaemorrhagic Escherichia coli O157: H7 cleaves human coagulation factor V. *Molecular microbiology,* 24**,** 767-778.

BRUNDER, W., SCHMIDT, H. & KARCH, H. J. M. M. 1997b. EspP, a novel extracellular serine protease of enterohaemorrhagic Escherichia coli O157: H7 cleaves human coagulation factor V. 24**,** 767-778.

BRÜSSOW, H., CANCHAYA, C. & HARDT, W.-D. 2004a. Phages and the evolution of bacterial pathogens: from genomic rearrangements to lysogenic conversion. *Microbiology and molecular biology reviews,* 68**,** 560-602.
BRÜSSOW, H., CANCHAYA, C., HARDT, W.-D. J. M. & REVIEWS, M. B. 2004b. Phages and the evolution of bacterial pathogens: from genomic rearrangements to lysogenic conversion. 68**,** 560-602.
BUDIMIR, A. 2011. Metal ions, Alzheimer's disease and chelation therapy. *Acta Pharmaceutica,* 61**,** 1.
BURLAND, V., SHAO, Y., PERNA, N. T., PLUNKETT, G., BLATTNER, F. R. & SOFIA, H. J. 1998a. The complete DNA sequence and analysis of the large virulence plasmid of Escherichia coli O157: H7. *Nucleic acids research,* 26**,** 4196-4204.
BURLAND, V., SHAO, Y., PERNA, N. T., PLUNKETT, G., BLATTNER, F. R. & SOFIA, H. J. J. N. A. R. 1998b. The complete DNA sequence and analysis of the large virulence plasmid of Escherichia coli O157: H7. 26**,** 4196-4204.
BUSH, K. & BRADFORD, P. A. 2019. Interplay between β-lactamases and new β-lactamase inhibitors. *Nature Reviews Microbiology,* 17**,** 295-306.
BUSH, K. & JACOBY, G. A. 2010. Updated functional classification of β-lactamases. *Antimicrobial agents and chemotherapy,* 54**,** 969-976.
CAHILL, J., RAJAURE, M., HOLT, A., MORELAND, R., O'LEARY, C., KULKARNI, A., SLOAN, J. & YOUNG, R. 2017. Suppressor analysis of the fusogenic lambda spanins. *Journal of virology,* 91**,** e00413-17.
CAMPBELL, A. 1994. Comparative molecular biology of lambdoid phages. *Annual review of microbiology,* 48**,** 193-222.
CAMPELLONE, K. G., ROBBINS, D. & LEONG, J. M. 2004. EspFU is a translocated EHEC effector that interacts with Tir and N-WASP and promotes Nck-independent actin assembly. *Developmental cell,* 7**,** 217-228.
CANCHAYA, C., FOURNOUS, G. & BRÜSSOW, H. 2004. The impact of prophages on bacterial chromosomes. *Molecular microbiology,* 53**,** 9-18.
CANO, V., MARCH, C., INSUA, J. L., AGUILÓ, N., LLOBET, E., MORANTA, D., REGUEIRO, V., BRENNAN, G. P., MILLÁN-LOU, M. I. & MARTÍN, C. 2015. K lebsiella pneumoniae survives within macrophages by avoiding delivery to lysosomes. *Cellular microbiology,* 17**,** 1537-1560.
CAPRIOLI, A., FALBO, V., RODA, L., RUGGERI, F. & ZONA, C. 1983. Partial purification and characterization of an Escherichia coli toxic factor that induces morphological cell alterations. *Infection and Immunity,* 39**,** 1300-1306.
CARON, E., CREPIN, V. F., SIMPSON, N., KNUTTON, S., GARMENDIA, J. & FRANKEL, G. 2006. Subversion of actin dynamics by EPEC and EHEC. *Current opinion in microbiology,* 9**,** 40-45.
CASTANIE-CORNET, M.-P., PENFOUND, T. A., SMITH, D., ELLIOTT, J. F. & FOSTER, J. W. 1999. Control of acid resistance in Escherichia coli. *Journal of bacteriology,* 181**,** 3525-3535.
CATALÃO, M. J., GIL, F., MONIZ-PEREIRA, J. & PIMENTEL, M. 2011. Functional analysis of the holin-like proteins of mycobacteriophage Ms6. *Journal of bacteriology,* 193**,** 2793-2803.
CAVA, F. & DE PEDRO, M. A. 2014. Peptidoglycan plasticity in bacteria: emerging variability of the murein sacculus and their associated biological functions. *Current opinion in microbiology,* 18**,** 46-53.

CHANG, C., MAHMOOD, M. M., TEUBER, S. S. & GERSHWIN, M. E. 2012. Overview of penicillin allergy. *Clinical reviews in allergy & immunology,* 43**,** 84-97.
CHAPUT, C., ECOBICHON, C., CAYET, N., GIRARDIN, S. E., WERTS, C., GUADAGNINI, S., PRÉVOST, M.-C., MENGIN-LECREULX, D., LABIGNE, A. & BONECA, I. G. 2006. Role of AmiA in the morphological transition of Helicobacter pylori and in immune escape. *PLoS pathogens,* 2**,** e97.
CHART, H. Toxigenic Escherichia coli. Symposium Series (Society for Applied Microbiology), 1998. 77S-86S.
CHEN, L., DENG, H., CUI, H., FANG, J., ZUO, Z., DENG, J., LI, Y., WANG, X. & ZHAO, L. J. O. 2018. Inflammatory responses and inflammation-associated diseases in organs. 9**,** 7204.
CHEN, S.-Y., JANE, W.-N., CHEN, Y.-S. & WONG, H.-C. 2009. Morphological changes of Vibrio parahaemolyticus under cold and starvation stresses. *International journal of food microbiology,* 129**,** 157-165.
CHONG, Y., FITZHENRY, R., HEUSCHKEL, R., TORRENTE, F., FRANKEL, G. & PHILLIPS, A. D. 2007. Human intestinal tissue tropism in Escherichia coli O157: H7–initial colonization of terminal ileum and Peyer's patches and minimal colonic adhesion ex vivo. *Microbiology,* 153**,** 794-802.
CHRISTIE, G. E., ALLISON, H., KUZIO, J., MCSHAN, M., WALDOR, M. & KROPINSKI, A. M. 2012. *Prophage-induced changes in cellular cytochemistry and virulence*, CABI Press, UK.
CLARKE, A. J. & DUPONT, C. 1992. O-acetylated peptidoglycan: its occurrence, pathobiological significance, and biosynthesis. *Canadian journal of microbiology,* 38**,** 85-91.
CLARKE, A. J., STRATING, H. & BLACKBURN, N. T. 2002. Pathways for the O-acetylation of bacterial cell wall polysaccharides. *Glycomicrobiology.* Springer.
CLARKE, C. A., SCHEURWATER, E. M. & CLARKE, A. J. 2010. The vertebrate lysozyme inhibitor Ivy functions to inhibit the activity of lytic transglycosylase. *Journal of biological chemistry,* 285**,** 14843-14847.
CLEMENTS, A., YOUNG, J. C., CONSTANTINOU, N. & FRANKEL, G. J. G. M. 2012. Infection strategies of enteric pathogenic Escherichia coli. 3**,** 71-87.
CLOKIE, M. R., MILLARD, A. D., LETAROV, A. V. & HEAPHY, S. J. B. 2011. Phages in nature. 1**,** 31-45.
COLOMER-LLUCH, M., JOFRE, J. & MUNIESA, M. 2011. Antibiotic resistance genes in the bacteriophage DNA fraction of environmental samples. *PloS one,* 6**,** e17549.
CONRADI, H. 1903. Über lösliche, durch aseptische Autolyse erhaltene Giftstoffe von Ruhr-und Typhusbazillen. *DMW-Deutsche Medizinische Wochenschrift,* 29**,** 26-28.
CONTROL, C. F. D. & PREVENTION 2013. Office of Infectious Disease. *Antibiotic resistance threats in the United States*.
COOKSON, S. T. & NATARO, J. P. 1996. Characterization of HEp-2 cell projection formation induced by diffusely adherentEscherichia coli. *Microbial pathogenesis,* 21**,** 421-434.
COURT, D. L., OPPENHEIM, A. B. & ADHYA, S. L. 2007. A new look at bacteriophage λ genetic networks. *Journal of bacteriology,* 189**,** 298-304.
COURVALIN, P. 2006. Vancomycin resistance in gram-positive cocci. *Clinical infectious diseases,* 42**,** S25-S34.

CRICHTON, R. R., DEXTER, D. & WARD, R. J. 2008. Metal based neurodegenerative diseases—from molecular mechanisms to therapeutic strategies. *Coordination Chemistry Reviews,* 252**,** 1189-1199.
D'ARI, R. 1985. The SOS system. *Biochimie,* 67**,** 343-347.
DAHAN, S., WILES, S., LA RAGIONE, R. M., BEST, A., WOODWARD, M. J., STEVENS, M. P., SHAW, R. K., CHONG, Y., KNUTTON, S. & PHILLIPS, A. 2005. EspJ is a prophage-carried type III effector protein of attaching and effacing pathogens that modulates infection dynamics. *Infection and Immunity,* 73**,** 679-686.
DALECKI, A. G., CRAWFORD, C. L. & WOLSCHENDORF, F. 2017. Copper and antibiotics: discovery, modes of action, and opportunities for medicinal applications. *Advances in microbial physiology,* 70**,** 193-260.
DAUTIN, N. 2010. Serine protease autotransporters of enterobacteriaceae (SPATEs): biogenesis and function. *Toxins,* 2**,** 1179-1206.
DAVIS III, A. E., LU, F., MEJIA, P. J. T. & HAEMOSTASIS 2010. C1 inhibitor, a multi-functional serine protease inhibitor. 104**,** 886-893.
DE GROOT, J. C., SCHLÜTER, K., CARIUS, Y., QUEDENAU, C., VINGADASSALOM, D., FAIX, J., WEISS, S. M., REICHELT, J., STANDFUß-GABISCH, C. & LESSER, C. F. 2011. Structural basis for complex formation between human IRSp53 and the translocated intimin receptor Tir of enterohemorrhagic E. coli. *Structure,* 19**,** 1294-1306.
DE OLIVEIRA, D. M., FORDE, B. M., KIDD, T. J., HARRIS, P. N., SCHEMBRI, M. A., BEATSON, S. A., PATERSON, D. L. & WALKER, M. J. 2020. Antimicrobial resistance in ESKAPE pathogens. *Clinical microbiology reviews,* 33**,** e00181-19.
DEAN, P. & KENNY, B. 2009. The effector repertoire of enteropathogenic E. coli: ganging up on the host cell. *Current opinion in microbiology,* 12**,** 101-109.
DELAHAY, R. M., FRANKEL, G. & KNUTTON, S. 2001. Intimate interactions of enteropathogenic Escherichia coli at the host cell surface. *Current opinion in infectious diseases,* 14**,** 559-565.
DEVINNEY, R., STEIN, M., REINSCHEID, D., ABE, A., RUSCHKOWSKI, S. & FINLAY, B. B. 1999. Enterohemorrhagic Escherichia coli O157: H7 produces Tir, which is translocated to the host cell membrane but is not tyrosine phosphorylated. *Infection and immunity,* 67**,** 2389-2398.
DIMMOCK, N. J., EASTON, A. J. & LEPPARD, K. N. 2015. *Introduction to modern virology*, John Wiley & Sons.
DONNENBERG, M. S., YU, J. & KAPER, J. 1993. A second chromosomal gene necessary for intimate attachment of enteropathogenic Escherichia coli to epithelial cells. *Journal of Bacteriology,* 175**,** 4670-4680.
DUBOS, R. J. & GEIGER, J. W. 1946. Preparation and properties of Shiga toxin and toxoid. *The Journal of experimental medicine,* 84**,** 143.
DZIVA, F., VAN DIEMEN, P. M., STEVENS, M. P., SMITH, A. J. & WALLIS, T. S. 2004. Identification of Escherichia coli O157: H7 genes influencing colonization of the bovine gastrointestinal tract using signature-tagged mutagenesis. *Microbiology,* 150**,** 3631-3645.
ELLIOTT, S. J., KREJANY, E. O., MELLIES, J. L., ROBINS-BROWNE, R. M., SASAKAWA, C. & KAPER, J. B. 2001. EspG, a novel type III system-secreted protein from enteropathogenic Escherichia coli with similarities to VirA of Shigella flexneri. *Infection and Immunity,* 69**,** 4027-4033.

ELLIOTT, S. J., SPERANDIO, V., GIRÓN, J. A., SHIN, S., MELLIES, J. L., WAINWRIGHT, L., HUTCHESON, S. W., MCDANIEL, T. K. & KAPER, J. B. 2000. The locus of enterocyte effacement (LEE)-encoded regulator controls expression of both LEE-and non-LEE-encoded virulence factors in enteropathogenic and enterohemorrhagic Escherichia coli. *Infection and immunity,* 68**,** 6115-6126.

EMANUELSSON, O., BRUNAK, S., VON HEIJNE, G. & NIELSEN, H. 2007a. Locating proteins in the cell using TargetP, SignalP and related tools. *Nature protocols,* 2**,** 953.

EMANUELSSON, O., BRUNAK, S., VON HEIJNE, G. & NIELSEN, H. 2007b. Locating proteins in the cell using TargetP, SignalP and related tools. *Nature protocols,* 2**,** 953-971.

ENDO, Y., TSURUGI, K., YUTSUDO, T., TAKEDA, Y., OGASAWARA, T. & IGARASHI, K. 1988. Site of action of a Vero toxin (VT2) from Escherichia coli O157: H7 and of Shiga toxin on eukaryotic ribosomes: RNA N-glycosidase activity of the toxins. *European Journal of Biochemistry,* 171**,** 45-50.

ENGLEY JR, F. B. 1952. The neurotoxin of Shigella dysenteriae (Shiga). *Bacteriological reviews,* 16**,** 153-178.

FAGUY, D. M. & DOOLITTLE, W. F. J. T. I. G. T. 2000. Horizontal transfer of catalase-peroxidase genes between archaea and pathogenic bacteria. 16**,** 196-197.

FARR, S. B. & KOGOMA, T. 1991. Oxidative stress responses in Escherichia coli and Salmonella typhimurium. *Microbiological reviews,* 55**,** 561-585.

FARRELL JR, R. E. 2009. *RNA Methodologies: laboratory guide for isolation and characterization*, Academic Press.

FEINER, R., ARGOV, T., RABINOVICH, L., SIGAL, N., BOROVOK, I. & HERSKOVITS, A. A. 2015. A new perspective on lysogeny: prophages as active regulatory switches of bacteria. *Nature Reviews Microbiology,* 13**,** 641-650.

FENG, P., LAMPEL, K. A., KARCH, H. & WHITTAM, T. S. 1998. Genotypic and phenotypic changes in the emergence of Escherichia coli O157: H7. *Journal of Infectious Diseases,* 177**,** 1750-1753.

FLECKENSTEIN, J. M., HARDWIDGE, P. R., MUNSON, G. P., RASKO, D. A., SOMMERFELT, H. & STEINSLAND, H. 2010. Molecular mechanisms of enterotoxigenic Escherichia coli infection. *Microbes and infection,* 12**,** 89-98.

FLEXNER, S. & SWEET, J. E. 1906. The pathogenesis of experimental colitis, and the relation of colitis in animals and man. *The Journal of experimental medicine,* 8**,** 514.

FOGG, P., RIGDEN, D., SAUNDERS, J., MCCARTHY, A. & ALLISON, H. 2010. Characterization of the relationship between integrase, excisionase and antirepressor activities associated with a superinfecting Shiga toxin encoding bacteriophage. *Nucleic acids research,* 39**,** 2116-2129.

FOGG, P., RIGDEN, D., SAUNDERS, J., MCCARTHY, A. & ALLISON, H. 2011. Characterization of the relationship between integrase, excisionase and antirepressor activities associated with a superinfecting Shiga toxin encoding bacteriophage. *Nucleic acids research,* 39**,** 2116-2129.

FOGG, P. C., GOSSAGE, S. M., SMITH, D. L., SAUNDERS, J. R., MCCARTHY, A. J. & ALLISON, H. E. 2007. Identification of multiple integration sites for Stx-phage Φ24B in the Escherichia coli genome, description of a novel integrase and evidence for a functional anti-repressor. *Microbiology,* 153**,** 4098-4110.

FRANKE, B., VESES-GARCIA, M., DIEDERICHS, K., ALLISON, H., RIGDEN, D. J. & MAYANS, O. 2020a. Structural annotation of the conserved carbohydrate esterase vb_24B_21 from Shiga toxin-encoding bacteriophage Φ24B. *Journal of Structural Biology,* 212**,** 107596.

FRANKE, B., VESES-GARCIA, M., DIEDERICHS, K., ALLISON, H., RIGDEN, D. J. & MAYANS, O. J. J. O. S. B. 2020b. Structural annotation of the conserved carbohydrate esterase vb_24B_21 from Shiga toxin-encoding bacteriophage Φ24B. 212**,** 107596.

FRANKEL, G., PHILLIPS, A. D., ROSENSHINE, I., DOUGAN, G., KAPER, J. B. & KNUTTON, S. 1998. Enteropathogenic and enterohaemorrhagic Escherichia coli: more subversive elements. *Molecular microbiology,* 30**,** 911-921.

FRANZIN, F. M. & SIRCILI, M. P. 2015. Locus of enterocyte effacement: a pathogenicity island involved in the virulence of enteropathogenic and enterohemorragic Escherichia coli subjected to a complex network of gene regulation. *BioMed research international,* 2015.

FRASER, M. E., CHERNAIA, M. M., KOZLOV, Y. V. & JAMES, M. N. 1994. Crystal structure of the holotoxino from Shigella dysenteriae at 2.5 Å resolution. *Nature structural biology,* 1**,** 59-64.

FRAUNHOLZ, M. & SINHA, B. 2012. Intracellular Staphylococcus aureus: live-in and let die. *Frontiers in cellular and infection microbiology,* 2**,** 43.

FRIEDBERG, D., UMANSKI, T., FANG, Y. & ROSENSHINE, I. 1999. Hierarchy in the expression of the locus of enterocyte effacement genes of enteropathogenic Escherichia coli. *Molecular microbiology,* 34**,** 941-952.

FRIEDRICH, A. W., BORELL, J., BIELASZEWSKA, M., FRUTH, A., TSCHÄPE, H. & KARCH, H. J. J. O. C. M. 2003. Shiga toxin 1c-producing Escherichia coli strains: phenotypic and genetic characterization and association with human disease. 41**,** 2448-2453.

FROST, L. S., LEPLAE, R., SUMMERS, A. O. & TOUSSAINT, A. 2005. Mobile genetic elements: the agents of open source evolution. *Nature Reviews Microbiology,* 3**,** 722-732.

GAASTRA, W. & SVENNERHOLM, A.-M. 1996. Colonization factors of human enterotoxigenic Escherichia coli (ETEC). *Trends in microbiology,* 4**,** 444-452.

GARCIA, E., NEDIALKOV, Y. A., ELLIOTT, J., MOTIN, V. L. & BRUBAKER, R. R. 1999. Molecular characterization of KatY (antigen 5), a thermoregulated chromosomally encoded catalase-peroxidase of Yersinia pestis. *Journal of bacteriology,* 181**,** 3114-3122.

GARRED, Ø., DUBININA, E., HOLM, P. K., OLSNES, S., VAN DEURS, B., KOZLOV, J. V. & SANDVIG, K. 1995a. Role of processing and intracellular transport for optimal toxicity of Shiga toxin and toxin mutants. *Experimental cell research,* 218**,** 39-49.

GARRED, Ø., DUBININA, E., POLESSKAYA, A., OLSNES, S., KOZLOV, J. & SANDVIG, K. 1997. Role of the disulfide bond in Shiga toxin A-chain for toxin entry into cells. *Journal of Biological Chemistry,* 272**,** 11414-11419.

GARRED, Ø., VAN DEURS, B. & SANDVIG, K. 1995b. Furin-induced cleavage and activation of Shiga toxin. *Journal of Biological Chemistry,* 270**,** 10817-10821.

GEORGOPAPADAKOU, N. 1993. Penicillin-binding proteins and bacterial resistance to beta-lactams. *Antimicrobial agents and chemotherapy,* 37**,** 2045-2053.

GILL, D. M. & RICHARDSON, S. H. 1980. Adenosine diphosphate-ribosylation of adenylate cyclase catalyzed by heat-labile enterotoxin of Escherichia coli: comparison with cholera toxin. *Journal of Infectious Diseases,* 141**,** 64-70.

GIOGHA, C., SCOTT, N. E., WONG FOK LUNG, T., POLLOCK, G. L., HARPER, M., GODDARD-BORGER, E. D., PEARSON, J. S. & HARTLAND, E. L. J. P. P. 2021. NleB2 from enteropathogenic Escherichia coli is a novel arginine-glucose transferase effector. 17**,** e1009658.
GIRARDIN, S. E., TOURNEBIZE, R., MAVRIS, M., PAGE, A. L., LI, X., STARK, G. R., BERTIN, J., DISTEFANO, P. S., YANIV, M. & SANSONETTI, P. J. 2001. CARD4/Nod1 mediates NF-κB and JNK activation by invasive Shigella flexneri. *EMBO reports,* 2**,** 736-742.
GLAUNER, B., HÖLTJE, J. & SCHWARZ, U. 1988. The composition of the murein of Escherichia coli. *Journal of Biological Chemistry,* 263**,** 10088-10095.
GLAUNER, B. J. A. B. 1988. Separation and quantification of muropeptides with high-performance liquid chromatography. 172**,** 451-464.
GOERING, R., DOCKRELL, H., ZUCKERMAN, M., ROITT, I. & CHIODINI, P. L. 2012. *Mims' medical microbiology*, Elsevier Health Sciences.
GOOSNEY, D. L., DEVINNEY, R. & FINLAY, B. B. 2001. Recruitment of cytoskeletal and signaling proteins to enteropathogenic and enterohemorrhagic Escherichia coli pedestals. *Infection and immunity,* 69**,** 3315-3322.
GOTTESMAN, M. M., GOTTESMAN, M. E., GOTTESMAN, S. & MARTIN, G. 1974. Characterization of bacteriophage λ reverse as an Escherichia coli phage carrying a unique set of host-derived recombination functions. *Journal of molecular biology,* 88**,** 471-487.
GRAVITZ, L. 2012. Turning a new phage. *Nature Medicine,* 18**,** 1318-1320.
GRIFFIN, P. M., OLMSTEAD, L. C. & PETRAS, R. E. 1990. Escherichia coli 0157: H7-associated colitis: a clinical and histological study of 11 cases. *Gastroenterology,* 99**,** 142-149.
GRUENHEID, S., DEVINNEY, R., BLADT, F., GOOSNEY, D., GELKOP, S., GISH, G. D., PAWSON, T. & FINLAY, B. B. 2001. Enteropathogenic E. coli Tir binds Nck to initiate actin pedestal formation in host cells. *Nature cell biology,* 3**,** 856-859.
GRYS, T. E., SIEGEL, M. B., LATHEM, W. W. & WELCH, R. A. 2005. The StcE protease contributes to intimate adherence of enterohemorrhagic Escherichia coli O157: H7 to host cells. *Infection and immunity,* 73**,** 1295-1303.
GRYS, T. E., WALTERS, L. L. & WELCH, R. A. 2006. Characterization of the StcE protease activity of Escherichia coli O157: H7. *Journal of bacteriology,* 188**,** 4646-4653.
GUIGNOT, J., SEGURA, A. & TRAN VAN NHIEU, G. 2015. The serine protease EspC from enteropathogenic Escherichia coli regulates pore formation and cytotoxicity mediated by the type III secretion system. *PLoS pathogens,* 11**,** e1005013.
HACKER, J., BLUM-OEHLER, G., MÜHLDORFER, I. & TSCHÄPE, H. 1997. Pathogenicity islands of virulent bacteria: structure, function and impact on microbial evolution. *Molecular microbiology,* 23**,** 1089-1097.
HADI, T., PFEFFER, J. M., CLARKE, A. J. & TANNER, M. E. 2011. Water-soluble substrates of the peptidoglycan-modifying enzyme O-acetylpeptidoglycan esterase (Ape1) from Neisseria gonorrheae. *The Journal of organic chemistry,* 76**,** 1118-1125.
HALE, T. & FORMAL, S. 1980. Cytotoxicity of Shigella dysenteriae 1 for cultured mammalian cells. Oxford University Press.

HALL, C. W. & MAH, T.-F. 2017. Molecular mechanisms of biofilm-based antibiotic resistance and tolerance in pathogenic bacteria. *FEMS microbiology reviews,* 41**,** 276-301.
HANKIN, E. H. 1896a. L'action bactericide des eaux de la Jumna et du Gange sur le vibrion du cholera. *Ann. Inst. Pasteur,* 10**,** ll.
HANKIN, E. H. 1896b. L'action bactericide des eaux de la Jumna et du Gange sur le vibrion du cholera. *Ann Inst Pasteur,* 10.
HAQUE, Q. M., SUGIYAMA, A., IWADE, Y., MIDORIKAWA, Y. & YAMAUCHI, T. 1996. Diarrheal and environmental isolates of Aeromonas spp. produce a toxin similar to Shiga-like toxin 1. *Current microbiology,* 32**,** 239-245.
HARRINGTON, S. M., DUDLEY, E. G. & NATARO, J. P. 2006. Pathogenesis of enteroaggregative Escherichia coli infection. *FEMS microbiology letters,* 254**,** 12-18.
HARRINGTON, S. M., SHEIKH, J., HENDERSON, I. R., RUIZ-PEREZ, F., COHEN, P. S., NATARO, J. P. J. I. & IMMUNITY 2009. The Pic protease of enteroaggregative Escherichia coli promotes intestinal colonization and growth in the presence of mucin. 77**,** 2465-2473.
HARRINGTON, S. M., STRAUMAN, M. C., ABE, C. M. & NATARO, J. P. 2005. Aggregative adherence fimbriae contribute to the inflammatory response of epithelial cells infected with enteroaggregative Escherichia coli. *Cellular microbiology,* 7**,** 1565-1578.
HASAN, R. J., PAWELCZYK, E., URVIL, P. T., VENKATARAJAN, M. S., GOLUSZKO, P., KUR, J., SELVARANGAN, R., NOWICKI, S., BRAUN, W. A. & NOWICKI, B. J. 2002. Structure-function analysis of decay-accelerating factor: identification of residues important for binding of the Escherichia coli Dr adhesin and complement regulation. *Infection and immunity,* 70**,** 4485-4493.
HASDEMIR, U. O., CHEVALIER, J., NORDMANN, P. & PAGÈS, J.-M. 2004. Detection and prevalence of active drug efflux mechanism in various multidrug-resistant Klebsiella pneumoniae strains from Turkey. *Journal of clinical microbiology,* 42**,** 2701-2706.
HASSAN, K. A., LIU, Q., HENDERSON, P. J. & PAULSEN, I. T. 2015. Homologs of the Acinetobacter baumannii AceI transporter represent a new family of bacterial multidrug efflux systems. *MBio,* 6**,** e01982-14.
HÄUSER, R., PECH, M., KIJEK, J., YAMAMOTO, H., TITZ, B., NAEVE, F., TOVCHIGRECHKO, A., YAMAMOTO, K., SZAFLARSKI, W. & TAKEUCHI, N. 2012. RsfA (YbeB) proteins are conserved ribosomal silencing factors. *PLoS genetics,* 8**,** e1002815.
HAYASHI, T., MAKINO, K., OHNISHI, M., KUROKAWA, K., ISHII, K., YOKOYAMA, K., HAN, C.-G., OHTSUBO, E., NAKAYAMA, K. & MURATA, T. 2001a. Complete genome sequence of enterohemorrhagic Eschelichia coli O157: H7 and genomic comparison with a laboratory strain K-12. *DNA research,* 8**,** 11-22.
HAYASHI, T., MAKINO, K., OHNISHI, M., KUROKAWA, K., ISHII, K., YOKOYAMA, K., HAN, C.-G., OHTSUBO, E., NAKAYAMA, K. & MURATA, T. J. D. R. 2001b. Complete genome sequence of enterohemorrhagic Eschelichia coli O157: H7 and genomic comparison with a laboratory strain K-12. 8**,** 11-22.
HE, B., XU, W., SANTINI, P. A., POLYDORIDES, A. D., CHIU, A., ESTRELLA, J., SHAN, M., CHADBURN, A., VILLANACCI, V. & PLEBANI, A. 2007. Intestinal bacteria trigger T cell-independent immunoglobulin A2 class switching by

inducing epithelial-cell secretion of the cytokine APRIL. *Immunity,* 26**,** 812-826.
HENDERSON, I. R., NATARO, J. P. J. I. & IMMUNITY 2001. Virulence functions of autotransporter proteins. 69**,** 1231-1243.
HENDRIX, R. W., LAWRENCE, J. G., HATFULL, G. F. & CASJENS, S. 2000. The origins and ongoing evolution of viruses. *Trends in microbiology,* 8**,** 504-508.
HENGEN, P. N. 1995. Purification of His-Tag fusion proteins from Escherichia coli. *Trends in biochemical sciences,* 20**,** 285-286.
HEROLD, S., KARCH, H. & SCHMIDT, H. 2004. Shiga toxin-encoding bacteriophages–genomes in motion. *International journal of medical microbiology,* 294**,** 115-121.
HILL, D., ROSE, B., PAJKOS, A., ROBINSON, M., BYE, P., BELL, S., ELKINS, M., THOMPSON, B., MACLEOD, C. & AARON, S. D. 2005. Antibiotic susceptibilities of Pseudomonas aeruginosa isolates derived from patients with cystic fibrosis under aerobic, anaerobic, and biofilm conditions. *Journal of clinical microbiology,* 43**,** 5085-5090.
HOFMANN, K. 1993. TMbase-A database of membrane spanning proteins segments. *Biol. Chem. Hoppe-Seyler,* 374**,** 166.
HØIBY, N., BJARNSHOLT, T., GIVSKOV, M., MOLIN, S. & CIOFU, O. 2010. Antibiotic resistance of bacterial biofilms. *International journal of antimicrobial agents,* 35**,** 322-332.
HOLM, L. 2019. Benchmarking fold detection by DaliLite v. 5. *Bioinformatics,* 35**,** 5326-5327.
HOLMGREN, J. 1981. Actions of cholera toxin and the prevention and treatment of cholera. *Nature,* 292**,** 413-417.
HOLT, A., CAHILL, J., RAMSEY, J., O'LEARY, C., MORELAND, R., MARTIN, C., GALBADAGE, D. T., SHARAN, R., SULE, P. & BETTRIDGE, K. 2019. Phage-encoded cationic antimicrobial peptide used for outer membrane disruption in lysis. *bioRxiv***,** 515445.
HOLT, G., LODGE, J., MCCARTHY, A., GRAHAM, A., YOUNG, G., BRIDGE, S., BROWN, A., VESES-GARCIA, M., LANYON, C. & SAILS, A. 2017a. Shigatoxin encoding Bacteriophage ϕ24 B modulates bacterial metabolism to raise antimicrobial tolerance. *Scientific reports,* 7**,** 1-14.
HOLT, G., LODGE, J., MCCARTHY, A., GRAHAM, A., YOUNG, G., BRIDGE, S., BROWN, A., VESES-GARCIA, M., LANYON, C. & SAILS, A. J. S. R. 2017b. Shigatoxin encoding Bacteriophage ϕ24 B modulates bacterial metabolism to raise antimicrobial tolerance. 7**,** 1-14.
HÖLTJE, J.-V. 1998. Growth of the stress-bearing and shape-maintaining murein sacculus of Escherichia coli. *Microbiology and molecular biology reviews,* 62**,** 181-203.
HOMMAIS, F., KRIN, E., COPPEE, J.-Y., LACROIX, C., YERAMIAN, E., DANCHIN, A. & BERTIN, P. 2004. GadE (YhiE): a novel activator involved in the response to acid environment in Escherichia coli. *Microbiology,* 150**,** 61-72.
HOOPER, D. C. 2001. Emerging mechanisms of fluoroquinolone resistance. *Emerging infectious diseases,* 7**,** 337.
HORINOUCHI, S. & WEISBLUM, B. 1980. Posttranscriptional modification of mRNA conformation: mechanism that regulates erythromycin-induced resistance. *Proceedings of the National Academy of Sciences,* 77**,** 7079-7083.
HYMAN, P. & ABEDON, S. T. 2009. Practical methods for determining phage growth parameters. *Bacteriophages.* Springer.

IGUCHI, A., THOMSON, N. R., OGURA, Y., SAUNDERS, D., OOKA, T., HENDERSON, I. R., HARRIS, D., ASADULGHANI, M., KUROKAWA, K. & DEAN, P. 2009. Complete genome sequence and comparative genome analysis of enteropathogenic Escherichia coli O127: H6 strain E2348/69. *Journal of bacteriology,* 191**,** 347-354.

JACEWICZ, M., CLAUSEN, H., NUDELMAN, E., DONOHUE-ROLFE, A. & KEUSCH, G. T. 1986. Pathogenesis of shigella diarrhea. XI. Isolation of a shigella toxin-binding glycolipid from rabbit jejunum and HeLa cells and its identification as globotriaosylceramide. *The Journal of experimental medicine,* 163**,** 1391-1404.

JACOBY, G. J. C. M. R. 2009. 2009. AmpC β-lactamases. 22**,** 664-689.

JAMES, C. E., STANLEY, K. N., ALLISON, H. E., FLINT, H. J., STEWART, C. S., SHARP, R. J., SAUNDERS, J. R. & MCCARTHY, A. J. 2001a. Lytic and lysogenic infection of diverse Escherichia coli and Shigella strains with a verocytotoxigenic bacteriophage. *Applied and environmental microbiology,* 67**,** 4335-4337.

JAMES, C. E., STANLEY, K. N., ALLISON, H. E., FLINT, H. J., STEWART, C. S., SHARP, R. J., SAUNDERS, J. R. & MCCARTHY, A. J. 2001b. Lytic and Lysogenic Infection of DiverseEscherichia coli and Shigella Strains with a Verocytotoxigenic Bacteriophage. *Applied and environmental microbiology,* 67**,** 4335-4337.

JANDHYALA, D. M., THORPE, C. M., MAGUN, B. J. R. & TOXINS, S. 2011. Ricin and Shiga toxins: effects on host cell signal transduction. 41-65.

JANDHYALA, S. M., TALUKDAR, R., SUBRAMANYAM, C., VUYYURU, H., SASIKALA, M. & REDDY, D. N. 2015. Role of the normal gut microbiota. *World journal of gastroenterology: WJG,* 21**,** 8787.

JARVIS, K. G., GIRON, J. A., JERSE, A. E., MCDANIEL, T. K., DONNENBERG, M. S. & KAPER, J. B. 1995. Enteropathogenic Escherichia coli contains a putative type III secretion system necessary for the export of proteins involved in attaching and effacing lesion formation. *Proceedings of the National Academy of Sciences,* 92**,** 7996-8000.

JARVIS, K. G. & KAPER, J. B. 1996. Secretion of extracellular proteins by enterohemorrhagic Escherichia coli via a putative type III secretion system. *Infection and immunity,* 64**,** 4826-4829.

JEON, J.-H., LEE, C.-H. & LEE, H.-S. 2009. Antimicrobial activities of 2-methyl-8-hydroxyquinoline and its derivatives against human intestinal bacteria. *Journal of the Korean Society for Applied Biological Chemistry,* 52**,** 202-205.

JIMÉNEZ, N., SENCHENKOVA, S. N., KNIREL, Y. A., PIERETTI, G., CORSARO, M. M., AQUILINI, E., REGUÉ, M., MERINO, S. & TOMÁS, J. M. 2012. Effects of lipopolysaccharide biosynthesis mutations on K1 polysaccharide association with the Escherichia coli cell surface. *Journal of bacteriology,* 194**,** 3356-3367.

JINDAL, S., THAMPY, H., DAY, P. J. & KELL, D. B. 2019. Very rapid flow cytometric assessment of antimicrobial susceptibility during the apparent lag phase of microbial (re) growth. *Microbiology,* 165**,** 439-454.

JOHANNES, L. & RÖMER, W. 2010. Shiga toxins—from cell biology to biomedical applications. *Nature Reviews Microbiology,* 8**,** 105-116.

JOHANSEN, B. K., WASTESON, Y., GRANUM, P. E. & BRYNESTAD, S. 2001. Mosaic structure of Shiga-toxin-2-encoding phages isolated from Escherichia coli O157: H7 indicates frequent gene exchange between lambdoid phage genomes. *Microbiology,* 147**,** 1929-1936.

JUHALA, R. J., FORD, M. E., DUDA, R. L., YOULTON, A., HATFULL, G. F. & HENDRIX, R. W. J. J. O. M. B. 2000. Genomic sequences of bacteriophages HK97 and HK022: pervasive genetic mosaicism in the lambdoid bacteriophages. 299**,** 27-51.

KAILASAN VANAJA, S., BERGHOLZ, T. M. & WHITTAM, T. S. 2009. Characterization of the Escherichia coli O157: H7 Sakai GadE regulon. *Journal of bacteriology,* 191**,** 1868-1877.

KANEHISA, M. & GOTO, S. 2000. KEGG: kyoto encyclopedia of genes and genomes. *Nucleic acids research,* 28**,** 27-30.

KAPER, J. B., NATARO, J. P. & MOBLEY, H. L. 2004a. Pathogenic escherichia coli. *Nature reviews microbiology,* 2**,** 123.

KAPER, J. B., NATARO, J. P. & MOBLEY, H. L. 2004b. Pathogenic escherichia coli. *Nature reviews microbiology,* 2**,** 123-140.

KARPMAN, D., HÅKANSSON, A., PEREZ, M.-T. R., ISAKSSON, C., CARLEMALM, E., CAPRIOLI, A. & SVANBORG, C. 1998. Apoptosis of renal cortical cells in the hemolytic-uremic syndrome: in vivo and in vitro studies. *Infection and immunity,* 66**,** 636-644.

KATSAMBA, P. & LAUGA, E. 2019. Hydrodynamics of bacteriophage migration along bacterial flagella. *Physical Review Fluids,* 4**,** 013101.

KAYE, S., LOUISE, C., BOYD, B., LINGWOOD, C. & OBRIG, T. 1993. Shiga toxin-associated hemolytic uremic syndrome: interleukin-1 beta enhancement of Shiga toxin cytotoxicity toward human vascular endothelial cells in vitro. *Infection and Immunity,* 61**,** 3886-3891.

KENNY, B. 2001. Mechanism of action of EPEC type III effector molecules. *International Journal of Medical Microbiology,* 291**,** 469-477.

KENNY, B., DEVINNEY, R., STEIN, M., REINSCHEID, D. J., FREY, E. A. & FINLAY, B. B. 1997. Enteropathogenic E. coli (EPEC) transfers its receptor for intimate adherence into mammalian cells. *Cell,* 91**,** 511-520.

KIM, C., SONG, S. & PARK, C. 1997. The D-allose operon of Escherichia coli K-12. *Journal of bacteriology,* 179**,** 7631-7637.

KLAPPROTH, J.-M. A., SCALETSKY, I. C., MCNAMARA, B. P., LAI, L.-C., MALSTROM, C., JAMES, S. P. & DONNENBERG, M. S. 2000. A large toxin from pathogenic Escherichia coli strains that inhibits lymphocyte activation. *Infection and immunity,* 68**,** 2148-2155.

KNUTTON, S., BALDWIN, T., WILLIAMS, P. & MCNEISH, A. 1989. Actin accumulation at sites of bacterial adhesion to tissue culture cells: basis of a new diagnostic test for enteropathogenic and enterohemorrhagic Escherichia coli. *Infection and immunity,* 57**,** 1290-1298.

KONOWALCHUK, J., SPEIRS, J. & STAVRIC, S. 1977. Vero response to a cytotoxin of Escherichia coli. *Infection and immunity,* 18**,** 775-779.

KORGAONKAR, A., TRIVEDI, U., RUMBAUGH, K. P. & WHITELEY, M. 2013. Community surveillance enhances Pseudomonas aeruginosa virulence during polymicrobial infection. *Proceedings of the National Academy of Sciences,* 110**,** 1059-1064.

KOTLOFF, K. L., NATARO, J. P., BLACKWELDER, W. C., NASRIN, D., FARAG, T. H., PANCHALINGAM, S., WU, Y., SOW, S. O., SUR, D. & BREIMAN, R. F. 2013. Burden and aetiology of diarrhoeal disease in infants and young children in developing countries (the Global Enteric Multicenter Study, GEMS): a prospective, case-control study. *The Lancet,* 382**,** 209-222.

KOTLOFF, K. L., WINICKOFF, J. P., IVANOFF, B., CLEMENS, J. D., SWERDLOW, D. L., SANSONETTI, P. J., ADAK, G. & LEVINE, M. 1999. Global burden of Shigella infections: implications for vaccine development and implementation of control strategies. *Bulletin of the World Health Organization,* 77**,** 651.

KOUDELKA, A. P., HUFNAGEL, L. A. & KOUDELKA, G. B. 2004a. Purification and characterization of the repressor of the Shiga toxin-encoding bacteriophage 933W: DNA binding, gene regulation, and autocleavage. *Journal of Bacteriology,* 186**,** 7659-7669.

KOUDELKA, A. P., HUFNAGEL, L. A. & KOUDELKA, G. B. J. J. O. B. 2004b. Purification and characterization of the repressor of the Shiga toxin-encoding bacteriophage 933W: DNA binding, gene regulation, and autocleavage. 186**,** 7659-7669.

KRAUS, A. J., BRINK, B. G. & SIEGEL, T. N. 2019. Efficient and specific oligo-based depletion of rRNA. *Scientific reports,* 9**,** 1-8.

KRAUS, R. 1905. *Ueber experimentelle Therapie der Dysenterie*.

KREBS, S. J. & TAYLOR, R. K. 2011. Nutrient-dependent, rapid transition of Vibrio cholerae to coccoid morphology and expression of the toxin co-regulated pilus in this form. *Microbiology,* 157**,** 2942.

KRISTICH, C. J., RICE, L. B. & ARIAS, C. A. 2014. Enterococcal infection—treatment and antibiotic resistance. *Enterococci: from commensals to leading causes of drug resistant infection [Internet]*.

KUEHN, M. J. & KESTY, N. C. 2005. Bacterial outer membrane vesicles and the host–pathogen interaction. *Genes & development,* 19**,** 2645-2655.

KUETE, V. 2014. Health effects of alkaloids from African medicinal plants. *Toxicological survey of African medicinal plants.* Elsevier.

KUMAR, A., TANEJA, N., KUMAR, Y. & SHARMA, M. J. J. O. A. M. 2012. Detection of S higa toxin variants among S higa toxin–forming E scherichia coli isolates from animal stool, meat and human stool samples in I ndia. 113**,** 1208-1216.

LAINHART, W., STOLFA, G. & KOUDELKA, G. B. 2009a. Shiga toxin as a bacterial defense against a eukaryotic predator, Tetrahymena thermophila. *Journal of bacteriology,* 191**,** 5116-5122.

LAINHART, W., STOLFA, G. & KOUDELKA, G. B. J. J. O. B. 2009b. Shiga toxin as a bacterial defense against a eukaryotic predator, Tetrahymena thermophila. 191**,** 5116-5122.

LAKHUNDI, S. & ZHANG, K. 2018. Methicillin-resistant Staphylococcus aureus: molecular characterization, evolution, and epidemiology. *Clinical microbiology reviews,* 31**,** e00020-18.

LAN, R. & REEVES, P. R. 2002. Escherichia coli in disguise: molecular origins of Shigella. *Microbes and infection,* 4**,** 1125-1132.

LAPOINTE, P., WEI, X. & GARIÉPY, J. 2005. A role for the protease-sensitive loop region of Shiga-like toxin 1 in the retrotranslocation of its A1 domain from the endoplasmic reticulum lumen. *Journal of Biological Chemistry,* 280**,** 23310-23318.

LASKOWSKI, R. A., WATSON, J. D. & THORNTON, J. M. 2005. ProFunc: a server for predicting protein function from 3D structure. *Nucleic acids research,* 33**,** W89-W93.
LATHEM, W. W., BERGSBAKEN, T. & WELCH, R. A. 2004. Potentiation of C1 esterase inhibitor by StcE, a metalloprotease secreted by Escherichia coli O157: H7. *The Journal of experimental medicine,* 199**,** 1077-1087.
LATHEM, W. W., GRYS, T. E., WITOWSKI, S. E., TORRES, A. G., KAPER, J. B., TARR, P. I. & WELCH, R. A. 2002. StcE, a metalloprotease secreted by Escherichia coli O157: H7, specifically cleaves C1 esterase inhibitor. *Molecular microbiology,* 45**,** 277-288.
LATINO, L. 2016. *Pseudolysogeny and sequential mutations build multiresistance to virulent bacteriophages in Pseudomonas aeruginosa.* Université Paris-Saclay.
LAW, D. 2000a. Virulence factors of Escherichia coli O157 and other Shiga toxin-producing E. coli. *Journal of Applied Microbiology,* 88**,** 729-745.
LAW, D. J. J. O. A. M. 2000b. Virulence factors of Escherichia coli O157 and other Shiga toxin-producing E. coli. 88**,** 729-745.
LEDERBERG, E. M. & LEDERBERG, J. J. G. 1953. Genetic studies of lysogenicity in Escherichia coli. 38**,** 51.
LI, J., ADAMS, V., BANNAM, T. L., MIYAMOTO, K., GARCIA, J. P., UZAL, F. A., ROOD, J. I. & MCCLANE, B. A. 2013. Toxin plasmids of Clostridium perfringens. *Microbiology and Molecular Biology Reviews,* 77**,** 208-233.
LI, X.-Z., PLÉSIAT, P. & NIKAIDO, H. 2015. The challenge of efflux-mediated antibiotic resistance in Gram-negative bacteria. *Clinical microbiology reviews,* 28**,** 337-418.
LIM, J. Y., YOON, J. W. & HOVDE, C. J. 2010. A brief overview of Escherichia coli O157: H7 and its plasmid O157. *Journal of microbiology and biotechnology,* 20**,** 5.
LINDBERG, A., BROWN, J., STRÖMBERG, N., WESTLING-RYD, M., SCHULTZ, J. & KARLSSON, K. 1987. Identification of the carbohydrate receptor for Shiga toxin produced by Shigella dysenteriae type 1. *Journal of Biological Chemistry,* 262**,** 1779-1785.
LINDGREN, S., MELTON, A., O'BRIEN, A. J. I. & IMMUNITY 1993. Virulence of enterohemorrhagic Escherichia coli O91: H21 clinical isolates in an orally infected mouse model. 61**,** 3832-3842.
LITTLE, J. W. 1984. Autodigestion of lexA and phage lambda repressors. *Proceedings of the National Academy of Sciences,* 81**,** 1375-1379.
LITTLE, J. W. 2007. *Prophage Induction of Phage λ*, Horizon Scientific Press.
LIVNY, J. & FRIEDMAN, D. I. 2004a. Characterizing spontaneous induction of Stx encoding phages using a selectable reporter system. *Molecular microbiology,* 51**,** 1691-1704.
LIVNY, J. & FRIEDMAN, D. I. J. M. M. 2004b. Characterizing spontaneous induction of Stx encoding phages using a selectable reporter system. 51**,** 1691-1704.
LLARENA, A.-K., ASPHOLM, M., O'SULLIVAN, K., WÊGRZYN, G. & LINDBÄCK, T. 2021. Replication Region Analysis Reveals Non-lambdoid Shiga Toxin Converting Bacteriophages. *Frontiers in microbiology,* 12.
LO, Y.-C., LIN, S.-C., SHAW, J.-F. & LIAW, Y.-C. 2003. Crystal structure of Escherichia coli thioesterase I/protease I/lysophospholipase L1: consensus sequence blocks constitute the catalytic center of SGNH-hydrolases through a conserved hydrogen bond network. *Journal of molecular biology,* 330**,** 539-551.

LOBANOVSKA, M. & PILLA, G. 2017. Focus: drug development: Penicillin's discovery and antibiotic resistance: lessons for the future? *The Yale journal of biology and medicine,* 90**,** 135.
LOESSNER, M. J., KRAMER, K., EBEL, F. & SCHERER, S. 2002. C-terminal domains of Listeria monocytogenes bacteriophage murein hydrolases determine specific recognition and high-affinity binding to bacterial cell wall carbohydrates. *Molecular microbiology,* 44**,** 335-349.
LORIS, R., HAMELRYCK, T., BOUCKAERT, J. & WYNS, L. 1998. Legume lectin structure. *Biochimica et biophysica acta (BBA)-Protein structure and molecular enzymology,* 1383**,** 9-36.
ŁOŚ, J., ŁOŚ, M., WĘGRZYN, A. & WĘGRZYN, G. 2008. Role of the bacteriophage λ exo-xis region in the virus development. *Folia microbiologica,* 53**,** 443-450.
ŁOŚ, J. M., ŁOŚ, M., WĘGRZYN, G. & WĘGRZYN, A. 2009. Differential efficiency of induction of various lambdoid prophages responsible for production of Shiga toxins in response to different induction agents. *Microbial pathogenesis,* 47**,** 289-298.
ŁOŚ, M. & WĘGRZYN, G. 2012. Pseudolysogeny. *Advances in virus research,* 82**,** 339-349.
LOUISE, C. B. & OBRIG, T. 1991. Shiga toxin-associated hemolytic-uremic syndrome: combined cytotoxic effects of Shiga toxin, interleukin-1 beta, and tumor necrosis factor alpha on human vascular endothelial cells in vitro. *Infection and Immunity,* 59**,** 4173-4179.
LOUISE, C. B. & OBRIG, T. G. J. J. O. I. D. 1995. Specific interaction of Escherichia coli 0157: H7-derived Shiga-like toxin II with human renal endothelial cells. 172**,** 1397-1401.
LOWY, F. D. 2000. Is Staphylococcus aureus an intracellular pathogen? *Trends in microbiology,* 8**,** 341-343.
MA, Z., GONG, S., RICHARD, H., TUCKER, D. L., CONWAY, T. & FOSTER, J. W. 2003. GadE (YhiE) activates glutamate decarboxylase-dependent acid resistance in Escherichia coli K-12. *Molecular microbiology,* 49**,** 1309-1320.
MACFARLANE, S. & MACFARLANE, G. T. 2003. Regulation of short-chain fatty acid production. *Proceedings of the Nutrition Society,* 62**,** 67-72.
MAKINO, K., ISHII, K., YASUNAGA, T., HATTORI, M., YOKOYAMA, K., YUTSUDO, C. H., KUBOTA, Y., YAMAICHI, Y., IIDA, T. & YAMAMOTO, K. 1998. Complete nucleotide sequences of 93-kb and 3.3-kb plasmids of an enterohemorrhagic Escherichia coli O157: H7 derived from Sakai outbreak. *DNA Research,* 5**,** 1-9.
MALININ, A., VOSTROV, A., VASIL'EV, A. & RYBCHIN, V. 1993. Characterization of bacteriophage N15 lysogenic conversion gene and identification of its product. *Soviet genetics,* 29**,** 202-208.
MARCHÈS, O., COVARELLI, V., DAHAN, S., COUGOULE, C., BHATTA, P., FRANKEL, G. & CARON, E. 2008. EspJ of enteropathogenic and enterohaemorrhagic Escherichia coli inhibits opsono-phagocytosis. *Cellular microbiology,* 10**,** 1104-1115.
MARINELLI, L. J., HATFULL, G. F. & PIURI, M. 2012. Recombineering: A powerful tool for modification of bacteriophage genomes. *Bacteriophage,* 2**,** 5-14.
MATSUSHIRO, A., SATO, K., MIYAMOTO, H., YAMAMURA, T. & HONDA, T. 1999. Induction of prophages of enterohemorrhagic Escherichia coli O157: H7 with norfloxacin. *Journal of bacteriology,* 181**,** 2257-2260.

MCDANIEL, T. K., JARVIS, K. G., DONNENBERG, M. S. & KAPER, J. B. 1995. A genetic locus of enterocyte effacement conserved among diverse enterobacterial pathogens. *Proceedings of the National Academy of Sciences,* 92**,** 1664-1668.
MCDANIEL, T. K. & KAPER, J. B. 1997. A cloned pathogenicity island from enteropathogenic Escherichia coli confers the attaching and effacing phenotype on E. coli K-12. *Molecular microbiology,* 23**,** 399-407.
MCEWEN, S. A. D. 2018. *Characterising the Adsorption Process of the Shigatoxigenic Bacteriophage, ϕ24 B, to Its Bacterial Host via an Essential Outer-Membrane Protein, BamA*, The University of Liverpool (United Kingdom).
MCGRATH, S., SEEGERS, J. F., FITZGERALD, G. F. & VAN SINDEREN, D. 1999. Molecular characterization of a phage-encoded resistance system in Lactococcus lactis. *Applied and environmental microbiology,* 65**,** 1891-1899.
MEHIO, W., KEMP, G. J., TAYLOR, P. & WALKINSHAW, M. D. 2010. Identification of protein binding surfaces using surface triplet propensities. *Bioinformatics,* 26**,** 2549-2555.
MELLIES, J. L., BARRON, A. M. & CARMONA, A. M. 2007. Enteropathogenic and enterohemorrhagic Escherichia coli virulence gene regulation. *Infection and immunity,* 75**,** 4199-4210.
MELLIES, J. L., ELLIOTT, S. J., SPERANDIO, V., DONNENBERG, M. S. & KAPER, J. B. 1999. The Per regulon of enteropathogenic Escherichia coli: identification of a regulatory cascade and a novel transcriptional activator, the locus of enterocyte effacement (LEE)-encoded regulator (Ler). *Molecular microbiology,* 33**,** 296-306.
MELLIES, J. L., NAVARRO-GARCIA, F., OKEKE, I., FREDERICKSON, J., NATARO, J. P. & KAPER, J. B. 2001. espC pathogenicity island of enteropathogenic Escherichia coli encodes an enterotoxin. *Infection and immunity,* 69**,** 315-324.
MELTON-CELSA, A. R., DARNELL, S. C., O'BRIEN, A. D. J. I. & IMMUNITY 1996. Activation of Shiga-like toxins by mouse and human intestinal mucus correlates with virulence of enterohemorrhagic Escherichia coli O91: H21 isolates in orally infected, streptomycin-treated mice. 64**,** 1569-1576.
MELTON-CELSA, A. R. J. M. S. 2014. Shiga toxin (Stx) classification, structure, and function. 2**,** 2.4. 06.
MÉNARD, L.-P. & DUBREUIL, J. D. 2002. Enteroaggregative Escherichia coli heat-stable enterotoxin 1 (EAST1): a new toxin with an old twist. *Critical reviews in microbiology,* 28**,** 43-60.
MERRELL, D. S. & FALKOW, S. 2004. Frontal and stealth attack strategies in microbial pathogenesis. *Nature,* 430**,** 250-256.
MO, K.-F., LI, X., LI, H., LOW, L. Y., QUINN, C. P. & BOONS, G.-J. 2012. Endolysins of Bacillus anthracis bacteriophages recognize unique carbohydrate epitopes of vegetative cell wall polysaccharides with high affinity and selectivity. *Journal of the American Chemical Society,* 134**,** 15556-15562.
MOHAISEN, M. R., MCCARTHY, A. J., ADRIAENSSENS, E. M. & ALLISON, H. E. 2020. The Site-Specific Recombination System of the Escherichia coli Bacteriophage Φ24B. *Frontiers in microbiology,* 11**,** 2467.
MØLGAARD, A., KAUPPINEN, S. & LARSEN, S. 2000. Rhamnogalacturonan acetylesterase elucidates the structure and function of a new family of hydrolases. *Structure,* 8**,** 373-383.

MOON, H., WHIPP, S., ARGENZIO, R., LEVINE, M. & GIANNELLA, R. 1983. Attaching and effacing activities of rabbit and human enteropathogenic Escherichia coli in pig and rabbit intestines. *Infection and immunity,* 41**,** 1340-1351.
MORABITO, S., TOZZOLI, R., OSWALD, E. & CAPRIOLI, A. 2003. A mosaic pathogenicity island made up of the locus of enterocyte effacement and a pathogenicity island of Escherichia coli O157: H7 is frequently present in attaching and effacing E. coli. *Infection and Immunity,* 71**,** 3343-3348.
MORAES, J. P., PAPPA, G. L., PIRES, D. E. & IZIDORO, S. C. 2017. GASS-WEB: a web server for identifying enzyme active sites based on genetic algorithms. *Nucleic acids research,* 45**,** W315-W319.
MOYNIHAN, P. J., SYCHANTHA, D. & CLARKE, A. J. 2014. Chemical biology of peptidoglycan acetylation and deacetylation. *Bioorganic Chemistry,* 54**,** 44-50.
MUNIESA, M., BLANCO, J. E., DE SIMÓN, M., SERRA-MORENO, R., BLANCH, A. R. & JOFRE, J. 2004. Diversity of stx2 converting bacteriophages induced from Shiga-toxin-producing Escherichia coli strains isolated from cattle. *Microbiology,* 150**,** 2959-2971.
MUNITA, J. M., ARIAS, C. A., UNIT, A. & SANTIAGO, A. 2016. HHS public access mechanisms of antibiotic resistance. *HHS Public Access,* 4**,** 1-37.
MUNIYAPPA, K. & RADDING, C. 1986. The homologous recombination system of phage lambda. Pairing activities of beta protein. *Journal of Biological Chemistry,* 261**,** 7472-7478.
MURASE, T., YAMAI, S. & WATANABE, H. 1999. Changes in pulsed-field gel electrophoresis patterns in clinical isolates of enterohemorrhagic Escherichia coli O157: H7 associated with loss of Shiga toxin genes. *Current microbiology,* 38**,** 48-50.
NADZIRIN, N., GARDINER, E. J., WILLETT, P., ARTYMIUK, P. J. & FIRDAUS-RAIH, M. 2012. SPRITE and ASSAM: web servers for side chain 3D-motif searching in protein structures. *Nucleic acids research,* 40**,** W380-W386.
NAKAMURA, A. M., NASCIMENTO, A. S. & POLIKARPOV, I. 2017. Structural diversity of carbohydrate esterases. *Biotechnology Research and Innovation,* 1**,** 35-51.
NATARO, J., YIKANG, D., GIRON, J., SAVARINO, S., KOTHARY, M. & HALL, R. 1993. Aggregative adherence fimbria I expression in enteroaggregative Escherichia coli requires two unlinked plasmid regions. *Infection and immunity,* 61**,** 1126-1131.
NATARO, J. P. 2005. Enteroaggregative Escherichia coli pathogenesis. *Current opinion in gastroenterology,* 21**,** 4-8.
NATARO, J. P. & KAPER, J. B. 1998. Diarrheagenic escherichia coli. *Clinical microbiology reviews,* 11**,** 142-201.
NATARO, J. P., MAI, V., JOHNSON, J., BLACKWELDER, W. C., HEIMER, R., TIRRELL, S., EDBERG, S. C., BRADEN, C. R., MORRIS JR, J. G. & HIRSHON, J. M. 2006. Diarrheagenic escherichia coli infection in Baltimore, Maryland, and New haven, Connecticut. *Clinical infectious diseases,* 43**,** 402-407.
NATARO, J. P., STEINER, T. & GUERRANT, R. L. 1998. Enteroaggregative Escherichia coli. *Emerging infectious diseases,* 4**,** 251.

NAVARRO-GARCíA, F., CANIZALEZ-ROMAN, A., LUNA, J., SEARS, C. & NATARO, J. P. 2001. Plasmid-encoded toxin of enteroaggregative Escherichia coli is internalized by epithelial cells. *Infection and Immunity,* 69**,** 1053-1060.

NEJMAN-FALEŃCZYK, B., BLOCH, S., LICZNERSKA, K., DYDECKA, A., FELCZYKOWSKA, A., TOPKA, G., WĘGRZYN, A. & WĘGRZYN, G. 2015. A small, microRNA-size, ribonucleic acid regulating gene expression and development of Shiga toxin-converting bacteriophage Φ24 B. *Scientific reports,* 5**,** 1-15.

NICKEL, J., RUSESKA, I., WRIGHT, J. & COSTERTON, J. 1985. Tobramycin resistance of Pseudomonas aeruginosa cells growing as a biofilm on urinary catheter material. *Antimicrobial agents and chemotherapy,* 27**,** 619-624.

NÜBLING, S., EISELE, T., STÖBER, H., FUNK, J., POLZIN, S., FISCHER, L. & SCHMIDT, H. 2014. Bacteriophage 933W encodes a functional esterase downstream of the Shiga toxin 2a operon. *International Journal of Medical Microbiology,* 304**,** 269-274.

NYAMBE, S., BURGESS, C., WHYTE, P. & BOLTON, D. 2016. The Survival of a Temperate vtx Bacteriophage and an Anti-Verocytotoxigenic Escherichia coli O157 Lytic Phage in Water and Soil Samples. *Zoonoses and public health,* 63**,** 632-640.

O'BRIEN, A., LIVELY, T., CHANG, T. & GORBACH, S. 1983. Purification of Shigella dysenteriae 1 (Shiga)-like toxin from Escherichia coli O157: H7 strain associated with haemorrhagic colitis. *Lancet (London, England),* 2**,** 573-573.

O'LOUGHLIN, E. V. & ROBINS-BROWNE, R. M. 2001. Effect of Shiga toxin and Shiga-like toxins on eukaryotic cells. *Microbes and infection,* 3**,** 493-507.

OCHOA, T. J. & CONTRERAS, C. A. 2011. Enteropathogenic E. coli (EPEC) infection in children. *Current opinion in infectious diseases,* 24**,** 478.

OHNISHI, M., KUROKAWA, K. & HAYASHI, T. 2001. Diversification of Escherichia coli genomes: are bacteriophages the major contributors? *Trends in microbiology,* 9**,** 481-485.

OPPENHEIM, A. B., KOBILER, O., STAVANS, J., COURT, D. L. & ADHYA, S. 2005. Switches in bacteriophage lambda development. *Annu. Rev. Genet.,* 39**,** 409-429.

PAGES, J.-M., JAMES, C. E. & WINTERHALTER, M. 2008. The porin and the permeating antibiotic: a selective diffusion barrier in Gram-negative bacteria. *Nature Reviews Microbiology,* 6**,** 893-903.

PANG, T., FLEMING, T. C., POGLIANO, K. & YOUNG, R. 2013. Visualization of pinholin lesions in vivo. *Proceedings of the National Academy of Sciences,* 110**,** E2054-E2063.

PANG, T., PARK, T. & YOUNG, R. 2010. Mutational analysis of the S21 pinholin. *Molecular microbiology,* 76**,** 68-77.

PANG, T., SAVVA, C. G., FLEMING, K. G., STRUCK, D. K. & YOUNG, R. 2009. Structure of the lethal phage pinhole. *Proceedings of the National Academy of Sciences,* 106**,** 18966-18971.

PAPP-WALLACE, K. M., ENDIMIANI, A., TARACILA, M. A. & BONOMO, R. A. 2011. Carbapenems: past, present, and future. *Antimicrobial agents and chemotherapy,* 55**,** 4943-4960.

PARK, J. T. & UEHARA, T. 2008. How bacteria consume their own exoskeletons (turnover and recycling of cell wall peptidoglycan). *Microbiology and Molecular Biology Reviews,* 72**,** 211-227.

PARK, T., STRUCK, D. K., DANKENBRING, C. A. & YOUNG, R. 2007. The pinholin of lambdoid phage 21: control of lysis by membrane depolarization. *Journal of bacteriology,* 189**,** 9135-9139.
PARSOT, C. 2005. Shigella spp. and enteroinvasive Escherichia coli pathogenicity factors. *FEMS microbiology letters,* 252**,** 11-18.
PATON, J. C. & PATON, A. W. 1998. Pathogenesis and diagnosis of Shiga toxin-producing Escherichia coli infections. *Clinical microbiology reviews,* 11**,** 450-479.
PEIFFER, I., BERNET-CAMARD, M. F., ROUSSET, M. & SERVIN, A. L. 2001. Impairments in enzyme activity and biosynthesis of brush border-associated hydrolases in human intestinal Caco-2/TC7 cells infected by members of the Afa/Dr family of diffusely adhering Escherichia coli. *Cellular microbiology,* 3**,** 341-357.
PEIFFER, I., SERVIN, A. L. & BERNET-CAMARD, M.-F. 1998. Piracy of decay-accelerating factor (CD55) signal transduction by the diffusely adhering strain Escherichia coli C1845 promotes cytoskeletal F-actin rearrangements in cultured human intestinal INT407 cells. *Infection and immunity,* 66**,** 4036-4042.
PERCIVAL, S. L., SULEMAN, L., VUOTTO, C. & DONELLI, G. 2015. Healthcare-associated infections, medical devices and biofilms: risk, tolerance and control. *Journal of medical microbiology,* 64**,** 323-334.
PERCIVAL, S. L. & WILLIAMS, D. W. 2014. Chapter Six - Escherichia coli. *In:* PERCIVAL, S. L., YATES, M. V., WILLIAMS, D. W., CHALMERS, R. M. & GRAY, N. F. (eds.) *Microbiology of Waterborne Diseases (Second Edition).* London: Academic Press.
PERNA, N. T., PLUNKETT, G., BURLAND, V., MAU, B., GLASNER, J. D., ROSE, D. J., MAYHEW, G. F., EVANS, P. S., GREGOR, J. & KIRKPATRICK, H. A. 2001a. Genome sequence of enterohaemorrhagic Escherichia coli O157: H7. *Nature,* 409**,** 529-533.
PERNA, N. T., PLUNKETT III, G., BURLAND, V., MAU, B., GLASNER, J. D., ROSE, D. J., MAYHEW, G. F., EVANS, P. S., GREGOR, J. & KIRKPATRICK, H. A. 2001b. Genome sequence of enterohaemorrhagic Escherichia coli O157: H7. *Nature,* 409**,** 529.
PHILPOTT, D. J., ACKERLEY, C. A., KILIAAN, A. J., KARMALI, M. A., PERDUE, M. H. & SHERMAN, P. M. 1997. Translocation of verotoxin-1 across T84 monolayers: mechanism of bacterial toxin penetration of epithelium. *American Journal of Physiology-Gastrointestinal and Liver Physiology,* 273**,** G1349-G1358.
PISABARRO, A. G., DE PEDRO, M. A. & VÁZQUEZ, D. 1985. Structural modifications in the peptidoglycan of Escherichia coli associated with changes in the state of growth of the culture. *Journal of bacteriology,* 161**,** 238-242.
PITOUT, J. D., PEIRANO, G., KOCK, M. M., STRYDOM, K.-A. & MATSUMURA, Y. 2019. The global ascendency of OXA-48-type carbapenemases. *Clinical microbiology reviews,* 33**,** e00102-19.
PITTS, B. J. & MEYERSON, L. R. 1981. Inhibition of Na, K-ATPase activity and ouabain binding by sanguinarine. *Drug Development Research,* 1**,** 43-49.
POHANE, A. A., JOSHI, H. & JAIN, V. 2014. Molecular dissection of phage endolysin: an interdomain interaction confers host specificity in Lysin A of Mycobacterium phage D29. *Journal of biological chemistry,* 289**,** 12085-12095.

POLLOCK, G. L., OATES, C. V., GIOGHA, C., WONG FOK LUNG, T., ONG, S. Y., PEARSON, J. S., HARTLAND, E. L. J. I. & IMMUNITY 2017. Distinct roles of the antiapoptotic effectors NleB and NleF from enteropathogenic Escherichia coli. 85**,** e01071-16.
POTLURI, L.-P., KANNAN, S. & YOUNG, K. D. 2012. ZipA is required for FtsZ-dependent preseptal peptidoglycan synthesis prior to invagination during cell division. *Journal of bacteriology,* 194**,** 5334-5342.
PRACHAYASITTIKUL, V., PRACHAYASITTIKUL, S., RUCHIRAWAT, S. & PRACHAYASITTIKUL, V. 2013. 8-Hydroxyquinolines: a review of their metal chelating properties and medicinal applications. *Drug design, development and therapy,* 7**,** 1157.
PROFT, T., SRISKANDAN, S., YANG, L. & FRASER, J. D. 2003. Superantigens and streptococcal toxic shock syndrome. *Emerging infectious diseases,* 9**,** 1211.
PUPO, G. M., LAN, R. & REEVES, P. R. 2000. Multiple independent origins of Shigella clones of Escherichia coli and convergent evolution of many of their characteristics. *Proceedings of the National Academy of Sciences,* 97**,** 10567-10572.
QADRI, F., SVENNERHOLM, A.-M., FARUQUE, A. & SACK, R. B. 2005. Enterotoxigenic Escherichia coli in developing countries: epidemiology, microbiology, clinical features, treatment, and prevention. *Clinical microbiology reviews,* 18**,** 465-483.
QUINN, J. P., DUDEK, E. J., DIVINCENZO, C. A., LUCKS, D. A. & LERNER, S. A. 1986. Emergence of resistance to imipenem during therapy for Pseudomonas aeruginosa infections. *Journal of Infectious Diseases,* 154**,** 289-294.
RAMIREZ, M. S. & TOLMASKY, M. E. 2010. Aminoglycoside modifying enzymes. *Drug resistance updates,* 13**,** 151-171.
RANGARAJAN, E. S., RUANE, K. M., PROTEAU, A., SCHRAG, J. D., VALLADARES, R., GONZALEZ, C. F., GILBERT, M., YAKUNIN, A. F. & CYGLER, M. 2011. Structural and enzymatic characterization of NanS (YjhS), a 9-O-Acetyl N-acetylneuraminic acid esterase from Escherichia coli O157: H7. *Protein Science,* 20**,** 1208-1219.
RAO, M. C. Toxins which activate guanylate cyclase: heat-stable enterotoxins. Ciba Foundation Symposium, 1985. 74-93.
RECKTENWALD, J. R. & SCHMIDT, H. 2002. The nucleotide sequence of Shiga toxin (Stx) 2e-encoding phage φP27 is not related to other Stx phage genomes, but the modular genetic structure is conserved. *Infection and immunity,* 70**,** 1896-1908.
REVA, O. & TÜMMLER, B. 2008. Think big–giant genes in bacteria. *Environmental microbiology,* 10**,** 768-777.
RILEY, L. M., VESES-GARCIA, M., HILLMAN, J. D., HANDFIELD, M., MCCARTHY, A. J. & ALLISON, H. E. 2012a. Identification of genes expressed in cultures of E. coli lysogens carrying the Shiga toxin-encoding prophage Φ24 B. *BMC microbiology,* 12**,** 1-14.
RILEY, L. M., VESES-GARCIA, M., HILLMAN, J. D., HANDFIELD, M., MCCARTHY, A. J. & ALLISON, H. E. 2012b. Identification of genes expressed in cultures of E. coli lysogens carrying the Shiga toxin-encoding prophage Φ24 B. *BMC microbiology,* 12**,** 42.
RILEY, L. M., VESES-GARCIA, M., HILLMAN, J. D., HANDFIELD, M., MCCARTHY, A. J. & ALLISON, H. E. J. B. M. 2012c. Identification of genes expressed in

cultures of E. coli lysogens carrying the Shiga toxin-encoding prophage Φ24 B. 12**,** 1-14.
RILEY, L. W., REMIS, R. S., HELGERSON, S. D., MCGEE, H. B., WELLS, J. G., DAVIS, B. R., HEBERT, R. J., OLCOTT, E. S., JOHNSON, L. M. & HARGRETT, N. T. 1983. Hemorrhagic colitis associated with a rare Escherichia coli serotype. *New England Journal of Medicine,* 308**,** 681-685.
RUIZ, J. 2019. Transferable mechanisms of quinolone resistance from 1998 onward. *Clinical microbiology reviews,* 32**,** e00007-19.
SAILE, N., SCHWARZ, L., EIßENBERGER, K., KLUMPP, J., FRICKE, F. W. & SCHMIDT, H. 2018a. Growth advantage of Escherichia coli O104: H4 strains on 5-N-acetyl-9-O-acetyl neuraminic acid as a carbon source is dependent on heterogeneous phage-borne nanS-p esterases. *International Journal of Medical Microbiology,* 308**,** 459-468.
SAILE, N., SCHWARZ, L., EIßENBERGER, K., KLUMPP, J., FRICKE, F. W. & SCHMIDT, H. J. I. J. O. M. M. 2018b. Growth advantage of Escherichia coli O104: H4 strains on 5-N-acetyl-9-O-acetyl neuraminic acid as a carbon source is dependent on heterogeneous phage-borne nanS-p esterases. 308**,** 459-468.
SAILE, N., VOIGT, A., KESSLER, S., STRESSLER, T., KLUMPP, J., FISCHER, L. & SCHMIDT, H. 2016a. Escherichia coli O157: H7 strain EDL933 harbors multiple functional prophage-associated genes necessary for the utilization of 5-N-acetyl-9-O-acetyl neuraminic acid as a growth substrate. *Applied and environmental microbiology,* 82**,** 5940-5950.
SAILE, N., VOIGT, A., KESSLER, S., STRESSLER, T., KLUMPP, J., FISCHER, L., SCHMIDT, H. J. A. & MICROBIOLOGY, E. 2016b. Escherichia coli O157: H7 strain EDL933 harbors multiple functional prophage-associated genes necessary for the utilization of 5-N-acetyl-9-O-acetyl neuraminic acid as a growth substrate. 82**,** 5940-5950.
SAMUEL, B. S., SHAITO, A., MOTOIKE, T., REY, F. E., BACKHED, F., MANCHESTER, J. K., HAMMER, R. E., WILLIAMS, S. C., CROWLEY, J. & YANAGISAWA, M. 2008. Effects of the gut microbiota on host adiposity are modulated by the short-chain fatty-acid binding G protein-coupled receptor, Gpr41. *Proceedings of the National Academy of Sciences,* 105**,** 16767-16772.
SANDKVIST, M. 2001. Type II secretion and pathogenesis. *Infection and immunity,* 69**,** 3523-3535.
SANGER, F., COULSON, A. R., HONG, G., HILL, D. & PETERSEN, G. D. 1982. Nucleotide sequence of bacteriophage λ DNA. *Journal of molecular biology,* 162**,** 729-773.
SÃO-JOSÉ, C., PARREIRA, R. & SANTOS, M. 2003. Triggering of host-cell lysis by double-stranded DNA bacteriophages: fundamental concepts, recent developments and emerging applications. *Recent Res Dev Bacteriol,* 1**,** 103-130.
SARTOR, R. B. 2008. Microbial influences in inflammatory bowel diseases. *Gastroenterology,* 134**,** 577-594.
SAUNDERS, J. R., ALLISON, H., JAMES, C. E., MCCARTHY, A. J. & SHARP, R. 2001. Phage-mediated transfer of virulence genes. *Journal of Chemical Technology & Biotechnology,* 76**,** 662-666.
SAVAGE, D. C. 1977a. Microbial ecology of the gastrointestinal tract. *Annual review of microbiology,* 31**,** 107-133.

SAVAGE, D. C. 1977b. Microbial ecology of the gastrointestinal tract. *Annual Reviews in Microbiology,* 31**,** 107-133.
SAXENA, S. K., O'BRIEN, A. & ACKERMAN, E. 1989. Shiga toxin, Shiga-like toxin II variant, and ricin are all single-site RNA N-glycosidases of 28 S RNA when microinjected into Xenopus oocytes. *Journal of Biological Chemistry,* 264**,** 596-601.
SCHEURWATER, E., REID, C. W. & CLARKE, A. J. 2008. Lytic transglycosylases: bacterial space-making autolysins. *The international journal of biochemistry & cell biology,* 40**,** 586-591.
SCHMIDT, H., BEUTIN, L. & KARCH, H. 1995. Molecular analysis of the plasmid-encoded hemolysin of Escherichia coli O157: H7 strain EDL 933. *Infection and immunity,* 63**,** 1055-1061.
SCHMIDT, H., GEITZ, C., TARR, P. I., FROSCH, M. & KARCH, H. J. T. J. O. I. D. 1999. Non-O157: H7 pathogenic Shiga toxin-producing Escherichia coli: phenotypic and genetic profiling of virulence traits and evidence for clonality. 179**,** 115-123.
SCHMIDT, H., HENKEL, B. & KARCH, H. 1997. A gene cluster closely related to type II secretion pathway operons of gram-negative bacteria is located on the large plasmid of enterohemorrhagic Escherichia coli O157 strains. *FEMS Microbiology Letters,* 148**,** 265-272.
SCHMIDT, H. & KARCH, H. 1996. Enterohemolytic phenotypes and genotypes of Shiga toxin-producing Escherichia coli O111 strains from patients with diarrhea and hemolytic-uremic syndrome. *Journal of clinical microbiology,* 34**,** 2364-2367.
SCHMIDT, H., KERNBACH, C. & KARCH, H. 1996. Analysis of the EHEC hly operon and its location in the physical map of the large plasmid of enterohaemorrhagic Escherichia coli O157: H7. *Microbiology,* 142**,** 907-914.
SCHMITT, C. K., MCKEE, M. L., O'BRIEN, A. D. J. I. & IMMUNITY 1991. Two copies of Shiga-like toxin II-related genes common in enterohemorrhagic Escherichia coli strains are responsible for the antigenic heterogeneity of the O157: H-strain E32511. 59**,** 1065-1073.
SCHMITZ, F.-J., JONES, M. E., HOFMANN, B., HANSEN, B., SCHEURING, S., LÜCKEFAHR, M., FLUIT, A., VERHOEF, J., HADDING, U. & HEINZ, H.-P. 1998. Characterization of grlA, grlB, gyrA, and gyrB mutations in 116 unrelated isolates of Staphylococcus aureus and effects of mutations on ciprofloxacin MIC. *Antimicrobial Agents and Chemotherapy,* 42**,** 1249-1252.
SCHWIDDER, M., HEINISCH, L. & SCHMIDT, H. J. T. 2019. Genetics, toxicity, and distribution of enterohemorrhagic Escherichia coli hemolysin. 11**,** 502.
SCOTLAND, S., DAY, N., CRAVIOTO, A., THOMAS, L. & ROWE, B. 1981. Production of heat-labile or heat-stable enterotoxins by strains of Escherichia coli belonging to serogroups O44, O114, and O128. *Infection and immunity,* 31**,** 500-503.
SCOTLAND, S., SMITH, H. & ROWE, B. 1985. Two distinct toxins active on Vero cells from Escherichia coli O157. *Lancet (London, England),* 2**,** 885-886.
SCOTLAND, S., SMITH, H., WILLSHAW, G. & ROWE, B. 1983. Vero cytotoxin production in strain of Escherichia coli is determined by genes carried on bacteriophage. *The Lancet,* 322**,** 216.
SEARS, C. L. & KAPER, J. B. 1996. Enteric bacterial toxins: mechanisms of action and linkage to intestinal secretion. *Microbiological reviews,* 60**,** 167-215.

SECOR, P. R., SWEERE, J. M., MICHAELS, L. A., MALKOVSKIY, A. V., LAZZARESCHI, D., KATZNELSON, E., RAJADAS, J., BIRNBAUM, M. E., ARRIGONI, A. & BRAUN, K. R. 2015. Filamentous bacteriophage promote biofilm assembly and function. *Cell host & microbe,* 18**,** 549-559.

SEILER, H. G., SIGEL, H., SIGEL, A. & TOWNSHEND, A. 1990. Handbook on toxicity of inorganic compounds: Marcel Dekker, New York, NY, 1988 (ISBN 0-8247-7727-1). xxiv+ 1069 pp. Elsevier.

SENDER, R. J. P. B. 2016. S. fuchs, R. Milo. 14**,** e1002533.

SHAM, H. P., SHAMES, S. R., CROXEN, M. A., MA, C., CHAN, J. M., KHAN, M. A., WICKHAM, M. E., DENG, W., FINLAY, B. B., VALLANCE, B. A. J. I. & IMMUNITY 2011. Attaching and effacing bacterial effector NleC suppresses epithelial inflammatory responses by inhibiting NF-κB and p38 mitogen-activated protein kinase activation. 79**,** 3552-3562.

SHAW, K., RATHER, P., HARE, R. & MILLER, G. 1993. Molecular genetics of aminoglycoside resistance genes and familial relationships of the aminoglycoside-modifying enzymes. *Microbiological reviews,* 57**,** 138-163.

SHEIKH, J., DUDLEY, E. G., SUI, B., TAMBOURA, B., SULEMAN, A. & NATARO, J. P. 2006. EilA, a HilA-like regulator in enteroaggregative Escherichia coli. *Molecular microbiology,* 61**,** 338-350.

SHEIKH, J., HICKS, S., DALL'AGNOL, M., PHILLIPS, A. D. & NATARO, J. P. 2001. Roles for Fis and YafK in biofilm formation by enteroaggregative Escherichia coli. *Molecular microbiology,* 41**,** 983-997.

SHIGA, K. 1898. Ueber den Erreger der dysenterie in Japan. *Zentralbl Bakteriol Mikrobiol Hyg (Vorläufige Mitteilung),* 23**,** 599-600.

SJOGREN, R., NEILL, R., RACHMILEWITZ, D., FRITZ, D., NEWLAND, J., SHARPNACK, D., COLLETON, C., FONDACARO, J., GEMSKI, P. & BOEDEKER, E. 1994. Role of Shiga-like toxin I in bacterial enteritis: comparison between isogenic Escherichia coli strains induced in rabbits. *Gastroenterology,* 106**,** 306-317.

SMITH, D. L. 2005. *Characterisation of the infection of E. coli by a Shiga-toxin encoding bacteriophage.* University of Liverpool.

SMITH, D. L., JAMES, C. E., SERGEANT, M. J., YAXIAN, Y., SAUNDERS, J. R., MCCARTHY, A. J. & ALLISON, H. E. 2007a. Short-tailed stx phages exploit the conserved YaeT protein to disseminate Shiga toxin genes among enterobacteria. *Journal of bacteriology,* 189**,** 7223-7233.

SMITH, D. L., ROOKS, D. J., FOGG, P. C., DARBY, A. C., THOMSON, N. R., MCCARTHY, A. J. & ALLISON, H. E. 2012a. Comparative genomics of Shiga toxin encoding bacteriophages. *BMC genomics,* 13**,** 1-10.

SMITH, D. L., ROOKS, D. J., FOGG, P. C., DARBY, A. C., THOMSON, N. R., MCCARTHY, A. J. & ALLISON, H. E. 2012b. Comparative genomics of Shiga toxin encoding bacteriophages. *BMC genomics,* 13**,** 311.

SMITH, D. L., WAREING, B. M., FOGG, P. C., RILEY, L. M., SPENCER, M., COX, M. J., SAUNDERS, J. R., MCCARTHY, A. J. & ALLISON, H. E. 2007b. Multilocus characterization scheme for Shiga toxin-encoding bacteriophages. *Applied and environmental microbiology,* 73**,** 8032-8040.

SMITH, H., DAY, N., SCOTLAND, S., GROSS, R. & ROWE, B. 1984. Phage-determined production of vero cytotoxin in strains of Escherichia coli serogroup O157. *Lancet (London, England),* 1**,** 1242-1243.

SMITH, T. J., BLACKMAN, S. A. & FOSTER, S. J. 2000. Autolysins of Bacillus subtilis: multiple enzymes with multiple functions. *Microbiology,* 146**,** 249-262.

SNIDER, J., THIBAULT, G. & HOURY, W. A. 2008. The AAA+ superfamily of functionally diverse proteins. *Genome biology,* 9**,** 1-8.
SPELLBERG, B. & GILBERT, D. N. 2014. The future of antibiotics and resistance: a tribute to a career of leadership by John Bartlett. *Clinical infectious diseases,* 59**,** S71-S75.
SPIEGELMAN, W. G., REICHARDT, L. F., YANIV, M., HEINEMANN, S. F., KAISER, A. & EISEN, H. 1972. Bidirectional transcription and the regulation of phage λ repressor synthesis. *Proceedings of the National Academy of Sciences,* 69**,** 3156-3160.
STAYROOK, S., JARU-AMPORNPAN, P., NI, J., HOCHSCHILD, A. & LEWIS, M. 2008. Crystal structure of the λ repressor and a model for pairwise cooperative operator binding. *Nature,* 452**,** 1022-1025.
STEENBERGEN, S. M., JIRIK, J. L. & VIMR, E. R. 2009. YjhS (NanS) is required for Escherichia coli to grow on 9-O-acetylated N-acetylneuraminic acid. *Journal of bacteriology,* 191**,** 7134-7139.
STEIN, P. E., BOODHOO, A., TYRRELL, G. J., BRUNTON, J. L. & READ, R. J. 1992. Crystal structure of the cell-binding B oligomer of verotoxin-1 from E. coli. *Nature,* 355**,** 748-750.
STEVENS, M. P., ROE, A. J., VLISIDOU, I., VAN DIEMEN, P. M., LA RAGIONE, R. M., BEST, A., WOODWARD, M. J., GALLY, D. L. & WALLIS, T. S. 2004. Mutation of toxB and a truncated version of the efa-1 gene in Escherichia coli O157: H7 influences the expression and secretion of locus of enterocyte effacement-encoded proteins but not intestinal colonization in calves or sheep. *Infection and immunity,* 72**,** 5402-5411.
STEVENS, M. P., VAN DIEMEN, P. M., FRANKEL, G., PHILLIPS, A. D. & WALLIS, T. S. 2002. Efa1 influences colonization of the bovine intestine by Shiga toxin-producing Escherichia coli serotypes O5 and O111. *Infection and immunity,* 70**,** 5158-5166.
STIBOROVÁ, M., ŠIMÁNEK, V. M., FREI, E., HOBZA, P. & ULRICHOVÁ, J. 2002. DNA adduct formation from quaternary benzo [c] phenanthridine alkaloids sanguinarine and chelerythrine as revealed by the 32P-postlabeling technique. *Chemico-biological interactions,* 140**,** 231-242.
STRATING, H., VANDENENDE, C. & CLARKE, A. J. 2012. Changes in peptidoglycan structure and metabolism during differentiation of Proteus mirabilis into swarmer cells. *Canadian journal of microbiology,* 58**,** 1183-1194.
STROCKBINE, N. A., MARQUES, L., NEWLAND, J. W., SMITH, H. W., HOLMES, R. K. & O'BRIEN, A. D. 1986. Two toxin-converting phages from Escherichia coli O157: H7 strain 933 encode antigenically distinct toxins with similar biologic activities. *Infection and immunity,* 53**,** 135-140.
SU, L., LU, C., WANG, Y., CAO, D., SUN, J. & YAN, Y. 2010. Lysogenic infection of a Shiga toxin 2-converting bacteriophage changes host gene expression, enhances host acid resistance and motility. *Molecular biology,* 44**,** 54-66.
SUSSKIND, M. M. & BOTSTEIN, D. J. M. R. 1978. Molecular genetics of bacteriophage P22. 42**,** 385-413.
SYKES, R. B., BONNER, D. P. & SWABB, E. A. 1985. Modern β-lactam antibiotics. *Pharmacology & therapeutics,* 29**,** 321-352.
TAKACS, C. N., POGGIO, S., CHARBON, G., PUCHEAULT, M., VOLLMER, W. & JACOBS-WAGNER, C. 2010. MreB Drives De N ovo Rod Morphogenesis in Caulobacter crescentus via Remodeling of the Cell Wall. *Journal of bacteriology,* 192**,** 1671-1684.

TANEIKE, I., ZHANG, H.-M., WAKISAKA-SAITO, N. & YAMAMOTO, T. J. F. L. 2002. Enterohemolysin operon of Shiga toxin-producing Escherichia coli: a virulence function of inflammatory cytokine production from human monocytes. 524**,** 219-224.
TATSUNO, I., HORIE, M., ABE, H., MIKI, T., MAKINO, K., SHINAGAWA, H., TAGUCHI, H., KAMIYA, S., HAYASHI, T. & SASAKAWA, C. 2001. toxB gene on pO157 of enterohemorrhagic Escherichia coli O157: H7 is required for full epithelial cell adherence phenotype. *Infection and immunity,* 69**,** 6660-6669.
TENAILLON, O., SKURNIK, D., PICARD, B. & DENAMUR, E. J. N. R. M. 2010. The population genetics of commensal Escherichia coli. 8**,** 207-217.
TESH, V. L., RAMEGOWDA, B. & SAMUEL, J. E. 1994. Purified Shiga-like toxins induce expression of proinflammatory cytokines from murine peritoneal macrophages. *Infection and Immunity,* 62**,** 5085-5094.
THORPE, C., HURLEY, B. P., LINCICOME, L. L., JACEWICZ, M. S., KEUSCH, G. T. & ACHESON, D. W. 1999. Shiga toxins stimulate secretion of interleukin-8 from intestinal epithelial cells. *Infection and Immunity,* 67**,** 5985-5993.
TOBE, T. J. T. F. J. 2010. Cytoskeleton-modulating effectors of enteropathogenic and enterohemorrhagic Escherichia coli: role of EspL2 in adherence and an alternative pathway for modulating cytoskeleton through Annexin A2 function. 277**,** 2403-2408.
TRABULSI, L. R., KELLER, R. & GOMES, T. A. T. 2002. 10.321/eid0805. Typical and Atypical Enteropathogenic Escherichia coli. *Emerging infectious diseases,* 8**,** 508.
TRAN VAN NHIEU, G., BOURDET-SICARD, R., DUMÉNIL, G., BLOCKER, A. & SANSONETTI, P. J. 2000. Bacterial signals and cell responses during Shigella entry into epithelial cells: Microreview. *Cellular microbiology,* 2**,** 187-193.
TROFA, A. F., UENO-OLSEN, H., OIWA, R. & YOSHIKAWA, M. 1999. Dr. Kiyoshi Shiga: discoverer of the dysentery bacillus. *Clinical infectious diseases,* 29**,** 1303-1306.
TSAI, K.-C., JIAN, J.-W., YANG, E.-W., HSU, P.-C., PENG, H.-P., CHEN, C.-T., CHEN, J.-B., CHANG, J.-Y., HSU, W.-L. & YANG, A.-S. 2012. Prediction of carbohydrate binding sites on protein surfaces with 3-dimensional probability density distributions of interacting atoms. *PloS one,* 7**,** e40846.
TSE, C. M., IN, J. G., YIN, J., DONOWITZ, M., DOUCET, M., FOULKE-ABEL, J., RUIZ-PEREZ, F., NATARO, J. P., ZACHOS, N. C. & KAPER, J. B. 2018. Enterohemorrhagic E. coli (EHEC)—Secreted Serine Protease EspP Stimulates Electrogenic Ion Transport in Human Colonoid Monolayers. *Toxins,* 10**,** 351.
UCHIDA, H., KIYOKAWA, N., HORIE, H., FUJIMOTO, J. & TAKEDA, T. 1999. The detection of Shiga toxins in the kidney of a patient with hemolytic uremic syndrome. *Pediatric research,* 45**,** 133-137.
UNKMEIR, A. & SCHMIDT, H. 2000. Structural analysis of phage-borne stx genes and their flanking sequences in Shiga toxin-producing Escherichia coli and Shigella dysenteriae type 1 strains. *Infection and immunity,* 68**,** 4856-4864.
VACA PACHECO, S., GARCıĆA GONZÁLEZ, O. & PANIAGUA CONTRERAS, G. L. 1997. The lom gene of bacteriophage λ is involved in Escherichia coli K12 adhesion to human buccal epithelial cells. *FEMS microbiology letters,* 156**,** 129-132.

VALLANCE, B. & FINLAY, B. 2000. Exploitation of host cells by enteropathogenic Escherichia coli. *Proceedings of the National Academy of Sciences,* 97**,** 8799-8806.
VAN DER POLL, T. & OPAL, S. M. 2008. Host–pathogen interactions in sepsis. *The Lancet infectious diseases,* 8**,** 32-43.
VAN DIEMEN, P. M., DZIVA, F., STEVENS, M. P. & WALLIS, T. S. 2005. Identification of enterohemorrhagic Escherichia coli O26: H− genes required for intestinal colonization in calves. *Infection and immunity,* 73**,** 1735-1743.
VAN SETTEN, P. A., MONNENS, L., VERSTRATEN, R., VAN DEN HEUVEL, L. & VAN HINSBERGH, V. 1996. Effects of verocytotoxin-1 on nonadherent human monocytes: binding characteristics, protein synthesis, and induction of cytokine release.
VANPARIA, S. F., PATEL, T. S., SOJITRA, N. A., JAGANI, C. L., DIXIT, B. C., PATEL, P. S. & DIXIT, R. B. 2010. Synthesis, characterization and antimicrobial study of novel 4-{[(8-hydroxyquinolin-5-yl) methyl] amino} benzenesulfonamide and its oxinates. *Acta Chim Slov,* 57**,** 600-667.
VARMA, A. & YOUNG, K. D. 2009. In Escherichia coli, MreB and FtsZ direct the synthesis of lateral cell wall via independent pathways that require PBP 2. *Journal of bacteriology,* 191**,** 3526-3533.
VARNADO, C. L., HERTWIG, K. M., THOMAS, R., ROBERTS, J. K. & GOODWIN, D. C. 2004. Properties of a novel periplasmic catalase–peroxidase from Escherichia coli O157: H7. *Archives of Biochemistry and Biophysics,* 421**,** 166-174.
VELARDE, J. J. & NATARO, J. P. 2004. Hydrophobic residues of the autotransporter EspP linker domain are important for outer membrane translocation of its passenger. *Journal of Biological Chemistry,* 279**,** 31495-31504.
VELARDE, J. J., VARNEY, K. M., INMAN, K. G., FARFAN, M., DUDLEY, E., FLETCHER, J., WEBER, D. J. & NATARO, J. P. 2007. Solution structure of the novel dispersin protein of enteroaggregative Escherichia coli. *Molecular microbiology,* 66**,** 1123-1135.
VESES-GARCIA, M., LIU, X., RIGDEN, D. J., KENNY, J. G., MCCARTHY, A. J. & ALLISON, H. E. 2015a. Transcriptomic analysis of Shiga-toxigenic bacteriophage carriage reveals a profound regulatory effect on acid resistance in Escherichia coli. *Applied and environmental microbiology,* 81**,** 8118-8125.
VESES-GARCIA, M., LIU, X., RIGDEN, D. J., KENNY, J. G., MCCARTHY, A. J. & ALLISON, H. E. 2015b. Transcriptomic analysis of shigatoxigenic bacteriophage carriage reveals a profound regulatory effect on E. coli acid resistance. *Applied and environmental microbiology***,** AEM. 02034-15.
VESES-GARCIA, M., LIU, X., RIGDEN, D. J., KENNY, J. G., MCCARTHY, A. J., ALLISON, H. E. J. A. & MICROBIOLOGY, E. 2015c. Transcriptomic analysis of Shiga-toxigenic bacteriophage carriage reveals a profound regulatory effect on acid resistance in Escherichia coli. 81**,** 8118-8125.
VESES GARCIA, M. 2010. *Identification of Shigatoxigenic bacteriophage genes expressed in their E. coli hosts.* University of Liverpool.
VOLLMER, W., BLANOT, D. & DE PEDRO, M. A. 2008. Peptidoglycan structure and architecture. *FEMS microbiology reviews,* 32**,** 149-167.
VON EICHEL-STREIBER, C., BOQUET, P., SAUERBORN, M. & THELESTAM, M. 1996. Large clostridial cytotoxins—a family of glycosyltransferases modifying small GTP-binding proteins. *Trends in microbiology,* 4**,** 375-382.

VOSTROV, A. A., VOSTRUKHINA, O. A., SVARCHEVSKY, A. N. & RYBCHIN, V. N. 1996a. Proteins responsible for lysogenic conversion caused by coliphages N15 and phi80 are highly homologous. *Journal of bacteriology,* 178**,** 1484-1486.

VOSTROV, A. A., VOSTRUKHINA, O. A., SVARCHEVSKY, A. N. & RYBCHIN, V. N. J. J. O. B. 1996b. Proteins responsible for lysogenic conversion caused by coliphages N15 and phi80 are highly homologous. 178**,** 1484-1486.

WAKIMOTO, N., NISHI, J., SHEIKH, J., NATARO, J. P., SARANTUYA, J., IWASHITA, M., MANAGO, K., TOKUDA, K., YOSHINAGA, M. & KAWANO, Y. 2004. Quantitative biofilm assay using a microtiter plate to screen for enteroaggregative Escherichia coli. *The American journal of tropical medicine and hygiene,* 71**,** 687-690.

WANG, G., MAIER, S. E., LO, L. F., MAIER, G., DOSI, S. & MAIER, R. J. 2010a. Peptidoglycan deacetylation in Helicobacter pylori contributes to bacterial survival by mitigating host immune responses. *Infection and immunity,* 78**,** 4660-4666.

WANG, J., SAROV, M., RIENTJES, J., HU, J., HOLLAK, H., KRANZ, H., XIE, Y., STEWART, A. F. & ZHANG, Y. 2006. An improved recombineering approach by adding RecA to λ red recombination. *Molecular biotechnology,* 32**,** 43-53.

WANG, S., KONG, J. & ZHANG, X. 2008. Identification and characterization of the two-component cell lysis cassette encoded by temperate bacteriophage ϕPYB5 of Lactobacillus fermentum. *Journal of applied microbiology,* 105**,** 1939-1944.

WANG, X., KIM, Y., MA, Q., HONG, S. H., POKUSAEVA, K., STURINO, J. M. & WOOD, T. K. 2010b. Cryptic prophages help bacteria cope with adverse environments. *Nature communications,* 1**,** 147.

WANG, X., KIM, Y., MA, Q., HONG, S. H., POKUSAEVA, K., STURINO, J. M. & WOOD, T. K. 2010c. Cryptic prophages help bacteria cope with adverse environments. *Nature communications,* 1**,** 1-9.

WEADGE, J. T. & CLARKE, A. J. 2006. Identification and characterization of O-acetylpeptidoglycan esterase: a novel enzyme discovered in Neisseria gonorrhoeae. *Biochemistry,* 45**,** 839-851.

WEADGE, J. T. & CLARKE, A. J. 2007. Neisseria gonorrheae O-acetylpeptidoglycan esterase, a serine esterase with a Ser-His-Asp catalytic triad. *Biochemistry,* 46**,** 4932-4941.

WEERASINGHE, P., HALLOCK, S., BROWN, R. E., LOOSE, D. S. & BUJA, L. M. 2013. A model for cardiomyocyte cell death: insights into mechanisms of oncosis. *Experimental and molecular pathology,* 94**,** 289-300.

WEI, J., GOLDBERG, M., BURLAND, V., VENKATESAN, M., DENG, W., FOURNIER, G., MAYHEW, G., PLUNKETT, G., ROSE, D. & DARLING, A. 2003. Complete genome sequence and comparative genomics of Shigella flexneri serotype 2a strain 2457T. *Infection and immunity,* 71**,** 2775-2786.

WEINBAUER, M. G. 2004. Ecology of prokaryotic viruses. *FEMS microbiology reviews,* 28**,** 127-181.

WEISBLUM, B. 1995. Erythromycin resistance by ribosome modification. *Antimicrobial agents and chemotherapy,* 39**,** 577-585.

WELCH, D. Role of catalase and superoxide dismutase of the virulence of Listeria monocytogenes. Annales de l'Institut Pasteur/Microbiologie, 1987. Elsevier, 265-268.

WHITE, R., CHIBA, S., PANG, T., DEWEY, J. S., SAVVA, C. G., HOLZENBURG, A., POGLIANO, K. & YOUNG, R. 2011. Holin triggering in real time. *Proceedings of the National Academy of Sciences,* 108**,** 798-803.
WONG, M. H. Y., CHAN, E. W. C. & CHEN, S. 2015. Evolution and dissemination of OqxAB-like efflux pumps, an emerging quinolone resistance determinant among members of Enterobacteriaceae. *Antimicrobial agents and chemotherapy,* 59**,** 3290-3297.
XIE, Z.-R., LIU, C.-K., HSIAO, F.-C., YAO, A. & HWANG, M.-J. 2013. LISE: a server using ligand-interacting and site-enriched protein triangles for prediction of ligand-binding sites. *Nucleic acids research,* 41**,** W292-W296.
YAMAMOTO, T., KOYAMA, Y., MATSUMOTO, M., SONODA, E., NAKAYAMA, S., UCHIMURA, M., PAVEENKITTIPORN, W., TAMURA, K., YOKOTA, T. & ECHEVERRIA, P. 1992. Localized, Aggregative, and Diffuse Adherence to HeLa Cells, Plastic, and Human Small Intestines by Escherichi coli Isolated from Patients with Diarrhea. *Journal of Infectious Diseases,* 166**,** 1295-1310.
YOSHIDA, H., BOGAKI, M., NAKAMURA, M., YAMANAKA, L. M. & NAKAMURA, S. 1991. Quinolone resistance-determining region in the DNA gyrase gyrB gene of Escherichia coli. *Antimicrobial agents and chemotherapy,* 35**,** 1647-1650.
YOSHIDA, S. & SASAKAWA, C. 2003. Exploiting host microtubule dynamics: a new aspect of bacterial invasion. *Trends in microbiology,* 11**,** 139-143.
YOUNG, K. D. 2006. The selective value of bacterial shape. *Microbiology and molecular biology reviews,* 70**,** 660-703.
YOUNG, R. 2013. Phage lysis: do we have the hole story yet? *Current opinion in microbiology,* 16**,** 790-797.
YOUNG, R., WANG, N. & ROOF, W. D. 2000. Phages will out: strategies of host cell lysis. *Trends in microbiology,* 8**,** 120-128.
ZHANG, X., CHENG, Y., XIONG, Y., YE, C., ZHENG, H., SUN, H., ZHAO, H., REN, Z. & XU, J. 2012. Enterohemorrhagic Escherichia coli specific enterohemolysin induced IL-1β in human macrophages and EHEC-induced IL-1β required activation of NLRP3 inflammasome. *PLoS One,* 7**,** e50288.
ZOU, J. & SHANKAR, N. 2016. The opportunistic pathogen Enterococcus faecalis resists phagosome acidification and autophagy to promote intracellular survival in macrophages. *Cellular microbiology,* 18**,** 831-843.
ZUPPI, M., TOZZOLI, R., CHIANI, P., QUIROS, P., MARTINEZ-VELAZQUEZ, A., MICHELACCI, V., MUNIESA, M. & MORABITO, S. 2020. Investigation on the evolution of Shiga toxin-converting phages based on whole genome sequencing. *Frontiers in Microbiology,* 11**,** 1472.